



Port, Jennifer Lynne Forbes (2018) *Investigating the therapeutic potential of NUAK1 for the treatment of colorectal cancer*. PhD thesis.

<https://theses.gla.ac.uk/9125/>

Copyright and moral rights for this work are retained by the author

A copy can be downloaded for personal non-commercial research or study,  
without prior permission or charge

This work cannot be reproduced or quoted extensively from without first  
obtaining permission in writing from the author

The content must not be changed in any way or sold commercially in any  
format or medium without the formal permission of the author

When referring to this work, full bibliographic details including the author,  
title, awarding institution and date of the thesis must be given

Enlighten: Theses

<https://theses.gla.ac.uk/>  
[research-enlighten@glasgow.ac.uk](mailto:research-enlighten@glasgow.ac.uk)



University  
of Glasgow

# Investigating the Therapeutic Potential of NUAK1 for the Treatment of Colorectal Cancer

**Jennifer Lynne Forbes Port**

This thesis is submitted to the University of Glasgow in fulfilment of the requirements of the Degree of Doctor of Philosophy.

**Institute of Cancer Sciences**  
College of Medical, Veterinary, and Life Sciences  
University of Glasgow

**The Beatson Institute for Cancer Research**  
Garscube Estate  
Glasgow

**September 2017**



CANCER  
RESEARCH  
UK

BEATSON  
INSTITUTE

## Abstract

NUAK1 (aka ARK5) is a member of the AMPK-related kinase family and has been associated with many essential cellular processes that are often perturbed in cancer. Elevated NUAK1 expression has been observed in advanced stages of colorectal cancer (CRC) and is further enriched in liver metastasis in human patients. Therefore, NUAK1 is a novel tumour progression-associated factor, however, its primary function in this context and its use as a potential therapeutic target remains unclear.

NUAK1 was previously identified as synthetic lethal in MYC-overexpressing tumour cells. This study shows that high NUAK1 levels correspond to poor patient survival in human CRC, and that increased NUAK1 RNA correlates with advanced tumour stages in a human TMA of CRC. Using mouse models of CRC, it is demonstrated that *Nuak1* deletion inhibits colon tumour initiation, and acute depletion of *Nuak1* by shRNA in established tumours significantly reduces tumour burden after just 7 days of shRNA activation. Interrogation of tumours acutely depleted of *Nuak1* showed decreased cell proliferation concurrent with increased ROS and cell death. Interestingly, the requirement for *Nuak1* did not extend to healthy wildtype intestine; depletion of *Nuak1* in mouse intestine had no impact on cell death, proliferation or differentiation, and wildtype 3D organoids were resistant to *Nuak1* inhibition. Using human CRC cell lines and transformed 3D organoid cultures, the study confirms that the NRF2 oxidative stress response is compromised in NUAK1 depleted cells, and treatment with a ROS scavenger can rescue the detrimental consequences of this *in vitro*, *ex vivo* and *in vivo*. Mechanistically, it was found that NUAK1 is necessary for the nuclear accumulation of NRF2 by counteracting negative regulation of this process by GSK3 $\beta$ , and that direct inhibition of GSK3 $\beta$  is able to restore NRF2 nuclear accumulation in NUAK1 deficient cells. Furthermore, it is shown that ROS-dependent activation of NUAK1 by cysteine oxidisation leads to the phosphorylation of MYPT1. Activation of MYPT1 results in the suppression of PP1 $\beta$  activity, which in turn inhibits dephosphorylation of GSK3 $\beta$  thus allowing NRF2 to accumulate in the nucleus and upregulate the anti-oxidant response pathway.

In summary, this thesis is proposing a fascinating, new and conserved mechanism of redox signal transduction in which activation of NUAK1 coordinates PP1 $\beta$ <sup>MYPT1</sup> inhibition, with AKT activation in order to suppress GSK3 $\beta$ -dependent inhibition of

NRF2 nuclear import. Exploiting the heightened sensitivity of tumour cells to ROS is emerging as a plausible strategy for cancer therapy and is implicated in the resistance to chemotherapy. Therefore, inhibiting the anti-oxidant response via transient inhibition of NUA1 may offer a new strategy for improving therapeutic outcomes in cancer.

# Table of Contents

List of Tables .....	7
List of Figures .....	8
Acknowledgements.....	10
Abbreviations .....	13
<b>Chapter 1 Introduction.....</b>	<b>18</b>
<b>1.1 Colorectal Cancer .....</b>	<b>18</b>
<b>1.2 CRC clinical manifestations.....</b>	<b>18</b>
<b>1.3 Clinical diagnosis and staging.....</b>	<b>18</b>
1.3.1 TNM Classification of Malignant Tumours (TNM) .....	19
1.3.2 The Dukes' staging system.....	22
<b>1.4 Current treatment of CRC .....</b>	<b>22</b>
<b>1.5 Normal Intestinal Homeostasis.....</b>	<b>23</b>
<b>1.6 Molecular characterization of CRC.....</b>	<b>25</b>
1.6.1 Adenomatous polyposis coli (APC), $\beta$ -Catenin and Wnt signalling.....	26
1.6.2 MYC deregulation in CRC.....	27
1.6.3 The 'adenoma-to-carcinoma' sequence.....	28
1.6.4 KRAS.....	31
1.6.5 Other common mutations in CRC.....	33
1.6.6 The consensus molecular subtypes of CRC .....	34
<b>1.7 Approaches to modelling CRC .....</b>	<b>35</b>
1.7.1 Human cell lines .....	35
1.7.2 Intestinal organoids.....	36
1.7.3 Genetically engineered mouse models (GEMMs).....	37
<b>1.8 AMPK-Related kinases .....</b>	<b>43</b>
1.8.1 AMPK.....	43
1.8.2 AMPK-related kinases.....	44
1.8.3 NUA1 and NUA2: structure, expression and a common target.....	46
1.8.4 NUA2: function and regulation.....	49
<b>1.9 NUA1 .....</b>	<b>50</b>
1.9.1 NUA1: function and regulation.....	50
1.9.2 NUA1 mouse models .....	51
1.9.3 NUA1 and cancer.....	52
1.9.4 NUA1 and synthetic lethality .....	54
<b>1.10 Aims of the project .....</b>	<b>58</b>
<b>Chapter 2 Materials &amp; Methods.....</b>	<b>60</b>
<b>2.1 Mouse experiments and analyses .....</b>	<b>60</b>
2.1.1 Colony Maintenance .....	60
2.1.2 Genotyping.....	60
2.1.3 Experimental Cohorts .....	60
2.1.4 Tissue preparation and scoring .....	64
2.1.5 Tissue stains and immunohistochemistry.....	64
<b>2.2 Crypt culture.....</b>	<b>68</b>
2.2.1 Organoid/spheroid preparation.....	68
2.2.2 Passaging spheroids/organoids in culture.....	69
2.2.3 Cryopreservation of spheroids/organoids.....	69
2.2.4 Thawing spheroids/organoids.....	69
2.2.5 Quantification of spheroids .....	70
2.2.6 Treatments .....	70
2.2.7 Cre recombination in vitro.....	70
2.2.8 ROS detection .....	70
2.2.9 Cell Viability .....	71

<b>2.3 Cell culture .....</b>	<b>71</b>
2.3.1 Passaging cells in culture.....	71
2.3.2 Cryopreservation of cell lines .....	71
2.3.3 Thawing cells in culture .....	72
2.3.4 Mouse Embryonic Fibroblast culture .....	72
2.3.5 Drug treatments .....	72
2.3.6 Transfection .....	73
2.3.7 ROS detection .....	73
2.3.8 Annexin V/PI staining.....	73
2.3.9 Protein isolation and Immunoblotting.....	74
2.3.10 Immunoprecipitation .....	76
2.3.11 Dimedone detection of cysteine oxidation .....	76
2.3.12 Iodoacetamide labelling .....	76
2.3.13 RNA isolation and analysis.....	77
<b>2.4 NUAK1 shRNA gene expression analysis.....</b>	<b>78</b>
<b>2.5 Human TMA analysis .....</b>	<b>79</b>
<b>2.6 <i>In situ</i> hybridization (RNA Scope) .....</b>	<b>79</b>
<b>2.7 Proteomic analysis .....</b>	<b>80</b>
2.7.1 SILAC labelling .....	80
2.7.2 Sample Preparation .....	80
2.7.3 MS analysis .....	81
<b>2.8 Data Analysis.....</b>	<b>82</b>
<b>Chapter 3 The relevance of NUAK1 in human CRC .....</b>	<b>83</b>
<b>3.1 Introduction .....</b>	<b>83</b>
<b>3.2 Results.....</b>	<b>85</b>
3.2.1 NUAK1 is a prognostic factor for survival in CRC.....	85
3.2.2 High NUAK1 mRNA levels are associated with more advanced CRC .....	88
3.2.3 NUAK1 is required for the survival of human CRC lines .....	91
<b>3.3 Discussion .....</b>	<b>95</b>
<b>Chapter 4 Investigating the role of NUAK1 using mouse models of CRC .....</b>	<b>98</b>
<b>4.1 Introduction .....</b>	<b>98</b>
4.1.1 Nuak1 Mouse models .....	99
<b>4.2 Results.....</b>	<b>102</b>
4.2.1 Nuak1 is dispensable in normal gut epithelium .....	102
4.2.2 Nuak1 is dispensable in wildtype organoid cultures.....	103
4.2.3 Nuak1 has no impact on c-MYC-dependent progenitor phenotype.....	104
4.2.4 Nuak1 is necessary for tumourigenesis in a GEMM of CRC.....	105
4.2.5 Nuak1 is necessary for 'stemness' in GEMM generated spheroid cultures .....	109
4.2.6 Nuak1 is necessary for the survival of established intestinal tumours in a GEMM model of CRC.....	112
4.2.7 Nuak1 is required for the survival of pre-formed spheroids .....	120
<b>4.3 Discussion .....</b>	<b>122</b>
<b>Chapter 5 NUAK1 is required for the detoxification of ROS.....</b>	<b>127</b>
<b>5.1 Introduction .....</b>	<b>127</b>
<b>5.2 Results.....</b>	<b>132</b>
5.2.1 NUAK1 suppression impairs the NRF2 antioxidant program .....	132
5.2.2 Tumour suppressive effect of Nuak1 depletion is a consequence of increased ROS, which can be reversed by exogenous provision of NAC in vivo .....	139
5.2.3 NUAK1 is required for the nuclear localisation of NRF2 protein.....	142
5.2.4 NUAK1 promotes nuclear translocation of NRF2 by antagonizing GSK3 $\beta$ .....	145
5.2.5 MYPT1 responds to ROS in a NUAK1 dependent manner .....	147
5.2.6 NUAK1 is activated by ROS oxidisation of cysteine residues .....	148
<b>5.3 Discussion .....</b>	<b>150</b>
<b>Chapter 6 Discussion, Conclusions and Future work.....</b>	<b>155</b>

**Bibliography .....163**

# List of Tables

## Chapter 1

Table 1. 1 - TNM stage definition and description for T stage, N stage and M stage. ....	20
Table 1. 2 - Duke' staging system with descriptions. ....	22
Table 1. 3 - The Consensus molecular subtypes for CRC .....	35

## Chapter 2

Table 2. 1 - Immunohistochemistry (IHC) antibodies and conditions.....	67
Table 2. 2 - Acrylamide gel composition.....	75

## Chapter 5

Table 5. 1 - Genes regulated by NRF2 involved in oxidant response and redox signalling. Figure adapted from Ma, 2013, supplementary table 1.....	129
---	-----

# List of Figures

## Chapter 1

Figure 1. 1 - Visual representation of tumour progression in colorectal cancer using the TNM classification of malignant tumours system.....	21
Figure 1. 2 - Normal intestinal homeostasis in the small intestine and the colon.....	24
Figure 1. 3 - The Wnt signalling pathway. ....	26
Figure 1. 4 - The Adenoma to Carcinoma sequence.....	30
Figure 1. 5 - The RAS signalling pathway.....	32
Figure 1. 6 - Murine -, small intestine - derived organoids.....	37
Figure 1. 7 - The Cre-Lox System. ....	40
Figure 1. 8 - The AMPK-related kinase family .....	45
Figure 1. 9 - Amino acid sequence homology between human NUA1 and NUA2 .....	47
Figure 1. 10 - Schematic representation of NUA1/NUA2's role in the regulation of myosin light chain phosphorylation.....	49
Figure 1. 11 - NUA1 alteration frequency across human cancer types.....	53
Figure 1. 12 - The TOR signalling pathway .....	57
Figure 1. 13 - A summary of NUA1 activators, downstream effects and pathways.....	59

## Chapter 3

Figure 3. 1 - NUA1 overexpression correlates with tumour progression, lymph node infiltrates, and reduced overall survival in human CRC.....	87
Figure 3. 2 - High NUA1 RNA correlates with increased tumour stage and lymph node metastasis in a human CRC TMA .....	90
Figure 3. 3 - NUA1 level does not correlate with survival in human TMA .....	91
Figure 3. 4 - Human CRC cell lines are sensitive to loss of NUA1 activity.....	94

## Chapter 4

Figure 4. 1 - <i>The Villin-CreER<sup>T2</sup>; Apc<sup>fl/+</sup>; LSL-KRas<sup>G12D</sup>; Nuak1<sup>fl/fl</sup></i> mouse model for sporadic intestinal cancer.....	100
Figure 4. 2 - The TET-ON DI-shNuak1.612/1533 mouse model.....	101
Figure 4. 3 - Nuak1 is dispensable in normal gut epithelium .....	103
Figure 4. 4 - Nuak1 is dispensable in wildtype organoid cultures .....	104
Figure 4. 5 - Nuak1 has no impact on c-MYC-dependent progenitor phenotype.....	105
Figure 4. 6 - Deletion of Nuak1 suppresses colorectal tumour formation .....	106
Figure 4. 7 - Inefficient deletion of Nuak1 in the small intestine .....	107
Figure 4. 8 - Interrogation of Nuak1 levels in VAK and VAKN colon normal tissue and tumour.....	108
Figure 4. 9 - Nuak1 depletion does not alter Kras or Apc status in colonic tumours. ....	109
Figure 4. 10 - Nuak1 is necessary for 'stemness' in GEMM generated spheroid cultures. ....	111
Figure 4. 11 - The DSS/DI-shNuak1 model experimental plan and validation .....	113
Figure 4. 12 - Acute Nuak1 depletion reduces colonic tumour number, burden and size. ....	114
Figure 4. 13 - Three days of Nuak1 depletion reduces colonic tumour number, burden and size.....	115
Figure 4. 14 - Tumours are enriched with Nuak1 mRNA and Nuak1 depletion is observed at 3 days but not 7 days.....	117
Figure 4. 15 - Nuak1 depletion leads to reduced cell proliferation and increase cell death .....	119
Figure 4. 16 - Spheroids require Nuak1 for survival <i>ex vivo</i> .....	121

## Chapter 5

Figure 5. 1 - NRF2 regulation .....	130
Figure 5. 2 - NUAk1 suppression impairs the NRF2 anti-oxidant program .....	133
Figure 5. 3 - NUAk1 suppression leads to increased cellular ROS .....	134
Figure 5. 4 - Small interfering RNA (siRNA) for the silencing of NUAk1 are on target	135
Figure 5. 5 - NUAk1 suppression sensitises cells to peroxide .....	136
Figure 5. 6 - HTH-induced cell death is rescued by addition of exogenous anti-oxidant	138
Figure 5. 7 - Acute loss of Nuak1 results in increased ROS in tumours .....	140
Figure 5. 8 - NUAk1 addicted tumours are rescued by addition of exogenous anti-oxidant .....	142
Figure 5. 9 - NUAk1 does not regulate NRF2 at protein level .....	143
Figure 5. 10 - NUAk1 is required for NRF2 localisation to the nucleus .....	144
Figure 5. 11 - NUAk1 is necessary for the inhibitory phosphorylation of GSK3 $\beta$ Ser-9	145
Figure 5. 12 - NUAk1's regulation of GSK3 $\beta$ is conserved to SW480 cells and is independent of upstream AKT signalling.....	146
Figure 5. 13 - Pharmacological or genetic abrogation of GSK3 $\beta$ rescues nuclear accumulation of NRF2.....	147
Figure 5. 14 - MYPT1 responds to peroxide treatment in a NUAk1 dependent manner.	148
Figure 5. 15 - NUAk1 is activated by ROS oxidation of cysteine residues .....	149
Figure 5. 16 - NUAk1 regulation of the anti-oxidant response pathway .....	154

## Chapter 6

Figure 6. 1 - NUAk1 and the anti-oxidant stress response .....	158
--	-----

## Acknowledgements

First and foremost, I would like to express my sincere gratitude to my supervisor Dr. Daniel Murphy for the constant support and guidance throughout my Ph.D study and for the opportunity to work in his lab on a truly exciting research project. I would like to thank him for his motivation and enthusiasm and I have grown tremendously as a scientist under his mentorship.

My sincere thanks also goes to the University of Glasgow, Institute for Cancer Sciences and to Marie Curie for funding my Ph.D studentship here at the Beatson Institute. Also to the Beatson Institute for Cancer Research for having me, it's been a dream to be part of such an impressive Institute.

I would also like to thank my student advisors, Professors Eyal Gottlieb, Robert Insall, and Martin Drysdale, for their insightful comments and encouragement in my project, and for always making our meetings stimulating and enjoyable.

I would like to thank our collaborators for their specialist help during this study, Dr. Sara Zanivan and the Beatson Institute Proteomics Facility, Billy Clark from Biological Services, Ann Hedley and Gabriela Kalna from Computational Biology and Professor Graeme Murray from University of Aberdeen. Thanks to the fantastic biological and histological services at the Beatson Institute, without these services this work would not have been possible. A special thanks goes to Colin, for always being enthusiastic to help with histology and the team in the BRU for all their help with animal experiments.

To my very dear friend and fellow PhD student, Tiziana. I feel so happy that we got to share in this amazing experience together, there have been some big highs and big lows, but together we have been unstoppable! She has been a constant source of laughter and support. To Nathiya, who has shown me such patience and guidance over the years, thanks goes to her for sharing all of her knowledge, experience and most importantly joy with me. It's been a privilege to work on this study with her. To Meera, I would like to thank her for sharing her immense scientific knowledge with me and mentoring me in the colon mouse models, without her, this project would not have progressed as it did. I am also grateful for her friendship and all the fun times we had! To Jacqueline, I would like to thank her for bringing laughter and fun to the lab, and for her mentorship in all things western blot!! I would like to thank my fellow colleagues in M10, Sarah, Björn, Katarina, Allan and all of

M06. I'm so grateful for all the times we spent together, for the stimulating scientific discussions, for the immense support in impending deadlines and for all the fun we have had in between. I would like to thank my students, Martina and Amy; I learned so much from being a mentor and both were an absolute joy to work with. A special thanks goes to Nathiya and Björn, who have spent hours looking over this thesis and providing great feedback. To my best friends, Dominika, Alessandra, Christin, thank you for always being there to listen, laugh, and have fun with! We've had some great adventures over the years, and I'm sure we'll have many more.

Last but certainly not least; I would like to thank my parents, John and Viveca, and my sister, Katrina, for their never-ending faith in me and my capabilities and for all of their love. I wouldn't be here today, without their support. To my wonderful boyfriend, Alasdair, who has been a pillar of strength when times have been challenging. Thanks to my best friends, Meghann and Amy, for being my family away from home. Finally, thanks goes to my small black cat, Coco, for always being excited to see me after a long day in the lab.

## Author's Declaration

“I declare that, except where explicit reference is made to the contribution of others, that this dissertation is the result of my own work and has not been submitted for any other degree at the University of Glasgow or any other institution.”

Printed Name: JENNIFER LYNNE FORBES PORT

Signature:

A handwritten signature in black ink, appearing to read 'J. Forbes Port', written in a cursive style.

# Abbreviations

## Mouse models

LSL = lox stop lox codon  
DI = doxycycline inducible  
TRE = tetracycline-responsive element  
UTR = untranslated region  
ES = embryonic stem cells  
VA = *Villin CreER<sup>T2</sup>;Apc<sup>fl/fl</sup>*  
VAN = *Villin CreER<sup>T2</sup>;Apc<sup>fl/fl</sup>;Nuak1<sup>fl/fl</sup>*  
VAK = *Villin CreER<sup>T2</sup>;Apc<sup>fl/fl</sup>;LSL-KRas<sup>G12D/+</sup>*  
VAKN = *Villin CreER<sup>T2</sup>;Apc<sup>fl/fl</sup>;LSL-KRas<sup>G12D/+</sup>;Nuak1<sup>fl/fl</sup>*  
TET-ON = tetracycline inducible system  
GFP = green fluorescent protein

## Symbols

O<sub>2</sub>•<sup>-</sup> = superoxide anion  
H<sub>2</sub>O<sub>2</sub> = hydrogen peroxide  
•OH = hydroxyl radical  
RO<sub>2</sub>• = alkoxy radical  
RO• = alkoxy radical  
<sup>1</sup>O<sub>2</sub> = singlet oxygen  
O<sub>3</sub> = ozone  
•NO = nitric oxide  
•NO<sub>2</sub> = nitrogen dioxide  
ONOO<sup>-</sup> = peroxynitrite  
°C = degrees Celsius  
µg = microgram  
mg = milligram  
g = gram  
kg = kilogram  
µl = microliter  
ml = millilitre  
nm = nanometre  
µm = micrometre  
mm = millimetre  
cm = centimetre  
nM = nanomolar  
µM = micromolar  
mM = millimolar  
M = molar

## A

ACF = aberrant crypt foci  
ACN = acetonitrile  
ADP = adenosine biphosphate  
AICAR = 5' aminoimidazole-4-carboxamide riboside  
AKT = protein kinase B  
AMP = adenosine monophosphate  
AMPK = AMP-activated protein kinase  
AMPK-RK – AMPK-related kinase  
AOM = azoxymethane

APC = adenomatous polyposis coli  
ARE = anti-oxidant response element  
ATP = adenosine triphosphate

## **B**

BCA = bicinchoninic acid  
BICR = Beatson Institute for Cancer Research  
BMP = bone morphogenetic protein  
BRSK1/2 = brain-specific kinases  
BSA = bovine albumin serum

## **C**

CaMKK $\beta$  = Ca<sup>2+</sup>/calmodulin-dependent PK kinase  $\beta$   
CBC = crypt-based columnar  
CDK2 = cyclin dependent kinase 2  
CDK4 = cyclin dependent kinase 4  
CIMP = CpG island methylator phenotype  
CIN = chromosomal instability  
CKI = casein kinase 1  
CME = complete mesocolic excision  
CNC = cap 'N' collar  
COX = cyclooxygenase  
CRC = colorectal cancer  
CREB = cAMP response element binding protein  
CT/CTC = Computed tomography-colonography  
CTCF = corrected total cell fluorescence

## **D**

DAB = 3,3'-diaminobenzidine  
DMEM = Dulbecco's modified Eagle's medium  
DMH = dimethylhydrazine  
DMSO = Dimethyl sulfoxide  
DNA = deoxyribonucleic acid  
DSS = dextran sodium sulphate

## **E**

EBV = Epstein-Barr virus  
ECM = extracellular matrix  
EDTA = Ethylenediaminetetraacetic acid  
EGF = epidermal growth factor  
EGFR = epidermal growth factor receptor  
ER = endoplasmic reticulum

## **F**

FACs = flow cytometry  
FAP = familial adenomatous polyposis  
FASP = filter-aided sample preparation  
FBS = foetal bovine serum  
FCS = foetal calf serum  
FDA = Food and Drug Administration  
FDR = false discovery rate  
FFPE = formalin fixed paraffin embedded  
FZD = frizzled receptor

## **G**

GCLG = Glutamate-Cysteine Ligase Catalytic Subunit  
GCLM = Glutamate-Cysteine Ligase Modifier Subunit  
GDP = guanosine-5'-biphosphate  
GEMM = genetically engineered mouse model  
GILK = Gly-Ile-Leu-Lys motif  
GSH = glutathione  
GSHR = glutathione reductase  
GSK3 $\beta$  = glycogen synthase kinase 3  $\beta$   
GTP = guanosine-5'-triphosphate

## **H**

H&E = hematoxylin and eosin  
HCC = hepatocellular carcinoma  
HEPES = 4-(2-Hydroxyethyl)piperazine-1-ethanesulfonic acid  
HFD = high fat diet  
HGSOC = high-grade serous ovarian cancer  
HRAS = Harvey rat sarcoma viral oncogene  
HRP = horseradish peroxidase  
HTH = HTH-01-015

## **I**

IBS = irritable bowel syndrome  
IGF = insulin-like growth factor  
IGF1R = insulin-like growth factor receptor 1  
IHC = immunohistochemistry  
IP = intraperitoneal  
ISC = intestinal stem cell  
IVCs = individually ventilated cages

## **K**

KEAP1 = kelch-like ECH-associated protein 1  
KRAS = Kirsten rat sarcoma viral oncogene

## **L**

LI = large intestine/colon  
LKB1 = liver kinase B1  
LMP1 = Epstein Barr virus (EBV) latent membrane protein 1  
LRP = low density lipoprotein receptor-related protein

## **M**

MAPK = mitogen-activated protein kinase  
MARK1/2/3 = MAP/microtubule affinity-regulating kinases  
MCM = minichromosome maintenance  
MELK = maternal embryonic leucine zipper kinase  
MGST = microsomal glutathione S-transferase 1  
MMP = matrix metalloproteinases  
MO25 = mouse protein 25  
mRNA = messenger ribonucleic acid  
MS = mass spectrometry  
MSH2 = MutS protein homolog 2  
MSI = microsatellite instability

mTOR = mechanistic target of rapamycin  
MYC-ER = c-MYC fused to the oestrogen receptor ligand binding domain  
MYPT1 = myosin phosphatase target subunit 1

## **N**

NAC = N-Acetyl-Cysteine  
NADPH = nicotinamide adenine dinucleotide phosphate  
NCI = National Cancer Institute  
NDR2 = nuclear Dbf2-related protein  
NES = nuclear export signal  
NHGRI = National Human Genome Research Institute  
NQO1 = quinone dehydrogenase  
NRAS = Neuroblastoma rat sarcoma viral oncogene  
NRF2 = nuclear factor erythroid 2 (NF-E2)-related factor 2  
NSCLC = non-small cell lung cancer  
NUAK1/ARK5 = NUA family SNF-like kinase 1/AMPK-related protein kinase 5  
NUAK2/SNARK = NUA family SNF-like kinase 2/ sucrose non-fermenting AMPK-related kinase

## **O**

OHT = 4'hydroxytamoxifen

## **P**

PAS = periodic acid Schiff  
PBS = Phosphate buffer saline  
PCR = polymerase chain reaction  
PDGFR = platelet-derived growth factor receptor  
PI = propidium iodide  
PI3K = phosphoinositide 3-kinase  
PIGF = placental growth factor  
PLL = poly-L-Lysine  
PP1 $\beta$  = protein phosphatase 1 catalytic subunit  $\beta$   
PRDX1 = Peroxiredoxin 1  
PTEN = phosphatase and tensin homolog

## **Q**

QIK = quiescence induced kinase  
qRT-PCR = quantitative real time polymerase chain reaction

## **R**

RAPTOR = regulatory-associate protein of mTOR  
RAS = rat sarcoma viral oncogene  
RIPA = Radioimmunoprecipitation assay buffer  
RNA = ribonucleic acid  
RNA = ribonucleic acid  
RNS = reactive nitrogen species  
ROS = reactive oxygen species  
RT = reverse transcriptase  
RT = room temperature

## **S**

SCF/ $\beta$ -TrCP = skip, cullin, F-box containing complex/F-box/WD repeat-containing protein 1A

SDS = Sodium dodecyl sulphate  
SDS-PAGE = Sodium dodecyl sulphate – polyacrylamide gel electrophoresis  
SEM = standard error of the mean  
shRNA = short hairpin ribonucleic acid  
SI = small intestine  
SIK/QSK = salt inducible kinases  
SNP = single nucleotide polymorphism  
SNRK = SNF-related serine/threonine-protein kinase  
STRAD = STE20-related kinase adaptor protein

## **T**

TA = transit amplifier  
TAK1 = TGF $\beta$ -activated kinase  
TBST = tris buffered saline tween solution  
TCF/LEF = T-cell factor/lymphoid enhancer factor  
TdT = terminal deoxynucleotidyl transferase  
TGCA = The Cancer Genome Atlas  
TGF $\beta$  = transforming growth factor  $\beta$   
TMA = tissue microarray  
TNF = tumour necrosis factor  
TNM = Tumour Node Metastasis for the classification of Malignant Tumours  
TOR = target of rapamycin  
TORC = target of rapamycin complex  
TP53/P53 = tumour protein 53  
TRAIL = tumour necrosis factor (TNF)-related apoptosis-inducing ligand  
TUNEL = Terminal deoxynucleotidyl transferase (TdT) dUTP Nick-End Labelling  
TXN = thioredoxin  
TXRND1 = thioredoxin reductase

## **U**

UBA = ubiquitin-associate  
UICC = Union for International Cancer Control

## **V**

VEGF = vascular endothelial growth factor  
VEGFR = vascular endothelial growth factor receptor

## **W**

WZ = WZ4003

## **Z**

ZP3 = zona pellucida 3

# Chapter 1 Introduction

## 1.1 Colorectal Cancer

Colorectal cancer (CRC), also known as bowel cancer and colon cancer, is the development of cancer in the colon or rectum. It is the fourth most common cancer in the UK with over 40,000 new cases annually, and 110 cases diagnosed daily (CRUK, 2013). More worryingly, this rate is expected to increase due to the adoption of westernised diet and lifestyle across the world. However, since the 1970s mortality rates have decreased by 43% in the UK and rates are projected to fall by a further 23% by 2035 due to more appropriate and available information, earlier diagnosis and improvements in surgical, adjuvant and palliative treatment (CRUK, 2013).

## 1.2 CRC clinical manifestations

Clinical manifestations tend to vary depending on the location of the tumour in the bowel. Thirty percent of patients present with sub/obstructing symptoms and are diagnosed in an acute stage of colorectal carcinoma; these symptoms include the passage of blood, also known as hematochezia, causing anaemia and fatigue and/or tenesmus, a continual or recurrent inclination to evacuate the bowels. Other symptoms include loss of appetite, nausea and vomiting. Metastasis in the liver or lung is present in 20-25% of colonic cancer patients and in 18% of rectal cancer at the time of first diagnosis (De Rosa et al., 2016).

## 1.3 Clinical diagnosis and staging

Accurate diagnosis and staging are essential to ensure an effective treatment strategy for the patient. The current gold standard for diagnosis is a complete colonoscopy up to the cecum, coupled with biopsy for histopathological examination and allows tumour localization and potentially the excision of polyps by endoscopy. Computed tomography-colonography (CT or CTC) can also be used in CRC diagnosis as an alternative to endoscopy and has been established as a highly sensitive and specific diagnostic modality (De Rosa et al., 2016).

Colorectal cancer can be classified using two distinct systems that will be discussed in detail in Sections 1.3.1 and 1.3.2; these provide a basis for prognosis and therapeutic decisions.

### **1.3.1 TNM Classification of Malignant Tumours (TNM)**

Pierre Denoix devised the TNM Classification of Malignant Tumours (TNM = Tumour Node Metastasis) between 1943 and 1952 and it is now the most commonly used staging system internationally (Motta et al., 1995). TNM is a cancer staging notation system that defines the stage of a cancer, which originates from a solid tumour, with alphanumeric codes. T describes the size of the primary tumour and local invasion depth, N describes the regional lymph node involvement, and M describes the presence of distant metastasis. TNM is now maintained by the Union for International Cancer Control (UICC) to achieve consensus on one globally recognised standard for classifying the extent of spread of cancer (Tobias Jeffrey S., 2013). See Table 1.1 and Figure 1.1 for stage definition, descriptions and visual representations.

Table 1. 1 - TNM stage definition and description for T stage, N stage and M stage.

Table adapted from (ASC, 2005-2007).

TNM Stage		Description
T stage	TX	The primary tumour cannot be evaluated.
	T0	No evidence of cancer in the colon or rectum.
	Tis	Refers to carcinoma <i>in situ</i> (also called cancer <i>in situ</i> ). Cancer cells are found only in the epithelium or <i>lamina propria</i> .
	T1	The tumour has grown into the submucosa.
	T2	The tumour has grown into the <i>muscularis propria</i> .
	T3	The tumour has grown through the <i>muscularis propria</i> and into the subserosa, or it has grown into tissues surrounding the colon or rectum.
	T4a	The tumour has grown into the surface of the visceral peritoneum.
	T4b	The tumour has grown into or has attached to other organs or structures.
N stage	NX	The regional lymph nodes cannot be evaluated.
	N0 (N plus zero)	There is no spread to regional lymph nodes.
	N1a	There are tumour cells found in 1 regional lymph node.
	N1b	There are tumour cells found in 2 to 3 regional lymph nodes.
	N1c	There are nodules made up of tumour cells found in the structures near the colon that do not appear to be lymph nodes.
	N2a	There are tumour cells found in 4 to 6 regional lymph nodes.
	N2b	There are tumour cells found in 7 or more regional lymph nodes.
	M stage	MX
M0 (M plus zero)		The disease has not spread to a distant part of the body.
M1a		The cancer has spread to 1 other part of the body beyond the colon or rectum.
M1b		The cancer has spread to more than 1 part of the body other than the colon or rectum.

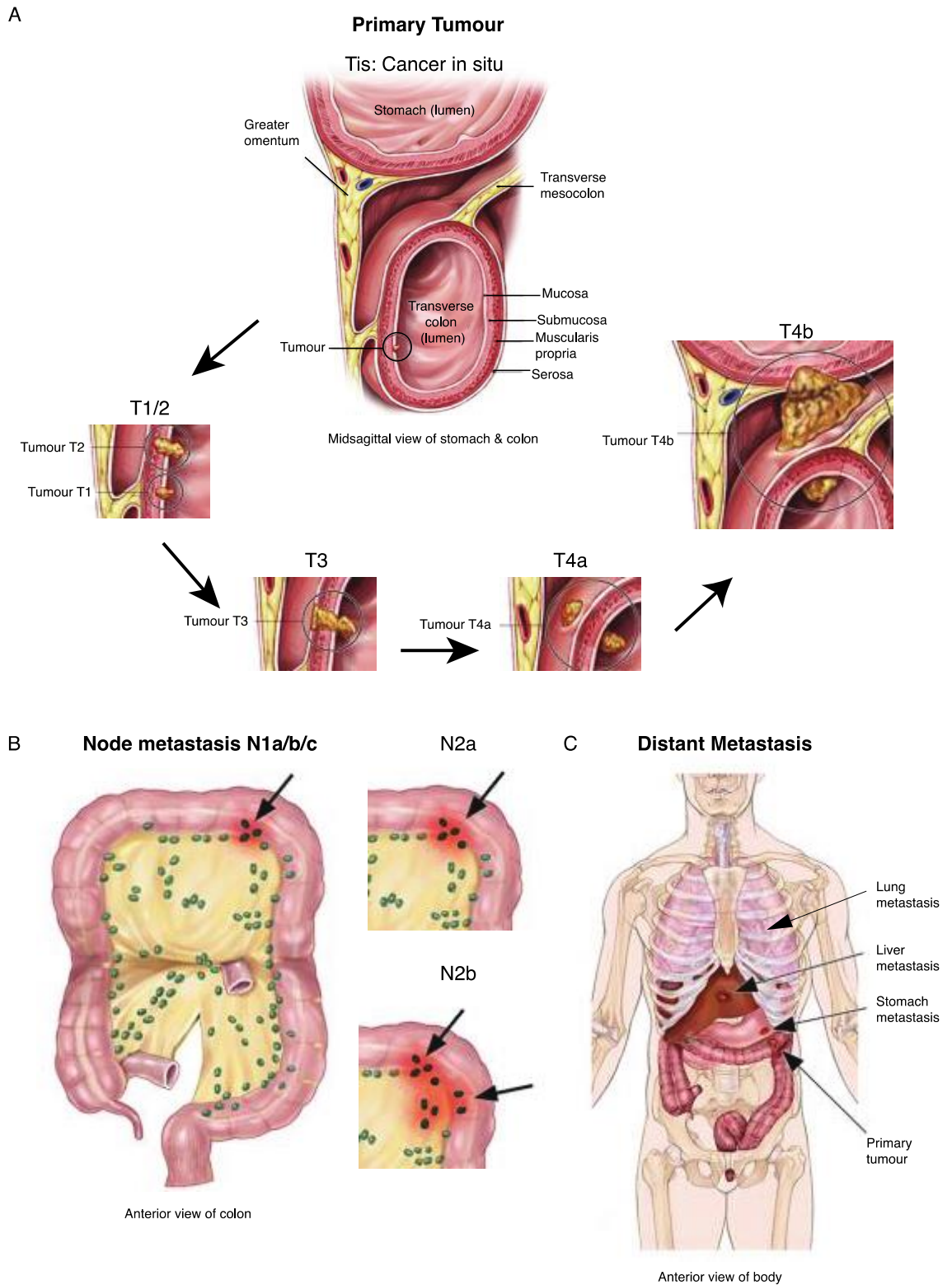


**Figure 1. 1 - Visual representation of tumour progression in colorectal cancer using the TNM classification of malignant tumours system**

(A) Progression of the primary tumour from cancer *in situ* where the cancer cells are found only in the epithelium or *lamina propria*, to T1/2 where the tumour has grown into the submucosa and/or *muscularis propria*, to T3 when the tumour has surpassed the *muscularis propria* and into the subserosa, to T4a and T4b where the tumour has a) grown into the surface of the visceral peritoneum and b) grown into or attached to other organs. (B) Lymph node metastasis from N1a/b/c, where tumour cells are found in 1-3 regional lymph nodes, to N2a/b, where tumour cells are found in 4-7 or more regional lymph nodes. (C) Distant metastasis in organs such as the lungs, liver, and stomach, M1a stage is where the cancer has spread to one other organ and M1b stage is where the cancer has spread to more than one other organ. Figure adapted from (ASC, 2005-2007).

### 1.3.2 The Dukes' staging system

In 1932, British pathologist Cuthbert Dukes devised the Dukes' staging system specifically for the specification of colorectal cancer (Kyriakos, 1985). The Dukes' staging system is no longer recommended for clinical use and has largely been replaced by the more detailed TNM system however some older patient data sets still provide this information. See Table 1.2 for description.

**Table 1. 2 - Dukes' staging system with descriptions.**

Dukes stage	Description
A	The tumour is limited to <i>muscularis propria</i> ; nodes not involved.
B	The tumour is extending beyond <i>muscularis propria</i> ; nodes not involved.
C	There are tumour cells in the nodes but highest (apical) node spared.
D	Distant metastatic spread.

## 1.4 Current treatment of CRC

Early stage primary colon cancers with no metastatic disease can be treated effectively by surgery with complete mesocolic excision (CME), with veins and arteries moved and ligated close to the main vascular trunk in order lower the local recurrence rate and improve survival (Hohenberger et al., 2009, Sehgal and Coffey, 2014). A similar procedure, total mesorectal excision can be performed for the treatment of early stage rectal cancer. Both treatments have an excellent oncological outcome with 5-year cancer specific survival rate of 70-90% (Sagar, 2011). In more locally advanced rectal cancers, neoadjuvant chemoradiotherapy such as infusional 5-fluorouracil or oral capecitabine is used to reduce local recurrence rates (De Rosa et al., 2016).

The current standard of care for unresectable metastatic disease is the combination of standard cytotoxic chemotherapy with biological agents. Standard chemotherapy schedules include 5-fluorouracil and leucovorin in combination with drugs such as oxaliplatin-FOLFOX and irinotecan-FOLFIRI. The biological agents can be separated into three distinct groups, the first is monoclonal antibodies against the epidermal growth factor receptor (EGFR) (i.e. cetuximab and panitumumab), which have shown success with commonly used treatment schedules in patients with advanced, chemotherapy-refractory CRC, in particular in wild-type KRAS tumours (Tveit et al., 2012, Peeters et al., 2010, Van Cutsem et al., 2009, Au et al., 2009). The second group are anti-angiogenic inhibitors targeting tumour vascularisation and include vascular endothelial growth factor (VEGF)-

A-targeted antibodies, bevacizumab and aflibercept and recombinant proteins that target VEGF-A, VEGF-B, and placental growth factor (PlGF) (Ciombor et al., 2015, Hurwitz et al., 2004, Van Cutsem et al., 2012, Taberero et al., 2014). The third and final group is regorafenib, an oral small molecule inhibitor of intracellular kinases involved in many signalling pathways including VEGFR2/3, RET, Kit, PDGFR and Raf kinases (Seow et al., 2016).

New therapeutic approaches currently under evaluation for the treatment of metastatic CRC include targeting signalling pathways including those above and MET, IGF1R, MEK, phosphoinositide 3-kinase (PI3K), Wnt, Notch, Hedgehog, and death receptor signalling pathways (Seow et al., 2016).

## **1.5 Normal Intestinal Homeostasis**

In order to understand CRC development and progression, we must first understand normal intestine homeostasis. The mammalian intestine consists of the large intestine, also known as the colon, and the small intestine, which can be further divided into the duodenum, jejunum and ileum. A single layer of epithelium cells (mucosa) lines the entire intestine and is renewed every 5 days in the human (3 days in the mouse). The epithelium of the small intestine can be separated into two morphologically and functionally distinct compartments, the crypts of Lieberkühn and the villi (see Figure 1.2). This architecture optimizes the absorption of nutrients by increasing the exchange interface with the intestinal lumen. On the other hand, the colon has much larger crypts and no villi, presenting a flat surface epithelium facing the lumen. The crypt is a submucosal invagination in which between one and six stem cells, also known as the crypt-based columnar (CBC) cells, reside at the bottom. These cells divide and give rise to transit amplifying (TA) or progenitor cells that proliferate at a high rate and expand into a non-proliferating population that migrates up the crypt walls towards the lumen. These non-proliferating cells then differentiate into four principal epithelial lineages: absorptive enterocytes, mucus-producing Goblet cells, hormone-secreting entero-endocrine cells, and antimicrobial and enzyme-secreting Paneth cells. Once the differentiated epithelial cells reach the peak of the villus, they undergo apoptosis and are shed into the lumen to make room for new cells migrating up from the crypt. This process of rapid renewal of the intestinal mucosa maintains the absorptive and barrier functions of the intestine and is the basis for intestinal homeostasis. In the colon, cells differentiate mainly to enterocytes and Goblet cells (Sancho et al., 2003, Schepers and Clevers, 2012).

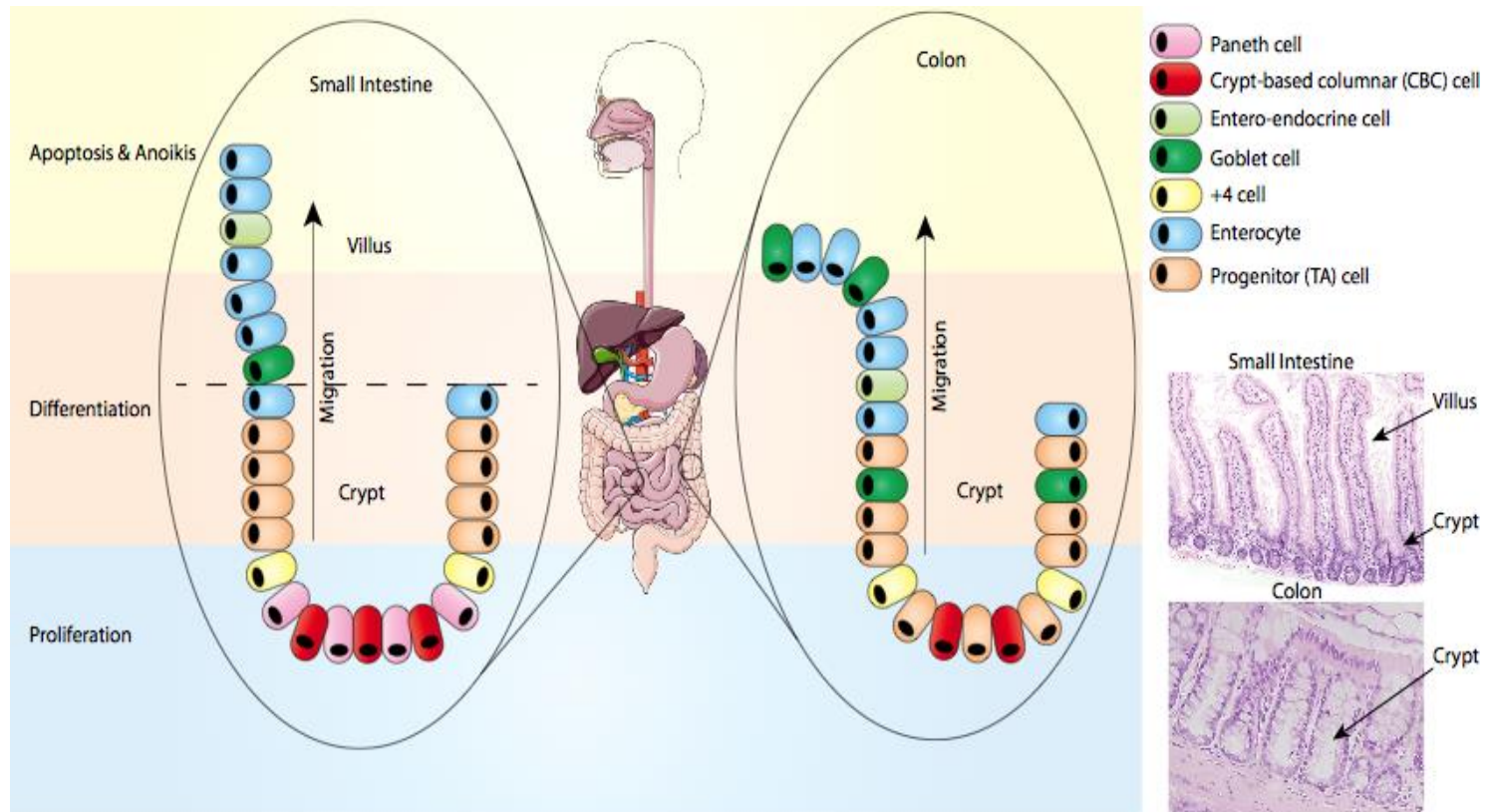


**Figure 1. 2 - Normal intestinal homeostasis in the small intestine and the colon.**

Crypt-based columnar (CBC) intestinal stem cells reside at the base of the crypts in both the small intestine and the colon. These cells divide rapidly producing progenitor or transit amplifying cells (TA) cells which have limited dividing capacity, and produce non-proliferating cells which differentiate into four principal epithelial lineages: enterocytes, Goblet cells, entero-endocrine cells, and Paneth cells. The small intestine and colon have slightly different cell type compositions; the small intestine is majorly enterocytes and fewer Goblet and entero-endocrine cells, the colon is majorly enterocytes and Goblet cells. The differentiated cells migrate up to the peak of the villus, undergo apoptosis and are shed into the lumen making room for ‘younger’ cells migrating up from the crypt. On the right is a haematoxylin and eosin (H&E) stained examples of murine small intestine and colon tissue, with villus and crypts indicated, scale bar = 100µm. Figure adapted from (Bloemendaal et al., 2016).

## 1.6 Molecular characterization of CRC

Intestinal homeostasis requires tightly controlled cell proliferation, differentiation, migration and cell death. If there is an imbalance of these mechanisms favouring cell proliferation, the resulting hyperproliferation may lead to tumourigenesis and CRC in patients. This process begins with epithelial hyperplasia which progresses, with increasing dysplasia, to aberrant crypt foci (ACF). These ACF then advance to benign tumours known as adenomas or adenomatous polyps that can eventually become malignant carcinoma (Pinto and Clevers, 2005).

CRC occurrence is usually attributed to sporadic mutations, which occur in 75% of cases, however germline-inactivating mutations in oncogenes or tumour suppressor genes can cause hereditary CRC (De Rosa et al., 2016). Between 2-5% of CRC can be attributed to inherited syndromes such as Lynch syndrome, familial adenomatous polyposis (FAP), MUTYH-associated polyposis, and certain hamartomatous polyposis conditions (Jasperson et al., 2010). Separately, up to one third of CRCs display increased familial risk, and several less penetrant susceptibility genes have been identified for this level of inheritance.

Familial adenomatous polyposis (FAP) is an autosomal dominant syndrome associated with the mutation of the tumour suppressor, adenomatous polyposis coli (APC) protein (Groden et al., 1991, Kinzler et al., 1991). Loss of APC leads to the onset of hundreds to thousands of adenomas within the large intestine and if left untreated, will progress to CRC by 40 years of age on average (Vasen et al., 2008). Treatment of FAP includes colonoscopy every 1-2 years starting from the age of 10-12 years, and in the case of adenomatous polyps, the patient will need annual endoscopic follow up. If polyps are endoscopically untreatable, surgical removal of the rectum and the entire or part of the colon can be considered (Jasperson et al., 2010).

Subsequently, somatic mutations in the same gene have been associated with the majority of sporadic CRCs. Extensive molecular characterization of CRC using both human tumour biopsies (Human Cancer Genome Atlas, 2012) and mouse models (Andreu et al, 2005; Sansom et al, 2004) has defined loss of functional APC as the initiating mutation in up to 81% of cases. In 90% of cases, the mutation results in a non-functional truncated protein (Fodde and Khan, 1995) and loss of both alleles is required for loss of tumour suppressing activity in FAP and CRC.

### 1.6.1 Adenomatous polyposis coli (APC), $\beta$ -Catenin and Wnt signalling

APC is an important component of Wnt signalling. In canonical Wnt signalling (Figure 1.3), WNT ligands bind to Frizzled and LRP5/6 co-receptors on the cell surface resulting in the dissociation of the multi-protein degradation complex composed of APC, AXIN, CKI and GSK3 $\beta$  (and others) which targets the transcription factor  $\beta$ -Catenin for ubiquitinylation and subsequent proteasomal degradation. This leads to  $\beta$ -Catenin accumulation and translocation to the nucleus where, by association with TCF/LEF factors, it transcriptionally activates Wnt target genes. In the absence of Wnt signalling,  $\beta$ -Catenin is degraded and therefore Wnt target genes are not transcribed. Loss of APC leads to loss of the degradation complex and uncontrolled, hyperactivated Wnt signalling resulting in the upregulation of proto-oncogenes, *c-MYC*, *CDK4* and *CYCLIN D1*.

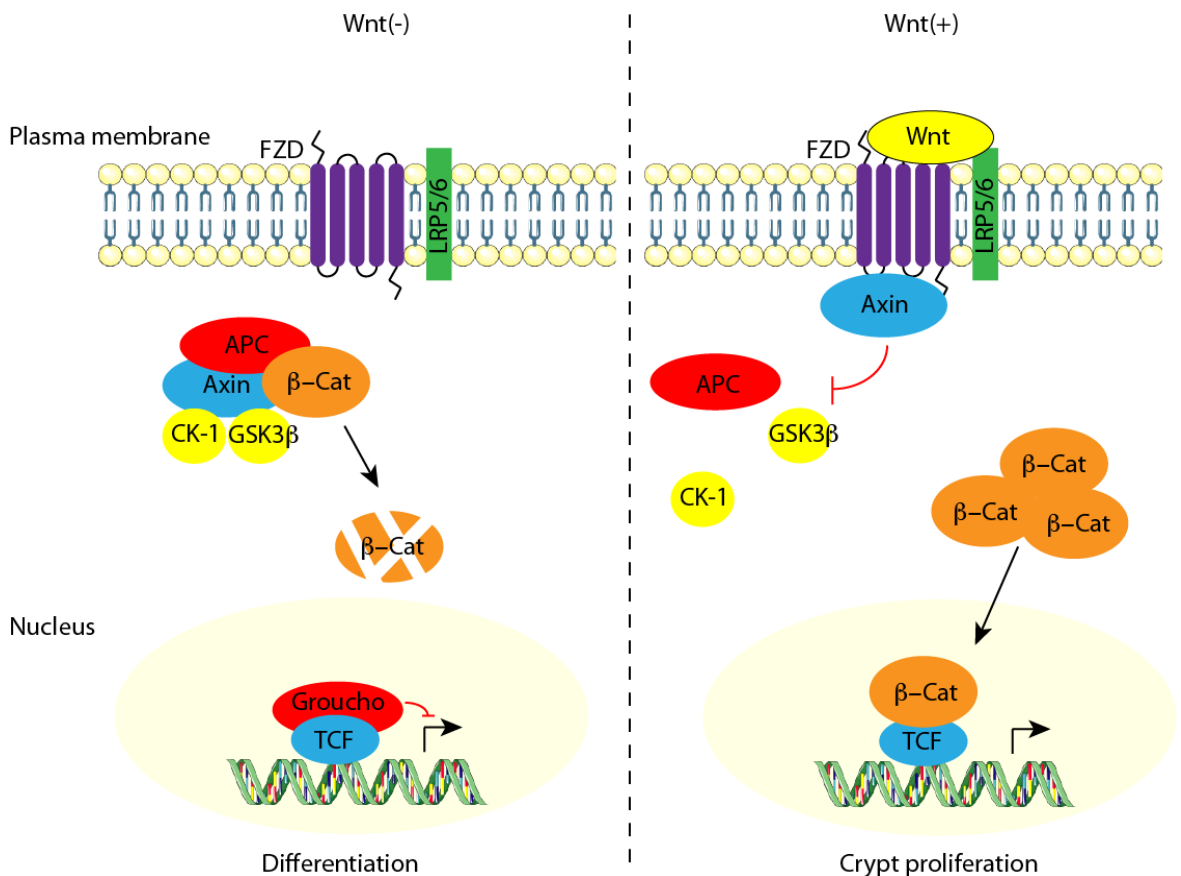


**Figure 1. 3 - The Wnt signalling pathway.**

In the absence of WNT ligands, the multi-protein degradation complex composed of APC, AXIN, CKI and GSK3 $\beta$  (and others) functions to target transcription factor,  $\beta$ -Catenin for ubiquitinylation and subsequent degradation by the proteasome. Without Wnt signalling, cells differentiate. In the presence of WNT ligands binding to the frizzled (FZD) and LRP5/6 co-receptors, the degradation complex is dissociated. This means that  $\beta$ -Catenin is free to accumulate and translocate to the nucleus where by association with TCF/LEF factors, it transcriptionally activates Wnt target genes. Constitutive Wnt signalling leads to continued crypt proliferation.

Activating mutations in the  $\beta$ -Catenin gene (*CTNNB1*) are also found in CRC, however, at a lower rate of 12.5% in adenomas and 1.4% in invasive carcinoma, and are less likely to progress to larger adenomas and invasive carcinoma (Inomata et al., 1996, Samowitz et al., 1999). *APC* and *CTNNB1* mutations are mutually exclusive (Sparks et al., 1998) and although they are not equivalent, evidence to date suggests that any mutation resulting in stabilised nuclear  $\beta$ -Catenin is enough to initiate neoplastic transformation in the colonic epithelium (Brabletz et al., 2002).

Currently there is no identified clinical use for *APC* or *CTNNB1* mutations for treatment selection, prognosis or early detection of cancer. The development of small molecule inhibitors of this pathway is underway, however most of these studies are still preclinical (Anastas and Moon, 2013, Fang et al., 2016, Hwang et al., 2016) and concerns have been raised for the predicted side effects of such drugs (Kahn, 2014). However it was recently shown that *APC* restoration in established invasive carcinomas led to rapid and widespread tumour cell differentiation and sustained regression without relapse in a mouse model of CRC, whereby *APC* is conditionally suppressed (or restored) with the use of a doxycycline-regulated shRNA (Dow et al. 2015). Furthermore, there is evidence to suggest that the WNTs themselves promote the outgrowth of metastatic lesions and cancer stem cells in lung, pancreatic and breast cancer (Malladi et al., 2016, Nguyen et al., 2009a, Yu et al., 2012, Tammela et al., 2017). Compounds impacting the stability of Axin (IWR and XAV939) and porcupine inhibitors (IWP2, C59, and LGK974) that lower  $\beta$ -Catenin to inhibit Wnt signalling, and that block WNT secretion respectively are currently being investigated. A promising study showed that inhibiting Porcupine led to reduced growth of transplanted and even autochthonous tumours in mouse models (Madan et al., 2016, Tammela et al., 2017). Furthermore, there is currently a clinical trial investigating the Porcupine inhibitor LGK974 in patients with malignancies dependent on WNT ligands including BRAF mutant colorectal cancer (2017).

### **1.6.2 MYC deregulation in CRC**

c-MYC is a basic helix-loop-helix transcription factor that is known to regulate, through activation or repression, almost 15% of genes in the human genome (Fernandez et al., 2003). Subsequently, c-MYC is involved in the regulation of many central cellular processes including proliferation, metabolism, differentiation, apoptosis and survival (Nesbit et al., 1999). c-MYC is a ubiquitously expressed proto-oncogene, which can act as a primary oncogene via mutation, in tumours such as Burkitt's lymphoma (Lombardi et al.,

1987), or more commonly, as a downstream effect of other activated oncogenes leading to its overexpression (Dang et al., 1999, Dang et al., 2009, Eilers and Eisenman, 2008). As mentioned previously activation of c-MYC is a downstream consequence of uncontrolled Wnt signalling, and it is also essential for CRC initiation and progression (Sansom et al., 2007). Characteristics of deregulated c-MYC include uninhibited cell proliferation and growth, DNA replication, protein biogenesis, angiogenesis, and a restriction of host immune response (Gabay et al., 2014). Furthermore, the requirement for nucleic acids, protein and lipids is higher in transformed cells due to rapid cellular proliferation and oncogenic c-MYC drives many of the required metabolic changes. At the same time, c-MYC overexpression leads to coordinated changes in gene expression resulting in increased proliferation. Therefore c-MYC acts as a major contributor to the ‘transformed phenotype’ (Miller et al., 2012).

In many studies, loss of c-MYC in c-MYC driven tumours has triggered rapid tumour regression by proliferative arrest, re-differentiation of tumour cells and collapse of tumour microenvironment (Arvanitis and Felsher, 2005, Felsher and Bishop, 1999, Flores et al., 2004, Sansom et al., 2007). This suggests it could be a successful therapeutic target however strategies to target c-MYC have been met with difficulty. Firstly, successful inhibitors of cancer-associated proteins have typically been developed based on their gain-of-function mutations that distinguish them from their normal counterparts however, this cannot be applied to c-MYC as it is rarely mutated in cancer despite its high expression. Secondly, c-MYC is a fundamental requirement in all proliferating cells therefore inhibition of the transcription factor would likely have unacceptable toxicities. Lastly, in order to inhibit c-MYC activity, a small molecule inhibitor would in theory, bind to c-MYC and block its ability to form protein-protein interactions, however, the surfaces at which these occur tend to be large, flat and relatively featureless. The lack of any recognizable motifs or clefts means that the design of small molecule inhibitors is difficult (Soucek et al., 2008).

### **1.6.3 The ‘adenoma-to-carcinoma’ sequence**

Loss of APC or activating mutations in  $\beta$ -Catenin and the consequent upregulation of the Wnt pathway and downstream c-MYC is fundamental to the initiation of colorectal carcinogenesis, however alone neither mutation is enough for the tumour to progress past the adenoma stage. For this, additional genetic and epigenetic alterations are needed. Loss of genomic and epigenomic integrity is a distinguishing feature of CRC and at least four

types have been described, these include chromosomal instability, microsatellite instability (MSI), CpG island methylator phenotype (CIMP) and global DNA hypomethylation (Sideris and Papagrigoriadis, 2014, Grady and Pritchard, 2014). These characteristics contribute to the increased rate of mutations in the development of CRC. These mutations include specific genes resulting in the deregulation of important signalling pathways such as the transforming growth factor  $\beta$  (TGF $\beta$ ) signalling pathway, and the phosphatidylinositol 3-kinase (PI3K) pathway. Additionally, many key tumour suppressor genes are often mutated, including TP53. These genetic and epigenetic alterations tend to occur in a preferred succession, however, the total accumulation of modifications rather than the order is accountable for determining the biological properties of the tumour (Fearon and Vogelstein, 1990). This provides clones of tumour cells a selective advantage at the given stage, necessary for the tumour to progress (Pinto and Clevers, 2005). Fearon and Vogelstein (1990) were the first to define such a sequential model for CRC, this has been defined as the ‘adenoma-to-carcinoma’ sequence (Figure 1.4) (Fearon and Vogelstein, 1990).

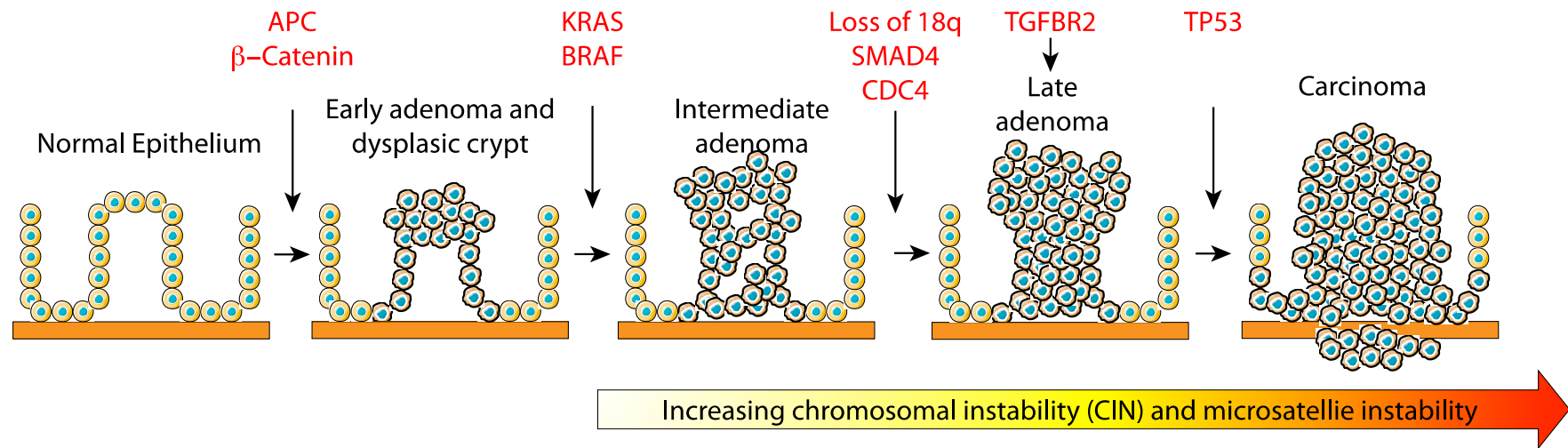


**Figure 1. 4 - The Adenoma to Carcinoma sequence.**

Fearon and Vogelstein published the ‘adenoma-to-carcinoma’ sequence in 1990, which was a sequential model for CRC. The normal epithelium acquires mutations in *APC* or  $\beta$ -catenin for the transformation to early adenoma and dysplastic crypts (also known as an aberrant crypt foci), subsequent mutations in *KRAS* or *BRAF* lead to the progression to an intermediate adenoma. Further mutations in TGF $\beta$  pathway including *SMAD4* and *TGFBR2* lead to late adenoma and then carcinoma and metastatic disease develops with the loss of *TP53* and increasing chromosomal and microsatellite instability.

#### **1.6.4 KRAS**

*KRAS* is a proto-oncogene and is the most frequently mutated gene in all human cancer types with CRC being no exception. Approximately 40% of CRC patients have tumour-associated *KRAS* mutations, with most mutations occurring at codons 12, 13 and 61 of the gene. The consequence of these mutations is the constitutive activation of *KRAS* signalling. The *KRAS* protein is one of three functionally distinct isoforms of the RAS family of small GTPases including *HRAS*, *KRAS*, and *NRAS*, which cycle between active guanosine triphosphate (GTP)-bound and inactive guanosine diphosphate (GDP)-bound forms (Figure 1.5). *KRAS* promotes proliferation and survival as a downstream effector of EGFR signalling, via RAS/RAF/MAPK signalling. Mutations in *KRAS* prevent the ability of GTPase activating proteins to hydrolyse *KRAS*-bound GTP and therefore *KRAS* cannot be 'switched off' (Downward, 2003). These activating mutations mean that even in the absence of growth factors, there is a sustained proliferation signal within the cell. Fearon and Vogelstein (1990) found that 50% of larger adenomas (more than 1cm in size) and colorectal carcinomas had *KRAS* mutations, however in contrast, such mutations were observed in less than 10% adenomas smaller than 1cm in size. Therefore, mutation of *KRAS* is considered a relatively early event in the adenoma-to-carcinoma progression sequence (Vogelstein et al., 1988). *KRAS* mutations are sustained throughout progression of the disease as shown by the concordance of *KRAS* status in primary and metastatic CRC (Artale et al., 2008).

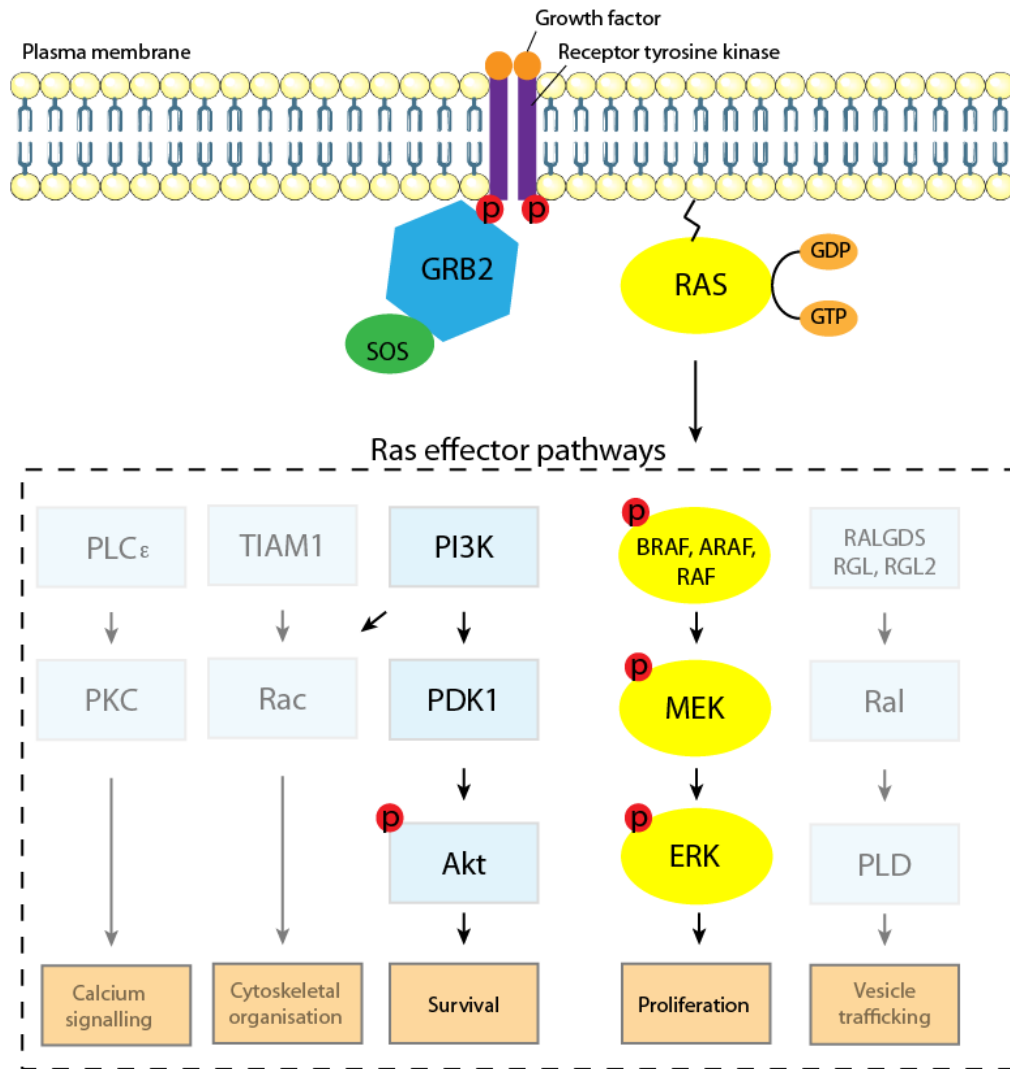


**Figure 1. 5 - The RAS signalling pathway.**

Growth factor binding to the cell-surface receptors results in activated receptor complexes, which contain adaptors such as growth-factor receptor bound protein 2 (GRB2). These proteins recruit SOS1 which in turn, increases RAS-guanosine triphosphate (RAS-GTP) levels by catalysing nucleotide exchange on RAS. The GTPase-activating protein (GAP) neurofibromin (NF1) binds to RAS-GTP and aids conversion to RAS-GDP (guanosine diphosphate) and terminates signalling. Several RAS effector pathways have been described, and some are depicted here. The RAS/RAF/MAPK signalling pathway regulates proliferation. RAS also activates the phosphatidylinositol 3-kinase (PI3K)-3-phosphoinositide-dependent protein kinase (PDK1)-Akt pathway that plays a crucial role in cell survival. Other RAS effector pathways include the regulation of calcium signalling, cytoskeletal organisation and vesicle trafficking. Figure adapted from (Schubbert et al., 2007).

The BRAF protein kinase is the direct downstream effector of KRAS in the RAS/RAF/MAPK signalling pathway and is mutated in 10-15% of CRC. *KRAS* and *BRAF* mutations are mutually exclusive suggesting that any mutation resulting in activated MAPK signalling is sufficient to support tumourigenesis. Mutations in EGFR ligands and the EGFR gene itself have also been observed in a subset of colorectal cancers (Grady and Pritchard, 2014).

Since discovery of KRAS's role in oncogenesis, there has been great effort to exploit it as a therapeutic target. Unfortunately these efforts have gone unrewarded, as the RAS proteins do not present suitable pockets to which drugs can bind. Furthermore inhibition of pathways downstream of RAS within the RAS/RAF/MAPK pathway and the PI3 Kinase pathway, have also been ineffective in patients with RAS driven tumours. Paradoxically RAF kinase inhibitors activate RAF/MAPK signalling, and MEK inhibitors activate upstream feedback mechanisms that render the inhibitors relatively ineffective (McCormick, 2015). Additionally, many studies have shown that patients with *KRAS* mutations do not benefit from upstream anti-EGFR therapy, either as a single agent (Amado et al., 2008) or in combination with chemotherapy (Bokemeyer et al., 2011, Bokemeyer et al., 2009).

### **1.6.5 Other common mutations in CRC**

Deregulation of the transforming growth factor  $\beta$  (TGF- $\beta$ ) pathway occurs in the majority of CRCs. The TGF- $\beta$  family are ubiquitous and multi-functional cytokines that are essential to cellular processes such as growth, development, inflammation, tissue repair and host immunity (Clark and Coker, 1998). Mutations have been observed in multiple components of the TGF- $\beta$  pathway including receptor genes, *TGFBR2* and *TGFBR1*, post receptor signalling pathway genes, *SMAD2* and *SMAD4*, and TGF- $\beta$  superfamily members such as *ACVR2* (Deacu et al., 2004, Eppert et al., 1996, Grady et al., 1999). Mutations in *TGFBR2* occur in 30% of CRC and have been associated with the progression of late adenomas to carcinoma, and in line with this loss of *SMAD4* has also been implicated in adenoma formation and the progression to carcinoma in mouse models (Takaku et al., 1998).

Fifty percent of CRCs have loss of function mutations in the *TP53* tumour suppressor gene which is associated with the development to carcinoma from adenoma. As with *APC*, *TP53* has been studied extensively as a possible therapeutic target however to date, it has no clinical or prognostic role in CRC patients (Walther et al., 2009). Notably, tumours harbouring mutations in *TP53* and *APC* are often associated with higher rates of chromosomal instability (CIN) (Drost et al., 2015, Rajagopalan et al., 2003, Pino and Chung, 2010).

The phosphatidylinositol 3-kinase pathway is mutated in up to 40% of CRC patients and has been associated with the progression from adenoma to carcinoma. The most common

mutations are found in the P10 $\alpha$  catalytic subunit of *PIK3CA* (32% of CRCs) (Samuels et al., 2004) and are also observed in *PTEN*, a negative regulator of PI3K signalling (Danielsen et al., 2008, Razis et al., 2008). EGFR signalling also has a role in modulating the PI3K pathway through KRAS activation and it has been suggested that mutations in *PIK3CA* and *PTEN* are predictive markers of anti-EGFR therapy (Razis et al., 2008, Sartore-Bianchi et al., 2009).

### **1.6.6 The consensus molecular subtypes of CRC**

CRC is a very heterogeneous disease accounting for the generation of drug resistance and relapse after therapy (De Rosa et al., 2016). On the other hand, as our understanding of CRC and the molecular alterations taking place increases, we can stratify tumours into subtypes and treat these differently, with a higher chance of success, making precision medicine a clinical reality for CRC (Guinney et al, 2015).

A recent study showed that all cases of CRC can be allocated to one of four consensus molecular subtypes (CMSs), each with distinguishing features and disease prognosis (Guinney et al., 2015) (Table 1.3). CMS1 is defined as microsatellite instability (MSI) immune, with features including hypermutations, microsatellite instability and a strong immune activation. CMS2 is defined as canonical, is epithelial and features increased Wnt and c-MYC signalling. CMS3 is defined as metabolic, is epithelial and features evident metabolic dysregulation. Finally, CMS4 is defined as mesenchymal and includes features such as prominent TGF- $\beta$  activation, stromal invasion and angiogenesis. Furthermore, the study found that CMS1 patients have worse survival after relapse and CMS4 patients have worse relapse-free and overall survival (Guinney et al., 2015).

**Table 1. 3 - The Consensus molecular subtypes for CRC**

Table adapted from (Guinney et al., 2015).

CMS1 MSI immune	CMS2 Canonical	CMS3 Metabolic	CMS4 Mesenchymal
14%	37%	13%	23%
MSI, CpG island methylator phenotype (CIMP) high, hypermutation	Chromosomal instability (CIN) high	Mixed MSI status, CIN low, CIMP low	CIN high
<i>BRAF</i> mutations		<i>KRAS</i> mutations	
Immune infiltration and activation	WNT and MYC activation	Metabolic deregulation	Stromal infiltration, TGF- $\beta$ activation, angiogenesis
Worse survival after relapse			Worse relapse-free and overall survival

## 1.7 Approaches to modelling CRC

In order to develop effective treatment strategies we need to understand key driver mutations and the cellular processes that are essential for tumourigenesis that could be targeted pharmacologically (Young et al., 2013).

### 1.7.1 Human cell lines

Cell lines that have been cultured directly from human patient tumours are used widely to model CRC. Advantages of using human cell lines include their direct relevance to the disease, and the ability to perform high-throughput experiments which are fast and relatively cheap. Cell lines mimic some tumour behaviour in culture, therefore basic measurements including cell growth, cell death, migration and invasion in response to a range of genetic modifications and drugs can be investigated.

The major disadvantage with human cell lines is that by culturing the cells in a monolayer on plastic, you remove the normal and crucial interaction of the cells and their environment. Time in culture also allows for genetic drift to occur resulting in the cell line no longer resembling the tumour from which it was generated. Furthermore, it is impossible to model an entire organism's response to the tumour with 2D culture, this

includes the immune system or angiogenesis, both of which are known to have an impact on tumour development (Young et al., 2013).

Taking these advantages and disadvantage into consideration, culturing CRC human cell lines is still an invaluable research tool that often allows the researcher to investigate genetic contributions to the disease and to clarify complex molecular mechanisms. Typically, *in vitro* investigation using cell lines lays the foundation for further *in vivo* work.

### **1.7.2 Intestinal organoids**

The development of 3D culturing systems has come closer to a better representation of the tumour environment and behaviour. It is now accepted that intestinal stem cells (ISCs) are the cell of origin of CRC and that mutations within the ISC population of crypt base columnar (CBC) cells act as the driving force behind tumour initiation (Barker et al., 2009). Studying this population of cells allows researchers to investigate the earliest stages of tumorigenesis.

The first description of culturing 3D rat intestinal organoids was published in 1992 (Evans et al., 1992, Fukamachi, 1992) and since then organoid culture systems have revolutionised CRC research. In 2009, a new and improved protocol for the 3D culture of self-renewing intestinal organoids was published by Hans Clever's lab (Sato et al., 2009). This technique was soon optimised for the generation of organoids from mouse and human colon, and colorectal adenoma tissue (Sato et al., 2011, Jung et al., 2011). In these protocols, epithelial cells are embedded within matrigel, which provides a laminin-rich 3D matrix for cells to grow in, and mimics the microenvironment found at the crypt base *in vivo* (Figure 1.6). Additionally, the cultures require culture media supplemented with growth factors to sustain the ISC population and for intestinal crypt growth. These include Noggin, a bone morphogenetic protein (BMP) inhibitor that blocks BMP inhibition of ISC self-renewal; epidermal growth factor (EGF), to support proliferation; and R-spondin, an activator of the Wnt signalling pathway, to sustain proliferation of the ISC population and inhibit their differentiation. Notably, organoids cultured from human CRC samples grow efficiently without the addition of growth factor supplements and can depend upon the mutational background and activated signalling pathways of the tumours from which they are generated (Matano et al., 2015, Fujii et al., 2016).

The organoid cultures contain all epithelial cell types found in the original intestinal system, including a ‘crypt’ region and migration of cells along a crypt-villus axis. Organoid culture has been referred to as ‘the missing link for researchers between *in vitro* and *in vivo* studies’ and is a more relevant model compared to traditional 2D cultures for the study of *in vivo* response. It overcomes disadvantages of 2D culturing including the lack of 3D cell/cell interactions and cell homology and maintains the advantages of experiments being quick and relatively cheap (Young and Reed, 2016).

As with any model system, there are limitations. It has been observed that CRC organoids are genetically stable, however during long-term culturing there is still the potential for genetic drift to occur as in 2D cell cultures. Furthermore, organoid culture does not include all other cell types found in a whole organism therefore differences in response between *ex vivo* and *in vivo* are unavoidable (Young and Reed, 2016).

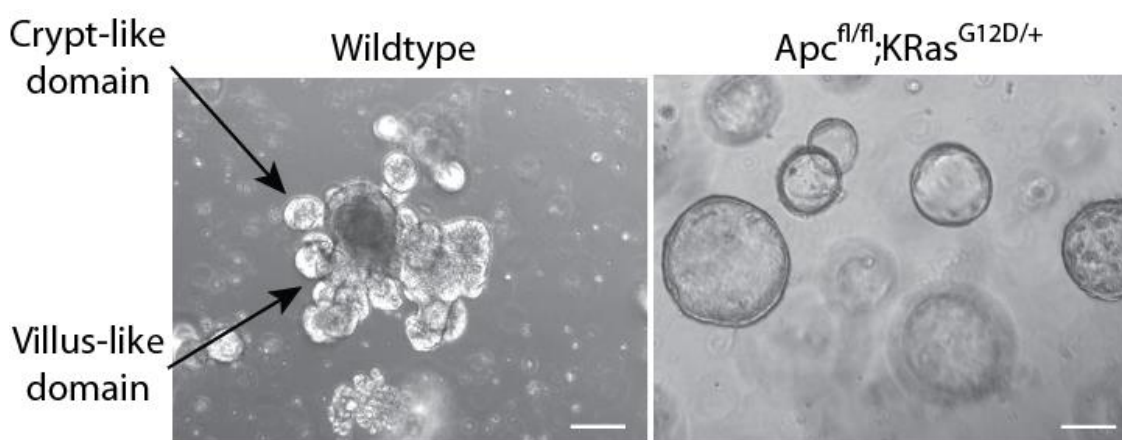


**Figure 1.6 - Murine -, small intestine - derived organoids.**

The left panel shows an organoid culture harvested from a wildtype mouse, with crypt-like and villus-like domains indicated. These cultures have all of the epithelial cell lineages including conserved migration of the differentiated cells along a crypt-villus axis. The right panel shows an organoid culture harvested from an intestinal tumour mouse model with deleted *Apc* gene and constitutively active *KRas* (genotype *Apc<sup>fl/fl</sup>;KRas<sup>G12D/+</sup>*). Due to loss of APC, these cells have high Wnt signalling. This means that they continually proliferate rather than differentiate, resulting in the formation of a spherical shape. Scale bar = 100µm.

### 1.7.3 Genetically engineered mouse models (GEMMs)

The arrival of gene targeting has enabled researchers to take a more controlled approach to creating models of CRC. The genetically engineered mouse model (GEMM) has become indispensable for the investigation of gene function, genetic contribution to disease, and for testing efficacy and toxicity of potential therapeutic treatments. Advantages of using GEMMs for the study of human disease include the availability of genomic information,

the ease of genetic manipulation using mutagenesis techniques and the ability to monitor the outcome on a whole organism (Young et al., 2013).

### 1.7.3.1 Mutant *Apc*-driven CRC mouse models

The first and still most widely used GEMM to investigate the loss of APC function and CRC development is derived from the FAP model, the ethylnitrosourea-induced *Min* mouse (Min for multiple intestinal neoplasia) (Moser et al., 1990). The *Min* mouse has a mutant allele of *Apc*, containing a nonsense mutation at codon 850 that results in a stably expressed truncated protein. *Min* homozygous mice are embryonic lethal and die *in utero* at approximately embryonic day 8 (Moser et al., 1992). *Min* heterozygous mice develop numerous (up to 100) intestinal adenomas within 3-4 months. Interestingly, all of these adenomas harbour allelic loss of the wild-type copy of the *Apc* allele as well as the *Min Apc* allele (Levy et al., 1994). These studies provided strong evidence that tumour initiation in the mouse requires bi-allelic loss of the gene, as observed in human patients developing CRCs (Powell et al., 1992). This model has been used for a range of studies that have been directly translated to humans, the most notable include chemoprevention studies and functional testing of genes that might modify intestinal tumourigenesis (Jackstadt and Sansom, 2016). The chemoprevention experiments have shown therapeutic benefit of non-steroidal anti-inflammatory drugs (NSAIDs) for e.g. celecoxib, a cyclooxygenase (COX) inhibitor and aspirin in both FAP patients and CRC patients respectively (Baron et al., 2003, Steinbach et al., 2000).

Additional *Apc* mutant alleles have since been constructed using homologous recombination including mutations at codons 1638, 716, 1309 and 474 (Fodde et al., 1994, Oshima et al., 1995, Quesada et al., 1998, Sasai et al., 2000). As with the *Apc Min* mice, homozygous mice all die *in utero* and heterozygous mice develop adenomas throughout the intestine, although the number varies as well as the average lifespan. Furthermore, these models corroborated loss of the second wild-type copy of *Apc* as the rate-limiting step in tumour development. Surprisingly, none of the tumours interrogated harboured *KRas* or *p53* mutations as in the human disease (Smits et al., 1997, Oshima et al., 1997).

Nevertheless, all of the above mouse models have shortcomings for studying CRC progression. To start with, the average lifespan of the animals is too short to permit the accumulation of driver mutations and progression of adenoma to advanced malignancies and secondly, the tumours are predominantly located within the small intestine rather than

the colon. These characteristics are not completely representative of human FAP or sporadic CRC in humans.

### **1.7.3.2 Conditional Apc models of CRC**

In the 1990s, *Cre-Lox (Cre)* technologies were developed and this enabled researchers to delete a gene of interest in any specific tissue at a specific time (Nagy, 2000). This is achieved by producing GEMMs with a *Cre recombinase* transgene under the control of an inducible tissue specific promoter alongside a modified version of the gene of interest, where *Lox P* recombination sites flank a region of the gene (Figure 1.7). In order to produce a conditional knockout the *Lox P* recombination sites often flank an essential exon so that when excised, the gene is non-functional. For the induction of an oncogene, such as *KRas*, the *Lox P* sites often flank a STOP codon so that the gene is only transcribed in the presence of *Cre recombinase*. Most commonly the induction of *Cre recombinase* is achieved by coupling the Cre enzyme to the oestrogen receptor, so that tamoxifen administration is required for activation of the *Cre recombinase* (Hayashi and McMahon, 2002). This technique also has the added benefit of overcoming the issue of homozygous embryonic lethal mutations.

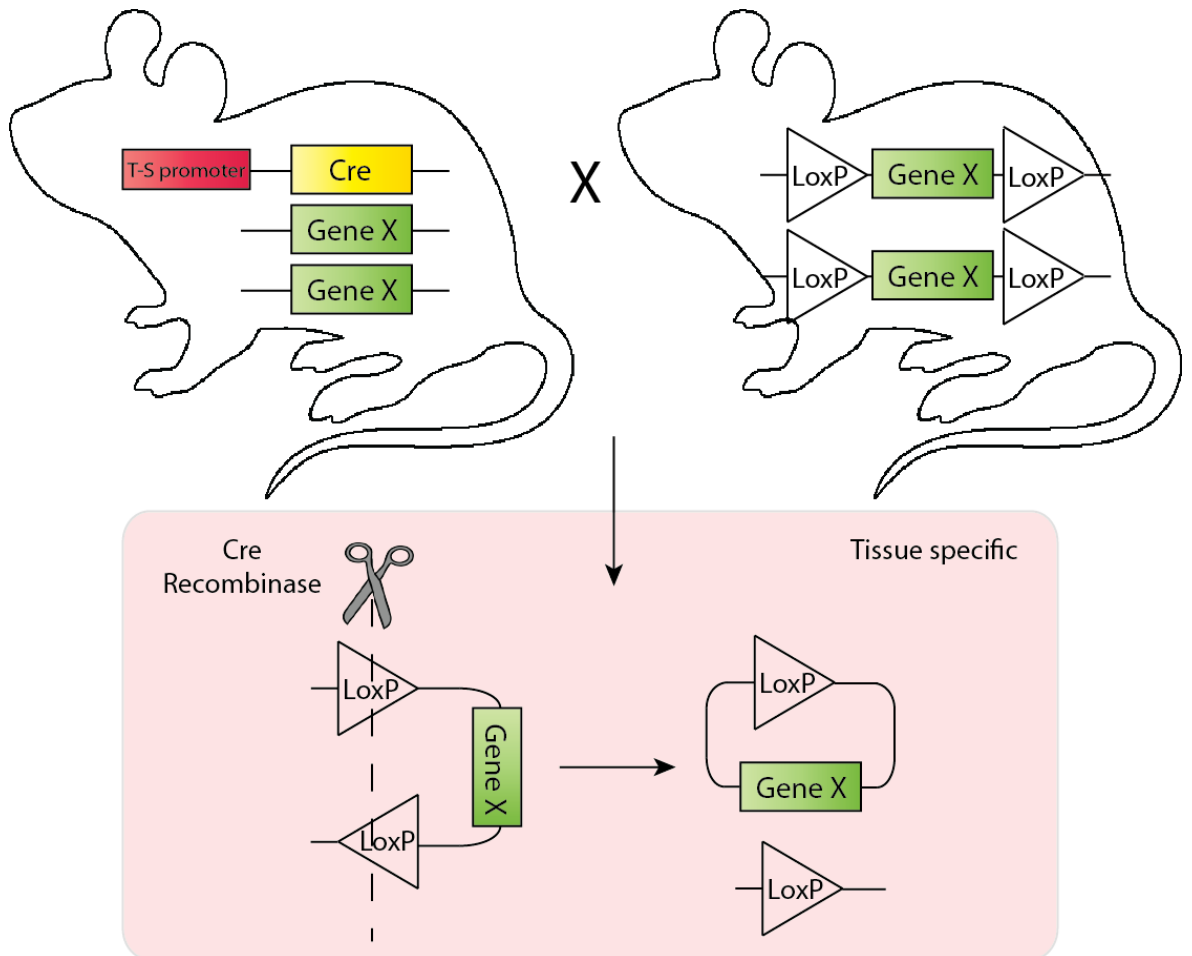


**Figure 1. 7 - The Cre-Lox System.**

The Cre-Lox system allows temporal and spatial control of gene expression *in vivo*. Two GEMMs are crossed, one contains the *Cre recombinase* transgene downstream of an inducible, tissue specific promoter, and the other contains the modified gene of interest, flanked by *Lox P* sites. In the F1 progeny, the *Cre recombinase* is expressed only in the tissue of interest and this result in the ‘floxing’ or excision of the gene of interest in that tissue only. In some cases only an essential exon of the gene of interest is flanked by *Lox P* sites, however this also results in a non-functional protein. Conversely, if the aim is to express a particular gene of interest rather than delete it, a STOP codon flanked by *Lox P* sites is placed upstream of the gene of interest.

The ability to acutely delete both copies of *Apc* has provided valuable insight into the mechanisms of early tumourigenesis. In 1997, Shibata and colleagues showed that delivering adeno-virus directly to the colon of homozygous *Apc* ‘floxed’ mice (where exon 14 is flanked by *Lox P* sites) was sufficient to instigate colon adenomas. Furthermore, homozygous deletion of *Apc* in the intestine using inducible *AhCre*, which is driven by the *Cyp1a1* promoter and is inducible by  $\beta$ -naphthoflavone and *VillinCreER<sup>T2</sup>*, drives massive morphological changes in intestinal homeostasis (Sansom et al., 2004, Andreu et al., 2005). Loss of *Apc* results in the crypt ‘progenitor’ phenotype, which is characterised by unrestricted proliferation and altered migration and differentiation within the intestinal crypt. The crypt progenitor phenotype is mediated by the Wnt target gene, *c-Myc* as additional loss of *c-Myc* in these mice was able to rescue this phenotype completely (Sansom et al., 2007). This result was repeated using *Villin-Cre*, which results in

recombination within the intestinal epithelium and requires induction by tamoxifen injection. In this case, mice cannot sustain homozygous deletion of *Apc* and need to be terminated at day 4-post induction (el Marjou et al., 2004, Andreu et al., 2005). Both of these short-term *Apc* models result in an increased number of undifferentiated cells within the intestine and so implicated a role for *Apc* in cancer development by dysregulation of the intestinal stem cells (ISCs). A fundamental study that used *Cre recombinase* under the control of stem cell specific *Lgr5* promoter, to conditionally delete *Apc* within ISCs, showed that ISCs are the cells of origin of CRC (Barker et al., 2009). This has significantly advanced our understanding of CRC tumourigenesis and tumour homeostasis.

Homozygous deletion has been crucial for our understanding of early tumourigenesis, however, the severe phenotype leads to a very short survival post induction and mice do not develop tumours. One possible method to overcome this is to use *Cre recombinases* that recombine in fewer cells, or even lower doses of induction reagent to achieve the same outcome. Another method is to heterozygously delete *Apc* and allow sporadic loss of the second allele to occur over the mouse's lifetime. Only the cells in which both copies of *Apc* are lost will form adenomas.

#### **1.7.3.4 KRas-driven mouse models of CRC**

Homozygous deletion of *KRas* results in embryonic lethality by day 12.5 (Koera et al., 1997) and a study investigating the whole body overexpression of activated *KRas* (*KRas<sup>LA</sup>*) observed a predisposition to a range of tumour types, particularly in the lungs, but mice also exhibited thymic lymphomas and skin papillomas. These mice did not develop adenomas in the colon but did show aberrant crypt foci (ACF), an early stage of dysplasia (Johnson et al., 2001). However, expression of activated *KRas* (*KRas<sup>V12G</sup>*) in the intestinal epithelium resulted in the development of lesions varying from ACF to adenocarcinoma (Janssen et al., 2002).

Heterozygous deletion of *Apc* can be combined with driver mutations such as activated *KRas* to investigate the contribution to CRC in a model that is more relevant to the human patient. Sansom et al. combined *Apc* deficiency with a conditional mutant allele of oncogenic *KRas*, *K-Ras (V12)* which is an activating mutation resulting in the amino acid substitution at position 12 in *KRas* from a glycine (G) to a valine (V). The allele is under the control of a floxed STOP transcriptional cassette so that until *Cre*-mediated recombination, the oncogenic allele remains transcriptionally silent. Activation of *KRas*

alone did not have an impact on normal intestinal homeostasis, however it co-operated with *Apc* deficiency to accelerate tumourigenesis and invasion (Sansom et al., 2006). The only limitation with this model is that the mice develop renal carcinomas before the intestinal tumours can fully invade and metastasise.

### **1.7.3.5 Chemical-induced mouse models of CRC**

Inflammation is also a known driver of CRC and therefore patients with ulcerative colitis and Crohn's disease are associated with high risk of cancer development that is estimated at 2%, 8% and 18% after 10, 20, and 30 years after diagnosis respectively. Furthermore, in a family with history of CRC, the condition irritable bowel syndrome (IBS) doubled the cumulative risk of developing dysplasia (Eaden et al., 2001).

Dextran sodium sulphate (DSS) is an inflammatory agent used in animal models to study colitis-induced carcinogenesis. DSS has direct toxic effects on the colonic epithelium resulting in chronic inflammation and is usually administered in the drinking water. After sufficient duration of DSS treatment alone, some mice will develop tumours exclusively in the colon, however, mice which are predisposed to tumourigenesis can be used to hasten tumour development and increase tumour number. This includes mice with mutations in *Apc*, *p53* and *Msh2* or in mice pre-treated with genotoxic agents such as 1,2-dimethylhydrazine (DMH) and azoxymethane (AOM) (Thaker et al., 2012). DMH is a metabolic precursor of methylazoxymethanol and has been reported to cause colon tumours in rodents that closely recapitulate the human disease (Haase et al., 1973, Martin et al., 1973, Shamsuddin and Phillips, 1981). AOM produces similar lesions in rodents but is more potent and stable than DMH (Bolt et al., 2000, Delker et al., 1999). Advantages of investigating CRC using chemical induced models include rapid and reproducible tumour initiation and the recapitulation of the adenoma-carcinoma sequences that occurs in humans (Rosenberg et al., 2009). Furthermore, tumours are located exclusively in the colon which better recapitulates the human disease compared to the models mentioned above. The combination of DSS with *Apc* mutation or AOM leads to the development of tumours in as little as 7-10 weeks whereas tumour development in other models usually requires several months (Thaker et al., 2012).

## 1.8 AMPK-Related kinases

### 1.8.1 AMPK

The AMP-activated protein kinase (AMPK) is a highly conserved serine/threonine protein kinase that is an essential energy sensor within cells. Many cellular functions require energy and most of these are driven by the hydrolysis of ATP to ADP, therefore a balance of ATP generation and ATP consumption in cells is required. The reversible reaction of  $2\text{ADP} = \text{ATP} + \text{AMP}$  leads to ATP generation and is normally maintained close to equilibrium. However, any rise in the ADP/ATP ratio causes the reaction to be shifted towards ATP and AMP production and thus falling energy status is not only associated with increased ADP but also AMP (Hardie and Hawley, 2001). A lower energy status is usually a result of cellular stresses that hinder ATP production such as hypoxia, glucose deprivation, and ischemia or mechanisms that increase ATP consumption such as cell growth or muscle contraction. Activation of AMPK results in the conservation of ATP by the inhibition of ATP-consuming processes such as the synthesis of lipids, carbohydrates and proteins, as well as the upregulation of catabolic processes for the generation of ATP (Hardie, 2003).

AMPK exists as a heterotrimeric complex comprising of a catalytic  $\alpha$ -subunit and regulatory  $\beta$  - and  $\gamma$ - subunits (Hardie et al., 2012). Regulation of AMPK is both mediated on allosteric and post-translational levels. ATP, ADP and AMP are all able to bind the  $\gamma$ -subunit of AMPK with similar affinity, however, allosteric activation of AMPK is only caused by AMP (Hardie et al., 1999). The binding of AMP and ADP to AMPK promote its phosphorylation and inhibit dephosphorylation of the protein by Liver kinase B1 (LKB1) in complex with STRAD and MO25 (Hawley et al., 2003, Shaw et al., 2004, Woods et al., 2003). It has been suggested that this provides a graded response of AMPK activity over a range of stress levels in the cells. ADP is usually present at higher levels, therefore the binding of ADP to AMPK may elicit a moderate stress response whereas binding of AMP suggests that ATP levels are very low and a more amplified response is elicited (Hardie et al., 2012). LKB1 phosphorylates the AMPK catalytic subunit at a conserved Threonine residue (referred to as Thr-172 due to its position in the original rat sequence) in the activation loop (Hong et al., 2003, Hawley et al., 1996).  $\text{Ca}^{2+}$ /calmodulin-activated protein kinase kinases such as CaMKK $\beta$  can also phosphorylate AMPK at Thr-172 in response to increases in cellular calcium independent of AMP or ADP levels (Hawley et al., 2005). Finally, TGF- $\beta$ -activated kinase 1 (TAK1) can also phosphorylate AMPK at this site in

response to Tumour necrosis factor (TNF)- related apoptosis- inducing ligand (TRAIL) activation (Herrero- Martín et al., 2009). In addition to the various metabolic stresses mentioned above that can activate AMPK, drugs and xenobiotics which involve increases in AMP, ADP or  $\text{Ca}^{2+}$  can also activate AMPK. These include antidiabetic drugs such as metformin, phenformin and thiazolidinediones (Zhou et al., 2001) and plant products reputed to have health benefits, such as resveratrol from grapes and red wine (Baur et al., 2006), which act by inhibiting mitochondrial ATP synthesis and thereby activate AMPK indirectly (Hawley et al., 2010). Direct AMPK activators are also available, such as 5-aminoimidazole-4-carboxamide riboside (AICAR), which acts as an AMP-mimetic and binds directly to the  $\gamma$ - subunit (Corton et al., 1995).

### **1.8.2 AMPK-related kinases**

The AMPK-related kinase (AMPK-RK) family was identified through their sequence homology with AMPK, specifically to the conserved active T loop located at the protein kinase domain (Manning et al., 2002). Currently twelve AMPK-related kinases (AMPK-RKs; BRSK1, BRSK2, NUAK1, NUAK2, QIK, QSK, SIK, MARK1, MARK2, MARK3, MARK4, and MELK) have been identified (Sun et al, 2013). Further sequence analyses have discovered that the SNRK kinase family are also distant relatives of AMPK (Figure 1.8).

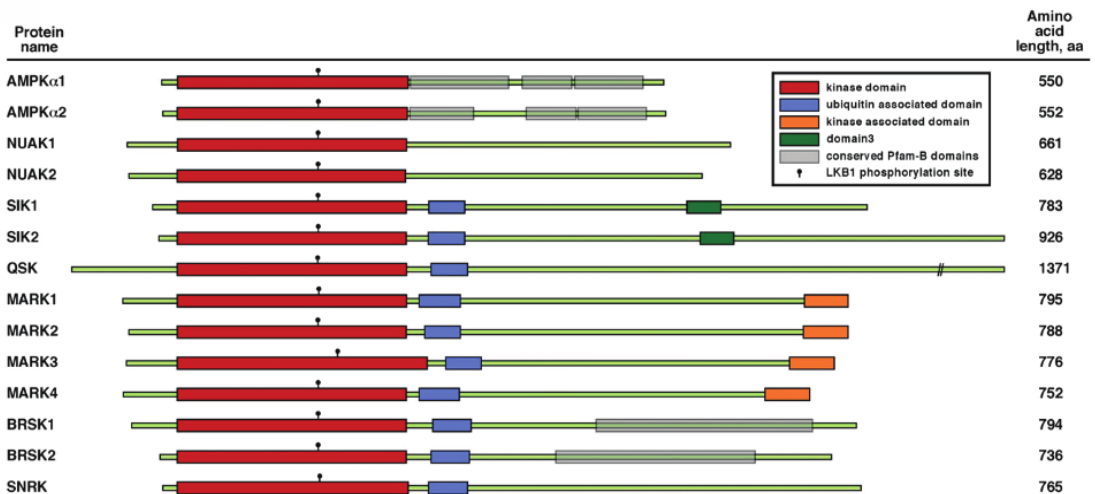
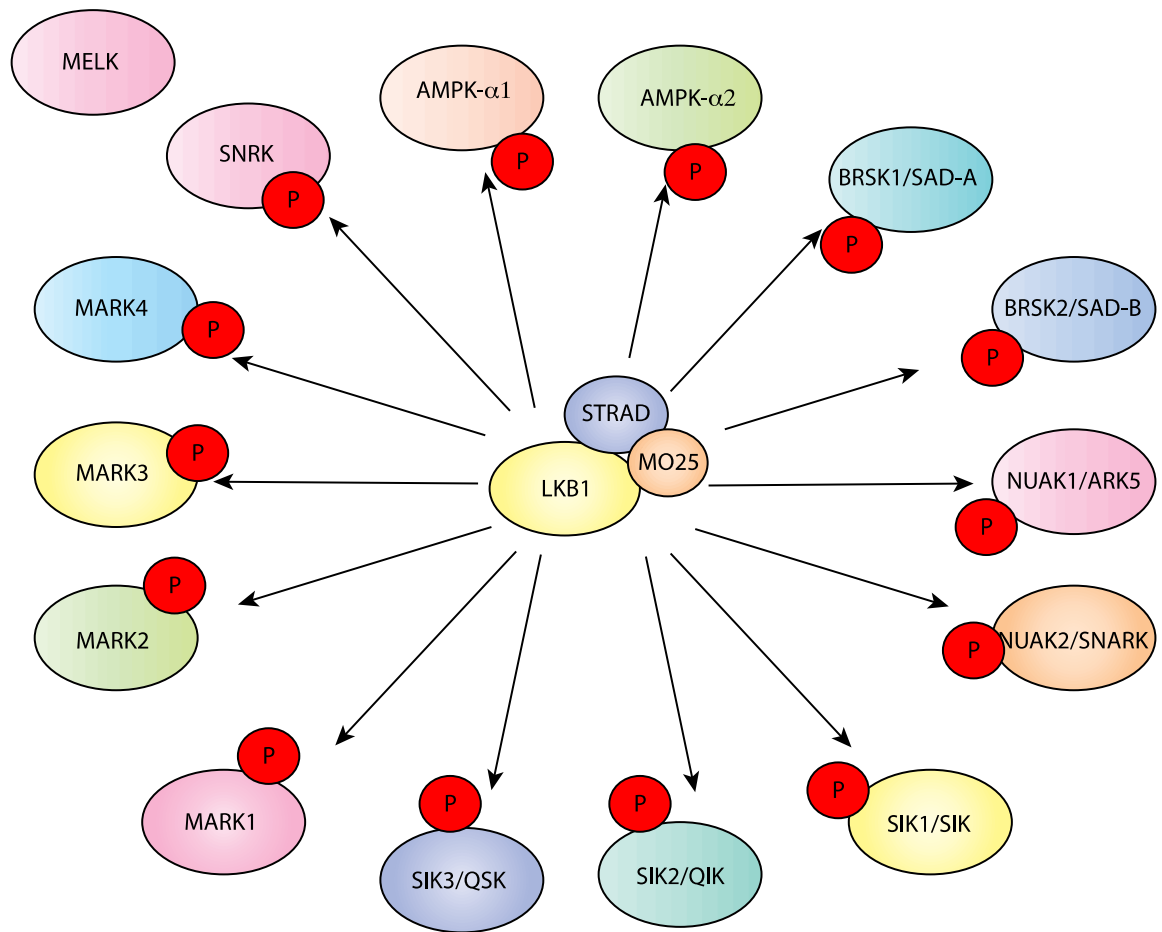


### Figure 1. 8 - The AMPK-related kinase family

Currently, there are 12 AMPK-related kinases identified. These include BRSK1, BRSK2, NUAK1, NUAK2, QIK, QSK, SIK, MARK1, MARK2, MARK3, MARK4, and MELK. In complex with STRAD and MO25, Liver Kinase B1 (LKB1) phosphorylates all AMPK-RKs at the conserved threonine residue excluding MELK. LKB1 is also known to phosphorylate one member of the SNRK kinase family at the same residue. The SNRK family are also distant relatives of AMPK according to sequence analyses. The bottom panel shows the domain organization of the human AMPK-RK. The amino acid length of each protein is indicated on the right (amino acid length, aa). Kinase domains, ubiquitin-associate domains (UBA), domain 3, kinase-associate domains (KA1), Pfam-B domains and conserved T-loop sites phosphorylated by LKB1 are indicated using key. Adapted from (Katajisto et al., 2007)

The AMPK-RKs have similar structural organization, comprising of an N-terminal catalytic domain, a C-terminal spacer sequence and in some cases, an ubiquitin-associated domain and a KA1 domain (Bright et al., 2009). Liver Kinase B1 (LKB1) is known to activate all family members (excluding MELK) at the conserved threonine residue when in complex with STRAD and MO25 (Lizcano et al., 2004). Evidence that other known activators of AMPK including AICAR, phenformin and upstream kinase, Ca<sup>2+</sup>/calmodulin-dependent PK kinase  $\beta$  (CaMKK $\beta$ ) can or cannot phosphorylate and/or activate the AMPK-RKs are conflicting but do suggest that regulation varies for individual AMPK-RK subfamilies (Lizcano et al., 2004, Sakamoto et al., 2004, Bright et al., 2008, Lefebvre et al., 2001). Indeed, we have recently shown that NUAK1 and NUAK2 are not regulated directly by CaMKK $\beta$  but are regulated by calcium signalling in LKB1 deficient conditions (Monteverde, Accepted for publication). Despite the vast amount of information about AMPK, many of the AMPK-RKs remain uncharacterized. Generally, the literature has associated the MAP/microtubule affinity-regulating kinases (MARKs) with the regulation of cell polarity (Drewes et al., 1997). The brain-specific kinases (BRSK1 & BRSK2) have been found to control neuronal polarity (Kishi et al., 2005). The salt inducible kinases (SIKs) have been implicated in various processes; SIK1 (SIK) has been related to the regulation of steroidogenic gene expression in adrenocorticotrophic hormone (ACTH) stimulation (Katoh et al., 2006), SIK2 (or QIK, Quin-induced kinase) may mediate insulin signal transduction (Horike et al., 2003) and inhibit CREB-mediated gene expression by phosphorylation of TORC2, at the same site as AMPK (Screaton et al., 2004). Finally, SIK3 (QSK) was found to regulate cell cycle progression in *Drosophila* (Bettencourt-Dias et al., 2004).

### **1.8.3 NUAK1 and NUAK2: structure, expression and a common target**

AMPK-regulated kinase novel (*nua*) family SNF-like kinases, NUAK1 (ARK5) and NUAK2 (SNARK) comprise of a serine/threonine-protein kinase domain at their N-terminus that is conserved among AMPK $\alpha$ 1/2 and the AMPK-RKs (Manning et al., 2002). Unlike the other AMPK-RKs, neither NUAK1 nor NUAK2 contain a ubiquitin-associated (UBA) domain, which has been associated with protein conformation and LKB1-mediated phosphorylation and activation (Jaleel et al., 2006). Interestingly, neither mammalian AMPK $\alpha$ 1 nor AMPK $\alpha$ 2 contain UBA domains either. The human *NUAK1* gene resides at chromosome 12q23.3 and encodes a protein of 661 amino acids with a molecular weight of 76kDa, whereas murine NUAK1 is 658 amino acids long. *Homo sapiens* NUAK1 is 91%

similar to *Mus musculus* NUA1, 75% to *Xenopus tropicalis* NUA1, and 65% similar to *C.elegans* UNC-82. NUA2 is located at chromosome 1q32.1 and encodes a 629 amino acid protein with a molecular weight of 69kDa (Lefebvre et al., 2001). The human NUA1 amino acid sequence shows 58% homology to NUA2 as a whole and 82% in the kinase domain (Suzuki et al., 2003a) (see Figure 1.9).

Range 1: 80 to 672		Graphics		▼ Next Match	▲ Previous Match
Score	Expect	Method	Identities	Positives	Gaps
648 bits(1672)	0.0	Compositional matrix adjust.	370/642(58%)	436/642(67%)	67/642(10%)
NUAK1	38	KPHGVKRHHHKKHNLKHYELQETLGKGYGKVKRATERFSGRVVAIKSIRKDKIKDEQDM			97
NUAK2	80	K VKRHHHKKHNL+HRYE ETLGKGYGKVK+A E SGR+VAIKSIRKDKIKDEQD+ KKQAVKRHHHKKHNLHRYEFLETLGKGYGKVKKARES-SGRLVAIKSIRKDKIKDEQDL			138
NUAK1	98	VHIRREIEIMSSLNHPHIIISYEVFENKDKIVIMEYASKGELYDYISERRRLSERETRH			157
NUAK2	139	+HIRREIEIMSSLNHPHII+I+EVFEN KIVI+MEYAS+G+LYDYISER++LSERE RH MHIRREIEIMSSLNHPHIIAIEVFENSSKIVIVMEYASRGDLYDYISERQQLSEREARH			198
NUAK1	158	FFRQIVSAVHYCHKNGVVRDLKLENILLDDNCNIKIADPGLSNLYQKDKFLQTFGGSPL			217
NUAK2	199	FFRQIVSAVHYCH+N VVHRDLKLENILLD N NIKIADPGLSNLY + KFLQTFGGSPL FFRQIVSAVHYCHQNRVVRDLKLENILLDANGNIKIADPGLSNLYHQGKFLQTFGGSPL			258
NUAK1	218	YASPEIVNGRYPYRGPVDSWALGVLLYTLVYGTMPFDGDFDHNLRQISSGEYREPTQPS			277
NUAK2	259	YASPEIVNG+PY GPEVDSW+LGVLLY LV+GTMPFDG DHK L++QIS+G YREP +PS YASPEIVNGKPYTGPVDSWSLGVLLYILVHGTMPPFDGHDHKILVKQISNGAYREPPKPS			318
NUAK1	278	DARGLIRWMLMVNPDRRATIEDIANHVVWVWGYKSSVDCDALHDSESP----LLARIID			333
NUAK2	319	DA GLIRW+LMVNP RRAT+ED+A+HVVWVWGY + V + +A H+ P A + D DACGLIRWMLMVNPTRRATLEDVASHVVWVWGYATRVGEQAPHEGGHPGSDSARASMD			378
NUAK1	334	WHHRSTGLQADTEAKMKGLAKP-----TTSEVMLERQRLKSKKENDFAQS----GQDA			384
NUAK2	379	W RS+ + AK+ K ++ LERQ SLKKS+KEND AQS D WLRSSSRPILLENGAKVCSFFKQHAPGGGSTTPGLERQHSKSKRKNEMAQSLHSDTADD			438
NUAK1	385	VPESPSKLSKRPKPKGILKRSNSEHRSHTGFIIEGVVGPALPSTFKMEQDLCRTGVLLPS			444
NUAK2	439	P K + K PKGILKK+ ++ EGV ++D TAHRPGKSNLKLKPKGILKKSAS-----AEGV-----QED-----			469
NUAK1	445	SPEAEVPGKLSPKQSA-TMPKKGILKKTQRESGYSSPERSESSELDSNDVMGSSIPS			503
NUAK2	470	P P SP Q+A +PKGILKK +QRESGYSSPE SES ELLD+ DV S P -PPELSPIPASPGQAAPLLPKKGIKPKRQRESGYSSPEPSESSELDDAGDVFVSGDPK			528
NUAK1	504	PSPDPARVTSHLSRCKRKGILKHSKYSAGTMDPALVSPPEMPTLESLEPGVPAEGLSR			563
NUAK2	529	P A L RKGILK + K+S ++ L +P T SL E P L+R EQKPPQAS----GLLLHRKGIKLNKFSQTAL--LAAPT--TFGSLDE-LAPPRPLAR			579
NUAK1	564	SYSRPSVISDDSVLSSDSFDLLDLQENRPARQIRSCVSAENFLQIQDFEGLQNRPRP-			622
NUAK2	580	+ SRPS +S+DS+LSS+SPD LDL E P +R CVS +N GL+ P A-SRPSGAVSEDSILSSESPDQLDLPERLP-EPPLRGCVSVDN-----LTGLEEPPSEG			631
NUAK1	623	--QYLKRYR-NRLADSSPFLLDMDVTVQYKQALEICSKLN			661
NUAK2	632	L+R+R + L DS FS LTD +VT Y+QAL +CSKL PGSCLRRWRQDPLGDSVCSF-S-LTDCQEVATYRQALRVCSKLT			672

Protein kinase domain

**Figure 1. 9 – Amino acid sequence homology between human NUA1 and NUA2**

Alignment of the amino acid sequences of human NUA1 and NUA2 proteins show that they share 58% sequence homology. The protein kinase domain is indicated, specifically NUA1 kinase domain can be found from aa55-306 and NUA2 can be found from aa53-303. The GILK motif is highlighted in yellow. Figure adapted from NCBI BLASTp analysis of NUA1 family SNF1-like kinase 1 [Homo sapiens], NCBI Reference Sequence: NP\_055655.1 and NUA2 family SNF1-like kinase 2 [Homo sapiens], NCBI Reference Sequence: NP\_112214.2.

NUA1 and NUA2 have distinct expression patterns although both are highly expressed in the brain. NUA1 is mainly expressed in highly oxidative tissues including the cerebrum, heart, soleus muscle in both human and mouse tissues (Inazuka et al., 2012, Nagase et al., 1998). NUA2 levels are greatest in the adrenal and brain tissue, however

expression has been detected in the thymus, spleen, kidney, stomach, liver, skin, testis, uterus and ovaries (Lefebvre and Rosen, 2005). However, Lefebvre and Rosen showed that NUA2 activity was relatively low in most tissues and highest in the kidneys. NUA1 and NUA2 have both been detected in the cytoplasm and the nucleus, however NUA2 is reported to be predominantly in the nucleus where it can alter gene expression as a transcriptional modulator in response to stress (Kuga et al., 2008, Hou et al., 2011).

To date, the best characterised substrate of NUA1 and NUA2 is the myosin phosphatase target subunit (MYPT1) (Yamamoto et al., 2008, Zagorska et al., 2010). MYPT1 is a component of the  $PP1\beta^{MYPT1}$  myosin phosphatase complex required for the catalysing dephosphorylation of myosin light chain, which in turn regulates many functions including smooth muscle contraction and cell adhesion (Ito et al., 2004). NUA1 and NUA2 are the only AMPK-RKs to contain a Gly-Ile-Leu-Lys (GILK) motif, which mediates direct binding to a regulatory pocket on the surface of  $PP1\beta$ . Downstream of LKB1 activation, NUA1 and NUA2 phosphorylate MYPT1 at three conserved residues, Ser-445, Ser-472, and Ser-910 in response to conditions that cause cell detachment (Banerjee et al., 2014b). Phosphorylation at these sites by NUA1 or NUA2 induces MYPT1 to bind to 14-3-3 isoforms, thereby suppressing phosphatase activity of  $PP1\beta$  towards the myosin light chain (Zagorska et al., 2010) (Figure 1.10).

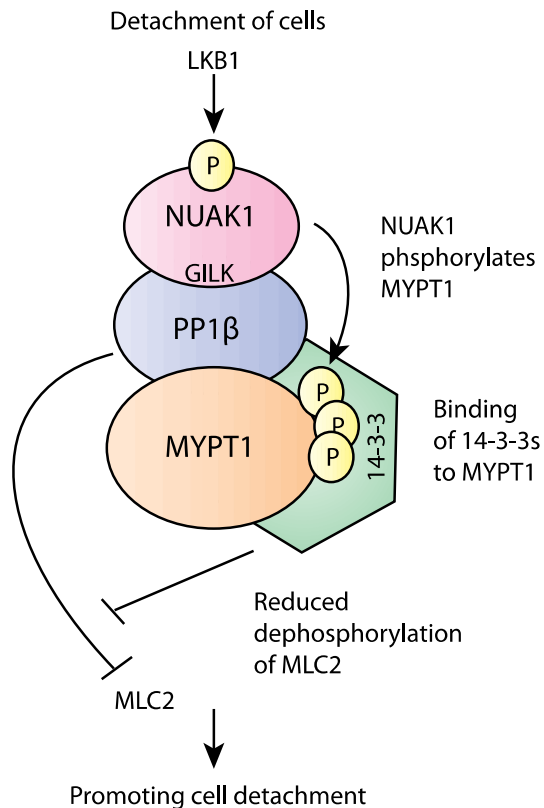


**Figure 1. 10 - Schematic representation of NUAKE1/NUAK2's role in the regulation of myosin light chain phosphorylation.**

LKB1 phosphorylates and activates the kinases NUAKE1 and NUAKE2, which are both able to interact with the MYPT1-PP1 $\beta$  myosin phosphatase complex through the ability to interact with the GILK-binding pocket on the PP1 $\beta$  catalytic subunit. Only one NUAKE is required to bind to PP1 $\beta$ . In response to cell detachment, the NUAKE1 isoforms can phosphorylate MYPT1, thereby inducing binding to 14-3-3. This inhibits interaction with myosin and leads to increased phosphorylation of MLC2 and activation of myosin II. Figure adapted from (Zagorska et al., 2010).

### **1.8.4 NUAKE2: function and regulation**

Several characteristics of NUAKE2 function and regulation have been compared to AMPK (Egan and Zierath, 2009) as NUAKE2 is also responsive to AMP and can be activated in response to glucose deprivation and chemical ATP production (Lefebvre et al., 2001, Lefebvre and Rosen, 2005, Kuga et al., 2008). It is unknown if NUAKE2 can function heterotrimerically as AMPK does, therefore it is currently unclear how NUAKE2 could be activated in response to AMP/ATP levels without regulatory  $\beta$  - and  $\gamma$ - subunits. LKB1 is also known to phosphorylate NUAKE2 at Thr-208, reportedly the NUAKE2 T-loop peptide is a better LKB1 substrate than AMPK $\alpha$  suggesting differential kinase binding affinity of LKB1 within the AMPK-RK family (Lizcano et al., 2004). NUAKE2 has been implicated in various studies as a regulator for cancer cell viability, migration and metastatic potential

for example, NUA2 has been related to cell motility associated with carcinogenesis (Lefebvre et al., 2001, Suzuki et al., 2003c) and separately, as a downstream kinases of the Epstein Barr virus (EBV) latent membrane protein 1 (LMP1), which has a role in resistance to cancer cell death (Kim et al., 2008). Additionally, NUA2 appears to protect cells from TNF-related apoptosis and is required for the CD-95 induced motility and invasiveness of breast cancer MCF-FB cells (Legembre et al., 2004). More recently, NUA2 has been associated with myocyte survival and the maintenance of muscle mass with age *in vivo* and *in vitro* by the downregulation of the Rho kinase signalling pathway (Lessard et al., 2016). Namiki et al. showed that the NUA2 gene is amplified in *PTEN*-deficient melanomas and that inhibition of CDK2 in this scenario was sufficient to suppress the growth of melanomas both *in vitro* and *in vivo* (Namiki et al., 2015).

## 1.9 NUA1

### 1.9.1 NUA1: function and regulation

As NUA1 and NUA2 share many characteristics, it is important to consider both during an investigation, however the focus of this thesis will be NUA1.

LKB1 is known to phosphorylate NUA1 at Thr-211 in response to metabolic stress (Suzuki et al., 2006). AKT can also phosphorylate NUA1 at Ser-600 in response to IGF signalling in tumour cells (Suzuki et al., 2003b). However, whether this is essential for kinase activity in all conditions is unclear as it was reported to be not required for a synthetic lethal response in combination with deregulated c-MYC (Liu et al., 2012). In 2006, Suzuki et al reported that Nuclear Dbp2-related protein (NDR2), an AGC kinase, activates NUA1 at Thr-211 upon IGF stimulation in a PDK1- and AKT-dependent manner (Suzuki et al., 2006).

NUA1 is stimulated *in vitro* by AMP, as NUA2 and AMPK, and is also able to phosphorylate SAMS peptide, a synthetic substrate for AMPK-RKs (Suzuki et al., 2003a, Suzuki et al., 2003b, Suzuki et al., 2006). As with NUA2, it is unknown if NUA1 can function heterotrimerically as AMPK, therefore, it is unclear how it can be stimulated in a similar manner to AMPK. As mentioned above NUA1 is activated downstream of growth factor signalling such as insulin and insulin-like growth factor 1 (IGF1) (Suzuki et al., 2003a, Suzuki et al., 2003b). Furthermore, Fisher et al. observed increased

phosphorylation of NUAK1 at Thr-211 in response to cell contraction or the AMPK activator AICAR in rat skeletal muscle (Fisher et al., 2005).

Publications to date have associated NUAK1 with many central cell processes such as proliferation, adhesion, ploidy, senescence, damage response, apoptosis and tumour progression. NUAK1 has been reported as a regulator of cellular senescence and ploidy by the modulation of phosphorylation of Large Tumour Suppressor Kinase 1 (LATS1) (Humbert et al., 2010). NUAK1 has also been observed to phosphorylate p53/TP53 leading to p21 mediated cell cycle arrest (Hou et al., 2011), however, conflicting reports have suggested that NUAK1 positively regulates cell cycle progression (Banerjee et al., 2014b, Liu et al., 2012). As mentioned previously, NUAK1 is known to interact with the myosin phosphatase targeting-1 (MYPT1)–protein phosphatase-1 $\beta$  (PP1 $\beta$ ) complex (PP1 $\beta$ <sup>MYPT1</sup>) and thereby regulate cell adhesion (Zagorska et al., 2010). Separately, NUAK1 has been associated with cellular survival under conditions of nutrient starvation by phosphorylation of cell survival factor AKT (Suzuki et al., 2003b).

### **1.9.2 NUAK1 mouse models**

Nuak1 null mice are embryonic lethal; by embryonic day 18.5 homozygous null mutants suffer omphalocele, which is a failure to close the developing ventral body wall (Hirano et al., 2006). It has also been reported that Nuak2 null mice have a high mortality rate and that embryos frequently exhibit exencephaly (Tsuchihara et al., 2008). Nuak1 and Nuak2 double mutants exhibit exencephaly, facial clefting, and spina bifida (Ohmura et al., 2012). In this study it was suggested that Nuak1 and Nuak2 showed complementary function in the development of the cranial neural plate. This is indicative of some over-lap in Nuak1 and Nuak2 function, at least during development.

Due to embryonic lethality, an inducible system is required to validate the physiological roles of Nuak1 in adult mice *in vivo*. After discovery that NUAK1 is preferentially expressed in highly oxidative tissues such as the brain, heart and soleus muscle, Inazuka et al. generated a muscle specific Nuak1 knock out (MNUAK1KO) mouse model. On a high fat diet it was observed that MNUAK1KO mice had a lower fasting blood glucose level, higher glucose tolerance, higher insulin sensitivity, and elevated concentration of muscle glycogen than wild type mice. Furthermore, phosphorylation of major components of the insulin signalling pathway, IRS1 (Tyr-608), and AKT were increased and insulin signalling was enhanced in MNUAK1KO mice. Consistent with this, phosphorylation of

IRS1 Ser-1097 (Ser-1101 in humans), which acts as an inhibitor of downstream insulin/AKT/mTOR signalling, was markedly decreased in the Nuak1-depleted tissues. They concluded that a physiological role of Nuak1 is to quash glucose uptake via negative regulation of insulin signal transduction in oxidative muscle.

### **1.9.3 NUAK1 and cancer**

NUAK1 has also been associated with tumour cell survival, invasion and metastasis, and poor prognosis in many tumour types including hepatocellular carcinoma (HCC) (Cui et al., 2013), glioma (Lu et al., 2013, Chang et al., 2012), breast (Chang et al., 2011), melanoma (Bell et al., 2014), and non-small cell lung cancer (NSCLC) (Chen et al., 2013).

The alteration frequency of NUAK1 in human cancer is relatively low, in a total of 164 studies (45709 samples) the highest alteration frequency for NUAK1 was in neuroendocrine prostate cancer at 18%. All other cancers had an alteration frequency within 0-6.9% (cBioPortal) (Figure 1.11). However, immunohistochemistry on human tissue showed elevated levels of NUAK1 expression in colon (38% of patient samples), pancreatic (57%) and hepatocellular carcinoma (66%) compared to non-tumour tissue (Liu et al., 2012). The Esumi lab also published that they observed increased NUAK1 expression in more advanced cases of CRC and much higher expression in liver metastasis (Kusakai et al., 2004).

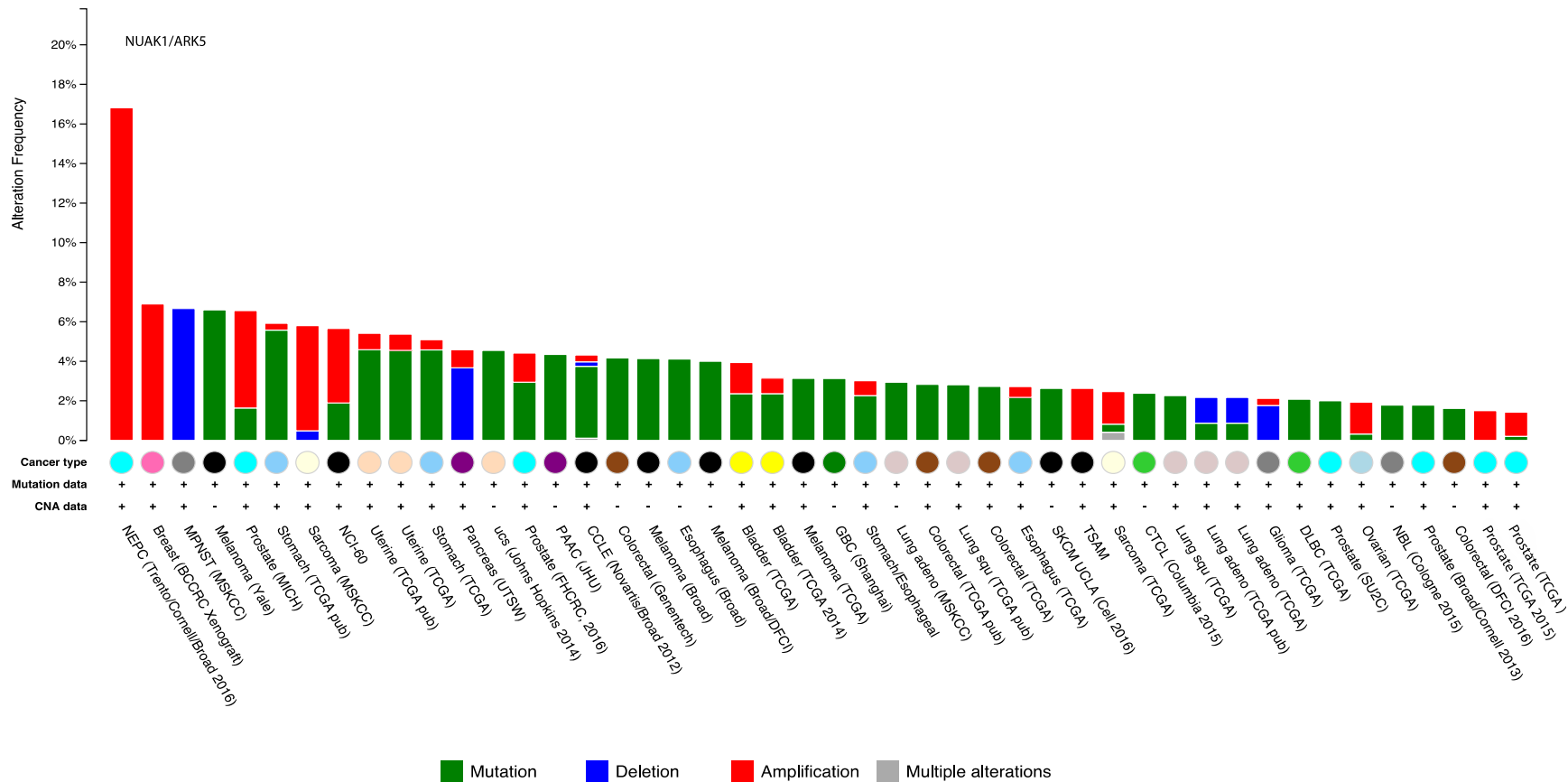


**Figure 1.11 - NUAK1 alteration frequency across human cancer types.**

Graph generated by cBioPortal (<http://www.cbioportal.org>) shows the cumulative frequency of genetic alterations in the *NUAK1* gene across a variety of human cancers. Green bars represent mutation (inclusive of activating and inactivating); red bars, represent gene amplification; blue bars represent gene deletion and grey bars represent multiple alterations at the same locus. Data are sourced from the TCGA, Trento/Cornell/Broad, BCCRC, MSKCC, Yale, MICH, UTSW, John Hopkins, FHCRC, JHU, Novartis/Broad, Genentech, Broad, Broad/DFCI, Shanghai, and SU2C. Published cohorts are indicated with a reference and date.

Most of the aforementioned studies have been correlative studies, however, NUA1 has been linked with several tumorigenic processes, such as promotion of tumour metastasis and invasion by increasing expression of matrix metalloproteinases (MMP-2, MMP-9 and MT1-MMP) downstream of AKT. MMPs play a key role in degrading the extracellular matrix and basement membrane and thus promote metastasis and angiogenesis in several cancers (Chang et al., 2012). Furthermore, NUA1 has a clear role in the regulation of cell adhesion via the phosphorylation of MYPT1 (Zagorska et al., 2010). In 2014, microRNA-211 was identified as a mediator of an invasive gene clusters in melanoma cells, and it was shown to inhibit loss of adhesion by directly down-regulating NUA1 expression (Bell et al., 2014).

#### **1.9.4 NUA1 and synthetic lethality**

As previously mentioned, c-MYC is notoriously difficult to target therefore many labs, including ours, have adopted the synthetic lethality approach to alternatively target c-MYC. Here, genome-wide interrogation using RNA interference has begun to identify genes that are specifically required for the fitness and survival of cells with overexpression of c-MYC (Kessler et al., 2012, Toyoshima et al., 2012, Liu et al., 2012). One such gene is NUA1 and our lab demonstrated that both human and mouse cell lines with high oncogenic levels of c-MYC require NUA1 specifically to maintain metabolic homeostasis. Initially it was observed that NUA1 restricts cell growth, and as AMPK is a negative regulator of cell growth via inhibition of the mammalian target of rapamycin (mTOR) pathway this caused speculation for a potential relationship of NUA1 with this signalling cascade.

mTOR is a protein serine/threonine kinase that regulates cell growth, proliferation, motility and survival in response to extracellular hormones, growth factors and nutrients (Zarogoulidis et al., 2014, Sabatini, 2006) (Figure 1.12). There are two known complexes of mTOR, termed mTOR complex 1 (mTORC1) and mTOR complex 2 (mTORC2), which are both structurally and functionally distinct (Zoncu et al 2011). mTORC1 includes mTOR, mLST8/Gbl, PRAS40, and the WD40 repeat-containing subunit raptor (Sancak et al., 2007, Sabatini, 2006) and is known to stimulate cellular growth, translation, transcription and autophagy. Amino acids, growth factors and energy are all potent stimuli for mTORC1 activity (Polak et al, 2009). Activation leads to an increase in p70S6 kinase activity and protein synthesis via phosphorylation of eukaryotic initiation factor 4E

(eIF4E) and ribosomal S6 protein (Polak et al, 2009). mTORC2 contains Rictor, mSin1, PRR5, and PRR5L and is less well characterised. Known functions include regulation of the actin cytoskeleton and phosphorylation of AKT on Ser-473 for complete activation (Courtney et al, 2010). mTORC1 signalling is regulated by inhibitory phosphorylation of the upstream kinases TSC1 and TSC2 by mitogen-activated kinases including AKT, ERK and RSK. Furthermore, PRAS40 is also a direct target of AKT and phosphorylation activates mTORC1 (Sancak et al., 2007, Vander Haar et al., 2007). mTOR signalling is active under nutrient-rich conditions and inactive under nutrient-poor conditions in contrast to AMPK, which is active in the inverse pattern. Upon LKB1 and AMP-dependent activation, AMPK phosphorylates TSC2 at Ser-1387 and Thr-1271 and inhibits downstream mTOR signalling to regain ATP homeostasis.

Oncogenic levels of c-MYC result in the activation of AMPK due to the increased consumption of cellular resources for cell growth, however Liu et al. showed that in the case of loss of NUA1, this response is diminished. Proteomic analysis suggested that NUA1 is required for the activation of AMPK as it protects the regulatory  $\beta$ 1 subunit of AMPK from proteasomal degradation. However, further analyses have failed to confirm this effect and recent data suggests that NUA1 can regulate mTOR independently of AMPK by phosphorylating the mTORC1 subunit RAPTOR (Monteverde, Accepted for publication).

Liu et al. concluded that raised energy consumption through unrestrained mTORC1 activity in cells expressing deregulated c-MYC led to a dependency on NUA1, which appears to restrict mTORC1 activity. Additionally, Liu et al. showed that NUA1 preserves high respiratory capacity via the stability of mitochondrial subunits that are necessary for the generation of ATP. It was unclear whether these two phenotypes are a direct influence of loss of NUA1 or that one is a consequence of the other, however in combination this led to a complete collapse in ATP levels preceding cell death (Liu et al., 2012). Loss of AMPK or an equivalent metabolic checkpoint has fatal consequences within a cell, as there is no mechanism to prevent the depletion of energy resources. This evidence suggests that NUA1 acts as a metabolic checkpoint in cells overexpressing c-MYC, however it is still unclear whether this mechanism is mediated via AMPK.

In the previous study, depletion of NUA1 by siRNA led to suppression of human tumour cell growth in 5/14 cases, two of which were CRC cell lines LS174T and Colo 320. Further interrogation of LS174T cells showed that cell death was accompanied by loss of

ATP and could be prevented by Rapamycin. LS174T colon carcinoma cells harbour a  $\beta$ -Catenin mutation that drives constitutive c-MYC expression (van de Wetering et al., 2002). Importantly, co-depletion of c-MYC also prevented cell death, confirming that the levels of c-MYC in LS174T are high enough for cells to establish a dependence of NUA1 that can be exploited. This was confirmed *in vivo* when the study showed that depletion of NUA1 suppresses LS174T xenograft growth. Finally, using an orthotopic model, NUA1 depleted murine  $p53^{-/-}$  hepatoma cells failed to develop hepatocellular carcinoma. In a separate intervention study where tumours were allowed to develop before NUA1 was lost, cells that retained NUA1 had a survival advantage relative to NUA1 wildtype controls (Liu et al., 2012). This data suggests that MYC-driven tumours might be particularly vulnerable to the disruption of metabolic checkpoints, such as NUA1, and provides the basis for this thesis.

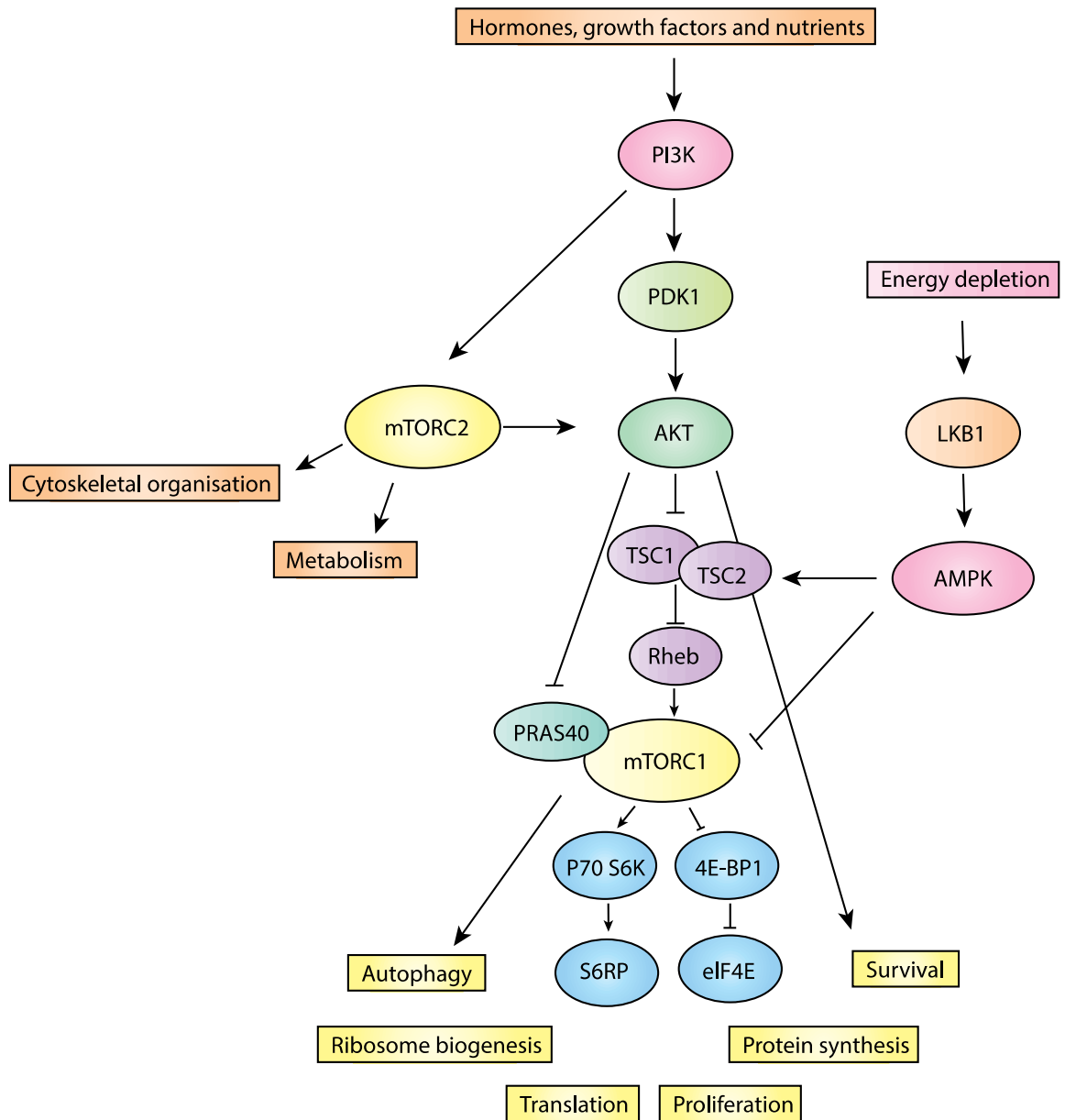


**Figure 1. 12 - The TOR signalling pathway**

A schematic showing a simplified version of the main components of the TOR signalling pathway. mTORC1 is activated in the presence of hormones, growth factors and nutrients via AKT phosphorylation of upstream inhibitory proteins, TSC1/TSC2. mTORC1 is then free to phosphorylate downstream proteins including p70S6 kinase and 4E-BP1 which leads to an increase in protein synthesis and other cellular processes such as glucose homeostasis, autophagy, stress response, and mitochondrial function. mTORC2 is activated by PI3kinase and is necessary for full activation of AKT, downstream cellular processes affected by mTORC1 include cytoskeletal organization and metabolism.

## 1.10 Aims of the project

Based on the current literature discussed in this introduction (summarised in Figure 1.13) and the lab's latest findings that tumour cells overexpressing c-MYC depend upon NUAK1 for survival, the main aim of this project is to investigate NUAK1 in the context of a c-MYC dependent tumour such as CRC. The hypothesis is that targeting NUAK1 in c-MYC dependent tumour cells may have therapeutic implications.

The first aim is to validate NUAK1's role as a tumour-associated protein in human CRC. To address this NUAK1 was investigated as a prognostic marker in human CRC using online patient data sets. Furthermore NUAK1 expression levels and patient outcome in different stages of CRC was examined using NUAK1 RNA scope on a Tissue Microarray (TMA) of human CRC. Next, NUAK1 levels were assessed in human CRC cell lines and the requirement for NUAK1 measured using small molecule inhibitors. These investigations are outlined in Chapter 3.

The second aim is to model Nuak1 in mouse models of CRC in order to investigate its role throughout tumorigenesis. Initially Nuak1's role in tumour development was addressed, therefore Nuak1 floxed mice (Inazuka et al., 2012) were bred onto a model for sporadic intestinal cancer, *Villin-CreER<sup>T2</sup>;Apc<sup>fl/+</sup>;LSL-KRas<sup>G12D/+</sup>*. Additionally, Nuak1's role in established colorectal tumours was addressed, therefore two independent doxycycline-inducible shRNA specific for Nuak1 were used in a carcinogen-induced mouse model for colorectal cancer. Importantly, the requirement for Nuak1 in normal healthy intestine was also investigated using the Nuak1 floxed allele under the control of *VillinCreER<sup>T2</sup>*. These investigations are outlined in Chapter 4.

The final aim is to investigate the molecular signalling pathways that require NUAK1 for tumour cell growth and survival using various *in vitro* approaches, including RNA sequencing and phospho-proteomic analysis, after NUAK1 depletion or inhibition in both U2OS and human CRC cell lines. These investigations are outlined in Chapter 5.

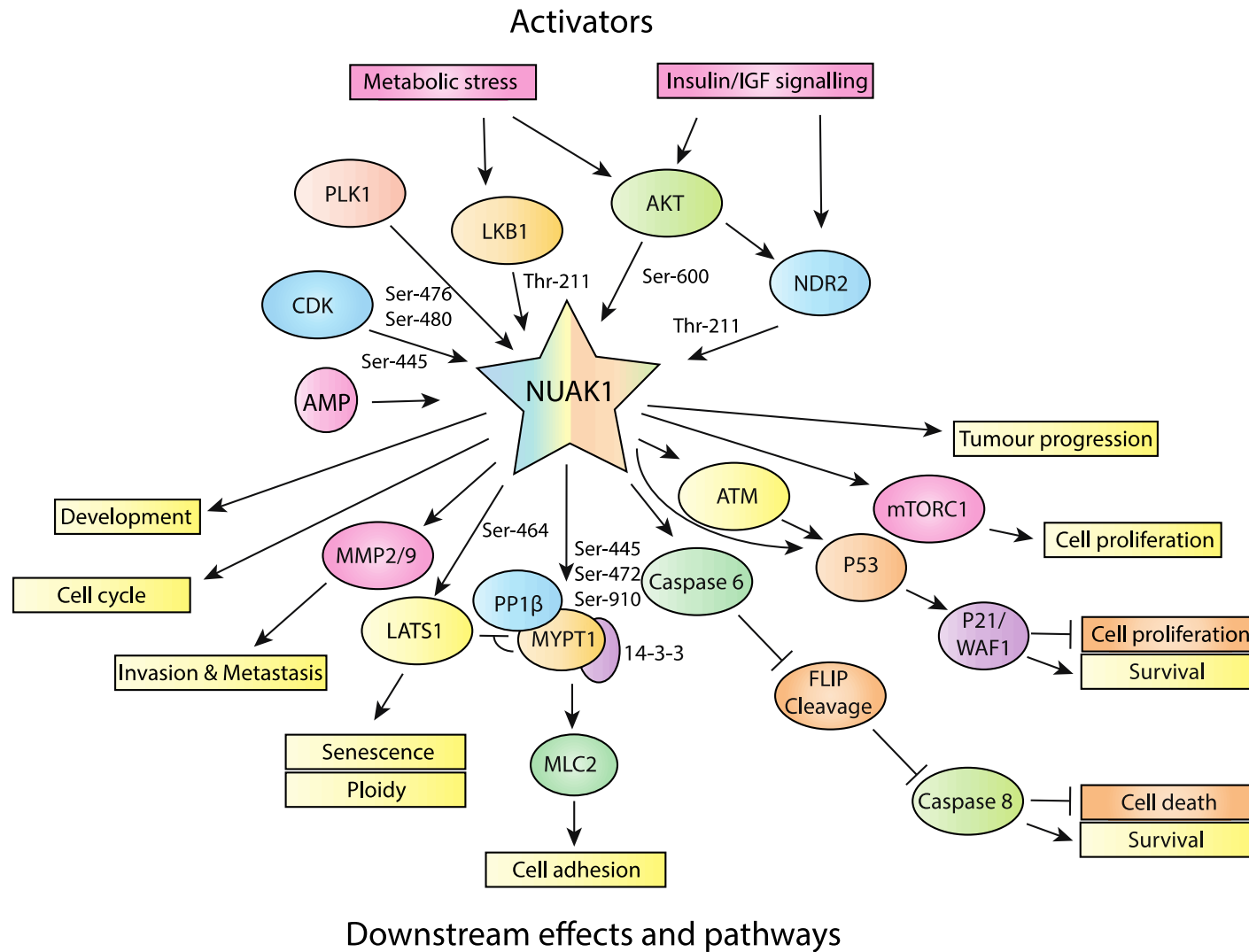


**Figure 1. 13 – A summary of NUA1 activators, downstream effects and pathways**

A schematic summary of NUA1 activators, downstream effects and pathways based on the current literature discussed in this introduction.

# Chapter 2 Materials & Methods

## 2.1 Mouse experiments and analyses

All experiments involving mice were approved by the local ethics committee and conducted in accordance with UK Home Office license numbers 70/7950 & 70/8646, and PIL I83E608A7 (CRUK BICR, UK).

### 2.1.1 Colony Maintenance

In order to generate experimental mice, breedings to generate the correct genotypes were set up between one male and one or two female mice. Pups were weaned at approximately 4 weeks of age and ear notched for identification and DNA genotyping. All transgenic mice were maintained in individually ventilated cages (IVCs) and handled in a laminar flow changing station. Experimental mice were moved to non-barrier cages once identified from genotyping. Mice were housed in a constant 12hr light/dark cycle, fed irradiated standard diet CRM (E) expanded diet from Special Diet Services; Cat 801730) and watered *ad libitum*.

### 2.1.2 Genotyping

Mice were ear-notched at 4 weeks of age and the tissue sent to Transnetyx (Cordova, TN, USA). Transnetyx currently uses a combination of quantitative PCR and DNA hybridization to determine the presence of specific alleles in the tissue samples provided.

### 2.1.3 Experimental Cohorts

The *Villin-CreER<sup>T2</sup>* (el Marjou et al., 2004); floxed *Apc* (Shibata et al., 1997); *LSL-KRas<sup>G12D</sup>* (Jackson et al., 2001); floxed *Nuak1* (Inazuka et al., 2012); and *Rosa26-CAAGS-lsl-rtTA<sup>3</sup>* (Premssirut et al., 2011) allelic mice have been described previously however they are summarised briefly below. The doxycycline-inducible shRNA alleles (*DI-shNUAK1*) targeting *Nuak1*, were generated by Mirimus Inc. This is the first description of these alleles to be published. All mice in these experiments were maintained on a mixed (FVBN x C57Bl/6 x 129/SV) background. All inductions were performed at 6-12 weeks when the mice reached a body weight of at least 20g. Mice were monitored at least 3 times weekly and sacrificed using a schedule 1 procedure by exposure to rising concentrations of carbon-dioxide gas followed by cervical dislocation. Mice were monitored for symptoms

including >15% weight loss, pale feet, lethargy, hunching, and/or bloody stool. Presentation of two or more symptoms was defined as a humane end point and mice were sacrificed immediately.

### **2.1.3.1 Villin-CreER<sup>T2</sup>; Nuak1<sup>fl/fl</sup> experiments**

*Villin-CreER<sup>T2</sup>* allows spatial-temporal control of transgenes downstream so that following recombination by tamoxifen induction, stable and homogenous expression is seen in the small intestine and colon, along the crypt villus axis, in both differentiated enterocytes and undifferentiated cells of the crypt (el Marjou et al., 2004). The *Nuak1 fl/fl* allele contains *lox P* sites at exon 3 at the endogenous locus and results in a non-functional protein after *Cre recombinase* excision.

Experimental mice used were all homozygous for the *Nuak1* floxed allele and controls were wildtype littermates. Mice were induced by once daily intraperitoneal (IP) injections of tamoxifen (Sigma) at 80mg/kg for four consecutive days and harvested on day 6-post induction. Experimental mice presented no symptoms in this time frame.

Experimental procedures were performed by Dr. Meera Raja, images taken by thesis author, Jennifer Port.

### **2.1.3.2 Villin-CreER<sup>T2</sup>; Apc<sup>fl/fl</sup>; Nuak1<sup>fl/fl</sup> experiments**

The floxed *Apc* allele (first described in Shibata et al, 1997) contains *lox P* sites on either side of exon 14 at the endogenous locus, so that *Cre* recombination results in a non-functional allele after excision.

Experimental mice used were all homozygous for both the floxed *Apc* and floxed *Nuak1* alleles and controls were wildtype littermates. Mice were induced by once daily IP injection of tamoxifen at 80mg/kg for two consecutive days and harvested on day 4-post induction. Mice were monitored for symptoms including >15% weight loss, pale feet, lethargy, hunching, and/or bloody stool.

Experimental procedures were performed by Dr. Meera Raja, images taken by thesis author, Jennifer Port.

### **2.1.3.3 Villin-CreER<sup>T2</sup>;Apc<sup>fl/+</sup>;LSL-KRas<sup>G12D/+</sup>;Nuak1<sup>fl/fl</sup> experiments**

The *LSL-KRas<sup>G12D</sup>* allele lies at the endogenous *KRas* locus and carries a LOX-STOP-LOX (LSL) termination sequence preceding the first exon and the *KRas G12D* point mutation in exon 1. *Cre* recombination allows the allele to be expressed constitutively (Jackson et al., 2001). Experimental mice used were all heterozygous for the floxed *Apc* allele, heterozygous for mutant *KRas*, and homozygous for the floxed *Nuak1* allele. Controls were wildtype littermates. Low tamoxifen dose survival cohorts were induced by one IP of tamoxifen at 50mg/kg and harvested at endpoint as above. High tamoxifen dose cohorts were induced with one day of 120mg/kg, then three consecutive days of 80mg/kg (high) and harvested as above.

Low tamoxifen dose experimental procedures were performed by Dr. Meera Raja, high tamoxifen dose experimental procedures were performed by Jennifer Port.

### **2.1.3.4 Zp3-Cre;Rosa26-CAAGS-LSL-rtTA<sup>3</sup>; DI-shNUAK1 experiments**

Expression of the *Zp3-Cre* allele is expressed exclusively in the oocyte prior to the first meiotic division; therefore following recombination all cells in the developed mouse should express downstream alleles, in this case the *Rosa26-CAAGS-rtTA<sup>3</sup>* (*rtTA3*).

The doxycycline-inducible shRNA alleles (*DI-shNUAK1*) targeting *Nuak1* were generated by Mirimus Inc., as described previously (Dow et al., 2012). In brief, shRNA candidates were selected using the sensor assay (Fellmann et al., 2011). Two shRNAs were chosen that scored >5 and produced knockdown >90%. The selected shRNA sequences were subsequently cloned in the miR-E backbone (Fellmann et al., 2013) within the 3'UTR of a turboGFP cDNA downstream of a tetracycline-responsive element (TRE) in the *Colla1* TtGM vector and targeted to the *Colla1* locus using standard protocols (Premssirut et al., 2011). Targeted embryonic stem (ES) cells were injected using blastocyst injection technique. Resulting shRNA mice were of mixed C57BL/6 × 129/SV background.

The *DI-shNUAK1* alleles were induced by daily gavage of 2mg doxycycline (Sigma; in H<sub>2</sub>O; 200ul at 10mg/ml). Mice were harvested at various time points including 3, and 7 days and 6 months of shRNA activation. Mice were always harvested 4 hours post the final treatment. Experimental mice used were all homozygous for both the *rtTA3* and *shNUAK1* alleles, controls were littermates that were wildtype for either allele.

### **2.1.3.5 Villin-CreER<sup>T2</sup>;Apc<sup>fl/+</sup>;DI-shNUAK1 mice experiments:**

To induce allele recombination, transient activation of *CreER<sup>T2</sup>* in the intestine was performed on mice by one IP injection of 80mg/kg tamoxifen. Experimental mice used were always heterozygous for the floxed *Apc* allele and included both heterozygous and homozygous genotypes for the *rtTA3* and shRNA alleles. Where indicated, 1.75 or 2.0% dextran sodium sulphate (DSS), m.w. 35k-50kDa (M.P. Biochemicals 0216011090/Sigma 42867) was administered in drinking water for five days, commencing four days post allele induction, followed by sterile water for one week, then tap water. Doxycycline was administered as above by oral gavage in 2mg daily boluses, from day 64 to day 70 post-induction. N-Acetyl-Cysteine or NAC (Sigma; 4% w/v) was administered in drinking water, starting three days before shRNA induction, and replaced every 3-4 days until sacrifice. The Licor ROSstar<sup>TM</sup> 800cW probe, a near-infrared hydrocyanine probe for imaging of extracellular ROS, was injected, via tail vein injection, 16 hours prior to harvest. Mice were then harvested, and the colon dissected and imaged using a Pearl Trilogy Small Animal Imaging System.

## ***2.1.4 Tissue preparation and scoring***

### **2.1.4.1 Tumour enumeration**

Small intestines and colons were flushed with PBS, cut open longitudinally in 10cm sections and tumours scored visually from fresh tissue. Tumour area was measured as width by length, omitting depth as negligible/immeasurable in many instances and the location of each tumour was noted.

### **2.1.4.2 Flash-frozen fresh tissue**

Prior to fixation and immediately upon harvest, a small number of representative tumours and adjacent normal tissue were dissected and flash-frozen in liquid nitrogen for RNA analysis or for visualization of fluorescence.

### **2.1.4.3 Tissue processing and sectioning**

Tissues were mounted 'en face' and fixed overnight in formalin at room temperature (RT). After this period, fixed tissue was rolled ('swiss roll method') and dehydrated in 70% Et OH. The tissues were then further processed by the BICR histology team using an automated processor (Thermo Scientific Excelsior ES). Finally tissues were embedded in paraffin and then cut into 4 $\mu$ M sections using a microtome. Sections were placed on poly-L-Lysine (PLL) coated slides and incubated at 58°C for 24 hours.

## ***2.1.5 Tissue stains and immunohistochemistry***

Formalin fixed paraffin embedded (FFPE) tissue sections were deparaffinized in 3 changes of xylene (5 mins each) and rehydrated in graded ethanol solutions (100%, 100%, 95%, 95%, 70%, 70%; 2 mins each). Sections were then incubated in dH<sub>2</sub>O in preparation for immunohistochemistry (IHC) or cell specific staining.

### **2.1.5.1 Hematoxylin and Eosin (H&E) staining**

The properties of H&E staining make it possible to visualize any morphological changes in tissue sections both at the level of tissue and cells. Hematoxylin is used to stain cell nuclei and Eosin to stain cell cytoplasm. Sections were stained with Gli1Haematoxyline (Sigma) for 13 mins, washed in running tap water for 5 mins, dipped 20 times in differentiation solution (Sigma), washed again for 30 secs, dipped 20 times in Scotts tap water substitute

(MgSO<sub>4</sub>+ sodium bicarbonate), washed for 30 secs, stained with 1% Eosin for 5 mins, and finally washed again for 2 mins. Slides were then dehydrated, incubated with xylene for 2x 5 mins and mounted.

### **2.1.5.2 Alcian blue/PAS staining**

Together, Alcian blue/Pas staining differentiates between neutral and acidic proteoglycans such as mucins. Alcian blue stains the acidic mucins present in the tissue a blue colour while PAS (periodic acid Schiff) is then used to stain basement membranes, glycogen and neutral mucins pink. In this study Alcian blue/PAS staining was used to identify goblet cells in the intestine. Sections were stained with Alcian blue solution (1% alcian blue in 3% acetic acid) for 30 mins, washed in running tap water, incubated with periodic acid for 10 mins, washed, incubated with Schiffs reagent for 20 mins and washed and dehydrated as before. Slides were then dehydrated, incubated with xylene for 2x 5 mins and mounted.

### **2.1.5.3 Immunohistochemistry**

IHC was used to visualise the distribution and localisation of specific proteins. FFPE tissues were sectioned, de-waxed and dehydrated as discussed in Section 2.1.5. Antigen retrieval was performed by microwaving the sections in 10mM Sodium Citrate, pH 6.0, at full power for 10 mins. Endogenous peroxidases were quenched in 3% H<sub>2</sub>O<sub>2</sub> for 15 mins, washed in dH<sub>2</sub>O and non-specific binding was blocked with 1 or 3% BSA solution. Sections were then incubated with the primary antibody (diluted in blocking solution) at an optimized concentration and duration (Table 2.1) and then washed 3x 5 mins in PBS or TBST before being incubated with the appropriate secondary antibody conjugated with HRP for 30-60 mins in blocking solution. The sections were then washed in PBS or TBST (3x 5 mins) and a signal amplification step was performed using the Vectastain Avidin-Biotin Complex (ABC) kit (Vector labs). This involved incubation with the A/B reagent (1:100 in PBS) for 30 mins and a further wash. In order to visualise the signal, sections were then incubated with 3,3'-diaminobenzidine (DAB) reagent until adequate staining was achieved. Excess DAB was removed and the slides washed with dH<sub>2</sub>O. For counterstaining, the sections were dipped in hematoxylin 5 times, washed in running tap water for 5 mins, dipped 20 times in differentiation solution, washed for 30 secs, dipped 20 times in Scotts tap water substitute and washed for 30 secs. The sections were then dehydrated with an alcohol gradient as above (70%, 70%, 95%, 95%, 100%, 100% EtOH

for 2 mins each) and then cleared in xylene (2x 5 mins). Sections were then mounted and sealed.

For manual quantification of IHC, used only in Chapter 4, Section 4.2.1: 50 crypt/villi sections were scored on representative sections from at least 3 mice of each genotype. Quantification was performed by undergraduate student Silvija Svambaryte.

For automatic quantification of IHC, HALO image analysis software (Indica Labs) was used. Only tumour regions were scored and comparisons made between control and experimental tumours.

Table 2. 1 - Immunohistochemistry (IHC) antibodies and conditions

Primary Antibody	Code/Clone	Supplier	Retrieval	Primary antibody dilution	Secondary antibody
Caspase 3 ASP-175	9661	Cell Signalling	Sodium Citrate pH6, water bath @ 98°C, 25 mins	1/50 @ RT, 35 mins	Rabbit Envision @ RT, 35 mins
Lysosome	A099	Dako	Proteinase K, 10 mins	1/1000 @ RT, 35 mins	Rabbit Envision @ RT, 35 mins
8-oxo-dG	AB10802	Abcam	TRIS-EDTA-Tween buffer pH9	1/50 @ 4°C, O.N.	Mouse Envision+ system @ RT, 30 mins
NUAK1	NUAK1 T211-1613187-KLH-GLUTA UNMODIFIED PEPTIDE	Eurogentec	Sodium Citrate pH6, microwave method, 10 mins	1/1000 @ 4°C, O.N.	Vector Labs, Anti-rabbit (1:1000) @ RT, 1hr
Phospho-ERK	sc-7383	Santa Cruz	Sodium Citrate pH6, microwave method, 10 mins	1/5000 @ 4°C, O.N.	Vector Labs, Anti-rabbit (1:1000) @ RT, 1hr
B-Catenin	610154	BD Biosciences	Sodium Citrate pH6, microwave method, 10 mins	1/50 @ RT, 2 hours	Mouse Envision+ system @ RT, 1hr
BrdU	MCA2060P	AbD Serotec	Sodium Citrate pH6, water bath @ 98°C, 25 mins	1/200 @ RT, 35 mins	Mouse Envision+ system @ RT, 30 mins

#### 2.1.5.4 TUNEL staining

TUNEL staining was performed on paraffin-embedded sections using the ApopTag peroxidase labeling kit (Millipore; S7100). The kit labels apoptotic cells by modifying DNA fragments using terminal deoxynucleotidyl transferase (TdT) for the detection of apoptotic cells. Digoxigenin-conjugated nucleotides are enzymatically added to free 3'OH DNA termini by TdT in a template free manner. The incorporated nucleotides form

an oligomer composed of digoxigenin-conjugated nucleotides. DNA fragments labelled with the digoxigenin-nucleotide are then allowed to bind an anti-digoxigenin antibody that is conjugated to a peroxidase reporter molecule. Signal was detected using DAB as a substrate as previously. Protocol was carried out according to manufacturers instructions and an additional blocking step (1% BSA for 1 hour at room temperature) was incorporated prior to the addition of peroxidase-conjugated anti-digoxigenin. Tissues were counterstained as described previously.

### **2.1.5.5 BrdU incorporation**

BrdU is incorporated into replicating DNA and can be detected using anti-BrdU antibodies using conditions shown above. Animals were injected with BrdU (Sigma) at a concentration of 100mg/kg and harvested at least 2 hours later. Tissues were fixed and processed as above and BrdU IHC performed to visualize BrdU incorporated cells (Table 2.1).

## **2.2 Crypt culture**

### **2.2.1 Organoid/spheroid preparation**

Primary organoid cultures of intestinal crypts were established as previously described (Sato et al., 2009) from the small intestine and colon of *Villin-CreER<sup>T2</sup>;Apc<sup>fl/fl</sup>;LSL-KRas<sup>G12D/+</sup>*, *Villin-CreER<sup>T2</sup>;Apc<sup>fl/fl</sup>;LSL-KRas<sup>G12D/+</sup>;Nuak1<sup>fl/fl</sup>*, *Vil-CreER<sup>T2</sup>;Apc<sup>fl/fl</sup>;LSL-KRas<sup>G12D/+</sup>;DI-shNUAK1* mice and from the small intestine of wildtype mice. Cultures from tumour models will be referred to as spheroids due to their spherical shape and deficiency in cell differentiation. This distinguishes them from wildtype organoids.

Adult mice were induced with one IP injection of tamoxifen at 80mg/kg and tissues harvested four days later. Intestines were flushed with ice-cold PBS, opened longitudinally and villi were removed using a glass coverslip. Intestines were incubated in EDTA/PBS (2mM for SI; 25mM for colon) for 30 min at 4°C. Excess solution was discarded and loose intestine fragments were collected by manual trituration in 3x PBS washes. The crypt-enriched fractions were passed through a 70µM cell strainer and pelleted at 600rpm for 2 min in a tabletop centrifuge. Re-suspended crypts were counted by haemocytometer, then seeded in Matrigel (BD Bioscience) with Advanced DMEM/F12 media (Invitrogen), supplemented with 10mM HEPES, 2mM Glutamine, 0.1% FBS, Pen/Strep, 1% N-2 & 2% B-27 supplements (1X, Invitrogen).

Alternatively, for quantification of primary spheroid formation, isolated crypts were further incubated in Cell Dissociation solution (Thermo; 5-15 mins) until a single cell suspension was achieved. Cells were then counted and seeded at normalised density as above.

Growth factors Noggin (100ng/ml; Peprotech) and EGF (50ng/ml; Peprotech) were added to primary cultures but removed from subsequent passages.

Wildtype organoid cultures were prepared using the same protocol but additionally supplemented with R-Spondin (500ng/ml; R&D systems) and all growth factors were re-added every 2-3 days in order to sustain cultures

### ***2.2.2 Passaging spheroids/organoids in culture***

Established crypt cultures were split 1-2 times per week by manual disruption followed by incubation in Cell Dissociation solution (Thermo) until a single cell suspension was achieved (5-15 mins). Cells were diluted 1:5 and re-suspended in matrigel. Wildtype organoids required addition of growth factors every 2-3 days.

### ***2.2.3 Cryopreservation of spheroids/organoids***

Established crypt cultures were disrupted manually and pelleted by centrifugation in a tabletop centrifuge for 3 mins, this was then repeated to disrupt the spheres further. The cells were then re-suspended in 500µl Advanced DMEM/F12 media, supplemented with 10mM HEPES, 2mM Glutamine, 0.1% FBS, Pen/Strep, 1% N-2 & 2% B-27 supplements plus 10µl R-spondin, 10µl Noggin and 25µl EGF growth factors and incubated for 30 mins at 37°C in 1ml cryovials. DMSO was then added to a final concentration of 10% and the vials transferred to a freezing container (Mr.Frosty™) to be stored at -80°C. The cells were moved to liquid nitrogen cold storage for long-term storage.

### ***2.2.4 Thawing spheroids/organoids***

Organoids/spheroids were thawed in a 37°C waterbath and then transferred to warm Advanced DMEM/F12 media supplemented as above. The cells were mixed and then pelleted by centrifugation at 1200rpm for 5 mins. The cells were then re-suspended in matrigel and plated. Transformed cells were fed EGF and Noggin after thawing for a

couple of passages until robust, wildtype cells also required R-spondin (all concentrations as above).

### **2.2.5 Quantification of spheroids**

The total number of spheroids was counted manually every 24 hours at 4x objective. In each experiment technical triplicates were used and each experiment was performed in biological triplicates using spheroids isolated from 3 independent animals unless otherwise stated.

### **2.2.6 Treatments**

NUAK1 inhibitors, HTH-01-015 (Apex Biotech) or WZ4003 (Medchem Express) in DMSO, were added to single cell suspensions at the indicated concentrations. Trolox [(±)-6-Hydroxy-2,5,7,8-tetramethylchromane-2-carboxylic acid] (Sigma) was added to single cell suspensions at a final concentration of 500µM for 16 hours prior to HTH-01-015 and replenished daily for three days. Doxycycline (Sigma) was added to single cell suspensions at various final concentrations (0.1, 0.5 & 1.0µg/ml) for 24 hours minimum. Other time points specified.

### **2.2.7 Cre recombination in vitro**

*Ad-Cre* (*Cre Recombinase Adenovirus*) was used to recombine the floxed alleles in *Villin-CreER<sup>T2</sup>;Apc<sup>fl/fl</sup>;Kras<sup>G12D/+</sup>;DI-shNUAK1.1533* spheroids in culture. Formed spheroids were incubated for 6hours with the virus (Uni. Iowa; MOI 300) and Polybrene (4mg/ml; Sigma).

### **2.2.8 ROS detection**

Reactive Oxygen species (ROS) detection was performed on live spheroids by confocal fluorescent microscopy with 5µM CellRox green (3 hours @ 37°C; Thermo) after overnight treatment of pre-formed spheroids with HTH-01-015. Quantification was performed using ImageJ to calculate the corrected total cell fluorescence (CTCF) = integrated density – (area of selected cell\*mean fluorescence of background).

### **2.2.9 Cell Viability**

Cell viability was measured using the CellTiter-Blue® Cell Viability Assay (Promega). The assay measures the ability of viable cells to reduce resazurin dye (7-hydroxy-3H-phenoxazin-3-one-10-oxide) into resorufin. It is believed that mitochondrial enzymes are responsible for the transference of electrons from NADPH + H<sup>+</sup> to resazurin to form resoflurin (O'Brien et al, 2000). The level of reduction can be quantified by spectrophotometer as resazurin has an absorption peak at 600nm and resoflurin at 570nm wavelengths. Resazurin was added directly to organoids/spheroids at 20µl reagent per 100µl media and incubated for 6 hours, after which the fluorescence could be measured using a Tecan Safire fluorometer.

## **2.3 Cell culture**

U2OS, HCT-116, SW620, LS174T and SW480 cells were obtained from the ATCC and maintained in DMEM (Invitrogen; 25mM Glucose) supplemented with 1% glutamine, Penicillin (50,000units), Streptomycin (50,000µg) and 10% FBS (full culture media). All cells were cultured at 37°C at 5% CO<sub>2</sub>. All cell lines were validated using an approved in-house validation service (CRUK-BICR) and tested periodically for mycoplasma.

### **2.3.1 Passaging cells in culture**

Confluent cells were passaged using standard techniques. Media was removed and cells washed with PBS, cells were then incubated with 10% trypsin (1ml for 10cm dish) for 5-15 mins at 37°C. Once cells were detached, trypsin was neutralised with full culture media and then cells split into the desired dilution factor. Alternatively, to seed a specific number of cells, cells were counted using an automated cell counter and seeded accordingly. Cell cultures were refreshed every 3-4 months.

### **2.3.2 Cryopreservation of cell lines**

Cells were trypsinised as above until detached and then re-suspended in full culture media. Cells were then pelleted by centrifugation at 1000rpm for 3mins, trypsin and media removed and then suspended in freezing media (90% FBS; 10% DMSO) and transferred to 1ml cryovials. These were then stored at -80°C in an Mr.Frosty and transferred to liquid nitrogen stores for long-term storage after 24 hours.

### **2.3.3 Thawing cells in culture**

Cells were thawed quickly at 37°C and then suspended in full culture medium and transferred to a 10cm culture dish. Medium was changed 24 hours later and culture established.

### **2.3.4 Mouse Embryonic Fibroblast culture**

Primary mouse embryonic fibroblasts (MEFs) were isolated from embryos at E13.5. The uterine horn was removed from the pregnant female and each embryo removed from the amniotic sac and placed in an individual dish. The embryo was then decapitated and the liver tissue removed. A small portion of the tissue from the head was sent to Transnetyx (USA) for genotyping. The embryo was then minced using a scalpel and suspended in 1ml sterile PBS, mixed and transferred to a 15ml falcon. 1ml of trypsin (1x) was then added to the embryo and incubated for 15 mins, with mixing every 5 mins. Trypsin was neutralized by adding (up to) 10mls full culture medium, then the solution was moved to a 10cm culture dish. Medium was changed after 24 hours. MEFs were cultured using the standard 3T3 protocol;  $1.3 \times 10^6$  cells were passaged every 3 days and cells were not passaged past P5.

NUAK1 depleted MEFs were generated by interbreeding Zp3 positive, heterozygous rtTA3; shNuak1 mice, generating a variety of genotypes including those shown in Figure 13D. To induce the shNuak1 alleles, MEFs were treated with Doxycycline (Sigma; 1µg/ml) for 72 hours. Fluorescence was then observed and cells harvested.

### **2.3.5 Drug treatments**

Cells were treated with the indicated concentrations of NUAK1 inhibitors (HTH-01-015 and WZ4003). Hydrogen peroxide (H<sub>2</sub>O<sub>2</sub>) solution [30 % (w/w) in H<sub>2</sub>O, stock solution], containing stabilizer (Sigma) was used at 500µM or 1mM for 30 mins to induce ROS response. Cells were pre-incubated with 500µM of Trolox for 8 hours prior to treatment with Nuak1 inhibitor. Equivalent volumes of DMSO were used as vehicle controls. Cells were incubated with GSK3β inhibitors BIO-acetoxime (Tochris; 1µM) or CHIR99021 (Tochris; 5µM) for 6 hours prior to H<sub>2</sub>O<sub>2</sub> treatment.

### **2.3.6 Transfection**

Cells were seeded at the following seeding densities: U2OS  $1 \times 10^6$ , SW480  $1.5 \times 10^6$ , SW620  $3 \times 10^6$ , HCT116 and LS174T  $2 \times 10^6$  in a 10cm plate and transfected the following day. Cells were transfected with the following siRNAs: siNUAK1 #1 (40 $\mu$ M; Hs\_ARK5\_1) and siNUAK1 #2 (20  $\mu$ M; Hs\_ARK5\_3) specific for NUAK1 using Opti-MEM medium and transfection agent, Lipfectamine iMAX (Qiagen) according to manufacturers directions. Cells were incubated with transfection mix, in antibiotic free DMEM supplemented with 1% glutamine and 10% serum only, overnight and then medium was changed to full culture medium. A scrambled control (referred to as siCon) was used in all experiments. All siRNAs were purchased from Qiagen.

### **2.3.7 ROS detection**

ROS were measured after 8 hours NUAK1 inhibition with 10 $\mu$ M HTH-01-015 using CellROX deep-red reagent (Thermo) according to the manufacturers directions, followed by FACS analysis. Cells were seeded at the following concentrations in a 6-well plate; U2OS and SW480  $8 \times 10^4$ , SW620  $1.6 \times 10^5$ , HCT116 and LS174T  $1.2 \times 10^5$ . Cells were treated with inhibitor 16 hours later, Cell ROX reagent was added to a final concentration of 5 $\mu$ M 10 mins before the measurement and incubated in dark at 37°C. The cells were then washed with PBS and trypsinised until cells were successfully detached. Trypsin was neutralised by 1% FCS, cells transferred to a FACs tube and pelleted by centrifugation at 300g for 5 mins. The pellet was then resuspended in PBS and analysed for fluorescence (Ex: 644nm, Em: 665nm) using the FACs Calibur. Background was corrected using unstained samples and 10,000 events were counted for each sample in technical triplicate, each experiment was performed at least three times for each cell line.

ROS experiments were performed by Dr. Nathiya Muthalagu.

### **2.3.8 Annexin V/PI staining**

Annexin V/PI staining was used to measure apoptosis. Cells were seeded at the following concentrations in a 6-well plate; U2OS and SW480  $8 \times 10^4$ , SW620  $1.6 \times 10^5$ , HCT116 and LS174T  $1.2 \times 10^5$  cells/well. After treatment incubation, cells were trypsinised until detached, quenched with 1% FCS, transferred to FACs tube with original supernatant, and centrifuged at 300 x G for 5 mins to pellet all cells. Annexin binding buffer (200 $\mu$ l; 10mM HEPES PH 7.40, 140mM NaCl, 2.5mM CaCl<sub>2</sub>) and Annexin V-APC (2 $\mu$ l, Biolegend

640920) were added to the pellet and incubated for 15 mins in the dark. Propidium iodide (PI, 10 $\mu$ g/ml) was added immediately prior to FACS analysis. FACS Calibur was used for analysis, Annexin V-APC was excited at 633nm and PI has excitation/emission maxima of 493/636 nm. As above, background was corrected using unstained samples and 10,000 events were counted for each sample in technical triplicate, each experiment was performed at least three times for each cell line.

## **2.3.9 Protein isolation and Immunoblotting**

### **2.3.9.1 Protein isolation**

Cells were seeded as following; U2OS 1x10<sup>6</sup>, SW480 1.5x10<sup>6</sup>, SW620 3x10<sup>6</sup>, HCT116 and LS174T 2x10<sup>6</sup> in a 10cm plate and treated according to the respective experimental set up. Cells were washed with ice-cold PBS and whole cell lysates were prepared in RIPA buffer (150mM NaCl, 50mM Tris, pH 7.5, 1% NP-40, 0.5% sodium deoxycholic acid, 1% SDS, plus complete protease and phosphatase inhibitor cocktails [Roche]) followed by sonication (40% Amp for 10 secs) and then incubated on ice for 15 mins.

Cytoplasmic and Nuclear fractions were prepared in low salt buffer (20mM KCL, 10mM HEPES, pH 7.5, 1mM MgCl<sub>2</sub>, 1mM CaCl<sub>2</sub>, 0.1% Triton X-100) followed by centrifugation at 3300 rpm for 3 mins. Cytoplasmic supernatant was removed and the nuclear pellet was re-suspended in RIPA buffer and incubated for 15 mins on ice. Separation was followed by sonication of both fractions as above.

### **2.3.9.2 Protein quantification**

Protein quantification was performed using the Bicinchoninic acid (BCA) method with the Pierce BCA protein assay kit in a clear 96-well plate. Protein samples were measured in duplicate in PBS at a 1:50 dilution. Bovine serum albumin (BSA; Sigma) was used as a standard and diluted from stock in PBS to generate a concentration range of 5-25 $\mu$ g/ml. Lysis buffer was added to the standard at 1:50 dilution to account for background effect. BCA reagents were prepared according to manufacturer's instructions and added to each sample. Following a 1 hour incubation at 37°C the absorbance of each sample was read using a spectrometer at 562nm. The concentration of each sample was calculated using the standard curve.

### 2.3.9.3 Sample preparation and SDS-PAGE

Samples (50µg) were denatured with 5X Laemlli buffer (30mM Tris [pH 6.8], 50% glycerol, 10% SDS, 4% β-mercapthoethanol, 0.5% Bromophenol blue) to a final concentration of 1X and heating for 5 mins at 95°C.

The samples were then resolved by SDS-PAGE, using polyacrylamide gels of varying acrylamide percentage (Table 2.2), and 1X SDS PAGE running buffer (1% SDS, 25mM Tris, 0.192M Glycine). A PageRuler Prestained Protein Ladder (Thermo) was used and the gels were run at 100V continuously until sufficient separation had occurred.

**Table 2. 2 - Acrylamide gel composition**

	Separating gel			Stacking gel
	8.50%	10%	12.50%	
Acrylamide	4.3ml	5.1ml	6.35ml	650µl
Tris 1M pH8.9	5.6ml	5.6ml	5.6ml	-
Tris 1M pH6.8	-	-	-	600µl
Water	5.0ml	4.2ml	2.95ml	3.6ml
SDS 10%	150µl	150µl	150µl	50µl
APS 20%	75µl	75µl	75µl	25µl
TEMED	15µl	15µl	15µl	5µl

### 2.3.9.4 Immunoblotting

Proteins were then transferred to nitrocellulose membrane (Protran) using the Hoefer transfer module (TE22) as per manufacturer's instructions with transfer buffer (0.1% SDS, 25mM Tris, 0.192M Glycine, 20% methanol). Transfer was ran at 230mA for 2hours at 4°C. To visualize proteins, the membrane was incubated in Ponceau S solution (0.1% Ponceau S in 5% acetic acid). The membrane was then washed in 1X TBST (20mM Tris, 0.137M Sodium Chloride, 0.1% Tween20, pH7.5), and incubated in 5% milk (Marvel Milk Powder) in 1X TBST for 30mins. Following this, the membrane was incubated in primary antibody in 5% BSA in 1X TBST overnight at 4°C.

Primary antibodies used: NUA1 (CST 4458, 1:750); NRF2 (Novus NB100-80011, 1:1000); pMYPT1 Ser-445 (MRC S5087, 1:400); MYPT1 (BD 612164, 1:1000); β-ACTIN (Sigma A5441, 1:5000); LAMIN A/C (Santa Cruz 6215, 1:5000); pAKT Ser-473 (Cell Signaling 4060S, 1:500), pAKT Thr-308 (Cell Signaling 13038, 1:500), pan AKT (Cell Signaling 4685S, 1:1000), pGSK3β Ser-9 (Cell Signaling 9322s, 1:1000), GSK3β

(Cell Signaling 9832S, 1:10,000), MYC (Abcam, ab32072, 1:1000); NUA2 (MRC PPU S225B, 1:1000) and  $\beta$ -CATENIN (BD Biosciences, 1:1000).

The next day, the membrane was washed 3x with 1X TBST and incubated with the appropriate HRP-conjugated secondary antibody ( $\alpha$ -mouse IgG NA931V;  $\alpha$ -rabbit NA934V, both GE Healthcare;  $\alpha$ -goat IgG, Vector Labs PI-9500, 1:5000) in 5% milk in 1X TBST for 1 hour at room temperature. After washing, the protein signal was detected by chemiluminescence (Pierce ECL western blotting substrate 32106) using X-ray films (Fuji film super RX) and developed with an automated X-ray processor (AGFA, Classic EOS).

### **2.3.10 Immunoprecipitation**

For immunoprecipitations (IPs),  $2.5 \times 10^6$  cells were seeded per 15cm dish. The next day, 5  $\mu$ g of NUA1-Flag or empty vector was transfected using Lipofectamine 3000 reagent (1:1.8 ratio for Lipofectamine, 1:2 for p3000 reagent). Forty eight hours post transfection, cells were trypsinized and  $5 \times 10^6$  cells were seeded per 15cm dish. The following day, cells were washed with ice cold PBS and scraped in 400  $\mu$ l of NP-40 lysis buffer (150mM NaCl, 50mM Tris Ph7.5, 1mM EDTA, 1mM EGTA, 1% NP-40, plus complete protease and phosphatase inhibitor cocktail). Lysates were incubated on ice for 10min and centrifuged at 12,000 rpm for 10 mins and the supernatant was used for IP. 1.5mg of total protein was used per condition. Lysates were incubated with Flag-M2 resin (20  $\mu$ l /  $\mu$ g of protein) overnight. Beads were pelleted at 3000rpm/5 minutes and washed 3X with the lysis buffer (3000 rpm/5mins/4°C). IP'ed proteins were eluted in 60  $\mu$ l of 1x Laemlli buffer.

### **2.3.11 Dimedone detection of cysteine oxidation**

USOS cells transiently overexpressing FLAG-tagged NUA1 were treated with H<sub>2</sub>O<sub>2</sub> for 5 minutes, then lysed in RIPA buffer containing 1mM dimedone (Sigma, D153303) followed by  $\alpha$ -FLAG IP. Dimedone incorporation was detected using  $\alpha$ -dimedone antibody (Millipore, 07-2139).

### **2.3.12 Iodoacetamide labelling**

Iodo-acetamide labelling was performed similarly by addition of 55mM labelled (<sup>13</sup>C<sub>2</sub>D<sub>2</sub>H<sub>2</sub>INO; Sigma-Aldrich/ Merck KGaA, 721328) or unlabelled (C<sub>2</sub>H<sub>4</sub>INO; Sigma-Aldrich/ Merck KGaA, I6125) iodoacetamide in RIPA buffer, followed by anti-FLAG IP. IPs were washed twice in lysis buffer, followed by H<sub>2</sub>O, prior to combining H<sub>2</sub>O<sub>2</sub> treated and untreated samples for mass spectrometry analysis (explained in detail in Section 2.7.3).

Label incorporation was normalized to the level of IP'ed NUAk1, measured by immunoblotting of 10% of each IP.

### **2.3.13 RNA isolation and analysis**

#### **2.3.13.1 RNA isolation**

Snap-frozen intestinal epithelial tissue or human cells were homogenized and RNA was isolated using TRIZOL (Invitrogen). Transfected cells were seeded as following; U2OS  $0.5 \times 10^6$ , SW480  $0.5 \times 10^6$ , SW620  $1 \times 10^6$ , HCT116 and LS174T  $0.75 \times 10^6$  in a 6cm plate. The following day, cells were washed once with ice-cold PBS and harvested in 1ml Trizol, mixed gently with 200 $\mu$ l Chloroform (Sigma) and then centrifuged at 14,000RPM for 15mins at 4°C. RNA isolation from tissue followed the same protocol with an additional centrifugation step of 14,000RPM for 10mins at 4°C prior to adding chloroform. The aqueous upper phase was then transferred to a new vial and incubated with an equal volume of isopropanol for 20mins on ice. The samples were then centrifuged at 14,000RPM for 15mins at 4°C and the supernatant aspirated to expose the RNA pellet. The pellet was washed twice with 70% Ethanol with a centrifugation step, 8000RPM for 5mins. The pellet was air-dried and then suspended in Nuclease free H<sub>2</sub>O (Thermo) and incubated for 10mins at 56°C.

#### **2.3.13.2 cDNA synthesis**

RNA quantity and quality was measured using Nanodrop (Thermo Scientific) and 100-500ng of RNA was used to synthesize cDNA using the Quantitect reverse transcription kit (Qiagen 205313). Firstly, genomic DNA contamination was removed in each sample by incubation with gDNA wipeout buffer for 2mins at 42°C. Following this, the RNA samples were incubated with reverse transcription reaction components including Quantiscript Reverse Transcriptase, Quantiscript RT buffer and RT primer mix for 15 mins at 42°C, then 3 mins at 95°C in order to synthesize cDNA.

#### **2.3.13.3 Primer design**

Intron-spanning primers were designed using Universal Probe Library Assay Design Centre (Roche). The following primer sets were used to detect indicated mRNA transcripts:

### ***Human***

GCLC F: 5'atgcatgggatttggaaat; R: 5'gatcataaagggtatctggcctca  
GCLM F: 5'gttgaacagctgtatcagtgg; R: 5'gttgaacagctgtatcagtgg  
GSHR F: 5'atgacagcaccactgcac; R: 5'ctccaagcccgacaaagt  
MGST F: 5'accacaccattgcatatttgac; R: 5'gcatggaaagagtaactcca  
TXN F: 5'ttacagccgctcgtcaga; R: 5'ggcttctgaaaagcagtctt  
β-ACTIN F, 5'ccaaccgcgagaagatga; R: 5'ccagaggcgtacagggatag  
NUAK1 F: 5'acatgatctcaatctctcgtctg; R: 5'acctacggcaaagtcaagc

### ***Mouse***

Gclc L: 5'agatgatagaacacgggaggag; R: 5'tgacctaagcgattgttcttc  
Gclm L: 5'tgactcacaatgacccgaaa; R: 5'tcaatgtcagggatgctttct  
Gshr L: 5'ctatgacaacatccctactgtggt; R: 5'cccatacttatgaacagcttctg  
Mgst L: 5'gcccttctccctggattc; R: 5'ggccatcaacacctcattgt  
Txn L: 5'tgaagctgatcgagagcaag; R: 5'agaagtccaccacgacaagc  
B2m F: 5'agccgaacatactgaactgctacg; R: 5'cggccatactgtcatgcttaactc  
Nuak1 F: 5'gagccacacaacctca; R: 5'tctgcatcgggattcac

#### **2.3.13.4 Realtime qPCR**

Realtime qPCR was performed using the SYBR Green method (VWR QUNT95072) as per manufacturer's instructions. 200µM primers were used with 0.5µl cDNA per 10µl reaction. The following cycling conditions were used: 95°C for 5 mins, 95°C for 30 secs, 60°C for 20 secs, go to step 2x 35 cycles, 72°C for 10 mins, 65°C for 10 secs, 95°C for 30 secs.

## **2.4 NUAK1 shRNA gene expression analysis**

U2OS cells were depleted of Nuak1 by shRNA-4977 as previously described (Liu et al., 2012) and selected on puromycin for 48 hours. Control cells were similarly selected after infection with non-targeting shRNA expressing retrovirus. 24 hours after re-seeding in the absence of selection, total RNA was isolated using the RNEasy Mini Kit (Qiagen) according to manufacturer's instructions and DNA was depleted with the RNase-Free DNase Set (Qiagen). RNA-integrity was checked using the RNA ScreenTape assay (Agilent Technologies) and cDNA was synthesized with the TruSeq Stranded mRNA Library Prep Kit (Illumina). Following library quantification (D1000 ScreenTape, Agilent

Technologies), libraries were standardized to 10nM, denatured, diluted to 10pM and analyzed by paired-end sequencing using an Illumina NextSeq500 platform. RNA-Sequencing reads were aligned to the GRCh37 version of the human genome and differential expression determined using DESeq2 (Love et al., 2014). Pathway modulation analysis was performed using Metacore GeneGO (Thompson Reuters).

The NUAK1 shRNA gene expression analysis was performed by Dr. Nathiya Muthalagu.

## 2.5 Human TMA analysis

A human CRC tissue micro-array comprising 650 tissue cores was stained for *NUAK1* mRNA expression by RNA-Scope (as described above) and scored blindly using HALO image analysis software (Indicalab). The tissue microarray contained primary colorectal cancer (Dukes A = 53, Dukes B = 104, Dukes C = 111), lymph node metastasis (from corresponding Dukes C cases = 111) and normal colonic mucosal samples (52). An exclusion criteria was adhered to and included partial or over-stained samples as well as samples in which less than 1% of cells were positive for PP1B RNA. Based on this, 47 samples were omitted. Results were subdivided into equal quartiles from low to high NUAK1 expression and P values were determined by Chi-Square test according to patient clinico-pathological data including age, gender, site of primary tumour, degree of tumour differentiation and tumour stage.

This work was done in collaboration with Professor Graeme Murray, Department of Pathology, University of Aberdeen.

## 2.6 *In situ* hybridization (RNA Scope)

*In situ* hybridization (RNA-Scope) was performed according to the manufacturers directions (Advanced Cell Diagnostics; ACD) by the Histology Team at the Beatson Institute for Cancer Research. 4µm FFPE tissue sections were incubated at 60°C for 1 hour, then de-paraffinized and rehydrated. Endogenous peroxidases were blocked in H<sub>2</sub>O<sub>2</sub>, followed by antigen retrieval (100°C for 8 mins.) and protease digestion (H<sub>2</sub>O<sub>2</sub> & Protease Plus kit, ACD). Sections were hybridized with ACD-designed probes for human NUAK1 (458101), mouse Nuak1 (434281), positive ctrl PP1β (313911) or negative ctrl DapB (322330) for 2 hours at 40°C. Probe detection was performed using RNA-Scope kit reagents (ACD 322310) and counterstained with Hematoxylin.

For quantification of ISH from mouse tissue, HALO image analysis software (Indica Labs) was used. Only tumour regions were scored and comparisons made between control and experimental tumours.

This work was done with Masters student, Amy Bryson.

## **2.7 Proteomic analysis**

### **2.7.1 SILAC labelling**

U2OS cells were cultured in light ( $^{12}\text{C}_{61}^4\text{N}_4$  L-arginine and  $^{12}\text{C}_{61}^4\text{N}_2$  L-lysine, Sigma) and heavy ( $^{13}\text{C}_{61}^5\text{N}_4$  L-arginine and  $^{13}\text{C}_{61}^5\text{N}_2$  L-lysine, Cambridge Isotope Laboratories) SILAC medium (SILAC DMEM, Life Technologies) supplemented with 10 kDa dialysed serum (Sigma) until full labeling (>98%) of the proteome was reached. For “forward analysis” heavy labeled cells were treated for 1 hour with 10  $\mu\text{M}$  HTH-01-015, and light labeled cells were vehicle treated. Cells were then harvested and lysates mixed in equal amounts. For the reverse replicate experiment, light labeled cells were treated for 1 hour with 10 $\mu\text{M}$  HTH-01-015, and heavy labeled cells were vehicle treated.

### **2.7.2 Sample Preparation**

1.5mg of each cell lysate from light and heavy SILAC labeled cells were mixed 1:1, light Ctl : heavy HTH in the forward experiment and light HTH and heavy Ctl in the reverse experiment. Proteins were precipitated overnight at  $-20^\circ\text{C}$  in acetone, re-dissolved in 8M Urea, 0.1M TrisHCl pH 8.5 buffer with phosphatase inhibitors (Halt phosphatase cocktail, Thermo Scientific) and digested with Lys-C (Alpha Laboratories) and Trypsin (Promega) using Filter-Aided Sample Preparation (FASP) (Wiśniewski et al., 2009). To remove salts, peptides were loaded onto C18 Sep-Pak column (Waters) and eluted with increasing concentration of acetonitrile (ACN, 10%, 15%, 20%, 25%, 30%, 40%, 60%) in 0.1% trifluoroacetic acid. ACN was removed using a speed vacuum centrifuge and peptides were resuspended in MOPS 50 mM, sodium phosphate 10 mM, sodium chloride 50 mM pH 7.2. Fresh ACN was added to 30% final concentration and TFA to pH down to 2.5. The enrichment for phosphorylated peptides was performed incubating the peptide solution with  $\text{TiO}_2$  beads, 5:1, peptide: $\text{TiO}_2$ , as previously described (van den Biggelaar et al., 2014). Four subsequent incubations with  $\text{TiO}_2$  were performed. Peptides were eluted from the  $\text{TiO}_2$  beads using a solution 15% ammonium hydroxide 40% ACN and loaded onto a

C18 StageTip (Rappsilber et al., 2007). Peptides were eluted from StageTip with 80% ACN, speed vac and resuspended in 1% ACN, 0.05% TFA for MS analysis. Peptides recovered from the four incubations were run separately at the MS.

SILAC labeling and sample preparation were performed by Tiziana Monteverde.

### **2.7.3 MS analysis**

This protocol was performed according to (Reid et al., 2017). Digested peptides were injected on an EASY-nLC system coupled on line to a LTQ-Orbitrap Elite via a nanoelectrospray ion source (Thermo Fisher Scientific). Peptides were separated using a 20cm fused silica emitter (New Objective) packed in house with reversed-phase Repronil Pur Basic 1.9 $\mu$ m (Dr. Maisch GmbH) and eluted with a flow of 200nl/min from 5% to 25% of buffer containing 80% ACN in 0.5% acetic acid, in a 190 min linear gradient. The top ten most intense peaks in the full MS were isolated for fragmentation with high collision energy dissociation. MS data were acquired using the XCalibur software (Thermo Fisher Scientific) and .RAW files processed with the MaxQuant computational platform (Cox and Mann, 2008) version 1.5.0.36 and searched with the Andromeda search engine (Cox et al., 2011) against the human UniProt database (2010) (release-2012 01, 88,847 entries). MaxQuant was run with the following settings: To search the parent mass and fragment ions a mass deviation of 4.5ppm and 20ppm was required. The minimum peptide length was 7 amino acids and maximum of two missed cleavages and strict specificity for trypsin cleavage were required. Carbamidomethylation (Cys) was set as fixed modification, and oxidation (Met), N-acetylation and phosphoSTY as variable modifications. For peptide and phosphorylation site identification, a false discovery rate (FDR) of 1% was required. The re-quantification and match between runs features were enabled and the relative quantification of the peptides against their SILAC-labeled counterparts was performed by MaxQuant. For phosphorylation sites to be quantified, at least two ratio counts were required. The MaxQuant output file Phospho (STY) Sites was analyzed with the Perseus software (Tyanova et al., 2016), the reverse and contaminant hits were excluded and only class I phosphorylation sites (localization probability = probability that the phosphorylation site has been accurately localized > 0.75 and score difference > 5) used for the analysis.

Proteomic analysis was performed in collaboration with Dr. Sara Zanivan and the proteomics core facility at the Beatson Institute, Glasgow.

## 2.8 Data Analysis

All experiments were performed at least 3 times except where noted in the legends. Raw data were copied into Prism (Graphpad) spreadsheets. All Mean & SEM values of biological replicates were calculated using the calculator function. Graphical representation of such data was also produced in Prism. Box & spider plots were generated using Prism. Statistical significance for pairwise data was determined by the Student's (Unpaired) or Paired T test, as indicated. For multiple comparisons, ANOVA was used with a post-hoc Tukey test. \* denotes  $P < 0.05$ ; \*\* denotes  $P < 0.01$ ; \*\*\* denotes  $P < 0.001$ . For Kaplan-Meier plots, Mantel Cox logrank P values are presented.

# Chapter 3 The relevance of NUAK1 in human CRC

## 3.1 Introduction

The 5-year survival rate of colorectal cancer (CRC) is currently 59% with 10-year survival at 57% (CRUK, 2010-2011). Survival rate has doubled in the last 40 years of cancer research. This can be attributed to our better understanding of the disease and its subtypes, and consequently, advancements in new treatments and earlier diagnosis. However, there were still 15,903 deaths from colorectal cancer in 2014 alone, and it is currently the fourth most common cancer in the UK and third most common cancer worldwide (CRUK, 2014).

CRC can be classified using two distinct systems; these provide a basis for prognosis and therapeutic decisions. The TNM Classification of Malignant Tumours (TNM = Tumour Node Metastasis) is a general cancer staging notation system that defines the stage of a variety of different cancers, with alphanumeric codes in ascending order to represent how progressed the disease is. T1-4 describes the size of the primary tumour and local invasion depth, N0-2 describes the number of regional lymph nodes involved, and M0-1 describes the presence of distant metastasis (Tobias & Hochhauser, 2013). The Dukes' staging system is specifically for the classification of colorectal cancer (Kyriakos, 1985). Dukes' A describes an *in situ* cancer, Dukes' B describes the invasion beyond the *muscularis propria*, Dukes' C describes the involvement of the regional lymph nodes and Dukes' D describes a cancer with distant metastasis (see Chapter 1, Section 1.3 for further detail).

The identification of therapeutic targets is crucial for the discovery of drug targets and allocation of appropriate personalised treatment strategies. Therefore, the aim was to assess whether or not NUAK1 could indeed be a therapeutic target for colorectal cancer.

In 2004, Hiroysai Esumi's lab proposed that NUAK1 overexpression is involved in tumour progression of colorectal cancer clinically. They utilised a DNA array constructed of 241 paired cDNAs from 13 different types of tumour and corresponding normal tissue biopsied from various cancer patients including breast, uterus, lung, colon and rectum. Higher levels of NUAK1 mRNA were observed in colon and rectal cancers when compared to corresponding normal tissues. Furthermore, surgically resected, flash frozen samples taken from colorectal cancers and their liver metastases were analysed for NUAK1 mRNA by qPCR, and showed that elevated NUAK1 levels were associated with tumour progression. Liver metastasis had higher NUAK1 mRNA expression than the CRC samples and these

had higher levels than the normal mucosa samples. This result was corroborated by *in situ* hybridisation performed on frozen sections of colorectal cancers, their liver metastases, and normal colon tissue. They did not observe a clear progressive Duke's stage dependent increase in NUA1 mRNA by qPCR however they did state a significant difference between Dukes' B and C/D stages (Kusakai et al., 2004).

In order to validate the specificity of NUA1 expression and further elucidate the function of NUA1, Esumi and colleagues investigated NUA1 in the context of six human colon cancer cell lines; DLD-1, WiDr, HCT15, SW620, LoVo and SW480. LoVo and SW480 cell lines showed high NUA1 expression at both the mRNA and protein level and the *NUA1* gene was not amplified in any of the lines. They associated these higher levels with their invasion abilities *in vitro* and confirmed this by overexpressing NUA1 in the low expressing cell line DLD-1 (D/NUA1). The parental cell line displayed very low ability to invade however the D/NUA1 cells showed high invasive capability. Transient expression of constitutively active AKT in the D/NUA1 cell line further accelerated invasion while it was abrogated with PI3K inhibitor, LY294002 suggesting a dependence on the AKT pathway.

In this chapter, the aim is to assess the suitability of NUA1 for a prognostic marker in human CRC using online patient data sets, and NUA1 RNA scope in a Tissue Microarray (TMA) of human CRC. Additionally the sensitivity of human CRC cell lines to NUA1 inhibition is assessed.

## 3.2 Results

### 3.2.1 *NUAK1 is a prognostic factor for survival in CRC*

With the arrival of new high-throughput technologies, such as genome-wide next generation sequencing, immense amounts of data are now being generated, making the systematic study of the cancer genome possible. Novel computational algorithms have been established to manage the large volume of information and make analysis increasingly efficient and online databases have been developed to store and disseminate these results allowing researchers to share and mine data from all over the world. These developments have shed new light on the cancer genome providing an unprecedented global view of cancer subtypes.

The web-based tool, SurvExpress was used to investigate NUAK1 expression levels in relation to CRC patient outcome. SurvExpress is a cancer-wide gene expression database that documents clinical outcomes and allows the researcher to look at survival analysis and ‘risk’ assessments of cancer datasets in relation to specific genes (Aguirre-Gamboa et al., 2013).

SurvExpress assigns each sample with a score based on the expression levels of the gene of interest, and this is then used to generate ‘risk groups’. The word risk is used with the assumption that either low or high expression of a certain gene comes with a risk for the patient.

SurvExpress was used to generate two ‘risk groups’ based on ‘High NUAK1’ expression and ‘Low NUAK1’ expression by splitting the samples, ordered low to high score, at the median so that there were equal sample numbers in each group.

The first analysis performed was a meta-analysis of 17 independent cohorts comprising of 947 human CRC samples (Aguirre-Gamboa et al., 2013) and revealed that high NUAK1 expression was associated with poor overall patient survival (Figure 3.1A). Further analysis of two large individual datasets, (290 patients; Figure 3.1B) (Jorissen et al., 2009) and Smith Beauchamp Lu Colon (177 patients; Figure 3.1C) (Smith et al., 2008) also corroborated this result. Expression levels for NUAK1 are plotted for each of the corresponding analysis, separated into the high and low groups used (Figure 3.1D, E & F). This data clearly suggests that NUAK1 is a prognostic biomarker for CRC.

The Cancer Genome Atlas (TCGA) project is another web-based platform in which users can access, query and download the TCGA datasets (Weinstein et al., 2013). This large-scale, US-based project is a collaboration between the National Cancer Institute (NCI) and the National Human Genome Research Institute (NHGRI) and aims to characterise the spectrum of genomic alterations associated with the initiation and progression of cancer (Weinstein et al., 2013). These alterations include DNA sequence changes, copy number alterations, chromosomal aberrations and epigenetic modifications and will all be collected, stored, analysed and distributed by the TCGA.

TCGA analysis confirmed that NUA1 levels are higher in more aggressive disease, specifically TNM stage, T3 & 4 when compared with 1 & 2 and furthermore, in patients with lymph node involvement (N1 & 2) when compared with none (Figure 3.1G).

This data suggests that high NUA1 levels correspond to poor patient survival in human CRC; it is therefore a prerequisite to further investigate NUA1's contribution to the disease and to extrapolate any therapeutic value.

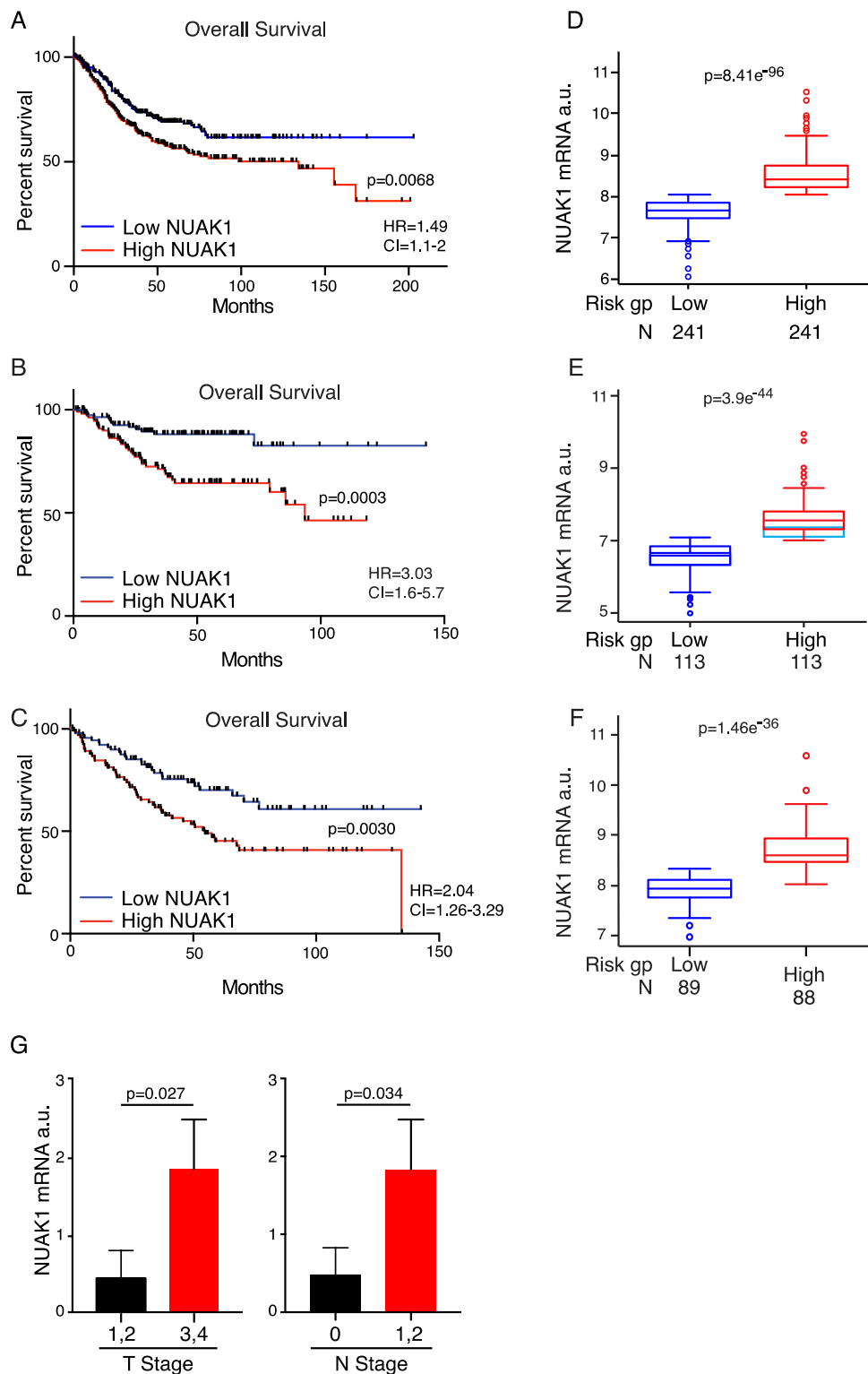


**Figure 3. 1 - NUAK1 overexpression correlates with tumour progression, lymph node infiltrates, and reduced overall survival in human CRC**

(A-C) Overall survival of human CRC patients separated by high (red) versus low (blue) NUAK1 expression. Logrank P value, hazard ratio (HR) and 95% confidence interval (CI) shown. Data were mined from Metabase SurvExpress (A), Jorissen et al, 2009 (B), and Smith et al, 2008 (C). All were then analysed and adapted using SurvExpress. (D-F) Box & whisker plots of NUAK1 mRNA levels in human CRC separated by expression group. Blue = low, Red = high. T-test P value shown. These graphs correspond to survival datasets (A&D), (B&E), (C&F). (G) Left panel: Mean  $\pm$  SEM values of NUAK1 mRNA expression in stage 1 or 2 (black bar, N=127) versus stage 3 or 4 (red bar, N=86) human CRC. Right panel: Mean  $\pm$  SEM values of NUAK1 mRNA expression in tumours of patients with (red bar, N=35) or without (black bar, N=178) lymph node infiltrates. T-test P values shown. Data are from the TCGA colorectal adenocarcinoma cohort accessed via Oncomine.

### **3.2.2 High NUAK1 mRNA levels are associated with more advanced CRC**

Genetically engineered mouse models (GEMMs) are essential to the understanding of basic biology and experiments investigating a whole-organism prior to human clinical trials, however patient-derived tissue samples allow researchers to corroborate their findings in the relevant disease and species *ex vivo* with no risk to the patient. Patient-derived samples can include tumour cell lines or organoids, blood/serum, and formalin-fixed paraffin-embedded (FFPE) tissue samples.

To further determine whether NUAK1 levels are clinically relevant to tumourigenesis in CRC, RNAscope *in situ* hybridisation (ISH) for NUAK1 was used on a human Tissue Microarray (TMA) of CRC (provided by Graeme Murray) (Duncan et al., 2008).

The tissue microarray is a novel advancement in the field of pathology, and contains hundreds of small representative FFPE tissue samples from different patient cases assembled on a single histologic slide. TMAs are constructed by isolating cylindrical tissue cores from different patient donor blocks and re-embedding these into a single block. This allows high throughput analysis of molecular targets such as DNA, mRNA and protein levels in multiple samples simultaneously using identical, standardised conditions thereby reducing variation and also allowing for maximal preservation of valuable and limited archival tissue samples (Jawhar, 2009).

The TMA was comprised of samples taken from 268 patients who were diagnosed with primary CRC and underwent elective surgery between 1994 and 2003. Clinicopathological data was collected including age, gender, site of primary tumour, degree of tumour differentiation and tumour stage, and follow-up was available up to 144 months for all patients. The tissue microarray contained primary colorectal cancer (Dukes A = 53, Dukes B = 104, Dukes C = 111), lymph node metastasis (from corresponding Dukes C cases = 111) and normal colonic mucosal samples (52).

After RNA scope hybridisation, NUAK1 expression level was scored using Halo image analysis software (Indicalab). Intestinal polyps or adenomas originate from epithelial cells however a tumour not only consists of neoplastic cells but also depends on an active stromal infrastructure and together these determine the behaviour of the tumour (Bosman et al., 1993). Therefore, each patient sample was analysed for the percentage of epithelial

or stromal cells expressing NUA1 mRNA. Interestingly, stromal cells had significantly higher levels of NUA1 (Figure 3.2A). In this context, when normal tissue was compared to tumour tissue there was no significant difference in NUA1 levels in either epithelium or stroma. Esumi and colleagues showed that NUA1 was overexpressed in more advanced colorectal disease (Kusakai et al., 2004) therefore it was hypothesised that any effect was being obscured by comparing all cancer stages with normal tissue and that separation into specific stages was necessary for a more detailed analysis.

Patients were split into four equal quartiles based on NUA1 expression level (Q1, Q2, Q3, Q4: low to high respectively) (Figure 3.2B) and then analysed against the clinico-pathological characteristics mentioned above.

Importantly, these results showed that increased NUA1 levels significantly correlated with advanced tumour stages using both the TNM and Dukes staging system in both epithelial cells and stromal cells (Figure 3.2C-F). Furthermore, increased lymph node metastasis (specifically N2) also correlated with higher NUA1 levels (Figure 3.2G & H). No correlations were made between NUA1 expression and patients' age, gender, site of primary tumour, or degree of tumour differentiation (data not shown).

In this context, it does not appear that the different levels of NUA1 in epithelial and stromal cells are having an impact on the overall outcome of the patient. Furthermore, it was assessed if high NUA1 levels affected the outcome of patient survival in this TMA cohort however it did not appear to correlate with lifespan (Figure 3.3).

Overall these results demonstrate an important role of NUA1 in late stage CRC and provide strong grounds for further analysis of the role of NUA1 in human CRC.

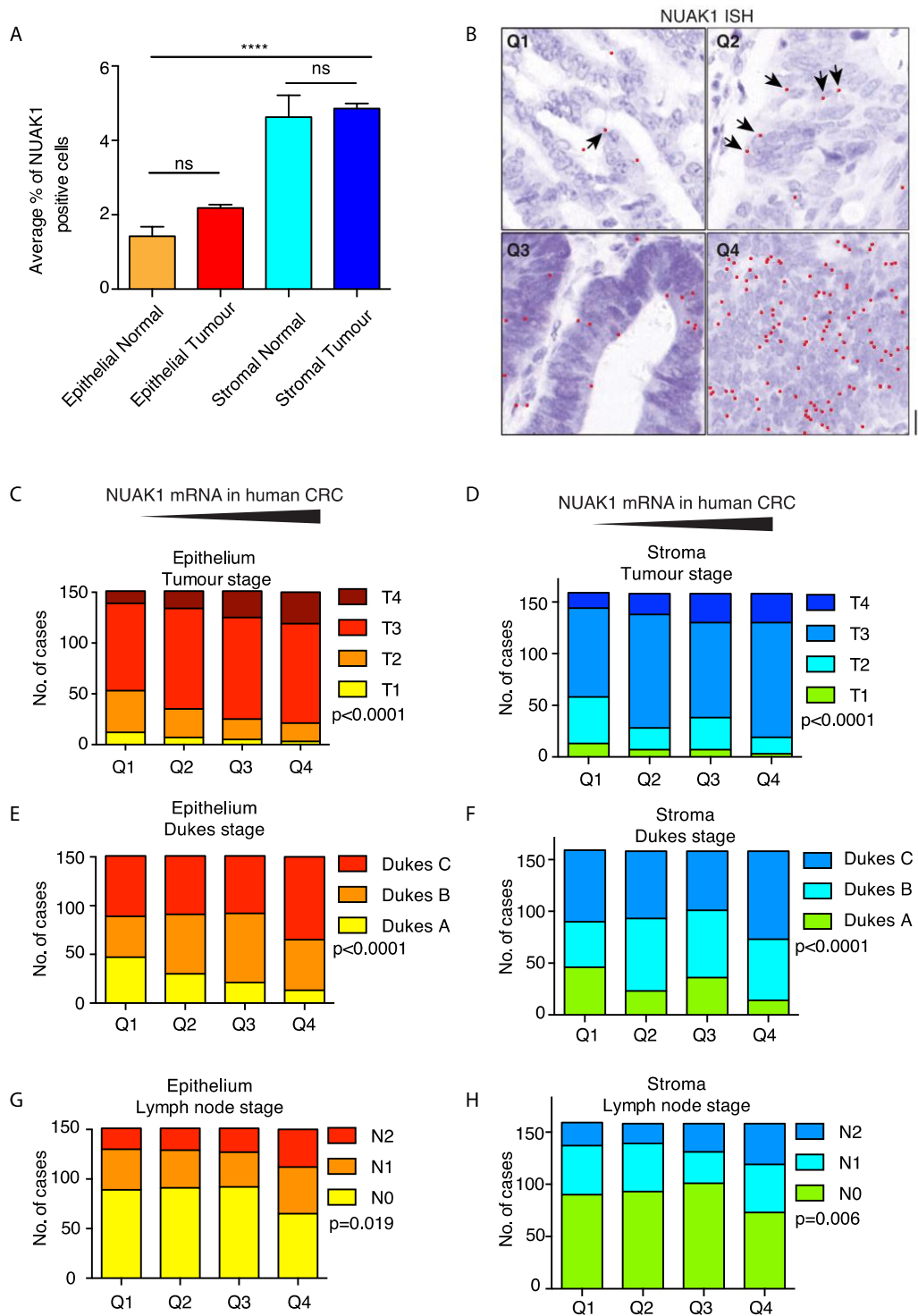


### Figure 3. 2 - High NUA1 RNA correlates with increased tumour stage and lymph node metastasis in a human CRC TMA

(A) Quantification (Mean±SEM) of cell types positive for NUA1 RNA based on the % of cells in each sample. One-way ANOVA followed by Tukey's multiple comparison test was used to calculate statistical significance, \*\*\*\*  $p < 0.0001$ . (B) Representative examples of NUA1 RNA levels detected by RNA scope ISH in each of the assigned quartiles (red dots [false colour], highlighted by arrowheads) counterstained with hematoxylin. Scale bar = 10µM. (C-H) Summary of NUA1 expression in both epithelial (C,E&G) and stromal (D,F&H) cells of a human CRC TMA. Data were divided into equal quartiles from lowest (Q1) to highest (Q4) expression and graphed by Tumour stage (C&D), Dukes' stage (E&F) and by Lymph node stage (G&H). Pearson Chi-Square P values shown.

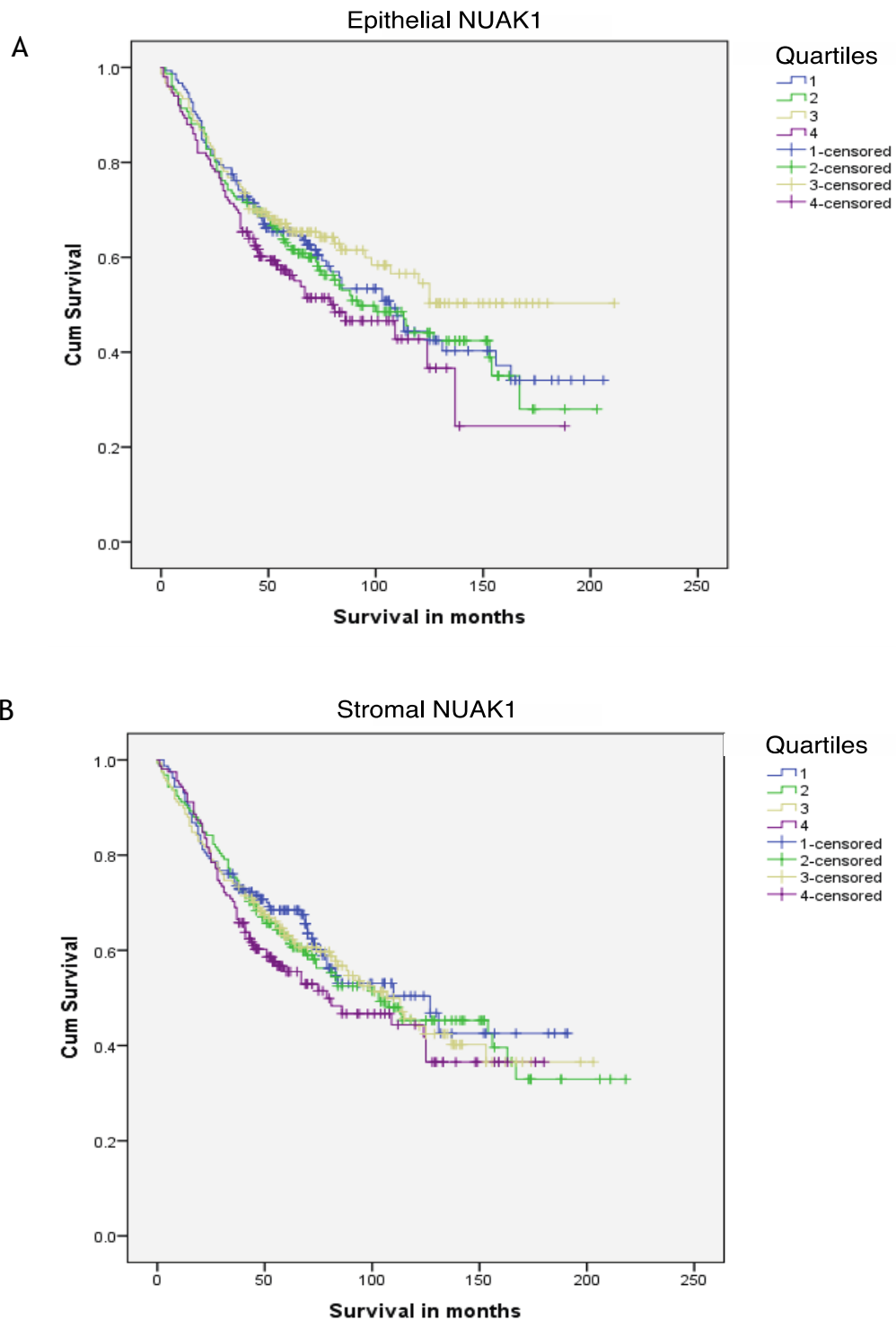


**Figure 3. 3 - NUAK1 level does not correlate with survival in human TMA**

(A&B) Overall survival of patients from human TMA plotted by NUAK1 expression level (Q1 = blue, Q2 = green, Q3 = yellow, Q4 = purple) in epithelial cells (A) and stromal cells (B). Log rank (Mantel Cox) statistics performed showing no significance. This work was performed with undergraduate student Amy Bryson.

**3.2.3 NUAK1 is required for the survival of human CRC lines**

NUAK1, NUAK2 and c-MYC protein levels were measured by western blot in four human CRC cell lines, SW480, SW620, LS174T and HCT116 and additionally in the

osteosarcoma tumour cell line, U2OS (Figure 3.4A). SW480 and U2OS had relatively high levels of NUA1, whereas HCT116 cells showed only low and SW620 and LS174T cell lines barely detectable NUA1 protein levels. Interestingly, SW480 and U2OS cells had the lowest NUA2 levels, HCT116 had moderate levels and SW620 and LS174T cells had the highest levels of NUA2. This may suggest that cells depend on one or the other NUA isoforms.

c-MYC levels were consistent across all of the cell lines however according to ATCC, each of the CRC cell lines used are positive for c-MYC overexpression, therefore it was hypothesised that these cell lines would likely be sensitive to loss of NUA1 activity based on NUA1's role in mediating MYC-driven tumorigenesis (Liu et al., 2012). The viability of these cells under pharmacological inhibition of NUA1 was investigated using two validated inhibitors; HTH-01-015 (HTH; Figure 3.4B) and WZ 4003 (WZ; Figure 3.4C) utilizing the Annexin V FITC/Propidium Iodide apoptosis assay and flow cytometry. Described as 'the first highly specific protein kinase inhibitors of NUA kinases', WZ4003 inhibits both NUA isoforms while HTH-01-015 is specific for NUA1 (Banerjee et al., 2014a). In a previous study, these compounds have demonstrated strong selectivity and did not inhibit the activity of 139 other kinases screened, including ten related members of the AMPK family. WZ4003 and HTH-01-015 were reported to inhibit the phosphorylation of the NUA1 and NUA2 substrate, MYPT1. NUA1 and NUA2 phosphorylate MYPT1 at three conserved residues, Ser-445, Ser-472, and Ser-910 in response to conditions that cause cell detachment, and it was shown that both inhibitors block phosphorylation at Ser-445 (Banerjee et al., 2014a). Additionally, Banerjee et al. reported that both HTH-01-015 and WZ4003 demonstrated *in vitro* efficacy against tumour cell proliferation and migratory potential of U2OS cells, making NUA1 an attractive therapeutic target for investigation in other tumour types.

The results of this study showed that a threshold of 10 $\mu$ M for HTH-01-015 was necessary to cause 50-70% of cell death in the CRC lines. WZ4003 showed a higher potency to induce apoptosis with 10 $\mu$ M causing 70-100% cell death in all three CRC cell lines with SW480 being the most sensitive. SW480 also had significant levels of cell death with 5 $\mu$ M WZ4003. This suggests that cells require NUA1 for survival however they are more sensitive to the loss of both NUA1 isoforms. Interestingly, HCT 116 were the least sensitive to WZ4003 although it was comparable with HTH-01-015 suggesting that they may be more dependent on NUA1. There does not appear to be any correlation between

sensitivity to the compounds and NUAKE1/NUAKE2 protein levels therefore specific dependency on either NUAKE isoform cannot be inferred from this data.

Western blot analysis of the phosphorylation status of MYPT1 confirmed that the concentrations of inhibitors used blocked NUAKE1 activity (Figure 3.4D & E). The phosphorylation of MYPT1 is further reduced in WZ4003 treated samples due to the additive effect of dual inhibition of NUAKE1 and NUAKE2.

Overall, this data suggests that NUAKE1 is essential for the survival of these cell lines and that NUAKE1 protein level does not necessarily predict NUAKE1 activity or dependence.

HTH-01-015 and WZ4003 have been shown to inhibit proliferation and migration in wildtype mouse embryonic fibroblasts (MEFs) and U2OS cells at 10 $\mu$ M therefore it was assessed if treatment with the two small molecule inhibitors would result in similar levels of cell death in the CRC cell lines. Figure 3.4F (left panel) shows that MEFs were not sensitive to HTH-01-015, and WZ4003 only led to 20-40% cell death. In U2OS cells a similar result was observed; HTH-01-015 had no effect on viability and WZ4003 treatment led to under 20% of cell death (Figure 3.4F, right panel). Inhibition of NUAKE1 activity was confirmed by western blot analysis of MYPT1 phosphorylation. Although the mechanism is not currently clear this data suggests that CRC cell lines are more dependent on active NUAKE1 for survival and that total protein levels do not correlate with this effect.

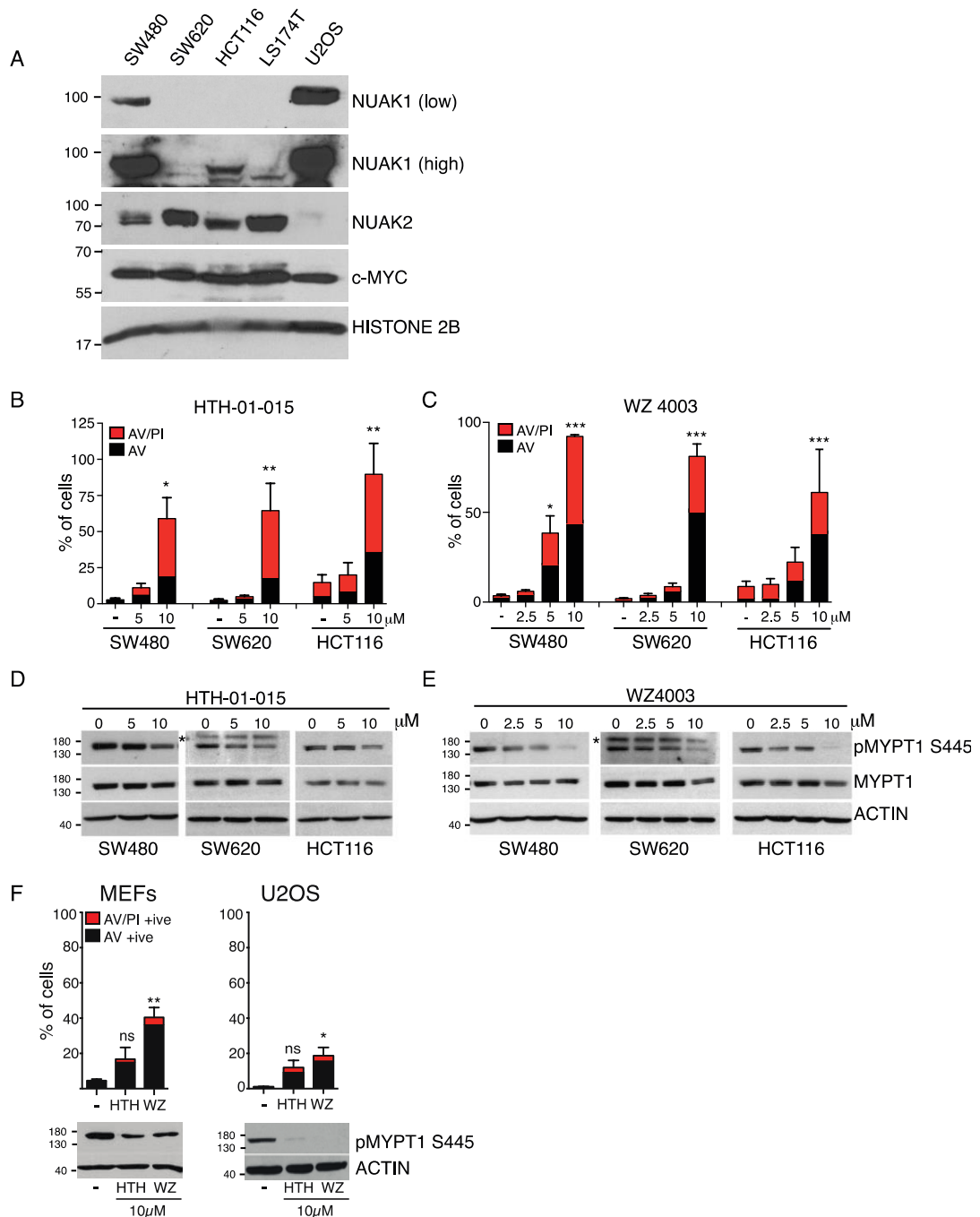


### Figure 3.4 - Human CRC cell lines are sensitive to loss of NUAK1 activity

(A) Immunoblot of NUAK1 (top panel = low exposure, bottom panel = high exposure), NUAK2 and c-MYC protein levels in human U2OS, LS174T, SW480, HCT116 and SW620 cells,  $n \geq 2$ . (B) CRC cell lines cultured in full serum conditions were treated with HTH-01-015 (vc, 5 & 10  $\mu$ M) (B) or WZ4003 (vc, 2.5, 5 & 10  $\mu$ M) (C) and apoptosis was measured at 48 hours post treatment. The graphs represent percentage of cells stained for Annexin V only (black bars) and for Annexin V/PI (red bars). Mean  $\pm$  SEM of three independent experiments, asterisks show significance (2-way ANOVA & post-hoc Tukey test, relative to vc controls) (D) Immunoblots of lysates from human CRC cell lines show reduction in MYPT1 Ser445 phosphorylation upon inhibition of NUAK1 (8hr) with HTH-01-015 (D) and WZ4003 (E). The asterisk indicates a non-specific band. (F) Apoptosis was measured at 48 hours as in B&C in immortalized MEFs and U2OS cells. Mean  $\pm$  SEM of three independent experiments, asterisks show significance (2-way ANOVA & post-hoc Tukey test, relative to vehicle controls). Figure 4A was performed with Master's student Martina Bruccoli. Figure 4B-E was performed by Dr. Nathiya Muthalagu.

### 3.3 Discussion

NUAK1 has been associated with tumour cell survival, invasion and metastasis in many tumour types such as hepatocellular carcinoma (HCC) (Cui et al., 2013), Glioma (Lu et al., 2013), Breast (Chang et al., 2012), Multiple Myeloma (Bell et al., 2014), and Non-Small Cell Lung Cancer (NSCLC) (Chen et al., 2013) making it an attractive therapeutic target for investigation. Furthermore, elevated NUAK1 was associated with poor survival as well as advanced stage in high-grade serous ovarian cancer (HGSOC) (Phippen et al., 2016), non-small cell lung cancer (NSCLC) (Chen et al., 2013) and gastric cancer (Ye et al., 2014). In gastric cancer, NUAK1 was positively correlated with depth of invasion, lymph node metastasis, pathological stage, surgical resection and histological differentiation. Here it is shown that NUAK1 is also a prognostic factor in human colorectal cancer using the online database SurvExpress. Patients with high NUAK1 expression had significantly reduced overall survival in three independent cohorts. Furthermore, TCGA analysis confirmed that NUAK1 levels are higher in more aggressive disease, and in patients with lymph node involvement. This suggests that this study has identified a valuable molecular biomarker for progressed CRC that may be used in the future as a diagnostic tool.

NUAK1 is rarely mutated in CRC (cBioPortal), however immunohistochemical analysis of NUAK1 protein expression in human CRC revealed elevated NUAK1 protein in 11/29 cases and detectable expression in 24/29 samples (Liu et al., 2012). In a separate study, NUAK1 expression was detected at higher levels in tumour cells than in adjacent normal epithelial cells in gastric cancer (Ye et al., 2014). Using RNAscope *in situ* hybridisation (ISH) for NUAK1 on a human Tissue Microarray (TMA) of CRC, this study has shown that NUAK1 expression is present in human CRC and strongly correlates with advanced tumour stage and increased lymph node metastasis. Surprisingly, NUAK1 expression level did not have an impact on overall patient survival in this patient cohort, which is in contrast to the three cohorts analysed by SurvExpress. This may suggest that there is variation between cohorts and that subtyping of patients is required to use NUAK1 expression as an indicator of outcome. Another point to make is that a large number of these patients are still alive, many patients will live 10-25 years post diagnosis, and additionally, none of the patients in the TMA had distant metastasis suggesting that there is a group of patients with very advanced disease that have not been included in this analysis, therefore it would be very interesting to follow with these patient groups.

A recent study suggested that the predictive power for prognostic outcome in CRC arises from the genes expressed by stromal cells rather than epithelial tumour cells (Calon et al., 2015). Here it is shown that NUA1 expression is at least 2-fold higher in stromal cells than epithelial cells within CRC tumours. Activation of the host stromal microenvironment is often referred to as 'reactive stroma' and has been shown to play a critical role in the progression of carcinoma in many tumour types. This 'reactive stroma' has been compared to the wound-healing process in normal tissue as stromal cells exhibit elevated production of extracellular matrix (ECM) components, growth factors and matrix-remodelling enzymes to create a tumour microenvironment that supports cancer cell survival, proliferation and invasion (Kalluri and Zeisberg, 2006). This is the first time NUA1 expression level has been shown to be elevated in the stroma compared to epithelial cells and might suggest an important NUA1-specific function in these cells. Interestingly, a recent study reported a distinct 'reactive stroma' gene signature that was specifically associated with primary chemoresistant tumours and was further upregulated in post-treatment recurrent tumours in ovarian cancer; NUA1 expression was strongly upregulated in these tumours (Ryner et al., 2015).

Multiple CRC cell lines demonstrated a dependence on NUA1 for survival when inhibition of NUA1, using inhibitors HTH-01-015 and WZ4003, led to substantial cell death that was not observed in normal fibroblasts or U2OS cells. This suggests that NUA1 is co-operating with specific characteristics of the CRC lines for the survival of these cells. CRC is dependent on the proto-oncogene c-MYC (Sansom et al., 2006) and according to ATCC, all three CRC cell lines investigated are positive for c-MYC overexpression. Despite this, similar total c-MYC protein levels were seen across all of the cells lines looked at, however this cannot always be used as a direct measure of protein activity. It has been demonstrated that tumour cells with elevated levels of c-MYC establish a dependence on NUA1 for maintaining metabolic homeostasis and for cell survival (Liu et al., 2012). Inhibition of NUA1 led to an mTOR dependent collapse in ATP levels followed by apoptosis that was also seen in an orthotopic mouse model of hepatocellular carcinoma. The study used U2OS cells expressing c-MYC fused to the oestrogen receptor ligand binding domain (MYC-ER) so that upon 4-hydroxytamoxifen (OHT) treatment, MYC-ER was activated resulting in a moderate increase in MYC activity. Only under these conditions, did the authors observe synthetic lethality. Furthermore, no correlation between absolute c-MYC levels and sensitivity to NUA1 was observed (unpublished). Therefore, CRC cell lines may depend on NUA1 for survival based on their high MYC activity however in order to investigate this further

acute perturbation of c-MYC levels would be required. This could be performed by using siRNA to target c-MYC or inducible c-MYC overexpression as was used by Liu et al. Notably, treatment of healthy fibroblasts with HTH-01-015 and WZ4003 led to very little cell death suggesting that it may be possible to target colorectal tumour cells with NUA1 inhibitors and not have a detrimental effect on healthy cells.

Furthermore, an additive effect on cell death was observed when cells were treated with the dual NUA1 and NUA2 inhibitor, WZ4003, compared to HTH-01-015, suggesting that both proteins have important functions in these cell lines and/or they are able to function at least partially redundantly. It has been suggested that the AMPK-related kinases share similar regulatory roles in the regulation of cellular physiology such as cell polarity and cell motility (Sun et al., 2013). The fact that both proteins are able to phosphorylate MYPT1 at Ser445 suggests that there may be some overlap in their functions. Furthermore, despite having differential functions, it is still possible that these proteins can complement one another in times of cellular stress if necessary. Ohmura et al. showed that NUA1 and NUA2 have complimentary functions in apical constriction and apico-basal elongation of the cranial neural plate during neural tube developments in mice (Ohmura et al., 2012).

In conclusion, this study has shown that NUA1 is a potential prognostic marker in human CRC that requires further investigation in order to extrapolate NUA1's effect on tumourigenesis and function in healthy and tumour cells. In the coming chapters, this investigation will strive to answer some of these questions.

# Chapter 4 Investigating the role of NUAK1 using mouse models of CRC

## 4.1 Introduction

In 1998, Nagase et al. characterised KIAA0537, a clone obtained from a human brain cDNA library which was later established to be NUAK1 (Nagase et al., 1998, Suzuki et al., 2003b). They showed that NUAK1 was predominantly expressed in the human heart and brain, followed by skeletal muscle, kidney, ovary, placenta, lung, and liver. This was later corroborated in the mouse by Inazuka et al. (Inazuka et al., 2012). Notably, normal small intestine and colonic tissue has very low basal levels of NUAK1 raising the question about the importance of NUAK1 in these tissues.

On the other hand, NUAK1 expression has been detected at higher levels in tumour cells than in adjacent normal epithelial cells in gastric cancer (Ye et al., 2014). Furthermore, in the previous chapter it was shown that NUAK1 is enriched in later stage colorectal tumours; consequently, this suggests that NUAK1 has an important role to play in CRC tumorigenesis. Publications to date have associated NUAK1 with many central cellular processes that are often perturbed in cancer such as proliferation and DNA damage response (Hou et al., 2011), adhesion (Zagorska et al., 2010), senescence (Humbert et al., 2010), apoptosis (Suzuki et al., 2003a, Suzuki et al., 2003b) and tumour progression. These observations have predominantly been made *in vitro*, whereas *in vivo* data on the physiological role of NUAK1 are lacking.

NUAK1 was first investigated in a mouse model in 2006, when Hirano et al. reported that *Nuak1* (aka *Omphk1*) homozygous mutants were non-viable, and presented omphalocele by E14.5 and died by E18.5 (Hirano et al., 2006). The first report of a conditional *Nuak1* knockout was made by Inazuka et al. in 2012. They generated the *Nuak1* floxed allele, which contains lox P sites at exon 3 at the endogenous locus and results in a non-functional protein after *Cre recombinase*-mediated excision. In this study, they investigated *Nuak1* function using a muscle specific knock out mouse model and reported that knock out mice were apparently normal but exhibited improved glucose homeostasis under high fat diet (HFD) conditions.

As discussed in depth previously, our lab published a study showing that *Nuak1* was required for both the initiation and survival of tumours in an orthotopic mouse model of

hepatocellular carcinoma (Liu et al., 2012). Using two doxycycline inducible shRNAs to target Nuak1, the study demonstrated that tumours did not develop in Nuak1 depleted mice. Furthermore, in an intervention study in which tumours were allowed to develop before doxycycline was added, shRNA expression (via fluorescent marker) could not be detected in the tumours of the treated cohort suggesting that Nuak1 retaining cells have a survival advantage and can out-compete Nuak1 depleted cells. Tumour relapse was accompanied by re-expression of Nuak1 mRNA. This effect was attributed to Nuak1 being an essential survival factor in Myc-driven tumours and loss of Nuak1 resulted in cell death and proliferative arrest *in vivo*.

Sansom et al. showed that loss of *Apc* in the small intestine leads to a “crypt progenitor” phenotype, which describes the unrestricted proliferation within the intestinal crypt and can only be sustained for 5 days in the mouse. Additional loss of *c-Myc* in these mice was able to rescue this phenotype completely therefore suggesting that c-MYC protein is a critical mediator in the early stages of intestinal neoplasia following *Apc* loss (Sansom et al., 2007). Due to the synthetic lethal relationship between c-Myc and Nuak1, it was speculated whether or not c-Myc-dependent cells in the intestine could be targeted by loss of Nuak1.

Based on these previous observations, the aim is to model loss of Nuak1 in a tumour mouse model of colorectal cancer (CRC) and address the following main questions:

- 1) Is Nuak1 necessary for normal intestinal homeostasis?
- 2) Is Nuak1 required for the process of tumourigenesis in the intestine?
- 3) Is Nuak1 required for the survival of established intestinal tumours?

#### **4.1.1 Nuak1 Mouse models**

In order to investigate the physiological role of Nuak1 in the intestine *in vivo*, the previously described conditional *Nuak1* floxed allele (*Nuak1 fl/fl*) was utilized (Inazuka et al., 2012). The *Nuak1 fl/fl* allele contains lox P sites at exon 3 at the endogenous locus and results in a non-functional protein after *Cre recombinase*-mediated excision (Figure 5A). In order to target our conditional transgenes to the intestine, *Villin-CreER<sup>T2</sup>* was used.

To investigate Nuak1’s contribution to tumourigenesis in the intestine two GEMMs for intestinal cancer were used:

In the first model, Nuak1's role in tumour development was investigated. To do this, *Nuak1* floxed mice were bred onto a mouse model for sporadic intestinal cancer: *Villin-CreER<sup>T2</sup>;Apc<sup>fl/+</sup>;LSL-KRas<sup>G12D/+</sup>* (VAK). The mice generated will be referred to as *Villin-CreER<sup>T2</sup>;Apc<sup>fl/+</sup>;LSL-KRas<sup>G12D/+</sup>;Nuak1<sup>fl/fl</sup>* (VAKN) (Figure 4.1). Here, transient tamoxifen-dependent activation of *CreER<sup>T2</sup>* in the intestines of adult mice drives widespread deletion of one copy of *Apc*, constitutive expression of oncogenic *KRas<sup>G12D</sup>* and deletion of *Nuak1* simultaneously. The floxed *Apc* allele contains lox P sites on either side of exon 14 at the endogenous locus, so that *Cre* recombination results in a non-functional allele after excision (Shibata et al., 1997). Tumour formation requires stochastic loss of the second copy of *Apc* during the lifespan of the mouse. The *LSL-KRas<sup>G12D</sup>* allele lies at the endogenous *KRas* locus and carries a LOX-STOP-LOX (LSL) termination sequence preceding the first exon and the *KRas G12D* point mutation in exon 1. *Cre* recombination allows the allele to be expressed constitutively (Jackson et al., 2001).

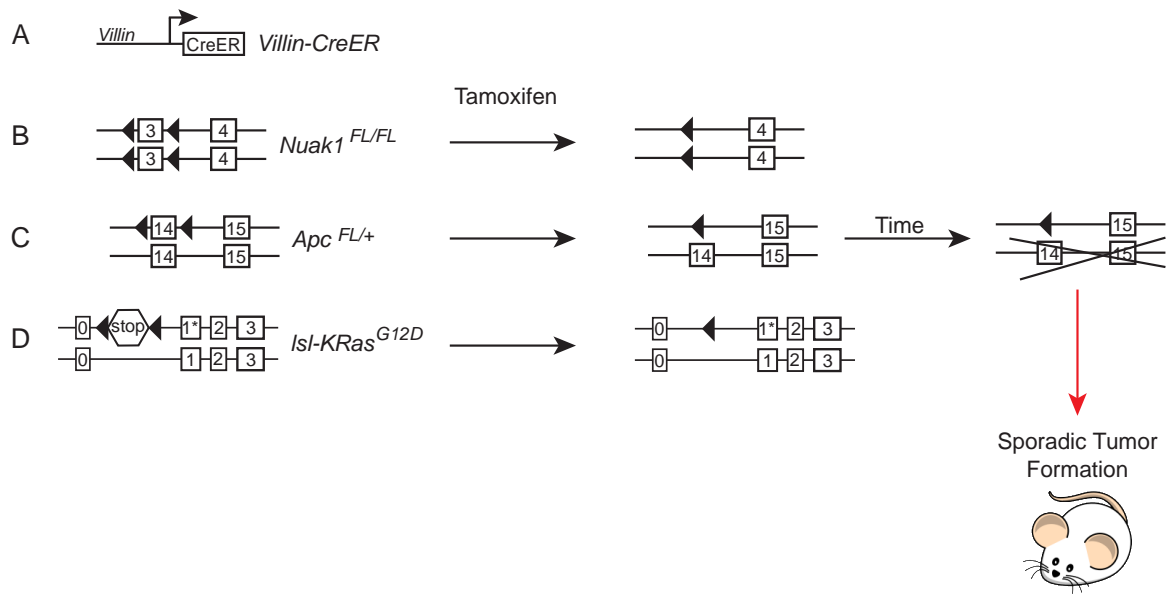


**Figure 4. 1 - The *Villin-CreER<sup>T2</sup>; Apc<sup>fl/+</sup>;LSL-KRas<sup>G12D</sup>;Nuak1<sup>fl/fl</sup>* mouse model for sporadic intestinal cancer**

Schematic of alleles present in our *Villin-CreER<sup>T2</sup>; Apc<sup>fl/+</sup>;LSL-KRas<sup>G12D/+</sup>;Nuak1<sup>fl/fl</sup>* mouse model of sporadic intestinal cancer. (A) represents the *Villin-CreER<sup>T2</sup>* allele, (B) represents the *Nuak1<sup>fl/fl</sup>* allele, (C) represents *Apc<sup>fl/+</sup>* allele and (D) represents the *LSL-KRas<sup>G12D</sup>* allele. Boxed numbers represent exons and black arrows represent lox p sites where recombination will occur, stop sign indicates a LSL termination sequence and an asterisk indicates the KRasG12D point mutation. Over time, loss of the wildtype *Apc* allele allows sporadic tumour development.

In the second model, Nuak1's role in established intestinal tumours was addressed. To achieve this, two independent doxycycline-inducible shRNA (*DI-shNuak1*) were used (purchased from MirimusTM) within a 'TET-ON' expression system. Analysis with two independent sequences specific for *Nuak1* (*shNUAK1.612* and *shNUAK1.1533*) can control

for potential off-target effects. The ‘TET-ON’ expression system delivers tissue-specific and robust expression of the reverse tet-transactivator (*rtTA3*) and thereby, reversible, tissue-restricted induction of tetracycline-responsive element (TRE)-controlled transgenes (Gossen and Bujard, 1992). The *rtTA3* includes a tetracycline repressor protein (TetR) and the VP16 protein by Herpes Simplex Virus and is placed under the control of the Rosa promoter, a locus used for constitutive and ubiquitous gene expression. The expressed *rtTA3* protein can bind to its target tetracycline operator (TetO) sequence within the TRE preceding the *DI-shNUAK1* allele as indicated, and allow expression. Expression of the TRE-regulated cassette is further controlled by the presence of a tetracycline derivative such as doxycycline. In order to trace expression of the *rtTA3* and *shNUAK1* transgenes, each is followed by an mKate and GFP cassette respectively (Figure 4.2).

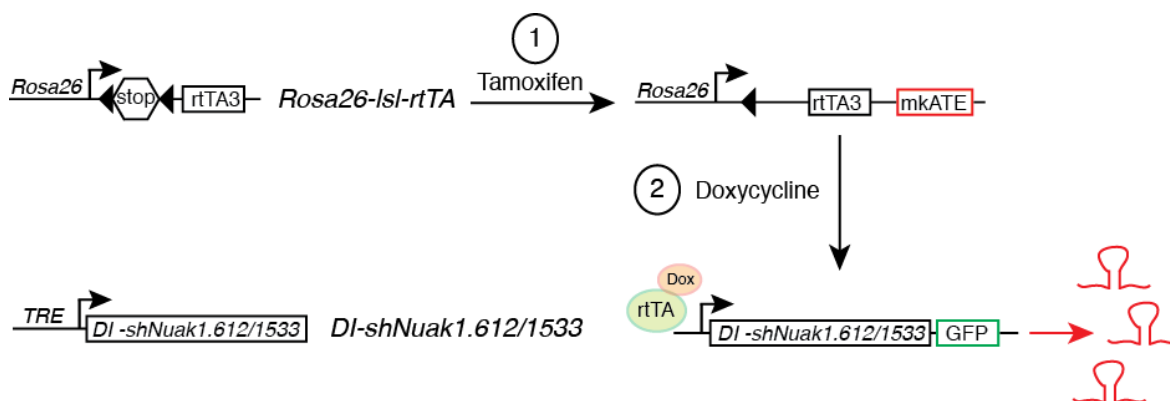


#### Figure 4. 2 - The TET-ON *DI-shNuak1.612/1533* mouse model

A schematic of the ‘TET-ON’ expression system used to deliver expression of the reverse tet-transactivator (*rtTA3*) and thereby, reversible induction of the tetracycline-responsive element (TRE)-controlled transgene, shRNA specific for Nuak1 (*DI-shNuak1.612/1533*). 1) After Cre-dependent activation, the *rtTA3* protein can bind to its target tetracycline operator sequence within the TRE preceding the *DI-shNuak1* allele as indicated, and allow expression. 2) The presence of a tetracycline derivative such as doxycycline is then required for the expression of the *DI-shNuak1* alleles. In order to trace expression of the *rtTA3* and *shNUAK1* transgenes, each is followed by an mKate and GFP cassette respectively.

The *DI-shNuak1* alleles were crossed onto *Villin-CreER<sup>T2</sup>;Apc<sup>fl/fl</sup>* mice so that the expression of the shRNA would be restricted to the epithelial cells of the intestine (see Figure 4.1 for *Villin-CreER<sup>T2</sup>* and *Apc<sup>fl/+</sup>* allele schematics). Transgene induction was initiated in adult *Villin-CreER<sup>T2</sup>;Apc<sup>fl/+</sup>;DI-shNUAK1* mice and tumours accelerated with dextran sodium sulphate (DSS) in the absence of shRNA expression. DSS is a chemical colitogen that induces colitis in the mice. Damage to the epithelial monolayer of the colon causes intestinal inflammation and increased bacterial invasion increasing the chance for neoplastic transformation and proliferation of dysplastic epithelium as the tissue regenerates. As a result sporadic loss of the second copy of *Apc* occurs and colonic tumours form within 10 weeks of induction (Thaker et al., 2012). Depletion of *Nuak1* by

*DI-shNuak1* was induced by doxycycline treatment for various timepoints (3 days, 7 days), immediately prior to harvest at 70 days post induction.

Separately, in order to investigate the effect of loss of *Nuak1* in a whole organism, the *DI-shNUAK1* alleles were used under control of the *ZP3 cre recombinase* allele. *ZP3 cre* is controlled by regulatory sequences from the mouse zona pellucida 3 (ZP3), which is expressed exclusively in the oocyte prior to the first meiotic division (Lewandoski et al., 1997). Therefore, following recombination, all cells in the developed mouse express the reverse *tet-transactivator* allele and the *DI-shNuak1* alleles.

## 4.2 Results

### 4.2.1 *Nuak1* is dispensable in normal gut epithelium

To investigate the *in vivo* requirement for *Nuak1* in the normal intestine, adult mice bearing the floxed *Nuak1* allele (*Nuak1 fl/fl*) under the control of *Villin-CreER<sup>T2</sup>* were induced. Induction involved four daily intraperitoneal injections (I.P) of tamoxifen (80mg/kg) and the mice were harvested 6 days post induction. Mice showed no visible symptoms of distress or discomfort due to *Nuak1* knockout in the intestine. According to Haematoxylin and Eosin (H&E) staining there was no difference in morphology between *Nuak1* knockout tissues and wildtype controls. Cell proliferation (measured by BrdU IHC) and death (measured by Cleaved Caspase 3 IHC) were also unchanged (Figure 4.3). Finally, no differences in differentiation were observed in regards to Paneth (measured by Lysozyme IHC) and Goblet cells (measured by PAS stain). Representative images can be seen in Figure 4.3. This data implies that, in the context of investigations performed here, *Nuak1* is not necessary for normal intestinal homeostasis in the mouse.

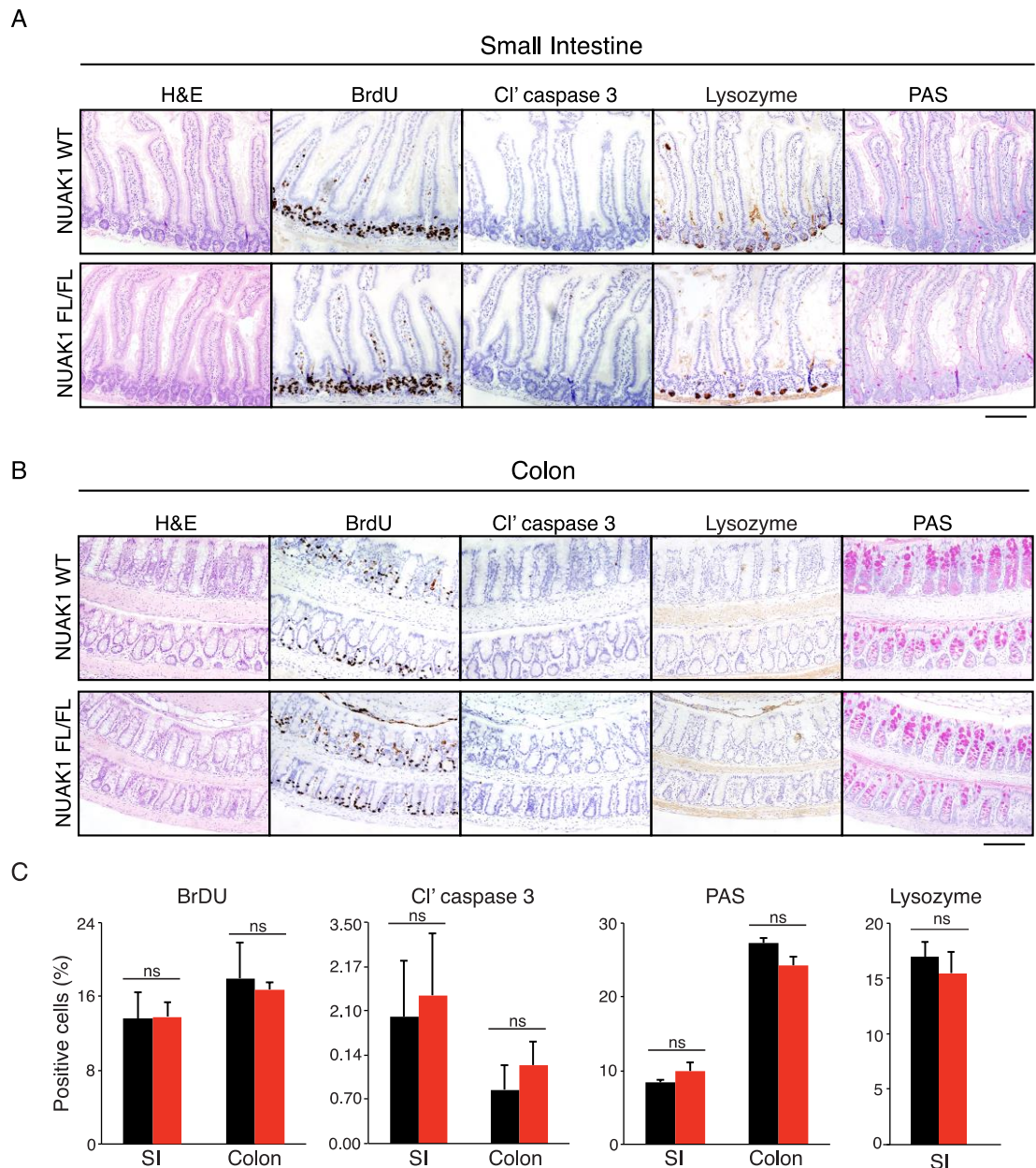


### Figure 4. 3 - Nuak1 is dispensable in normal gut epithelium

(A&B) Representative images of small intestine (SI) (A) and colon (B) from wildtype (top panels) or homozygous floxed NUAK1 (lower panels), stained for histology (H&E); proliferation (BrdU); apoptosis (Cleaved caspase 3); and differentiation (Lysozyme and PAS). N=3 Nuak1 wt/wt and 3 Nuak1 fl/fl. Scale bar = 100 $\mu$ M. (C) Quantification of staining from (A&B), SI: 50 villi-cypts regions counted per mouse, Colon: 50 crypt regions counted per mouse. Black bars = Nuak1 wt/wt; red bars = Nuak1 fl/fl. Mean $\pm$ SEM shown; One-way ANOVA used followed by Tukey's multiple comparison test, ns = not significant. Figure 5A-C experimental procedures and quantification was performed by Dr. Meera Raja and undergraduate student, Silvija Svambaryte.

### 4.2.2 Nuak1 is dispensable in wildtype organoid cultures

*In vitro* the use of three-dimensional 'Organoid' culture was adopted. This is a protocol established by Hans Clevers in which it is possible to grow stem cell containing crypts in a laminin-rich matrigel with essential growth factors and replicate the structure of cells lining the intestine. The wildtype crypts are able to form villus-like epithelial domains that

contain all differentiated cells of the normal intestine (Sato et al., 2009). Using this experimental system, pre-formed small intestine-derived wildtype organoids were treated with the NUA1 inhibitor, HTH-01-015 (Banerjee et al., 2014a) for 48 hours and performed a CellTiter-Blue® Cell Viability Assay (Promega). In this assay, viable cells reduce resazurin to resorufin, which is highly fluorescent. Nonviable cells cannot metabolise the indicator dye therefore do not generate a fluorescent signal. Wildtype organoid cell viability was unaffected by acute Nuak1 inhibition (Figure 4.4A & B).

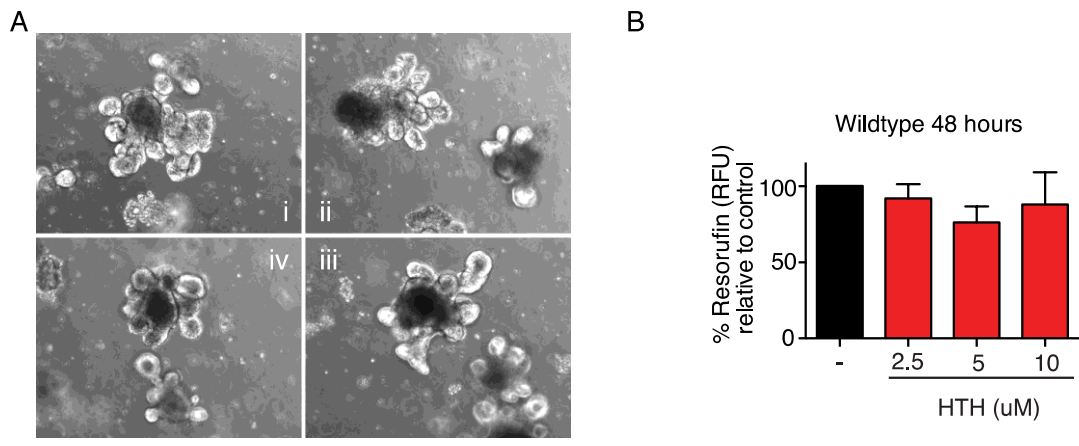


#### Figure 4.4 - Nuak1 is dispensable in wildtype organoid cultures

(A) Organoid cultures from wildtype intestines treated with vehicle (i), 2.5μM (ii), 5μM (iii) and 10μM (iv) NUA1 inhibitor HTH-01-015 for 48 hours. Scale bar = 100μm. (B) CellTiter-Blue® Cell Viability Assay performed at 48 hours post drug treatment, resazurin treatment for 6 hours, mean±SEM of 3 independent experiments shown.

#### 4.2.3 Nuak1 has no impact on c-MYC-dependent progenitor phenotype

The phenotype that results from loss of *Apc* in the small intestine is known as the ‘progenitor’ phenotype. This leads to an increase in BrdU incorporation, Minichromosome maintenance (MCM) staining and a dramatic enlargement of crypts by four days post *Apc* loss (Sansom et al., 2007). Additional loss of c-Myc in these mice could rescue this phenotype completely; therefore it was assessed whether c-Myc-dependent cells could be targeted with loss of Nuak1. In order to test this, adult *Villin-CreER<sup>T2</sup>;Apc<sup>fl/fl</sup>;Nuak1<sup>fl/fl</sup>* (VAN) mice were induced with a daily IP injection for two consecutive days of tamoxifen (80mg/kg) and harvested at four days post induction. *Villin-CreER<sup>T2</sup>;Apc<sup>fl/fl</sup>* mice were used as controls and will be referred to as VA. In this scenario, Nuak1 loss did not alter the *Apc fl/fl* progenitor phenotype (Figure 4.5). As before, cell proliferation (measured by BrdU IHC), death (measured by Cleaved Caspase 3 IHC) and cell differentiation,

specifically in Paneth cells (measured by Lysozyme IHC) and Goblet cells (measured by PAS stain) were investigated and no differences were observed.

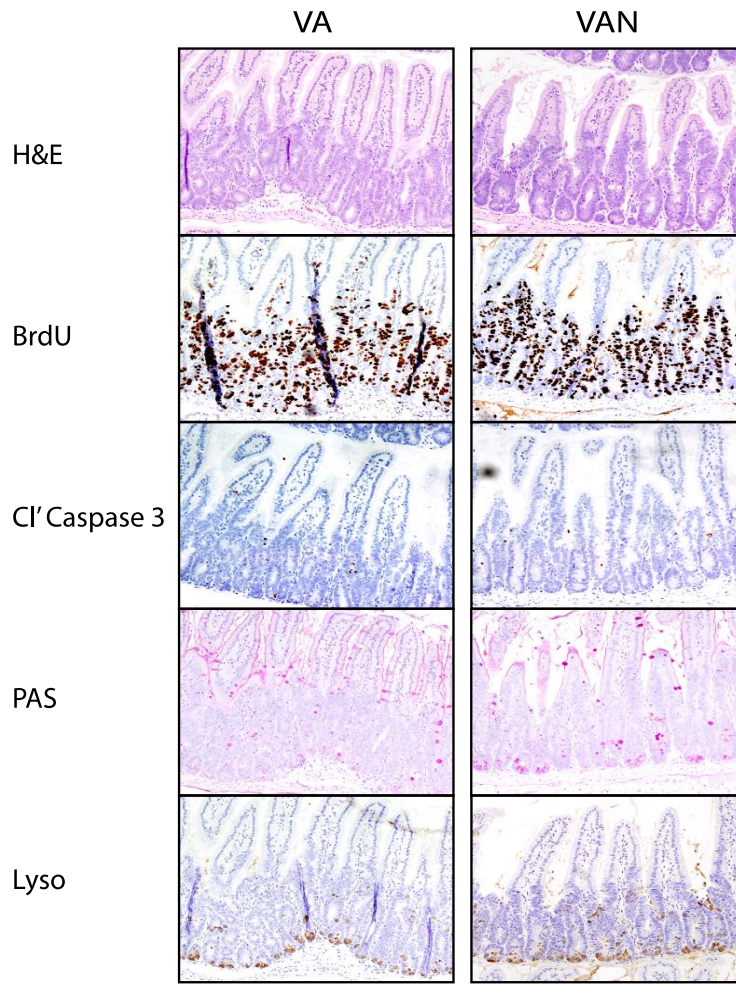


**Figure 4.5 - Nuak1 has no impact on c-MYC-dependent progenitor phenotype**

Representative images of small intestine from *Villin-CreER<sup>T2</sup>;Apc<sup>fl/fl</sup>* (VA; top panels) or *Villin-CreER<sup>T2</sup>;Apc<sup>fl/fl</sup>;Nuak1<sup>fl/fl</sup>* (VAN; lower panels), stained for histology (H&E); proliferation (BrdU); apoptosis (Cleaved caspase 3); and differentiation (Lysozyme and PAS). N=3 VA wt/wt and 3 VAN. Scale bar = 100µM.

**4.2.4 Nuak1 is necessary for tumourigenesis in a GEMM of CRC**

This study has shown that Nuak1 is not necessary for normal intestinal homeostasis. In order to investigate whether Nuak1 is necessary for tumourigenesis within the intestine, *Villin-CreER<sup>T2</sup>;Apc<sup>fl/+</sup>;LSL-KRas<sup>G12D/+</sup>;Nuak1<sup>fl/fl</sup>* (VAKN) adult mice were induced with one IP injection of tamoxifen (50mg/kg) and harvested at a defined endpoint of the presentation of two symptoms (defined in Section 2.1.3). Interestingly, dramatic suppression in colon tumour number (Figure 4.6A), burden (Figure 4.6B) and tumour size

(Figure 4.6C) was observed in *Nuak1* floxed mice (VAKN). Representative images can be seen in Figure 4.6D.

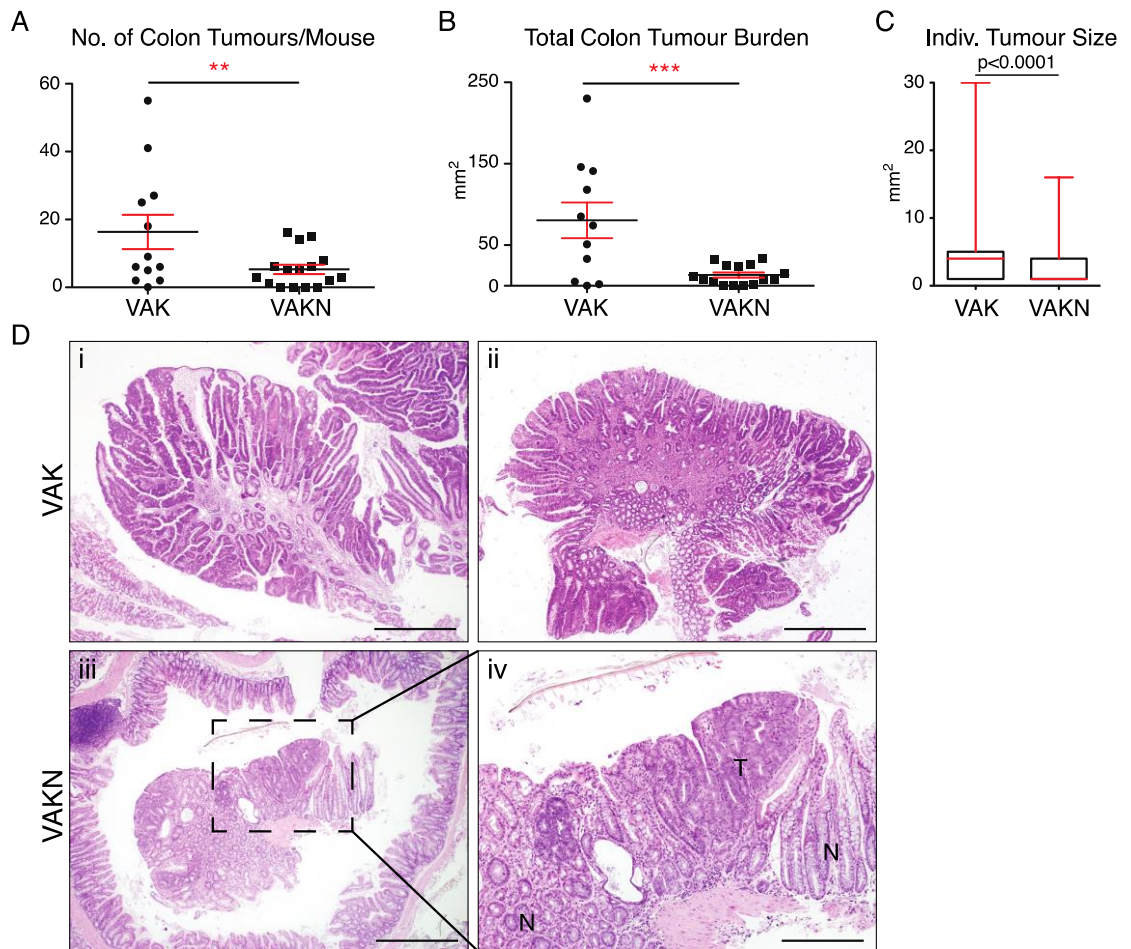


#### Figure 4. 6 - Deletion of *Nuak1* suppresses colorectal tumour formation

(A) Number of colon tumours per mouse in VAK (N=12) and VAKN (N=16) mice, harvested at end-point. Black bar indicates Mean tumour number while red bars indicate SEM. (B) Total tumour burden (area) per mouse of the indicated genotypes. Mean & SEM shown. (C) Size of individual tumours in mice of the indicated genotypes. Box plots depict the median (red bar) and interquartile range of individual tumour area; whiskers reflect maximum observed tumour size. N=192 (VAK) & 119 (VAKN). (B-D) P values from unpaired T-tests shown. (D) Representative H&E stained images of tumours from VAK (top panels) and VAKN (lower panels) mice. Panels i-iii: scale bar =500µm. Panel iv: zoom of inset from iii, scale bar =200µm, T=tumour, N=normal tissue. This work was performed by Dr. Meera Raja.

Surprisingly however, there was no overall survival benefit in these mice compared to controls (Figure 4.7A). This is likely due to there being no significant difference in small intestine tumour number (Figure 4.7B), burden (Figure 4.7C) or tumour size (Figure 4.7D) between VAK and VAKN mice. Upon further investigation, *Nuak1* expression was still retained in the tumours of the *Nuak1* floxed (VAKN) small intestine tumours (Figure 4.7E) but not in the colonic tumours (Figure 4.7F). Firstly, this suggests that the *Cre recombinase* has not been completely efficient or that access to the *Nuak1* locus is limited,

and secondly that Nuak1 retaining tumour cells have a survival advantage over Nuak1 depleted cells.

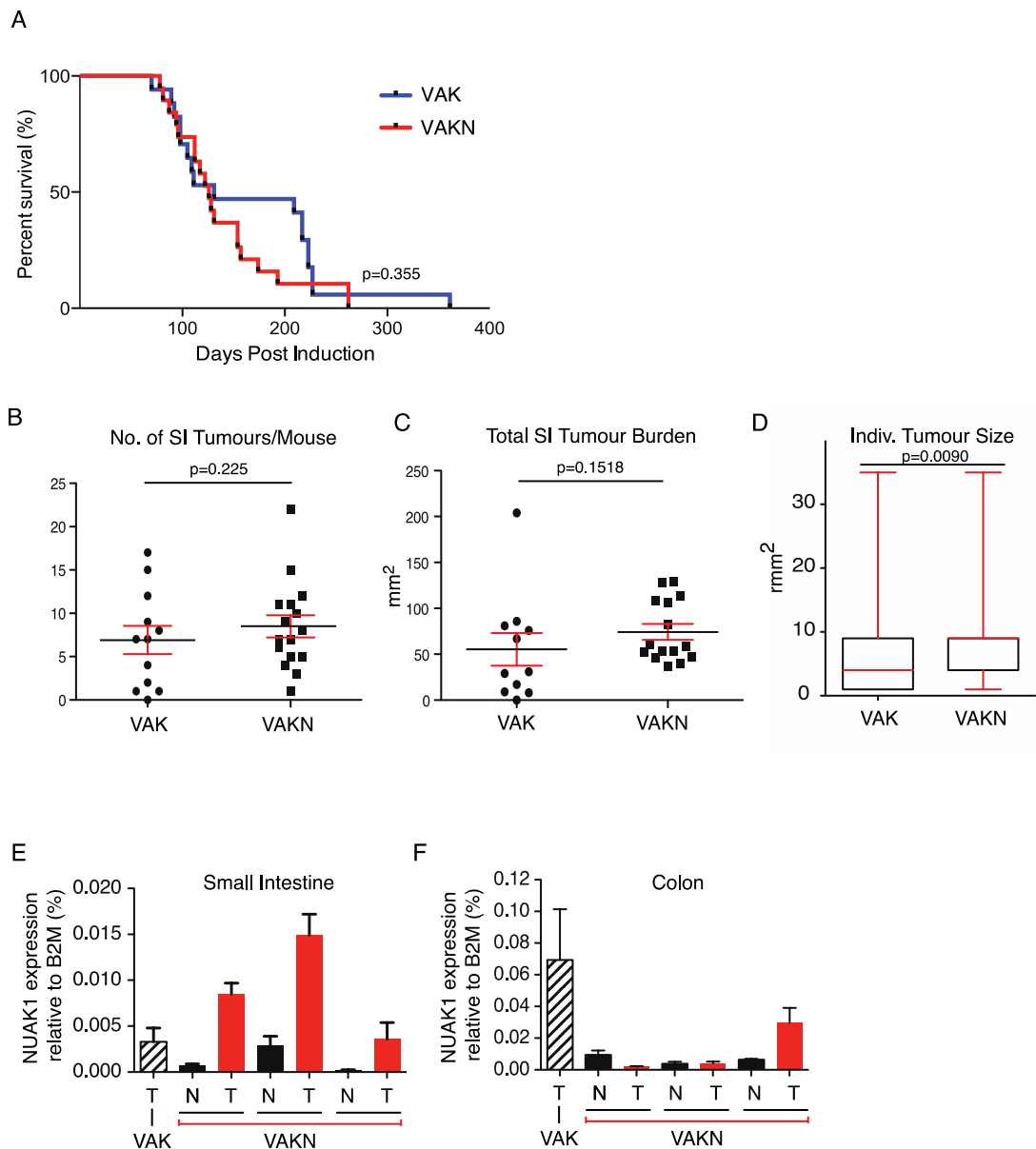


### Figure 4. 7 - Inefficient deletion of Nuak1 in the small intestine

(A) Kaplan Meier survival plot of VAK (n=14) and VAKN (n=22) mice measured from day of tamoxifen injection. P value shown for Logrank Test. (B) Number of small intestine (SI) tumours per mouse in VAK (n=12) and VAKN (n=16) mice harvested at end point. (C) Total SI tumour burden in mice of the indicated genotypes. (D) Size of individual tumours in mice of the indicated genotypes. Box plots depict the median (red bar) and interquartile range of individual tumour area; whiskers reflect maximum observed tumour size. N=176 (VAK) & 102 (VAKN). (E) Nuak1 mRNA in individual SI tumours and adjacent normal SI tissue taken from individual VAK and VAKN mice, as indicated. Error bars represent SEM of technical triplicates. (F) Nuak1 mRNA in individual Colonic tumours as in (E). This work was performed by Dr. Meera Raja.

Small intestinal normal tissue analysed had very low levels of Nuak1 RNA when compared to tumours (Figure 4.7E) and interestingly, control colonic tumours had much higher Nuak1 mRNA expression than small intestine tumours. Therefore, Nuak1 expression in the colon was investigated further. Nuak1 RNA *in situ* hybridisation (ISH)

and Nuak1 immunohistochemistry (IHC) was used (Figure 4.8). The Nuak1 IHC was inconclusive as background levels were high, there was signal in the wildtype tissue and no apparent depletion in the Nuak1 floxed tissues was observed. However, the Nuak1 ISH corroborated the previous RT q-PCR data to suggest that there are very low levels of Nuak1 present in normal colon epithelium, and that expression is enriched in tumour epithelium. Thus, there is a requirement for Nuak1 in tumour cells that is not present in wildtype tissue. Notably, Nuak1 floxed VAKN tumours had considerably less Nuak1 ISH staining than wildtype Nuak1 VAK tumours.

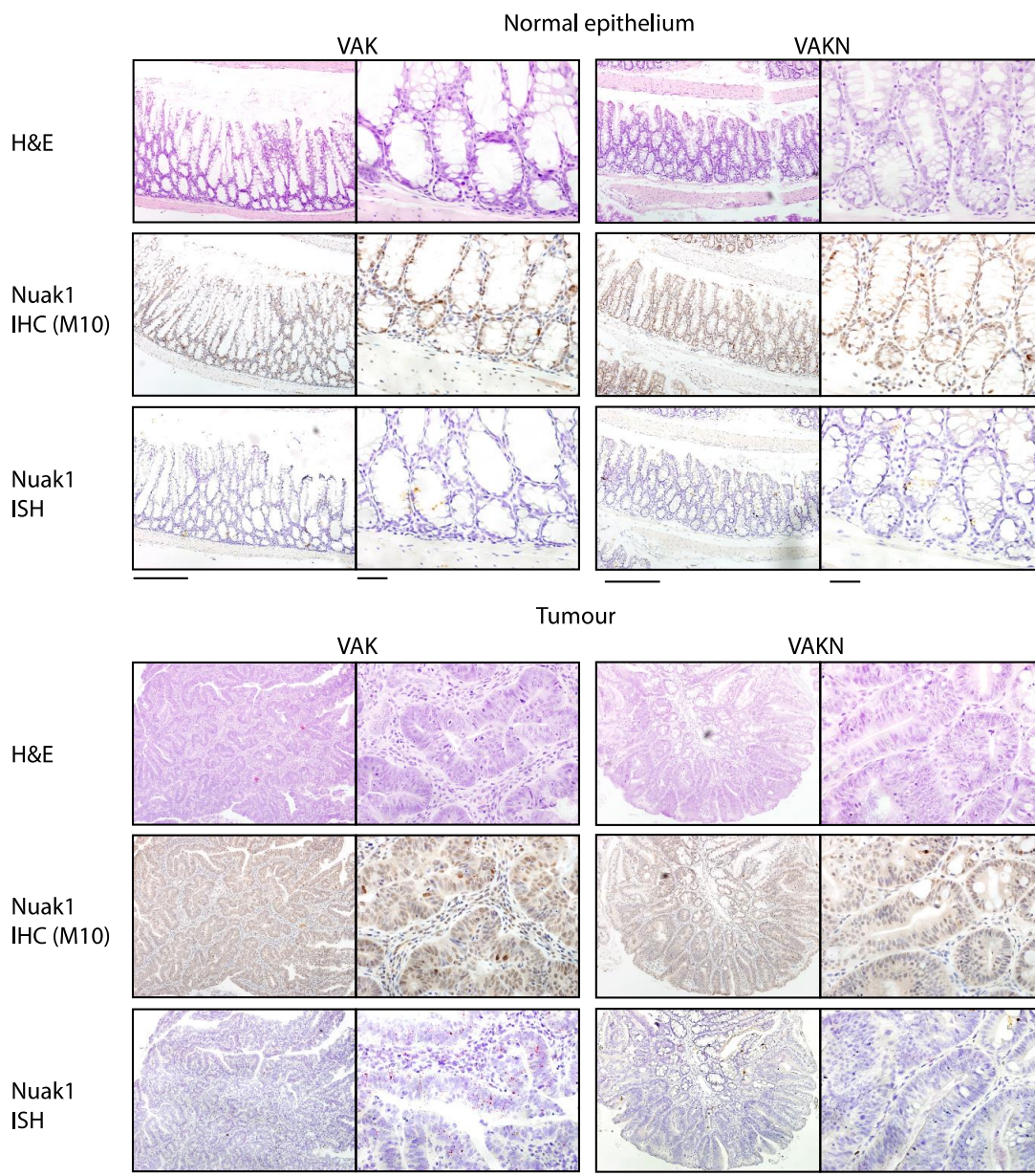


**Figure 4. 8 - Interrogation of Nuak1 levels in VAK and VAKN colon normal tissue and tumour**

Representative images of normal epithelium from VAK (top, left panels) and VAKN (top, right panels) and tumour epithelium from VAK (bottom, left panels) and VAKN (bottom, right panels) for H&E staining, Nuak1 IHC (in house antibody) and Nuak1 ISH. In Nuak1 RNA ISH, each red dot represents the probe binding to one copy of target Nuak1 mRNA. On the left side of each panel scale bar = 100µm, on the right side of each panel scale bar = 10µm.

Next *Apc* and *KRas* status was characterised in *Nuak1* wildtype (VAK) and depleted (VAKN) tumours. To achieve this, nuclear  $\beta$ -Catenin was used as a readout for loss of *Apc* and phosphorylation of ERK1 at Tyr-204 was used as a readout for *KRas* activation (Figure 4.9). This is one of two phosphorylation sites necessary for the full enzymatic activation of ERK, which is phosphorylated by MEK, as part of the RAS-RAF-MEK-ERK pathway (Downward, 2003). See Chapter 1, Section 1.6.1 (Figure 1.3) for *Apc* and  $\beta$ -Catenin relationship and 1.6.3 (Figure 1.5) for RAS-RAF-MEK-ERK pathway. IHC was performed on both cohorts, however, *Nuak1* did not appear to modulate either nuclear  $\beta$ -Catenin or phosphorylation of ERK1 in this context.

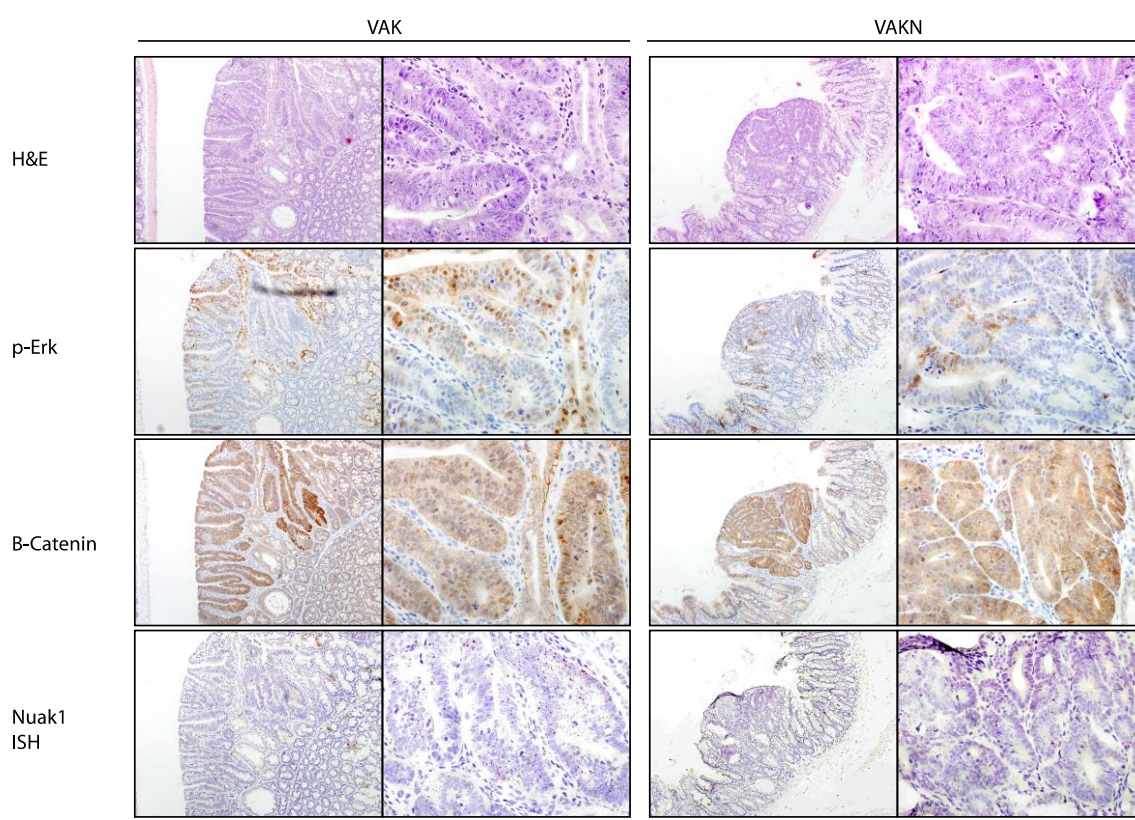


**Figure 4. 9 - *Nuak1* depletion does not alter *Kras* or *Apc* status in colonic tumours.**

Representative images of VAK (left panels) and VAKN (right panels) tumour stained for H&E, p-Erk IHC,  $\beta$ -Catenin IHC, and *Nuak1* *in situ* hybridisation (ISH). On the left side of each panel scale bar = 100 $\mu$ m, on the right side of each panel scale bar = 10 $\mu$ m. Phospho-ERK and  $\beta$ -Catenin IHCs were performed by Katarína Gyurászová.

#### **4.2.5 *Nuak1* is necessary for ‘stemness’ in GEMM generated spheroid cultures**

It is possible to generate organoids from *Apc* transformed (null) mouse crypts which are often referred to as ‘spheroids’. This describes the cystic organoid structures that result from high Wnt signalling, a consequence of loss of *Apc*. Wnt signalling has a central role in the maintenance of the undifferentiated crypt progenitor state (Sato et al., 2009), and as

a result, spheroids are composed primarily of stem cells. Unlike most cells in the human body, which are inherently limited in their proliferative capacity, stem cells have a long life span coupled with extensive proliferation potential. It has also been reported that organoids, including spheroids, undergo a considerably higher number of cell division than reported for other adult human epithelial culture systems (Dey et al., 2009, Garraway et al., 2010).

This study has shown that *Nuak1* is required for the formation of colonic tumours *in vivo* therefore it was necessary to confirm this result *ex vivo* using both a genetic and pharmacological approach. Initially, spheroids were generated from both the small intestine and the colon from *Villin-CreER<sup>T2</sup>;Apc<sup>fl/fl</sup>;LSL-Kras<sup>G12D/+</sup>* mice (VAK), which had been induced with 80mg/kg tamoxifen, four days prior. In order to investigate whether or not *Nuak1* is necessary for the ‘stemness’ of spheroids, the formation of spheroids from single cell suspension was analysed in the presence of NUAKE1 inhibitors, WZ4003 and HTH-01-015 (Banerjee et al, 2014). Compared to controls, spheroid formation was severely compromised in both the small intestine (Figure 4.10A) and colon (Figure 4.10B) spheroids in a dose dependent manner. As seen in the CRC cell lines, WZ4003 had a greater effect and significantly reduced spheroid growth at 2.5µM in both small intestine and colon-derived spheroids. HTH-01-015 was also effective in both, however only 5µM and 10µM significantly reduced spheroid numbers. Consistent with this, inhibition of *Nuak1* markedly reduced cell viability as measured by the Resazurin assay (Figure 4.10C).

In order to investigate this using an alternative genetic approach, spheroids from *Villin-CreER<sup>T2</sup>;Apc<sup>fl/fl</sup>;LSL-KRas<sup>G12D/+</sup>;Nuak1<sup>fl/fl</sup>* mice were generated. Mice were induced *in vivo* by tamoxifen injection and then harvested four days later as above. Compared to controls, *Nuak1* floxed spheroids from both small intestine and colon were compromised (Figure 4.10D&E). At least 50% *Nuak1* depletion was confirmed by mRNA analysis (Figure 4.10F).

This data proposes that transformed stem cells depend on *Nuak1* for cell viability and the ‘stemness’ properties characteristic of spheroids. This is in contrast to wildtype organoids where *Nuak1* appears to be dispensable.

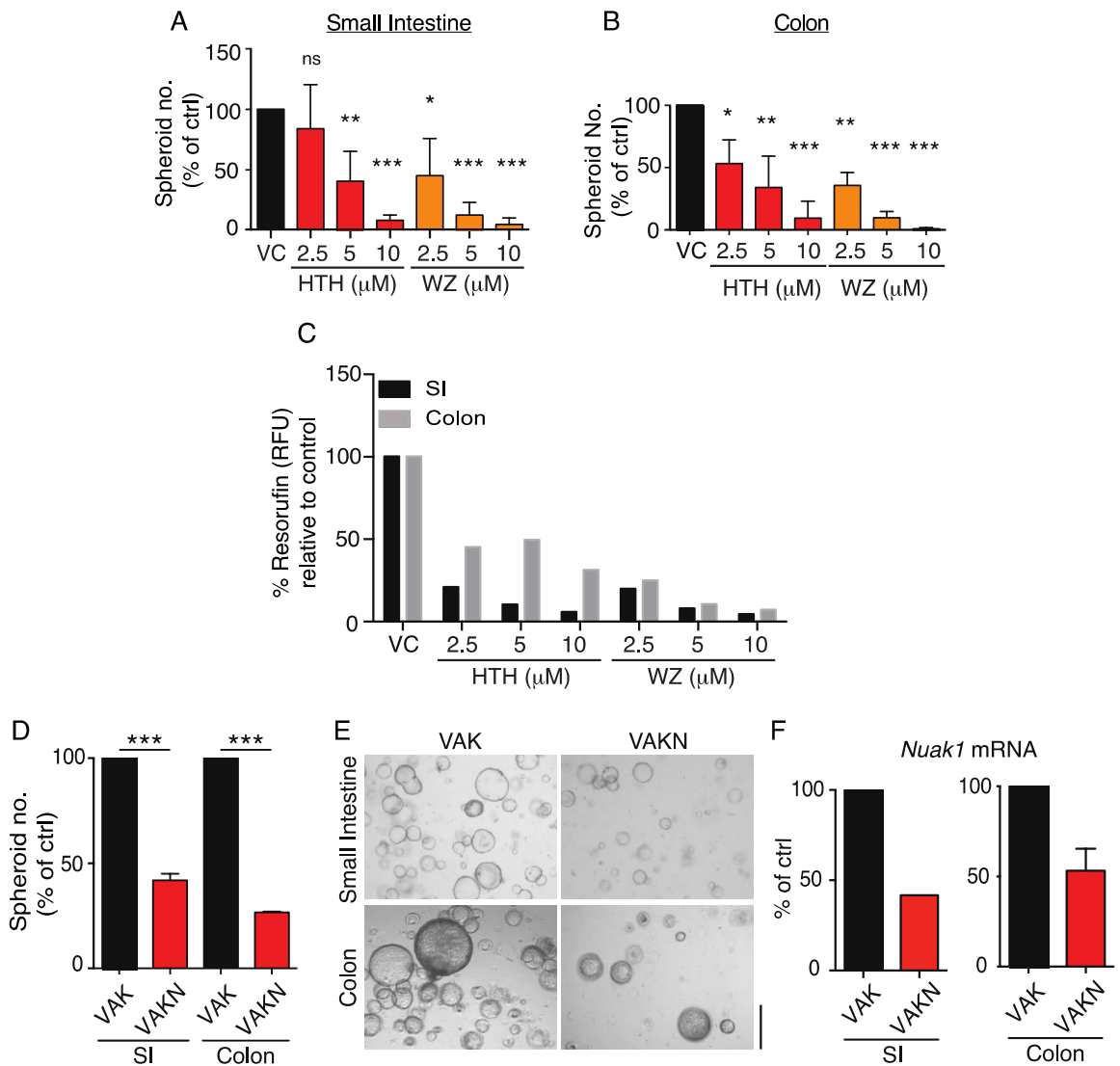


**Figure 4.10 - Nuak1 is necessary for 'stemness' in GEMM generated spheroid cultures.**

(A) Numbers of VAK small intestine-derived spheroids after treatment with Nuak1 inhibitors HTH-01-015 (HTH) or WZ4003 (WZ) for 48 hours, normalized to vehicle treated control (vc). Mean  $\pm$  SEM of 3 independent experiments shown; asterisks show significance (1-way ANOVA & post-hoc Tukey test, relative to vc controls). (B) Numbers of VAK large intestine-derived spheroids treated and graphed as per (A). (C) Representative experiment of CellTiter-Blue® Cell Viability Assay performed at 72 hours post drug treatment, n=3, resorufin treatment 6 hours normalised to vc controls. (D) Number of spheroids arising from freshly isolated VAKN small and large intestine, normalized to VAK controls seeded on the same day, cells counted 72 hours post harvest. Mean  $\pm$  SEM from VAK (N=4) and VAKN (N=6) mice shown. \*\*\* denotes significance (Unpaired T-test). (E) Representative images of spheroids from (D). Scale bar = 500μm. (F) Detection of Nuak1 mRNA in SI and colonic spheroids from VAKN mice relative to Nuak1 transcript levels in VAK spheroids. SI: Mean of 2 VAK and 2 VAKN mice shown. Colon: Mean of 4 VAK and 6 VAKN mice shown. Error bar indicates SEM. Figure 4.10D-F experimental procedures were performed by Dr. Fatih Ceceti.

## **4.2.6 Nuak1 is necessary for the survival of established intestinal tumours in a GEMM model of CRC**

From this study, it is clear that wildtype tissue is unaffected by the loss of Nuak1 and furthermore, it has been shown that colonic tumours require Nuak1 to form. Next, the loss of Nuak1 in pre-existing colonic tumours was investigated. Additionally, a model in which tumours are located exclusively in the colon was utilised as this better recapitulates the human disease and excludes variation caused by the small intestine in the previous investigation.

### **4.2.6.1 Acute Nuak1 depletion significantly reduces colonic tumour burden**

*Villin-CreER<sup>T2</sup>;Apc<sup>fl/fl</sup>;DI-shNuak1* adult mice were induced by tamoxifen injection (80mg/kg) and tumours accelerated by dextran sodium sulphate (DSS) treatment, in the absence of shRNA expression. Induction of the *DI-shNuak1* was performed by doxycycline treatment of the mice, for either three or seven days, immediately prior to harvest at 70 days post induction (Figure 4.11A). As mentioned previously, the *rtTA3* and *DI-shNuak1* transgenes are followed by an mKate and GFP cassette respectively, and allows easy visualisation of transgene expression. Frozen sections were harvested at both time points and both the mKate2 and GFP reporter proteins could be visualised (Figure 4.11B). This confirmed dual expression of the *rtTA3* and the *DI-shNuak1* alleles. Additionally, mouse embryonic fibroblasts (MEFs) were isolated from *DI-shNUAK1* mice where *Cre recombinase* was driven by regulatory sequences from the mouse zona pellucida 3 (ZP3), which is expressed exclusively in the oocyte prior to the first meiotic division (Lewandoski et al., 1997). Induction of each *DI-shNuak1* allele was performed *in vitro* by doxycycline treatment (1µg/ml, 72 hours). Figure 4.11C shows successful depletion of Nuak1 protein in the MEFs compared to a wildtype littermate, where doxycycline has no effect on Nuak1 expression. NUA2 protein levels were also unaffected by doxycycline-mediated activation of the *DI-shNuak1* alleles.

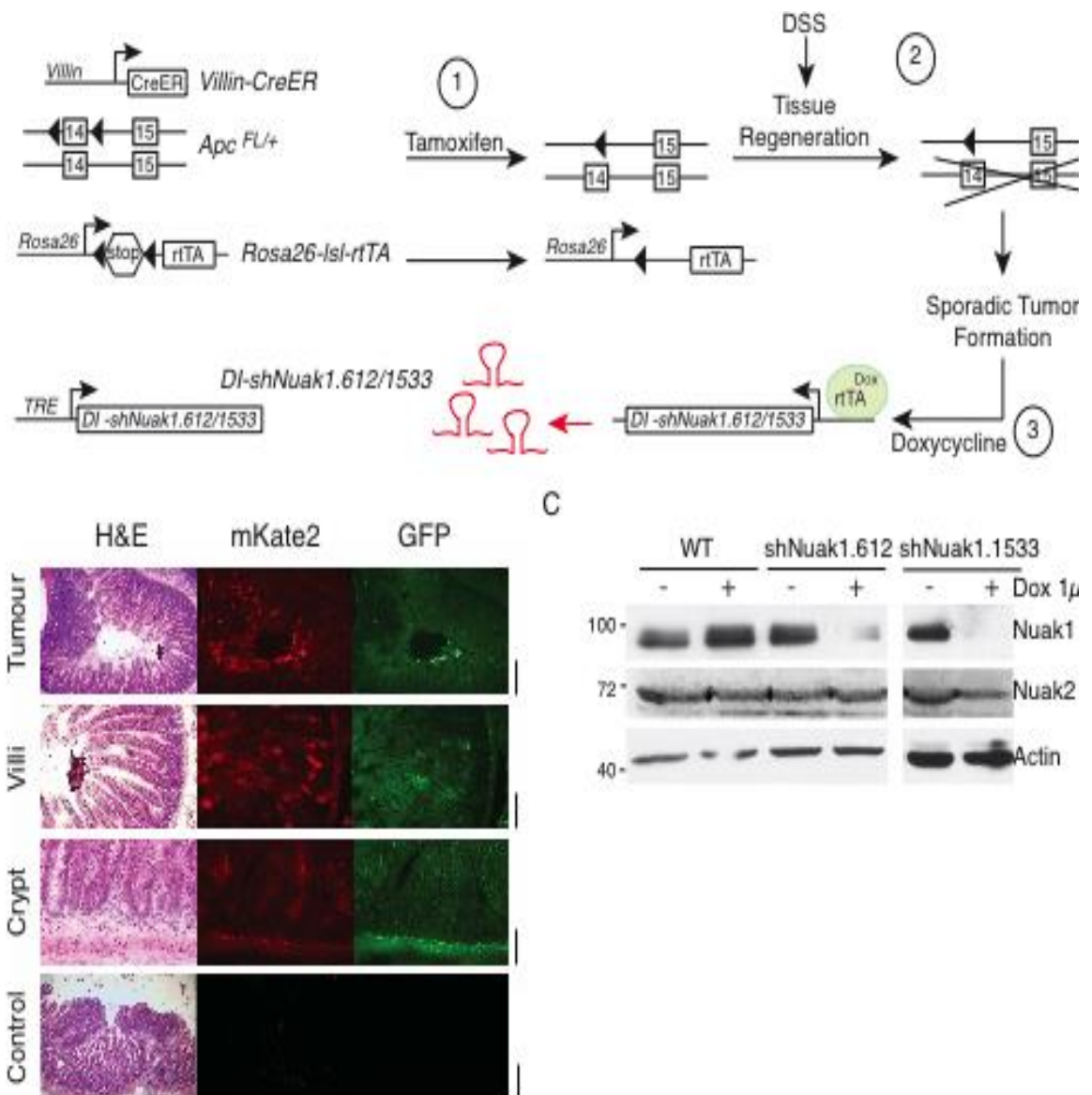


**Figure 4.11 - The DSS/*DI-shNuak1* model experimental plan and validation**

(A) Schematic of the experimental setup: 1) transient activation of CreER by tamoxifen injection (80mg/kg) at 6-12 weeks deletes the floxed *Apc* alleles and initiates gut restricted expression of *rtTA*<sup>3</sup>. 2) Four days post induction mice are administered 1.75 or 2% dextran sodium sulphate (DSS) in drinking water for 5 days to aggravate the colonic epithelium leading to the sporadic mutation of the remaining wildtype *Apc* allele and tumour initiation. 3) Mice were administered doxycycline (2mg by daily gavage) to induce expression of shNUAK1 at various timepoints preceding harvest. 4) Mice were harvested for examination after 3-7 days of Nuak1 depletion (70 days post induction). (B) Frozen sections of *Villin-CreER*<sup>T2</sup>; *Apc*<sup>fl/+</sup>; *DI-shNUAK1* intestine after 3 days of doxycycline treatment. Visualisation of both mKate2 and GFP reported proteins. Scale bars; upper = 500µm, middle (villi) = 200µm, middle (crypt) = 50µm. The lower panels show a *Villin-CreER*<sup>T2</sup>; *Apc*<sup>fl/+</sup> control intestine for comparison. (C) Nuak1 and NUAK2 immunoblot of MEFs carrying the shNuak1.612, shNuak1.1533 or wildtype alleles (genotypes specified) after treatment with doxycycline (1µg/ml) for 72 hours.

Remarkably, after only seven days of *DI-shNuak1* activation, there was a significant reduction in colon tumour number, burden and tumour size per mouse in the cohorts of both *DI-shNuak1* alleles (Figure 4.12).

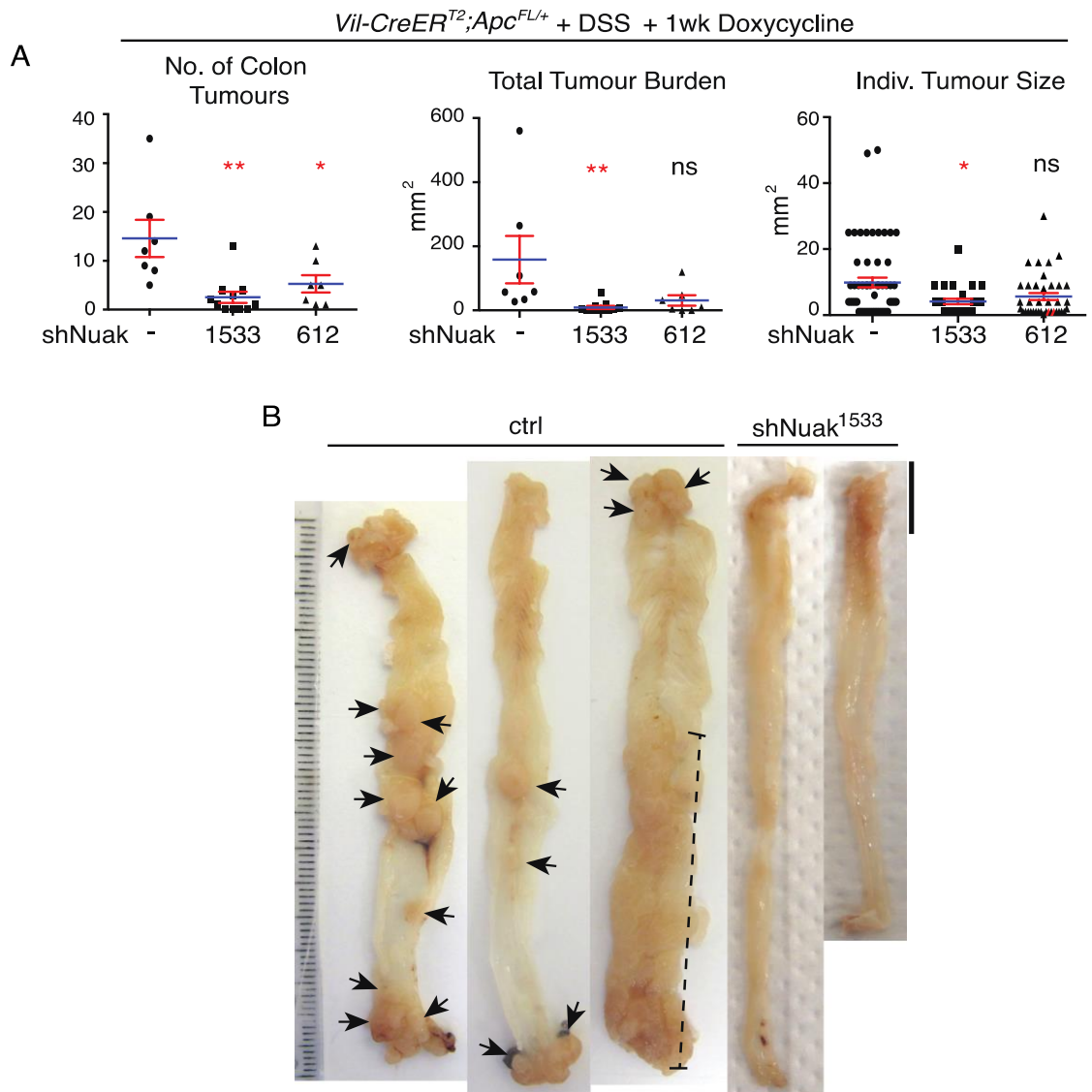


**Figure 4. 12 - Acute Nuak1 depletion reduces colonic tumour number, burden and size.**

(A) Colonic tumour number per mouse (left panel), total tumour burden (centre panel) and individual tumour size (right panel), in DSS-treated VA mice after 7 days of Nuak1 depletion in the gut using either of 2 doxycycline-inducible shRNAs (1533, N=10; or 612, N=7), compared with doxycycline treated controls lacking either shRNA or the rtTA3 allele (-, N=7). Graphs depict Mean (blue lines) and SEM (red bars). Red asterisks indicate significance (1-way ANOVA & post-hoc Tukey test). (B) Representative images of dissected colon tissue from mice in (A). Arrowheads indicate individual tumours; the dashed line denotes a continuous string of tumours. Scale bar =1cm.

In the same experimental context, tumours were also harvested after three days of doxycycline treatment to investigate acute Nuak1 loss. Confirming data from seven days of treatment, mice had lower colon tumour burden than the controls although it was not significant (Figure 4.13).

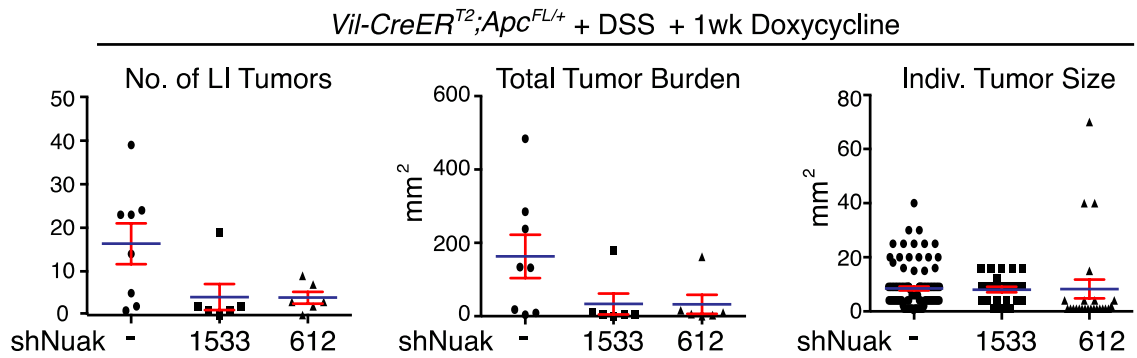


**Figure 4. 13 - Three days of Nuak1 depletion reduces colonic tumour number, burden and size.**

Colonic tumour number per mouse (left panel), total tumour burden (centre panel) and individual tumour size (right panel), in DSS-treated VA mice after 3 days of Nuak1 depletion in the gut using either of 2 doxycycline-inducible shRNAs (1533, N=6; or 612, N=6), compared with doxycycline treated controls lacking either shRNA or the rtTA3 allele (-, N=8). Graphs depict Mean (blue lines) and SEM (red bars). One-way ANOVA & post-hoc Tukey test were performed and no significance was observed.

Despite low tumour numbers in the *DI-shNuak1* mice, tumours present at both three and seven days doxycycline treatment were interrogated for Nuak1 mRNA using RNA Scope *in situ* hybridisation (ISH). NUAK1 RNA Scope ISH revealed a range of Nuak1 mRNA levels within the tumours present at three days. When quantified, there appeared to be a slight reduction in Nuak1 mRNA levels overall, however, it was not significant due to low cohort numbers. This suggests that activation of the *DI-shNuak1* alleles has indeed occurred, although it is not complete (Figure 4.14A&B).

On investigation of the tumours still present in the *DI-shNuak1* mice at seven days, Nuak1 mRNA was elevated (Figure 4.14C & D). There was significantly more Nuak1 mRNA in both *DI-shNuak1* alleles than control tumours. This is a surprising result and provides further evidence to support that colonic tumours require Nuak1 to survive and that tumours Nuak1 retaining tumour cells have the survival advantage.

Notably, Nuak1 mRNA levels were very low in both wildtype controls and *DI-shNuak1.1533* normal colon tissue. In the wildtype controls, it was evident that the

tumours were enriched as in Figure 4.7 & 4.8, suggesting once again, that Nuak1 is upregulated during tumorigenesis.

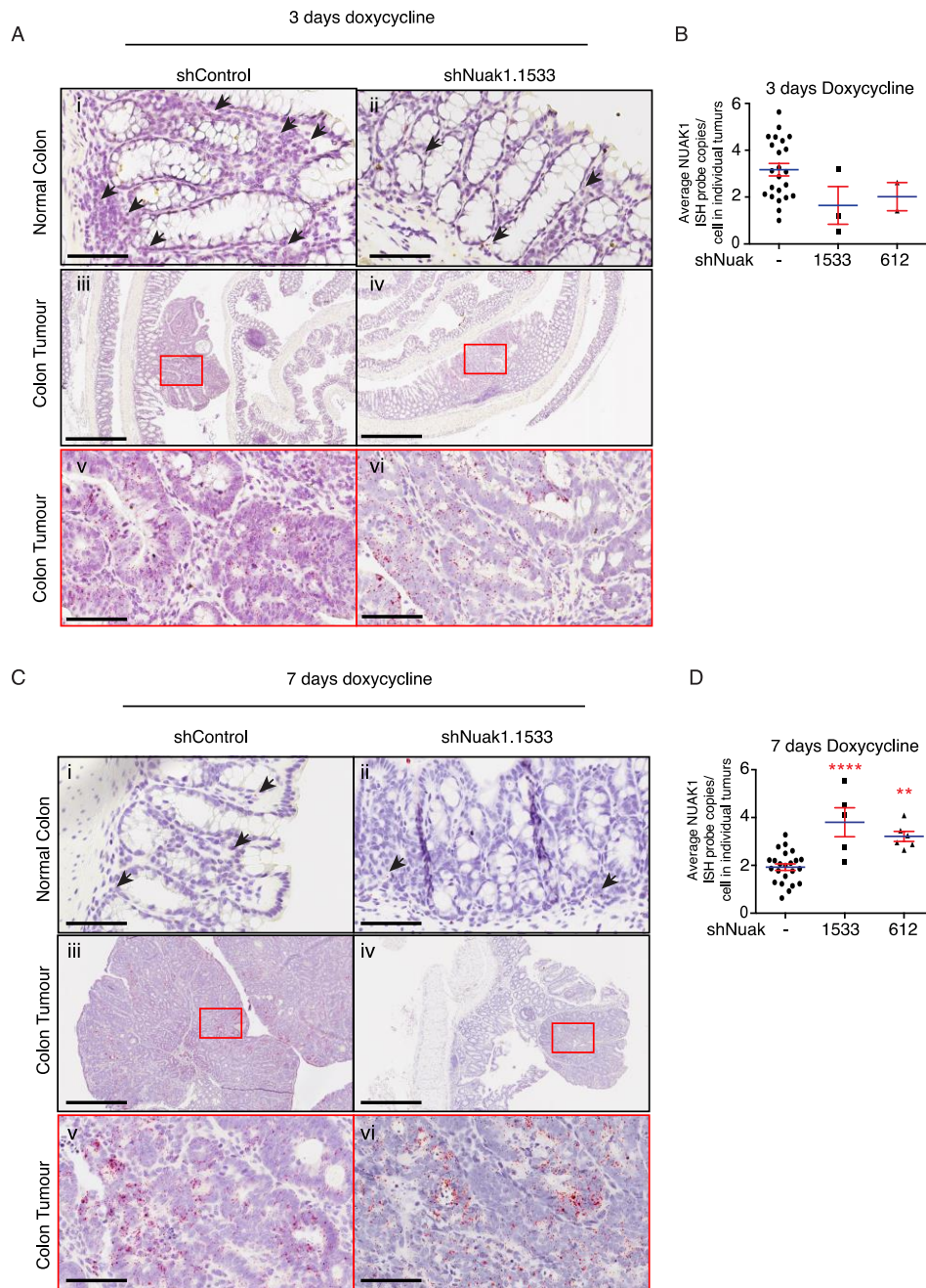
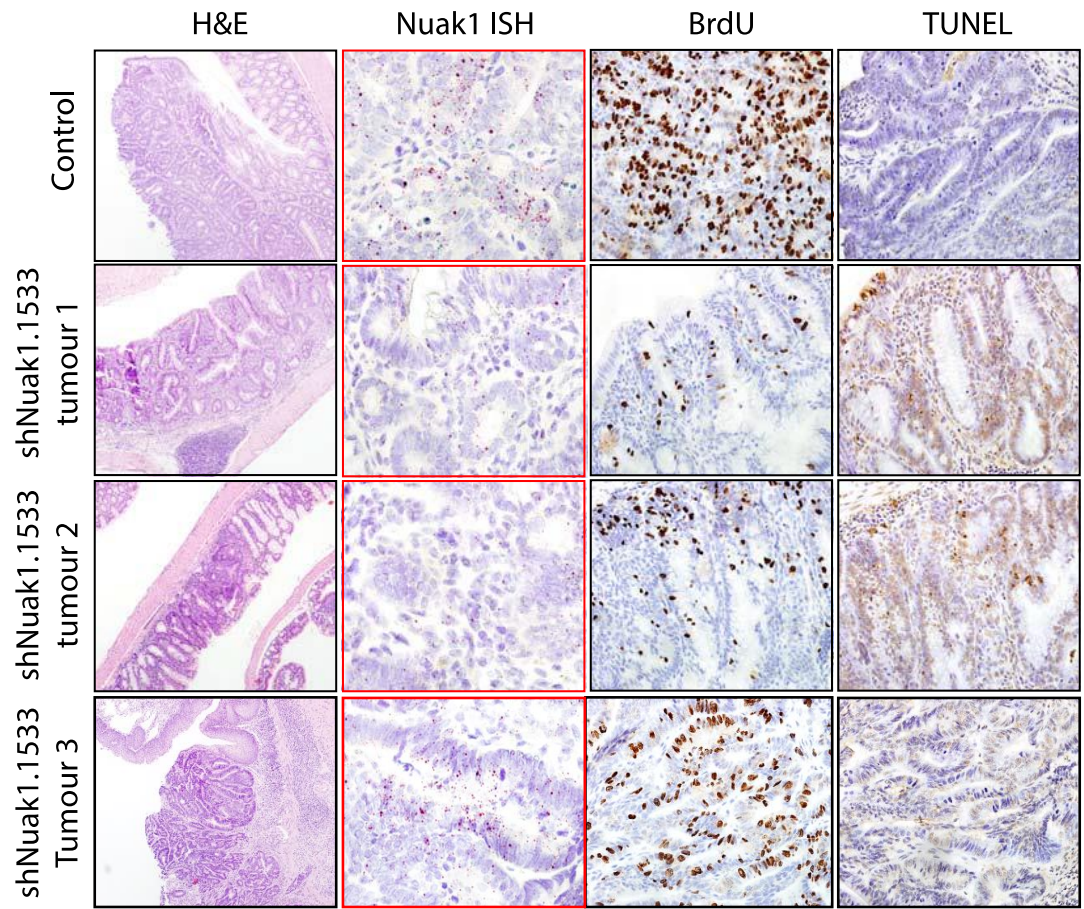


**Figure 4. 14 - Tumours are enriched with Nuak1 mRNA and Nuak1 depletion is observed at 3 days but not 7 days**

(A) Representative images of Nuak1 RNA scope ISH (red stain, indicated by black arrows in top panels) in (i) normal colon tissue in control mice, (ii) normal colon tissue in shNuak1.1533 mice. (iii) colon tumour in control mice, (iv) colon tumour in shNuak1.1533 mice, (v) zoom of inset from (iii), and (vi) zoom of inset from (iv). All harvested at 3 days post shRNA induction. Scale bars; i & ii = 200 $\mu$ m, iii & iv = 500 $\mu$ m, v & vi = 50 $\mu$ m. (B) Quantification of the average Nuak1 ISH probe copies per cell in individual tumours harvested at 3 days for controls (n=23 tumours), shNuak1.1533 (n=3 tumours) and shNuak1.612 (n=2 tumours). Each point on the graph represents a tumour that was scored individually for Nuak1 RNA. (C) As in (A) but with tumours harvested at 7 days post shRNA induction. Scale bars; i & ii = 200 $\mu$ m, iii & iv = 500 $\mu$ m, v & vi = 50 $\mu$ m. (D) As in (B), quantification of the average Nuak1 ISH probe copies per cell in individual tumours harvested at 7 days for controls (n=23 tumours), shNuak1.1533 (n=5 tumours) and shNuak1.612 (n=6 tumours).

Next, tumours present in *DI-shNuak1* mice at three days post shRNA induction were characterised for markers of cell death (TUNEL IHC) and proliferation (BrdU IHC) in order to understand the mechanism by which loss of Nuak1 is leading to such a significant reduction in tumour number by seven days post shRNA induction. Total quantification of BrdU incorporation and TUNEL positive cells in individual tumours showed a significant decrease in BrdU positive cells and a significant increase in TUNEL positive cells in *DI-shNuak1* tumours compared to controls (Figure 4.15A & B). Notably, tumours retaining Nuak1 mRNA appeared to have visually higher levels of BrdU incorporation and lower levels of TUNEL positive cells (see figure 4.15B *DI-shNuak1.1533* tumour 3 compared to tumour 1 & 2). Intriguingly, this data suggests that acute loss of Nuak1 results in increased cell death and reduced proliferation in intestinal tumours.

A



B

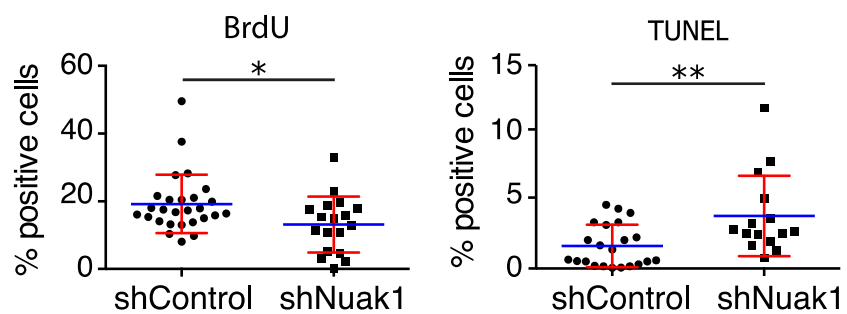


**Figure 4. 15 – Nuak1 depletion leads to reduced cell proliferation and increase cell death**

(A) Representative images of H&E staining, Nuak1 RNA *in situ* hybridisation (ISH), BrdU incorporation and TUNEL IHC for an shControl tumour (top panel) and *DI-shNuak1.1533* tumours 1-3 (middle and bottom panels). All tumours were harvested 3 days post shRNA induction, 70 days post tamoxifen induction. Scale bars from left to right = 100µm, 5µm, 10µm, 10µm. (B) Quantification of % positive BrdU and TUNEL cells by IHC in individual tumours harvested at 3 days for controls (n=22 tumours), shNuak1 (combined alleles; n=18 tumours). Each point on the graph represents a tumour that was scored individually, errors bars show SEM. Red asterisks indicate significance (Mann Whitney Test).

#### **4.2.7 Nuak1 is required for the survival of pre-formed spheroids**

In this chapter it has been shown that Nuak1 is required for the survival of established tumours *in vivo* therefore this result was further investigated *ex vivo* using both a genetic and pharmacological approach. Firstly, pre-formed *Villin-CreER<sup>T2</sup>;Apc<sup>fl/fl</sup>;LSL-KRas<sup>G12D/+</sup>* spheroids were treated with the NUAK1 inhibitors, HTH-01-015 and WZ4003, and spheroid number analysed over 48 hours. In the small intestine, pre-formed spheroids were sensitive to Nuak1 inhibition at 10µM HTH-01-015 and at both 5 and 10 µM WZ4003 in which there was more than 50% loss of spheroid number (Figure 4.16A). In comparison, the effect was reduced in colonic spheroids, however, there was still a significant reduction in spheroid number by 48 hours in 10µM HTH-01-015 and 5 and 10µM WZ4003 (Figure 4.16B).

In order to validate this result using a genetic approach, spheroids were generated from *Villin-CreER<sup>T2</sup>;Apc<sup>fl/fl</sup>;LSL-Kras<sup>G12D/+</sup>;DI-shNuak1.1533* mice, which were induced by tamoxifen (80mg/kg) three days prior, from both the small intestine and the colon. Initially spheroids were allowed to form in culture and then treated with doxycycline to induce activation of the *DI-shNUAK1.1533* allele. However, very few cells expressed the GFP reporter and after days in culture, these green fluorescent spheres disappeared (data not shown). Therefore, this suggested that the *Cre recombinase* was not 100% effective within the mouse, and that the escaping stem cell population were able to colonise more effectively than Nuak1 depleted spheroids. To maximise the activation of the *DI-shNuak1 in vivo*, adeno-viral induction of *Cre recombinase* was utilised, with GFP visualisation as a measure of success. In order to investigate the survival advantage of Nuak1 wildtype versus Nuak1 depleted stem cells, pre-formed spheroids were cultured in the presence of 1µg/ml doxycycline, to induce expression of the GFP-linked *DI-shNuak1* allele, and both fluorescent and non-fluorescent spheroids were counted daily up to 72 hours for both small intestine and colon-derived spheroids. Doxycycline treated small intestine-derived spheroids had reduced total spheroid numbers compared to untreated controls and furthermore, over 72 hours the number of GFP fluorescing spheroids was also reduced suggesting that Nuak1 depleted spheroids indeed have a survival disadvantage (Figure 4.16C). In the colon-derived spheroids there were no GFP positive spheroids until 48 hours suggesting that this was the time frame necessary for the doxycycline induction of the shRNA (Figure 4.16D). Pre-formed spheroids treated with HTH-01-015 and WZ4003 shown previously also displayed a delayed effect suggesting that it takes longer for reagents to penetrate the spheroid structure. There was also a reduction in spheroid

number at 48 and 72 hours, although the number of GFP positive spheroids remained constant. Figure 4.16E shows representative images of fluorescent spheroids after a doxycycline titration.

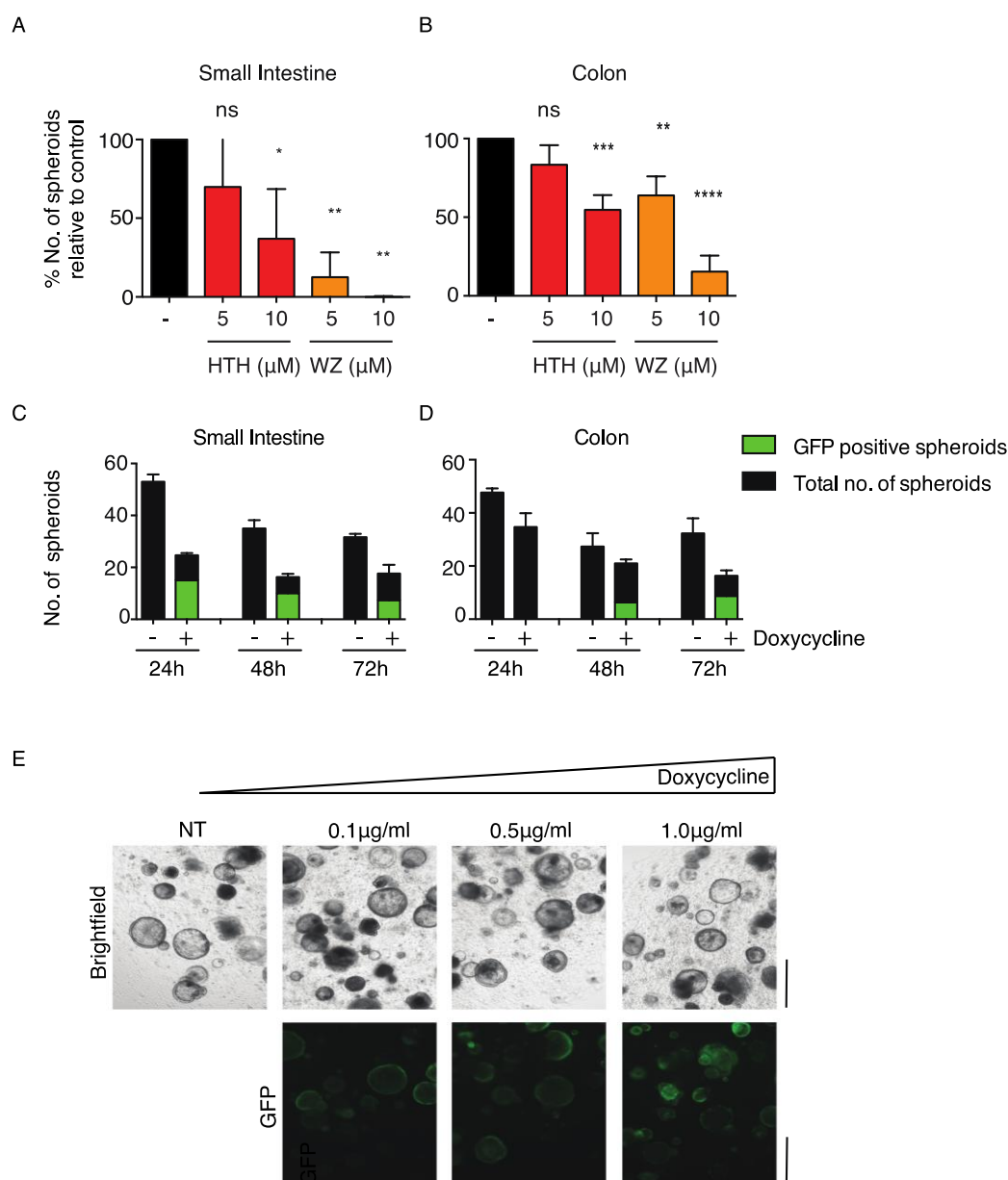


### Figure 4. 16 - Spheroids require Nuak1 for survival *ex vivo*

(A) Numbers of VAK small intestine-derived spheroids after treatment of pre-formed spheroids with Nuak1 inhibitors HTH-01-015 (HTH) or WZ4003 (WZ), normalized to vehicle treated control (vc). Mean  $\pm$  SEM of 3 independent experiments shown with spheroids isolated from 3 mice; asterisks show significance (1-way ANOVA & post-hoc Tukey test, relative to vc controls). (B) Numbers of VAK colon-derived spheroids treated and graphed as per (A). (C) Number of VAKshNuak1 small intestine-derived spheroids after shNuak1.1533 induction by 1  $\mu$ g/ml doxycycline treatment (+) for 24, 48 and 72 hours compared to untreated controls (-). Black bars represent the total number of spheroids counted; green bars represent the number of GFP positive spheroids counted. Representative experiment shown, N=2. (D) Number of VAKshNuak1 colon-derived spheroids treated and graphed as per (C). (E) Representative images of brightfield and GFP in small intestine-derived spheroids treated for 24 hours with doxycycline as indicated. Scale bars = 500  $\mu$ m.

## 4.3 Discussion

In the investigations of this chapter, it has been shown that Nuak1 has a minimal role in mouse normal intestinal homeostasis. No alterations in proliferation, cell death, or differentiation and cell lineage composition were observed in either the small intestine, or the colon by acute loss of Nuak1. To corroborate this data, wildtype organoid cultures were resistant to inhibition of Nuak1 by small molecule inhibitor, HTH-01-015 up to 48 hours and furthermore, both short term and long term whole body induction of DI-shNuak1 *in vivo* presented no obvious detrimental phenotypes. Together, this data strengthens Nuak1's position as a targeted therapy, suggesting that inhibition of NUA1 in cancer patients would have limited side effects.

On the other hand, NUA1 expression has been detected at higher levels in tumour cells than in adjacent normal epithelial cells in gastric cancer (Ye et al., 2014). The data in this chapter supports this finding as a drastic upregulation of Nuak1 mRNA was observed in intestinal tumour epithelium compared to normal intestinal epithelium.

It is now well accepted that the changes following loss of APC during the initiation of tumorigenesis are entirely dependent on functional c-MYC (Sansom et al., 2007), therefore this study aimed to investigate Nuak1's role in this context considering previous findings that NUA1 is synthetic lethal with overexpressed c-MYC (Liu et al., 2012). Surprisingly, no morphological changes were observed in *VillinCreER<sup>T2</sup>;Apc<sup>fl/fl</sup>;Nuak1<sup>fl/fl</sup>* compared to *VillinCreER<sup>T2</sup>;Apc<sup>fl/fl</sup>* controls after acute activation of transgenes. However, it is important to note that synthetic lethality may be a context dependent phenomenon that relies heavily on the level of c-Myc overexpression. For example, Liu et al. did not observe synthetic lethality in osteosarcoma sarcoma cell line, U2OS until c-Myc levels were acutely deregulated by activation of c-MYC fused to the oestrogen receptor ligand binding domain (MYC-ER). It may be that a threshold of c-Myc overexpression is required for dependence upon Nuak1, which is not reached in the Apc null conditions. It would be very interesting to add an additional method of c-Myc activation to investigate the effect of increasing levels of c-Myc expression in this experimental context.

MYC can regulate up to 15% of all human genes and therefore is involved in a complex network of cellular processes including proliferation, apoptosis, cell cycle regulation, protein synthesis, metabolism and differentiation (Fernandez et al., 2003, Orian et al., 2003). Therefore, c-MYC is required to function in many different contexts and it is

possible that the requirement for Nuak1 is not present in the context of acute loss of Apc in the mouse small intestine. Moreover, Liu et al. found that AMPK was also synthetic lethal with deregulated c-MYC, so it may be that AMPK or another member of the AMPK-RKs such as NUA2, is able to compensate for NUA1's role here. This seems plausible due to the very low basal levels of Nuak1 expression in wildtype small intestine, however the effect of acute loss of APC on NUA1, AMPK and NUA2 expression has not yet been investigated.

Importantly, Nuak1 is necessary for the formation of colonic tumours in the *Villin-CreER<sup>T2</sup>;Apc<sup>fl/+</sup>;LSL-KRas<sup>G12D/+</sup>* (VAK) mouse model for sporadic intestinal cancer. Nuak1 depletion in these mice caused dramatic suppression in the development of colon tumours as measured by tumour number, total burden and individual tumour size. However, this did not convey a survival benefit as Nuak1 depleted mice were harvested at a clinical endpoint due to their small intestine tumour burden, which remained unchanged from controls. Interestingly, all tumours isolated from the small intestine of the Nuak1 depleted cohort retained Nuak1 mRNA suggesting that *Cre*-mediated recombination had not been completely efficient. Additionally, this study has presented strong evidence in multiple experimental settings to suggest that there is a selective pressure for cells to retain Nuak1, which then conveys a survival advantage in tumour development where these cells can out-compete Nuak1 depleted cells. This is not the first time it has been shown that Nuak1 conveys a survival advantage; as previously mentioned Liu et al. showed in an intervention study where tumours were allowed to develop before Nuak1 was targeted by shRNA, the tumours that survived retained Nuak1. Furthermore, tumour relapse was accompanied by re-expression of Nuak1 mRNA (Liu et al.2012).

In order to overcome cells 'escaping' *Cre recombinase*-mediated excision in the intestine, an increased tamoxifen induction of one day of 120mg/kg, and then 3 consecutive days of 80mg/kg injections was performed. As expected, the increased tamoxifen induction initiated *Apc* loss in a higher number of epithelial cells than with the low tamoxifen dose. However, this led to increased hyperplasia throughout the intestine that the mouse could not sustain and resulted in a reduced median survival from 110 days post induction (dpi) to 69 dpi in VAK controls and 127 dpi to 116 dpi for VAKN Nuak1 floxed mice. Additionally, this reduced the number of developed tumours observed, as the mice needed to be sacrificed at an earlier stage. Therefore, it was not possible to recapitulate the previous data due to technical issues, however, this data does imply that the *Cre* recombinase is efficient in the induction of at least the *Apc* and *KRas* alleles as the related

phenotype escalated with the increased tamoxifen dose. It cannot confirm however, whether *Cre recombinase*, expressed from the Villin promoter, has sufficient access to the Nuak1 floxed allele locus for efficient and high frequency recombination and this may be an explanation for the presence of Nuak1 retaining cells after excision. It has been reported that the efficiency of *Cre recombinase* to recombine different alleles varies depending on several factors including the distance between Lox P sites, target gene expression levels, and the chromatin structure of target genes (Vooijs et al., 2001).

Measurable Nuak1 mRNA levels were observed in VAKN mouse tissues by RT q-PCR analysis, however, due to the nature of this experiment, the analysis is performed on a piece of tissue that includes a mixture of many cell types for example, epithelial, stromal, muscle etc. As *Villin-CreER<sup>T2</sup>* is only expressed in epithelial cells, Nuak1 depletion will only occur in these cells. All other cell types in the intestine will retain Nuak1 resulting in increased variation, the possibility of data distortion and an inaccurate representation of Nuak1 depletion in epithelial cells. Therefore, Nuak1 immunohistochemistry (IHC) and Nuak1 RNA *in situ* hybridization (ISH) was performed on paraffin embedded tissue samples. Unfortunately, the Nuak1 IHC appeared inconclusive, as background levels were high, there was signal in the wildtype tissue and no apparent depletion in the Nuak1 floxed tissues was observed. However, the Nuak1 ISH (Figure 4.8) corroborated with the previous realtime Q-PCR data (Figure 4.7E and F) to suggest that there are very low levels of Nuak1 present in normal colon epithelium and expression is enriched drastically in tumour epithelium. Although some Nuak1 ISH was observed in the Nuak1 floxed VAKN tumours it was considerably lower than the wildtype VAK tumours suggesting that depletion has occurred. Similarly, reduced levels of Nuak1 mRNA were observed in the *Villin-CreER<sup>T2</sup>;Apc<sup>fl/fl</sup>;DI-shNuak1* after 72 hours of shRNA activation. The principle of *in situ* hybridization (ISH) is the specific annealing of a labelled probe to complementary sequences of a target nucleic acid (DNA or mRNA), followed by detection and visualization (Carter et al., 2010). The *Nuak1 fl/fl* allele contains lox P sites at exon 3 at the endogenous locus and results in a non-functional protein after *Cre recombinase* excision however it is possible that some mRNA is still transcribed. Additionally, shRNA targets complementary mRNA for degradation as it is transcribed, therefore 'knockdown' is never 100% complete. It is important in these cases to have multiple methods of Nuak1 detection to measure depletion. For example, in the *Villin-CreER<sup>T2</sup>;Apc<sup>fl/fl</sup>;DI-shNuak1* cohorts it was possible to trace shRNA expression via fluorescent markers and observe efficient depletion of Nuak1 in MEFs derived from these mice confirming that the shRNA is on target. Nuak1 ISH in the mouse tissues also confirmed that Nuak1 mRNA is present in the

epithelium as well as the stroma corroborating the human TMA data in Chapter 1 (see Section 3.2.2).

The data in this chapter confirms that Nuak1 is necessary for the survival of established colorectal tumours and downregulation of Nuak1 by doxycycline inducible-shRNA in the *Villin-CreER<sup>T2</sup>;Apc<sup>fl/+</sup>;DI-shNuak1*, DSS model for colon carcinogenesis worked therapeutically to reduce tumour number, burden, and tumour size within 72 hours. This is a crucial result as cancer patients always present with established tumours and this strengthens the argument that NUAK1 could be a therapeutic target for colorectal cancer. The analysis of tumours harvested 72 hours post shRNA induction suggests that loss of Nuak1 leads to increased cell death and decreased cell proliferation. Once again, tumours retaining Nuak1 expression were identified and these appeared to have a survival advantage over Nuak1 depleted tumours. Furthermore, spheroids generated from *Villin-CreER<sup>T2</sup>;Apc<sup>fl/fl</sup>;KRas<sup>G12D/+</sup>;DI-shNuak1* provided additional evidence that Nuak1 depleted spheroids are selected against over 72 hours.

Despite increased apoptosis and reduced proliferation, the mechanism by which Nuak1 is required by tumour cells remains unclear. Nuak1 clearly has an important role in the regulation of cell proliferation. Liu et al. showed that depletion of NUAK1 by siRNA led to suppression of human tumour cell proliferation in 5/14 cell lines, two of which were CRC cell lines LS174T and Colo 320. Additionally, depletion of NUAK1 delayed progression through all phases of the cell cycle demonstrating that NUAK1 regulates cell growth (Liu et al., 2012). Another study revealed that NUAK1 inhibitors, WZ4003 and HTH-01-015, NUAK1 knockout and NUAK1 shRNA knockdown are able to inhibit proliferation of MEFs and U2OS cells *in vitro* (Banerjee et al., 2014a). In conclusion, these studies demonstrate that NUAK1 is required for the positive regulation of cell proliferation. Hou et al. also suggested that NUAK1 regulates cell proliferation in tumour cells however the proposed mechanism was that NUAK1 exerts tumour suppression through direct interaction with p53. This is contradictory to the phenotype presented in this study, however, this was dependent upon tumour suppressor, LKB1 activation and may be context dependent (Hou et al., 2011).

Interestingly, it appears that healthy wildtype stem cells both *in vivo* and *ex vivo* do not require Nuak1 for cell proliferation. Therefore it is clear that there is a requirement for Nuak1 in transformed tumour cells that is not present in healthy wildtype cells. This data suggests that tumour cells are able to upregulate NUAK1 expression during

tumourigenesis in order to maintain a survival advantage. During the process of carcinogenesis, cancer cells acquire many traits that differentiate them from normal healthy cells. Some of these hallmarks include sustained proliferation, deregulated metabolism, the ability to resist cell death, and activation of invasion and metastasis, many of which NUA1 has previously been associated with. Solid tumours develop hostile microenvironments characterised by poor oxygen, low nutrient supply and irregular vascularization. Healthy cells can modulate anabolic and catabolic pathways in response to changes in nutrient availability. Cancer cells, on the other hand, upregulate growth even under nutrient scarcity and constitutive activation of growth-promoting pathways often results in the dependence on certain pathways or proteins (Ackerman and Simon, 2014). Only cancer cells that have acquired the ability to survive in this unfavourable microenvironment will persist. AMPK is activated under various stress conditions where the cellular ATP concentration decreases and plays a key role in cellular adaptive responses to maintain energy balance; it may be that NUA1 is activated in a similar manner within a tumour environment only. Previous studies have observed NUA1 activation in response to increased AMP levels and nutrient starvation (Suzuki et al., 2003b). NUA1, AKT, and AMPK appear to be required for the mechanism of tolerance to nutrient starvation (Izuishi et al., 2000, Esumi et al., 2002, Hashimoto et al., 2002). AKT is well-known as a cell survival factor, and is activated by several growth factors via phosphatidylinositol-3 kinase, PDK1, or Rac/Cdc42 (Kennedy et al., 1997, Delcommenne et al., 1998, Datta et al., 1997, Higuchi et al., 2001, Brazil et al., 2002). Activated AKT subsequently inhibits cell death-promoting factors, including Bad, Forkhead, caspase 9, and Mdm2 (Brazil et al., 2002). Additionally, AMPK also acts as a cell survival factor, however, it is unclear how activation confers tolerance to nutrient starvation (Izuishi et al., 2000, Esumi et al., 2002, Hashimoto et al., 2002, Kato et al., 2002). Suzuki et al., (2003) reported that AKT phosphorylates NUA1 in response to nutrient starvation independently of AMPK. Activated NUA1 resulted in induction of cell survival via inhibition of cell-death-associated factor, caspase 8 suggesting that NUA1 itself is also a cell survival factor in conditions of nutrient starvation. This mechanism may also play a role in tumour cells requirement for Nuak1 during tumourigenesis, however, further analysis is required to prove or disprove this hypothesis.

In the next chapter this study will address the mechanism by which intestinal tumour cells depend upon NUA1 for survival.

# Chapter 5 NUAK1 is required for the detoxification of ROS

## 5.1 Introduction

In normal cells, reactive oxidants are produced in a controlled manner and some serve as signalling molecules to regulate functions such as cell division, inflammation, immune function, autophagy, and stress response. Reactive oxidants include reactive oxygen species or ROS (i.e.  $O_2^{\bullet-}$ ,  $H_2O_2$ ,  $\bullet OH$ ,  $RO_2\bullet$ ,  $RO\bullet$ ,  $^1O_2$ , and  $O_3$ ) and reactive nitrogen species or RNS (i.e.  $\bullet NO$ ,  $\bullet NO_2$ , and  $ONOO^-$ ). ROS is predominantly produced in the mitochondria as a consequence of aerobic respiration and in addition to this, most enzymes produce ROS as a by-product when they use molecular oxygen as a substrate. RNS are formed during the reaction of nitric oxide synthesis (NO) by NO synthase. NO can then react with other molecules to generate other RNS with stronger oxidant properties (Ma, 2013). Uncontrolled production of ROS results in oxidative stress that disrupts cellular processes and contributes to tumourigenesis, chronic disease and toxicity. Therefore in order to maintain the redox homeostasis, cells depend on the activation of the NRF2-antioxidant response pathway to detoxify and eliminate ROS and electrophilic agents (Nguyen et al., 2009b).

The transcription factor nuclear factor erythroid 2 (NF-E2)-related factor 2 (NRF2) is a member of the Cap 'N' Collar (CNC) family that contains a conserved basic leucine zipper (bZIP) structure. Studies investigating Nrf2 knockout mice have demonstrated that loss of Nrf2 increases susceptibility to a broad range of chemical toxicity and disease conditions related to oxidative pathology (Ma, 2013). The primary role of NRF2 is to induce the transcription of a wide array of genes that are able to detoxify ROS and thereby prevent the harmful effects of extrinsic and intrinsic insults (Moi et al., 1994). NRF2 binds to a common DNA sequence called antioxidant response element (ARE) in its transcriptional targets, and a genomic-scale search for NRF2 target genes identified many ARE-containing genes with known roles in oxidant homeostasis in addition to drug metabolism (Hayes et al., 2010). The ARE-regulated genes can be divided into three distinct groups: 1) drug metabolising enzymes (DMEs) by which NRF2 is able to control the metabolic fate of numerous pro-oxidants and electrophiles in an organism, 2) anti-oxidant defence genes which allow NRF2 to maintain homeostasis of ROS and RNS via several defence mechanisms, and 3) oxidant signalling proteins that influence a number of programmed

cellular functions such as autophagy, apoptosis and inflammation (See Table 5.1 for more information).

Under basal conditions, NRF2 has a rapid half-life of ~20 min, which results in low protein abundance in many cell types (Zhang et al., 2004). The canonical NRF2 regulator is KEAP1 (Figure 5.1A). NRF2 is sequestered in the cytoplasm by KEAP1, which results in its continuous ubiquitinyation and subsequent degradation by the proteasome (Itoh et al., 1999). KEAP1 contains cysteine residues that are targeted for oxidation in the presence of ROS or electrophilic cell stress, resulting in the release of NRF2 and its translocation to the nucleus. Here it can activate its transcriptional targets, which are mentioned above (Dinkova-Kostova et al., 2002).

In the KEAP1/NRF2 system, GSK3 $\beta$  is known to be a major regulator in the export of NRF2 from the nucleus (Figure 5.1B). GSK3 $\beta$  activates Fyn, which subsequently phosphorylates NRF2 at Y568, a prerequisite for nuclear export of NRF2 (Salazar et al., 2006, Rojo et al., 2008). Independently, GSK3 $\beta$  has also been shown to phosphorylate NRF2 directly at a cluster of serines. This allows the ubiquitin E3 ligase complex SCF/ $\beta$ -TrCP to associate with NRF2 and present it for KEAP1-independent proteasomal degradation (Chowdhry et al., 2013, Rada et al., 2011) (Figure 1A). In both mechanisms, either by supporting nuclear export or degradation in the cytosol, active GSK3 $\beta$  turns off NRF2 signalling.

**Table 5.1 - Genes regulated by NRF2 involved in oxidant response and redox signalling.** Figure adapted from Ma, 2013, supplementary table 1.

Drug metabolism and disposition		Antioxidant defense		Oxidant signaling and function	
Function	Gene Product	Function	Gene Product	Function	Gene Product
<b>Oxidation</b>		<b>Drug Transport</b>		<b>Stress response protein</b>	
Cytochrome P450	CYP2A5	Multidrug resistance-associated protein	MRP2, MRP3	Heme oxygenase	HO-1
Aldehyde dehydrogenase	ALDH3A1	<b>ROS catabolism</b>		<b>Autophagy</b>	
Alcohol dehydrogenase 7	ADH7	Superoxide dismutase 3	SOD3	p62 protein	p62
<b>Reduction</b>		Glutathione peroxidase	GPx2, 3, 6, 8	<b>Mitochondrial apoptosis</b>	
NAD(P)H:quinone oxidoreductase	NQO1	Peroxioredoxin	Prx1, Prx6	Parkinson disease 7	PARK7 (DJ-1)
Aldo-keto-reductase	AKR1B3, 1B8, 1C2	<b>Regeneration of oxidised factor</b>		<b>Mitochondrial biogenesis</b>	
<b>Conjugation</b>		Glutathione reductase	GSR1	Nuclear respiratory factor 1	NRF-1
UDP-glucuronosyltransferase	UGT1A1, 1A6, 1A9, 2B7	Thioredoxin	TrxR1	<b>Growth factor signaling</b>	
Sulfotransferase	SULT3A1	Sulfiredoxin	Srx1	Protein tyrosine phosphatase	PTP1
<b>Nucleophilic trapping</b>		<b>Synthesis of reducing factor</b>		Protein tyrosine phosphatase receptor	PTPRB
Glutathione S-transferase	GSTA2, A1, A3, P1, MGST1	Glutamate-cysteine ligase	GCLC (catalytic), GCLM (regulatory)	<b>Inflammation (COPD)</b>	
Epoxide hydrolase	EPHX1 (mEH)	Glucose-6-phosphate dehydrogenase	G6PDH	a1-antitrypsin	A1AT
Esterase	ES-10	Phosphogluconate dehydrogenase	6PGD	Secretory leukoprotease inhibitor	SLP1
		<b>Antioxidant protein and inhibitor</b>			
		Thioredoxin	Trx		
		Thioredoxin interacting protein	TXNIP		
		<b>Redox transport</b>			
		Cystine/glutamate transporter	SLC7A11 (xCT)		
		<b>Metal-binding protein</b>			
		Metallothionein	MT1, MT2		
		Ferritin	FTL (light chain), FTH (heavy chain)		

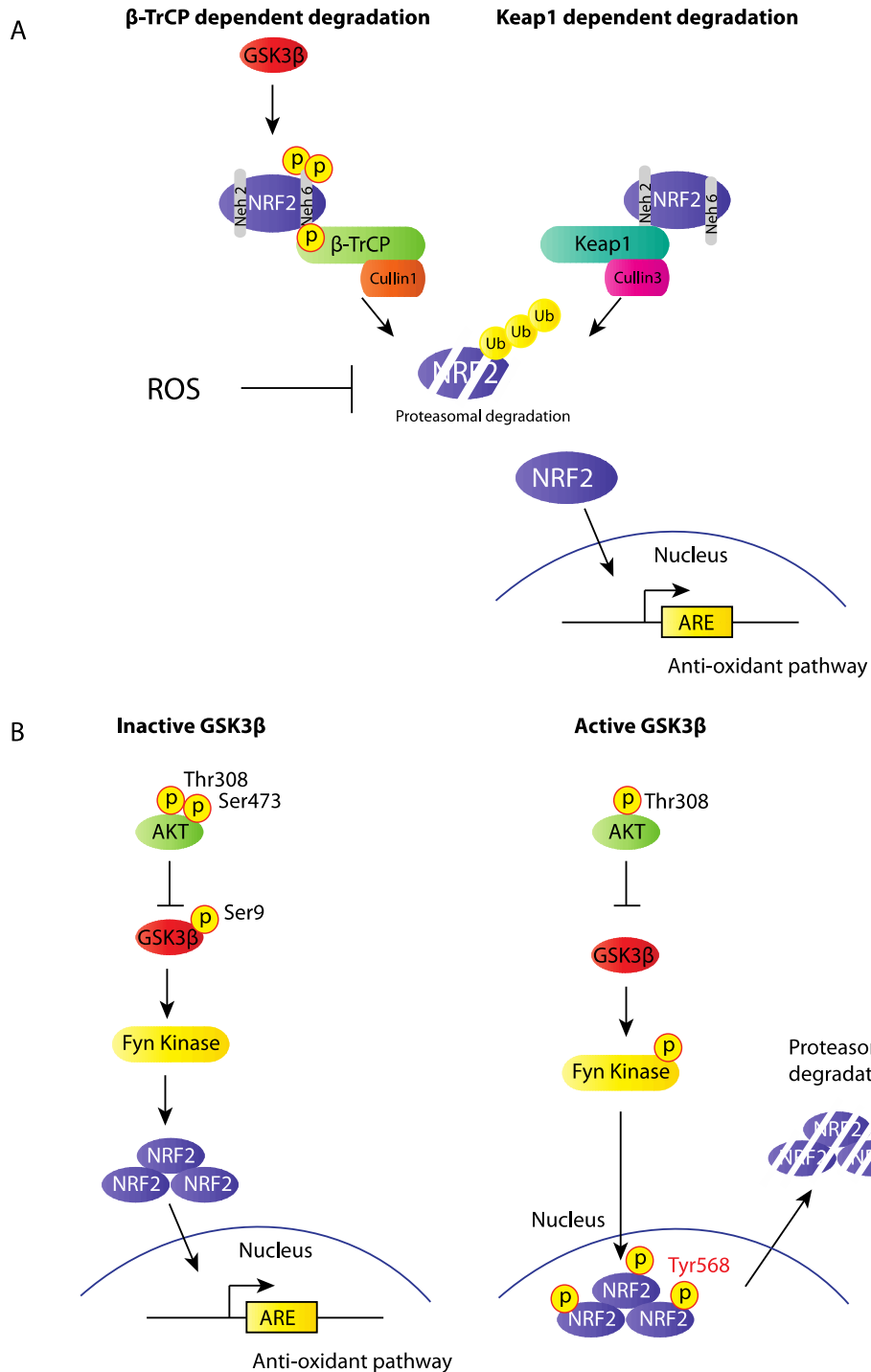


### Figure 5. 1 - NRF2 regulation

(A) Schematic of β-TrCP dependent (left) and KEAP1 dependent (right) degradation of NRF2. In β-TrCP dependent degradation, GSK3β phosphorylates NRF2 at a cluster of serines within the Neh 6 domain of NRF2 that overlaps with an SCF/β-TrCP destruction motif and promotes its degradation by the proteasome in a KEAP1-independent manner. Without GSK3β phosphorylation, NRF2 is free to localise to the nucleus and upregulate the oxidative response. In KEAP1 dependent degradation, in the absence of ROS or electrophiles KEAP1 associates with NRF2 and targets it for proteasomal degradation. In the presence of ROS or electrophiles, three cysteine residues on KEAP1 are modified leading to altered conformation of KEAP1 so that it can no longer associate with NRF2, NRF2 is then free to localise to the nucleus. (B) Schematic of another GSK3β mechanism in NRF2 control. In the KEAP1/NRF2 system, GSK3β is known to be a major regulator in the export of NRF2 from the nucleus. GSK3β phosphorylates and activates Fyn, which subsequently phosphorylates NRF2 at Tyr-568, a prerequisite for NRF2 export from the nucleus. After export, NRF2 is targeted for proteasomal degradation by KEAP1 as above.

NRF2 can act as both a tumour suppressor and an oncogene in tumourigenesis. This can be attributed to the pro-tumourigenic effects of low levels of ROS, for example the induction of sporadic mutations, and the anti-tumourigenic effects of high levels of ROS, which become cytotoxic if uncontrolled.

Several studies have demonstrated that Nrf2 prevents the formation of tumours in the stomach, bladder and skin in homozygous Nrf2 knockout mice treated with a chemical carcinogen (Ramos-Gomez et al., 2001, Osburn et al., 2007b, Khor et al., 2008, Fahey et al., 2002). It has been hypothesised that NRF2-mediated protection is due to the control of ROS and DNA damage in cells (Hirayama et al., 2003, Morito et al., 2003). Interestingly, a single nucleotide polymorphism (SNP) has been identified in the human *NRF2* gene that predisposes the patient to developing non-cell lung cancer (NSCLC) (Suzuki et al., 2013).

On the other hand, prolonged activation of NRF2 has been demonstrated in several types of cancer such as lung, breast, head and neck, ovarian and endometrial carcinomas (Singh et al., 2006, Shibata et al., 2011, Shibata et al., 2008b, Wang et al., 2008a, Jiang et al., 2010, Kim et al., 2010, Solis et al., 2010a, Zhang et al., 2010). Furthermore, high levels of NRF2 in tumours have been correlated with poor prognosis in cancer patients partly due to an increase in NRF2 dependent cell proliferation and resistance to chemotherapy and radiotherapy (Shibata et al., 2008a, Solis et al., 2010b, Sasaki et al., 2013).

It is also known that oncogene transformation is able to direct an increased activation of NRF2 and thereby suppress high ROS within tumours. NRF2 modulation was shown to impede K-Ras<sup>G12D</sup> – induced proliferation and tumourigenesis in a mouse model of Pancreatic Ductal Adenocarcinoma (DeNicola et al., 2011).

In the previous chapter it was demonstrated that Nuak1 is essential for the formation and survival of colorectal tumours and that acute loss of Nuak1 results in reduced proliferation and increased cell death. Based on these findings, the investigations of this chapter will strive to address the mechanism by which tumour cells depend upon NUAK1.

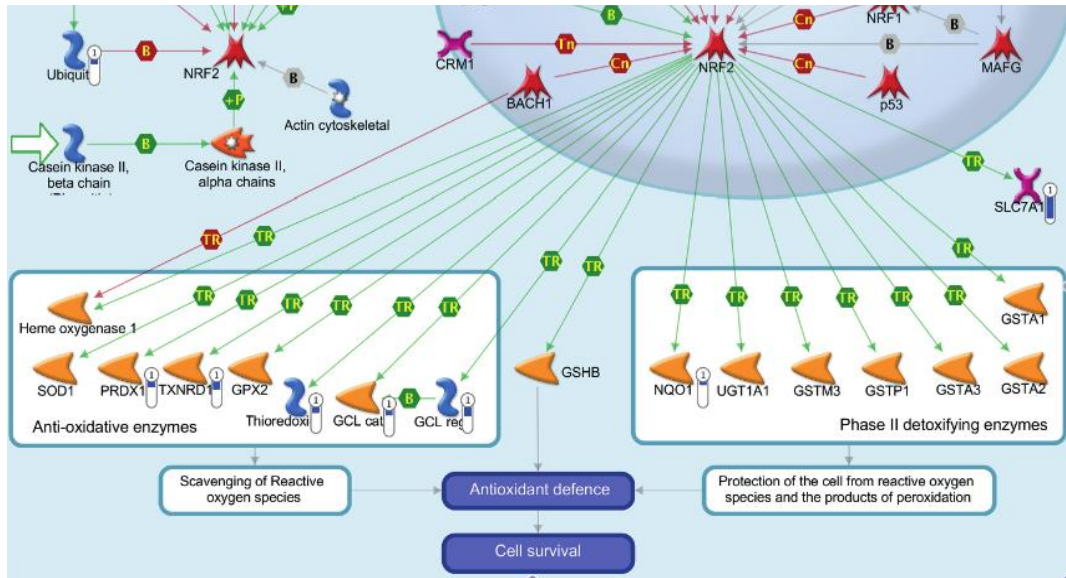
## 5.2 Results

### 5.2.1 NUAK1 suppression impairs the NRF2 antioxidant program

RNA-SEQ analysis showed that on suppression of NUAK1 by shRNA in U2OS cells, multiple NRF2 transcriptional targets are downregulated. This included a sub-set of antioxidant enzymes such as PRDX1, TXRND1, Thioredoxin, glutamate–cysteine ligase complex modifier subunit (GCLM) and GCL catalytic subunit (GCLC) and a sub-set of Phase II detoxifying enzymes such as NQO1 (Figure 5.2A). Metacore GeneGO pathway analysis revealed regulation of cholesterol synthesis, cell adhesion, NRF2 regulation of the oxidative stress response and glutathione metabolism were amongst the topmost pathways modulated upon NUAK1 depletion (Figure 5.2B). Encouragingly, NUAK1's role in the regulation of cell adhesion via PP1 $\beta$ <sup>MYPT1</sup> has been described previously (Zagorska et al., 2010), however modulation of NRF2 regulation of the oxidative stress response and glutathione metabolism suggested a novel role for NUAK1 in the oxidative stress response pathway. Figure 5.2C shows the downregulation of specific NRF2 transcriptional targets, GLCL, GCLM, GSHR, MGST and TXN.

Based on the finding above, the relationship between NUAK1 and NRF2 regulation was investigated using *in vitro* analysis of human colorectal cancer (CRC) cell lines, *ex vivo* mouse intestine-derived crypt cultures and *in vivo* analysis of our doxycycline inducible shNUAK1 colon tumour model introduced in Chapter 4.

A



B

Rank	Regulated Pathway	P-Value	FDR
1	SREBP Transcriptional control of Cholesterol & FA synthesis	1.89e-13	1.15e-10
2	Cell Adhesion, ECM Remodeling	1.25e-12	3.81e-10
3	Development, Role of IL8 in Angiogenesis	6.74e-8	1.37e-5
4	Oxidative stress, Role of Sirtuin1 and PGC1a	3.15e-7	4.81e-5
5	Cell Adhesion, Chemokines & Adhesion	8.34e-7	1.01e-4
6	<b>NRF2 regulation of Oxidative Stress response</b>	1.25e-6	1.27e-4
7	Regulation of Lipid Metabolism	9.92e-6	8.65e-4
8	<b>Glutathione Metabolism</b>	4.41e-5	3.35e-3
9	<b>Glutathione Metabolism, human version</b>	4.94e-5	3.35e-3
10	Cell Adhesion, Plasmin Signaling	6.72e-5	4.10e-3

C

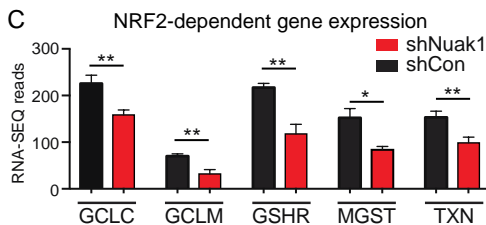


## Figure 5. 2 - NUAK1 suppression impairs the NRF2 anti-oxidant program

(A) Schematic from MetaCore GeneGO analysis from Thomson Reuters of RNA-Seq data to show modulation of targets downstream of Nrf2 in U2OS cells after depletion of NUAK1 by shRNA. (B) Top 10 pathways modulated in U2OS cells after depletion of NUAK1 by shRNA, identified by Metacore GeneGO analysis of RNA-Seq data. FDR = False discovery rate. Genes with corresponding Entrez ID's were entered into MetaCore and tested for enrichment in Maps, Diseases, GO processes, and GeneGO processes. Metacore uses a hypergeometric model to determine the significance of enrichment. (C) RNA-Seq read counts of select NRF2 targets from (A&B) Mean & SEM of 3 biological replicates shown; asterisks denote significance, unpaired T-test used. This work was performed by Dr. Nathiya Muthalagu.

### 5.2.1.1 NUAK1 suppression leads to increased cellular ROS

Transcriptional analysis of NUAK1 knockdown in U2OS cells revealed that NUAK1 has a role in the regulation of NRF2 and its downstream transcriptional targets, therefore it was hypothesised that increased cellular ROS levels would result as a consequence. Thus, using CellROX® Deep Red Reagent, ROS levels were measured in U2OS and the CRC cell lines after 8 hours of treatment with NUAK1 inhibitor, HTH-01-015 (10µM) by flow

cytometry. The CellROX® Deep Red reagent is a cell-permeant dye that does not fluoresce while in a reduced state and becomes fluorescent upon oxidation by ROS. HTH-01-015 caused a significant increase in oxidative stress in all cell lines suggesting that 8 hours of acute NUAK1 inhibition is enough to compromise the oxidative stress response (Figure 5.3A). In addition to this, *Villin-CreER<sup>T2</sup>;Apc<sup>fl/fl</sup>;Kras<sup>G12D/+</sup>* (VAK) small intestine-derived spheroids were incubated with HTH-01-015 (5 $\mu$ M) for 16 hours and oxidative stress measured using CellROX® green. It was necessary to change reagent as CellROX® green signal is stable for up to 24 hours, contrary to CellROX® deep red which is stable for up to 2 hours. While staining with 2D cells is instant, it takes longer for the stain to penetrate the matrigel in 3D cultures. Treatment with HTH-01-015 induced significantly more ROS than vehicle treated spheroids (Figure 5.3B & C).

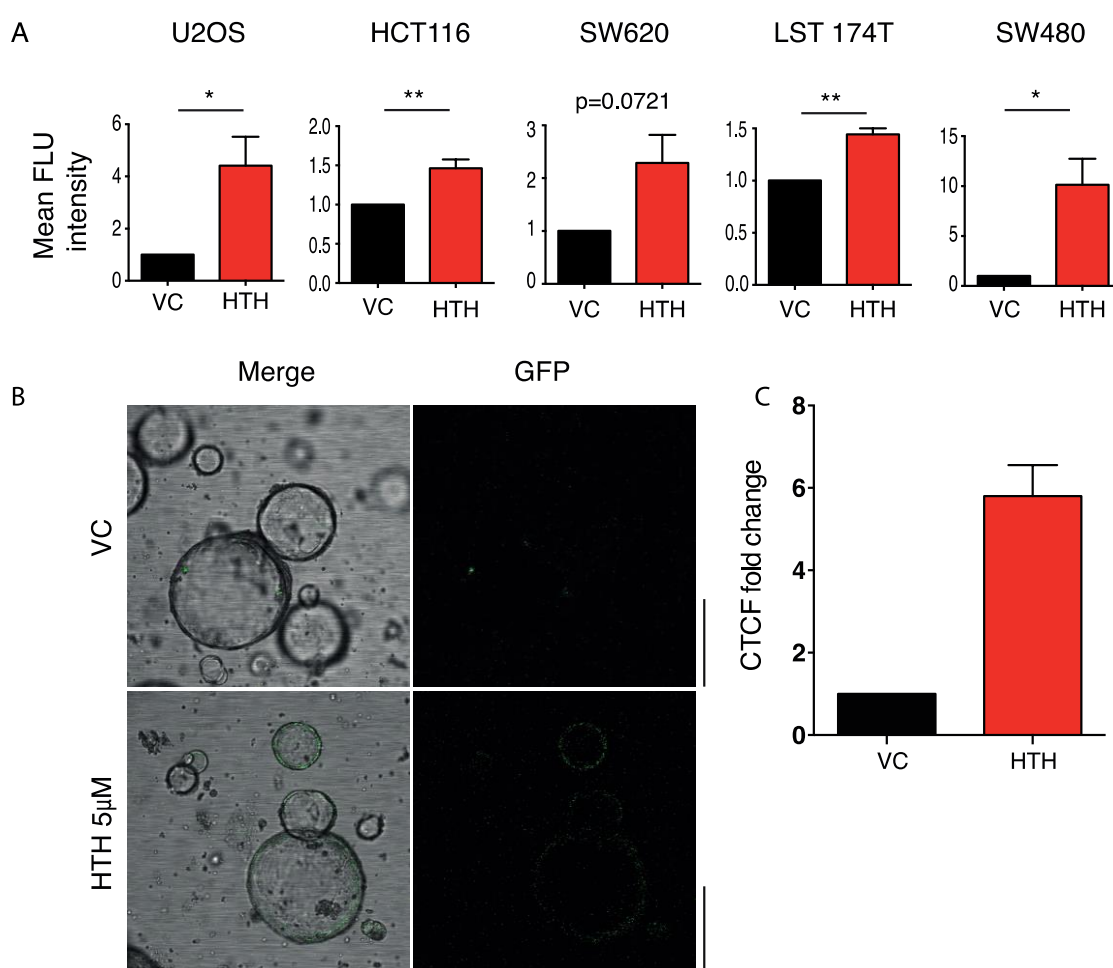


### Figure 5.3 - NUAK1 suppression leads to increased cellular ROS

(A) ROS levels in U2OS and CRC cell lines, HCT116, SW620, LS174T, and SW480 measured by FACS analysis of CellRox staining intensity upon acute inhibition of NUAK1 with HTH-01-015 10 $\mu$ M for 8 hours. Mean $\pm$ SEM from 3 independent experiments shown, asterisks denote significance, unpaired t-tests used. (B) Representative images of CellRox fluorescence of VAK spheroids after treatment with HTH-01-015 5 $\mu$ M for 16 hours. Scale bars = 200 $\mu$ m. (C) Quantification of spheroid fluorescence using ImageJ, corrected total cell fluorescence (CTCF) = Integrated density-(area of selected cell\*mean fluorescence of background). Representative experiment shown, N=41 spheroids counted per group from 3 technical triplicates, N=2. Figure 3 A was performed by Dr. Nathiya Muthalagu.

### 5.2.1.2 NUA1 suppression sensitises cells to hydrogen peroxide

Throughout this study two small interfering RNA (siRNA) sequences have been utilised for inducing silencing of NUA1 by RNA interference (RNAi). Initially both were investigated for on-target silencing of NUA1 protein as well as off-target silencing of fellow AMPK-RKs, AMPK and NUA2 proteins in SW480 cells. Both induced efficient silencing of NUA1 and did not affect AMPK or NUA2 at protein level (Figure 5.4).

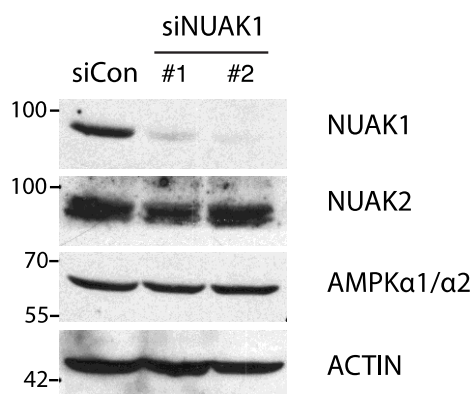


**Figure 5.4 - Small interfering RNA (siRNA) for the silencing of NUA1 are on target**  
Immunoblot showing NUA1 protein silencing by two siRNA sequences, #1 and #2 in SW480 cells. Neither siRNA showed silencing of NUA2 or AMPK $\alpha$ 1/ $\alpha$ 2. siRNA #1 was used at 40nM and siRNA #2 was used routinely at 10nM, samples were harvested 48 hours post transfection.

Oxidative stress is a consequence of the imbalance between rising ROS levels and the cells ability to scavenge them. Uncontrolled ROS will eventually result in cell death. To investigate whether the cells requirement for NUA1 is related to the inability to scavenge ROS, U2OS and the CRC cell lines were challenged with H<sub>2</sub>O<sub>2</sub> (1mM, 24 hours), 48 hours post transfection with siRNA for NUA1 (siNUAK1 #2) (Figure 5.5A-E). siNUAK1 #2 was used in this analysis as NUA1 depletion was more effective than siNUAK1 #1. Depletion of NUA1 alone did not lead to the substantial levels of cell death seen previously with the pharmacological inhibitors in Chapter 3, Section 3.2.3. However, NUA1 depleted cells were more sensitive to H<sub>2</sub>O<sub>2</sub> challenge resulting in at least a two-fold increase in cell death. This effect was observed in all cell lines and was measured by Annexin V FITC/Propidium Iodide apoptosis assay with flow cytometry.

As previously shown in Chapter 3, NUA1 can be detected easily at protein level only U2OS and SW480 cell lines, therefore NUA1 silencing was confirmed in U2OS cells by immunoblot (Figure 5.5B) and in the CRC cell lines by realtime qPCR analysis (Figure 5.5F). RNAi-mediated knockdown in U2OS and SW480 was successful, however, there

was only a two-fold reduction in SW620 and LS174T cells. Despite this, NUAK1 depletion was sufficient to result in a sensitisation to H<sub>2</sub>O<sub>2</sub> none the less.

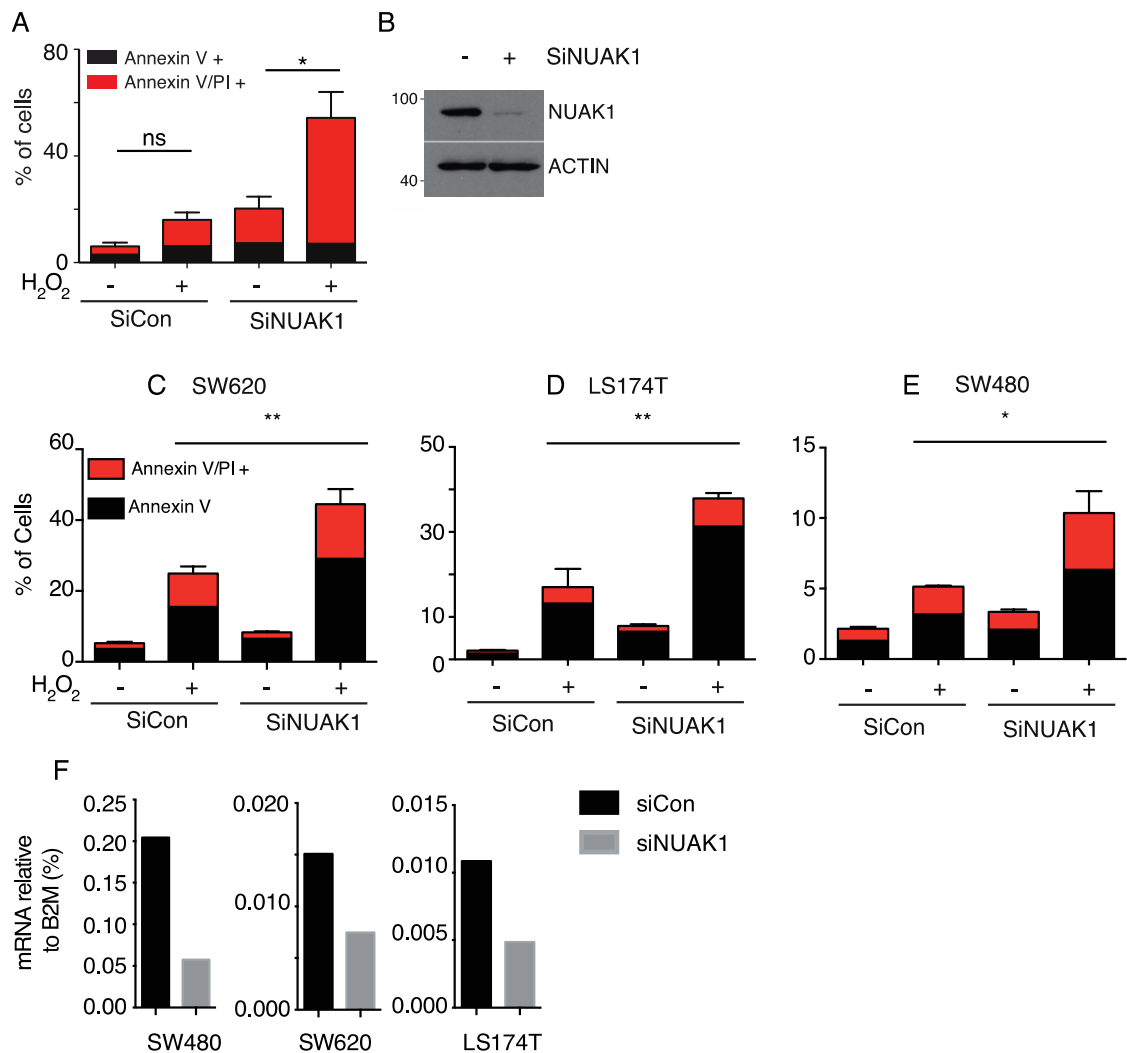


**Figure 5.5 - NUAK1 suppression sensitises cells to peroxide**

**(A)** Apoptosis induced by treatment of U2OS cells with 500μM H<sub>2</sub>O<sub>2</sub>, with and without prior depletion of NUAK1, measured at 24 hours. Mean±SEM of 3 independent experiments shown. **(B)** The immunoblot confirms depletion of NUAK1 by siNUAK1 #2. **(C-E)** Apoptosis induced by treatment of human CRC lines, SW620 **(C)**, LS174T **(D)** and SW480 **(E)** with 1mM H<sub>2</sub>O<sub>2</sub>, with and without prior depletion of NUAK1, measured at 24 hours. Mean & SEM of a representative result from 1 of 3 independent experiments are shown for each cell line. Asterisks denote significance, significance, 1-way ANOVA & post-hoc Tukey test used. **(F)** Real time qPCR analysis of NUAK1 expression after siRNA transfection in each of the CRC cell lines used above, β2-microglobulin (B2M) was used as the housekeeping gene control, one representative experiment of n>3 shown. Figures (5A+B) were performed by Dr. Nathiya Muthalagu.

### 5.2.1.3 HTH-induced cell death is rescued by addition of exogenous anti-oxidant *in vitro*

In order to confirm that suppression of ROS defences is the leading cause for cell death upon NUAK1 inhibition using HTH-01-015 in the CRC cell lines and spheroids, cells were pre-treated with an exogenous anti-oxidant.

Thus, SW620 and SW480 cells were pre-treated with Trolox (6-hydroxy-2,5,7,8-tetramethylchromane-2-carboxylic acid) for 8 hours and then treated with HTH-01-15 (48 hours; 10 $\mu$ M). Trolox is a derivative of vitamin E and is known to scavenge intracellular ROS (Hamad et al., 2010). Cell death was measured as before by Annexin V FITC/Propidium Iodide apoptosis assay with flow cytometry at 48 hours post drug addition. HTH-01-015 alone led to 80% cell death in SW620, and 60% cell death in SW480, corresponding to data in Chapter 3, Section 3.2.3, and combination with Trolox significantly reduced cell death to 40% in both cell lines (Figure 5.6A & B).

In addition to the 2D cell cultures, single cell suspensions of small intestine and colon-derived VAK stem cells were pre-treated with Trolox (500 $\mu$ M) for 16 hours, followed by treatment with 5 $\mu$ M HTH-01-015 (in the presence of Trolox or vehicle control) and analysed spheroid formation over 72 hours. Trolox was able to rescue spheroid number by more than two fold in both small intestine- and colon-derived spheroids. Interestingly, no HTH-01-015 effect was observed on the size of small intestine-derived spheroids, as measured by spheroid diameter, however the drug severely compromise colon-derived spheroid size as well as number. This was not rescued by the provision of Trolox indicating that there may be other Nuak1 functions contributing to this phenotype. Representative images show all experimental conditions (Figure 5.6C & D).

Overall this demonstrates that cytotoxic levels of ROS are the major reason for the cell death observed under suppression of NUA1.

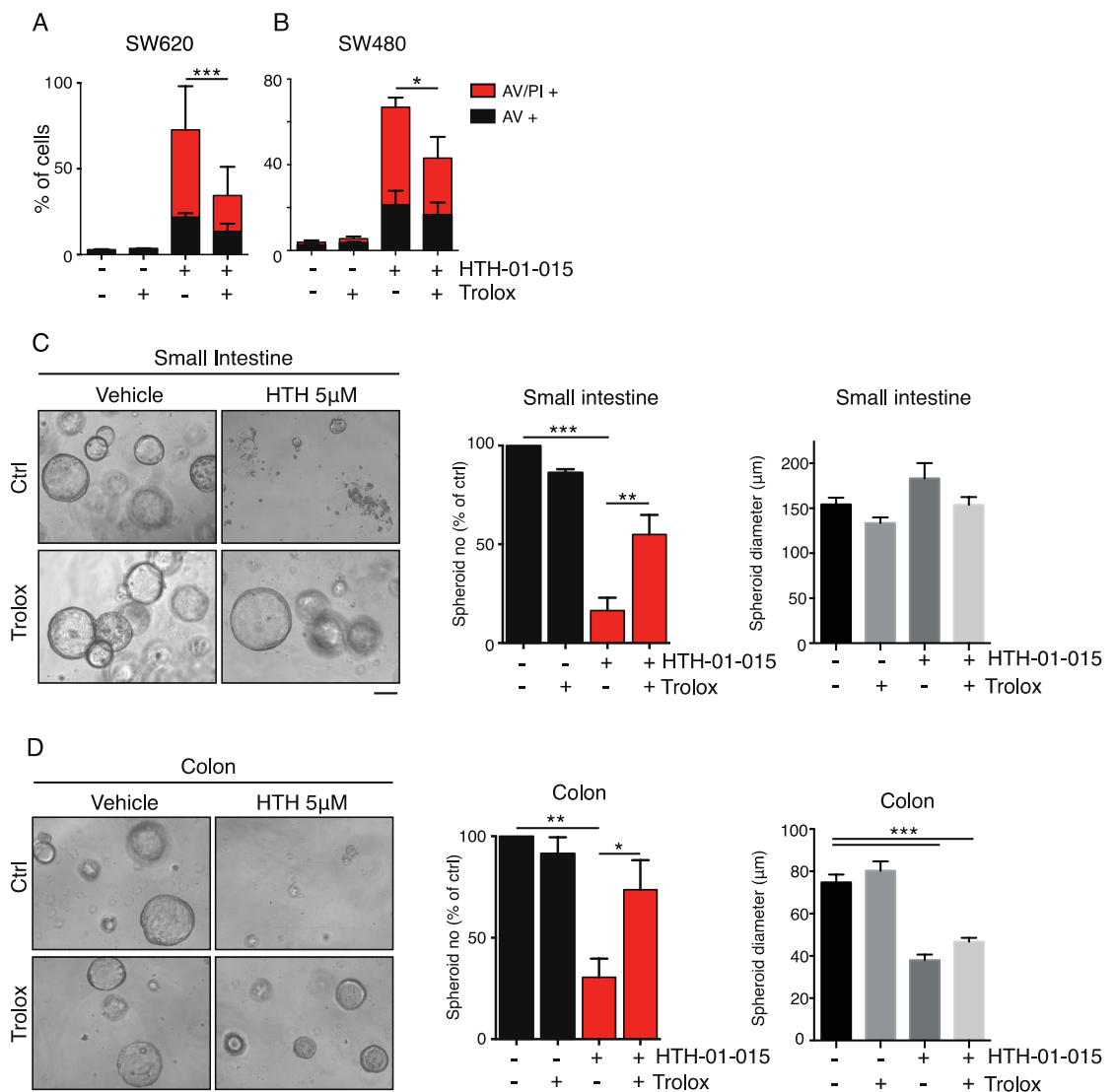


**Figure 5. 6 - HTH-induced cell death is rescued by addition of exogenous antioxidant**

Provision of exogenous antioxidant Trolox attenuates HTH-01-015-induced killing in human CRC lines SW620 (A) and SW480 (B). Mean±SEM of 3 independent experiments shown. Asterisks denote significance (1-way ANOVA & post-hoc Tukey test). (C) Representative images showing Trolox rescues growth of Small Intestine-derived VAK spheroids from Nuak1 inhibition (72 hours). Scale bar =100μm. Left panel shows quantification of spheroids after Nuak1 inhibition in the presence and absence of Trolox (500μM). Asterisks denote significance (1-way ANOVA & post-hoc Tukey test). Right panel shows average spheroid diameter, mean±SEM of 3 independent experiments, normalized to vehicle treated controls are shown. Right panel shows average spheroid diameter (μm), mean±SEM of control, Trolox, Trolox + HTH-01-015 n>50, HTH-01-05 n=24 from one representative experiment, one-way ANOVA & post-hoc Tukey test found no significance. (D) Same as in (C) but for Colon-derived spheroids, control, Trolox, Trolox + HTH-01-015 n>100, HTH-01-05 n=53, asterisks denote significance, 1-way ANOVA & post-hoc Tukey test performed. Figures (6A+B) were performed by Dr. Nathiya Muthalagu.

### **5.2.2 Tumour suppressive effect of Nuak1 depletion is a consequence of increased ROS, which can be reversed by exogenous provision of NAC *in vivo***

In the previous chapter, Nuak1 depletion by *DI-shNuak1* resulted in reduced proliferation and increased cell death in tumours. The data within this chapter strongly suggests that NUAK1 is promoting the NRF2 anti-oxidant defence system in tumours cells *in vitro* and *ex vivo* therefore it was assessed whether this mechanism was responsible for the reduced tumour burden after acute Nuak1 suppression *in vivo* (see Chapter 4, Section 4.2.6.2).

Initially, tumours were assessed for 8-Oxo-2'-deoxyguanosine (8-oxo-dG), which is an oxidized derivative of deoxyguanosine. 8-Oxo-dG is one of the major products of DNA oxidation and can be used as a measurement of oxidative stress (de Souza-Pinto et al., 2001). Total quantification of individual tumours for 8-oxo-dG staining showed that there was a significant increase in 8-oxo-dG positive cells in tumours derived from shNuak1 mice compared to controls (Figure 5.7A & B). Visually it was also apparent that Nuak1 retaining *DI-shNuak1* tumours had levels of 8-oxo-dG staining comparable to controls.

In order to investigate ROS in a more physiologically relevant context, tumours were investigated for ROS immediately prior to harvest (*ex vivo*) using the Licor ROSstar<sup>TM</sup> 800cW probe, a near-infrared hydrocyanine probe for imaging of extracellular ROS. In its reduced state, the probe is cell-impermeable and non-fluorescent, however upon oxidation by ROS, produces fluorescence making it suitable for *in vivo* imaging. *Villin-CreER<sup>T2</sup>;Apc<sup>fl/+</sup>;DI-shNUAK1.1533* mice were induced as before, with one 80mg/kg tamoxifen, followed by DSS treatment. At 68 days post induction, mice were treated with Doxycycline to activate the shRNA specific for Nuak1 for two days preceding harvest. Sixteen hours prior to harvest, mice were injected with the Licor ROSstar<sup>TM</sup> 800cW probe. Mice were then harvested, and the colon dissected and imaged using a Pearl Trilogy Small Animal Imaging System. Imaging of tumour bearing shNuak1 and control mice revealed elevated ROS levels in colonic tumours *in situ* after just two days of NUAK1 depletion compared to controls (Figure 5.7C).

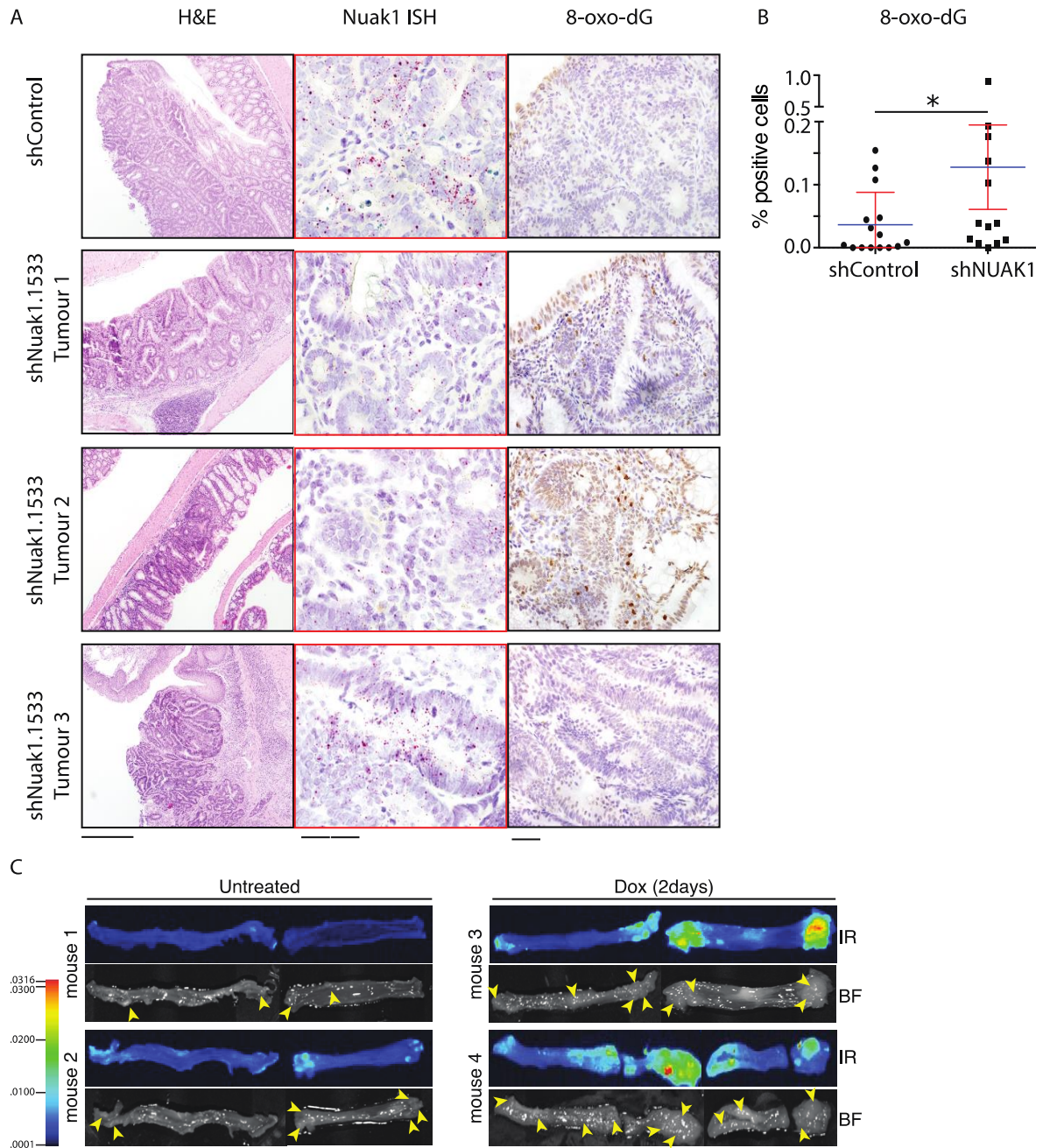


### Figure 5.7 - Acute loss of Nuak1 results in increased ROS in tumours

(A) Representative images of H&E staining, Nuak1 RNA *in situ* hybridisation (ISH) with inset zoom (200%) highlighted in red, and 8-Oxo-2'-deoxyguanosine (8-oxo-dG) IHC for an shControl tumour (top panel) and *DI-shNuak1.1533* tumours 1-3 (middle and bottom panels). All tumours were harvested 3 days post shRNA induction, 70 days post tamoxifen induction. Scale bars from left to right =100µm, 20µm, 10µm. (B) Quantification of % positive 8-oxo-dG cells by IHC in individual tumours harvested at 3 days for controls (n=22 tumours), and shNuak1 (combined alleles; n=18 tumours). Each point on the graph represents a tumour that was scored individually, errors bars show SEM. Red asterisks indicate significance (Mann Whitney Test). (C) Licor ROSStar<sup>TM</sup> *ex vivo* detection of ROS in colonic tumours induced to express shNuak1.1533 for 2 days, compared with non-induced controls.

Finally, *Villin-CreER<sup>T2</sup>;Apc<sup>fl/+</sup>;DI-shNUAK1.1533* mice, induced as above, were pre-treated with antioxidant N-Acetyl-Cysteine (NAC) in drinking water (4%) at 60 days post induction. At 63 dpi, the shRNA was induced by doxycycline treatment for 1 week preceding harvest. NAC exhibits direct and indirect antioxidant properties as it can detoxify ROS itself, as well as act as a precursor for Glutathione (GSH), another crucial antioxidant for the protection of cells against toxic agents (Dekhuijzen, 2004). Mice were harvested at 70 days post induction and tumours analysed. Results showed that exogenous provision of NAC reversed the tumour suppressive effect of Nuak1 depletion (Figure 5.8A & B) and had no effect on Nuak1 wildtype controls (Figure 5.8C).

These results suggest that impairment of the cellular anti-oxidant defence pathway is the underlying mechanism of tumour loss after acute Nuak1 suppression in the colon, and that current findings *in vitro*, translate *in vivo*.

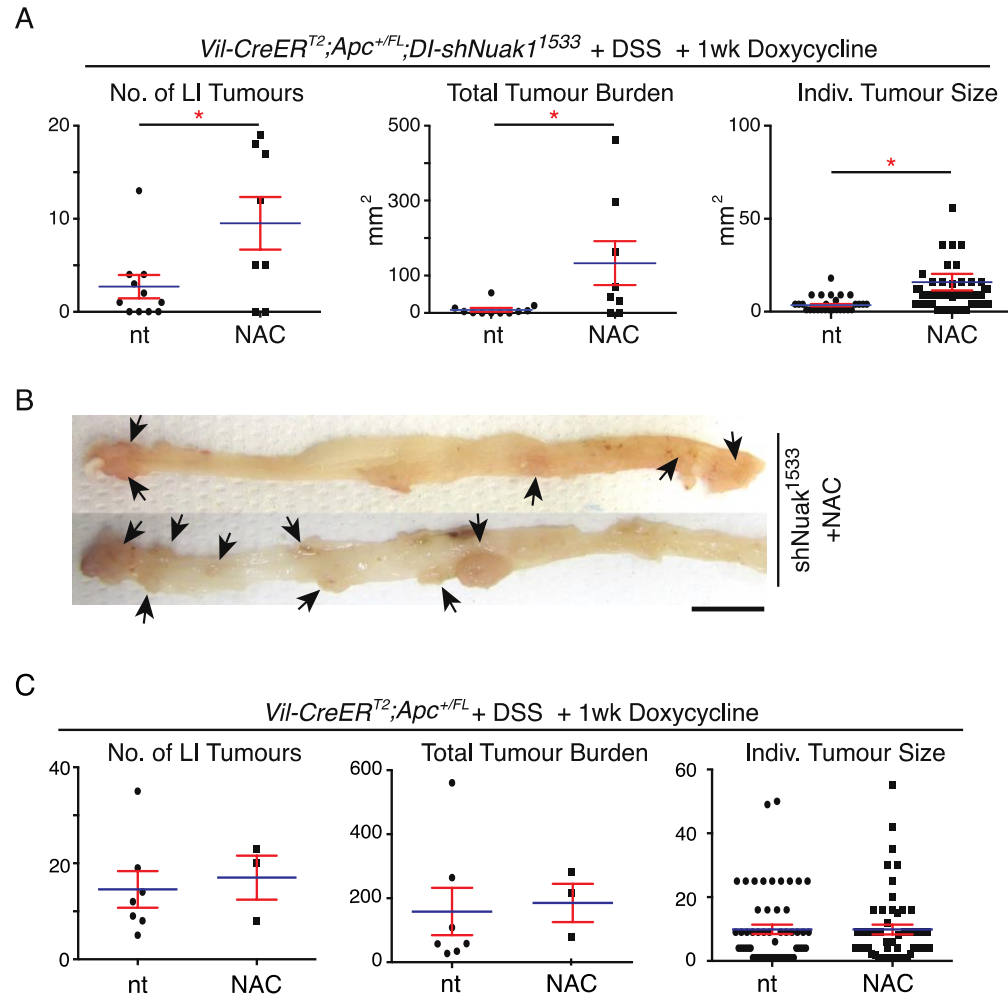


**Figure 5. 8 - NUAK1 addicted tumours are rescued by addition of exogenous anti-oxidant**

(A) Tumour number, total tumour burden and individual tumour size in DSS-treated *Vil-CreER<sup>T2</sup>;Apc<sup>fl/+</sup>* (VA) mice after 7 days of Nuak1 depletion in the gut using *DI-shNuak1.1533*, in mice given N-Acetyl-Cysteine (NAC, N=8) compared with no exogenous anti-oxidant (nt). Note that the nt data are the same used in Section 4.2.6.2, Figure 16. Red asterisks indicate significance (1-way ANOVA & post-hoc Tukey test). (B) Representative images of dissected colons from NAC treated *DI-shNuak1.1533* expressing mice. Arrowheads indicate tumours. Scale bar =1cm. (C) As in (A) but with control mice (WT for *rtTA3* or *DI-shNUAK1* allele).

### 5.2.3 NUAK1 is required for the nuclear localisation of NRF2 protein

The previous data suggests that NUAK1 is a key mediator in the upstream regulation of NRF2 targets and the anti-oxidant response pathway within a tumour environment; however the underlying mechanism by which NUAK1 regulates NRF2 remains elusive.

### 5.2.3.1 NUAK1 does not modulate NRF2 at protein level

One level of NRF2 regulation is targeted proteosomal degradation. Firstly, it was investigated if NUAK1 depletion modulates basal NRF2 protein levels however, no change at protein level was observed after knockdown by siNUAK1 #2 at 48 hours post transfection (Figure 5.9). This suggests that regulation of NRF2 by NUAK1 is not via protein stabilisation or inhibition of degradation.

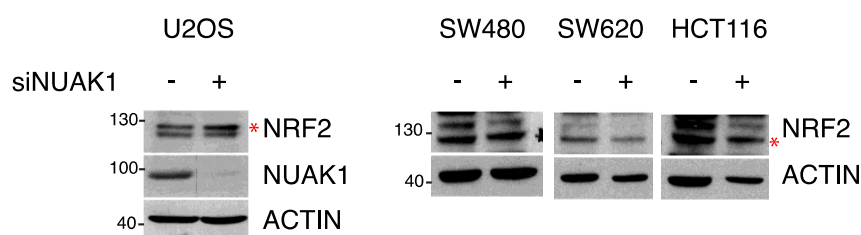


**Figure 5. 9 - NUAK1 does not regulate NRF2 at protein level**

Immunoblots showing NRF2 protein level in whole cell extract after NUAK1 depletion using siRNA sequence #2 in U2OS (left panel), and SW480, SW620 and HCT116 (right panels). The asterisk indicates the correct NRF2 band.

### 5.2.3.2 NUAK1 is required for the nuclear localisation of NRF2 protein

Next, NRF2 accumulation in the nucleus was examined after acute hydrogen peroxide treatment in NUAK1 depleted U2OS and CRC cell lines, SW480, SW620, HCT116 and LS174T (Figure 5.10). Depletion of NUAK1 strongly suppressed translocation of NRF2 into the nucleus when compared to non-targeting controls in all cell lines. This result was further confirmed in U2OS with NUAK1 inhibitor, HTH-01-015 for 8 hours at 10 $\mu$ M (Figure 5.10B) and in CRC cell line, SW480, using two independent siRNA sequences (referred to as #1 and #2 in figure 5.10C). Basal levels of nuclear NRF2 protein also appeared to be modulated by NUAK1 depletion before peroxide stimulation (see SW620 and HCT116 cells), thus NUAK1 is necessary for NRF2's localisation to the nucleus even under basal conditions. Finally, a H<sub>2</sub>O<sub>2</sub> time course was performed to assess the temporal dynamics of NRF2 localisation to the nucleus upon NUAK1 depletion. This showed that the response is reduced at all time points rather than delayed (Figure 5.10E).

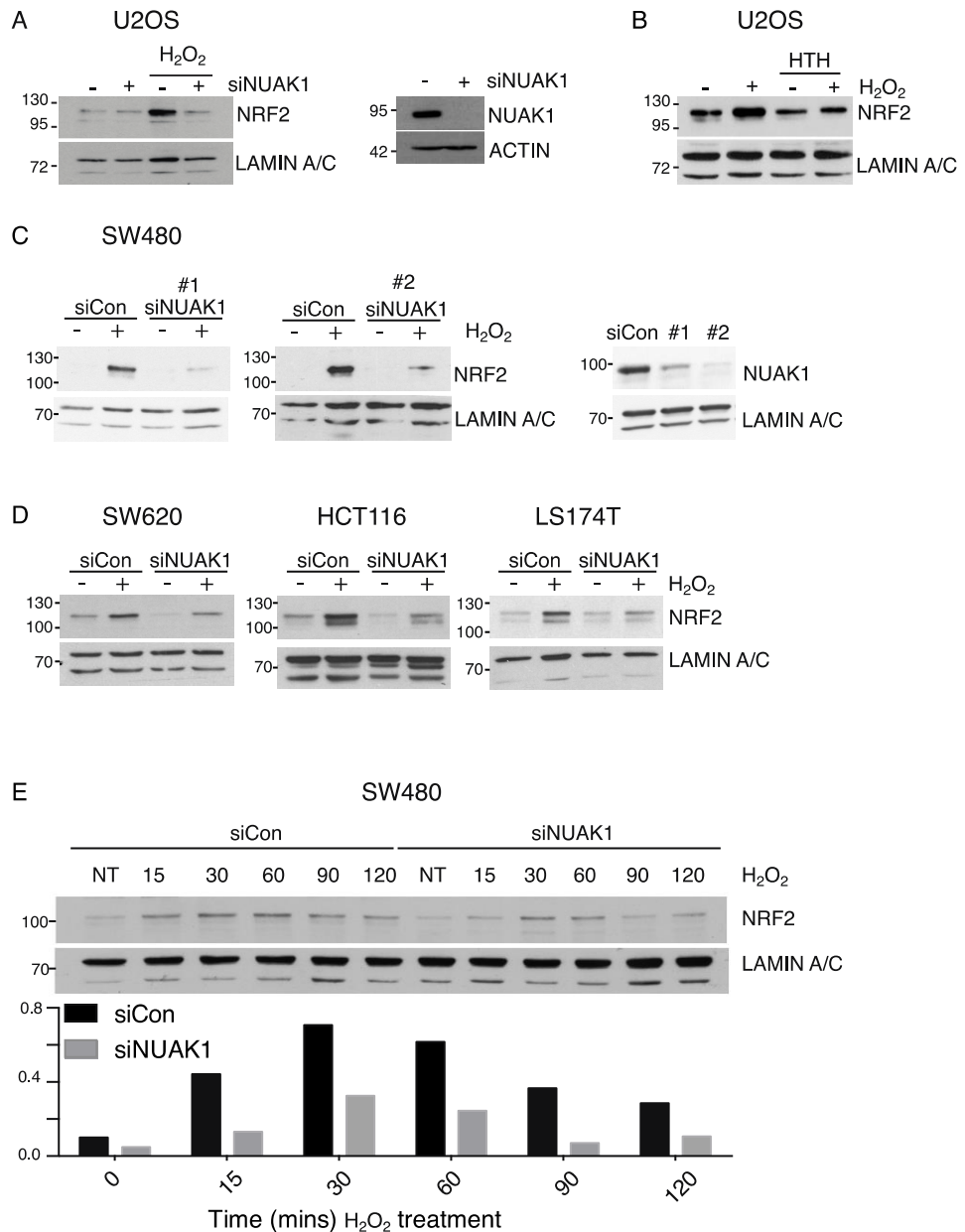


**Figure 5.10 - NUA1 is required for NRF2 localisation to the nucleus**

(A) Left panel: Immunoblot of NRF2 protein levels in nuclear extracts from U2OS cells after acute (30 mins) treatment of cells with 500µM H<sub>2</sub>O<sub>2</sub>, with and without prior depletion of NUA1 with siRNA #2. Right panel: confirmation of NUA1 depletion by siRNA #2. Nuclear protein LAMIN A/C is used as a loading control. (B) Immunoblot of NRF2 protein levels in nuclear extracts from U2OS cells after acute (30 mins) treatment of cells with 500µM H<sub>2</sub>O<sub>2</sub>, with and without 8 hours pre-treatment with 10µM HTH-01-015. (C) Left panel: As in (A) but with SW480 cells and siRNA sequence #1. Middle panel: As in (A) with S480 cells and siRNA sequence #2. Right panel: Nuclear extracts show confirmation of NUA1 knockdown with each siRNA sequence. (D) As in (A) but with SW620 (left panel), HCT116 (middle panel) and LS174T (right panel). (E) Immunoblot of NRF2 protein levels in nuclear extracts from SW480 cells after indicated timepoints of 500µM H<sub>2</sub>O<sub>2</sub> treatment with and without prior deletion of NUA1 with siNUAK1 #2. Below shows the densitometry of the immunoblot using ImageJ. All blots (A-E) are representative of at least 3 independent experiments. Figures (10A+B) were performed by Dr. Nathiya Muthalagu.

## 5.2.4 NUAK1 promotes nuclear translocation of NRF2 by antagonizing GSK3 $\beta$

### 5.2.4.1 NUAK1 is necessary for the phosphorylation of GSK3 $\beta$ Ser-9

Unbiased, SILAC-based phospho-proteomics was utilised to recognise mediators of NRF2 regulation upon NUAK1 inhibition with HTH-01-015 in U2OS cells. Phosphorylation of MYPT1 at Ser-445, the most validated target of NUAK1 was reduced in HTH-01-015 treated samples as expected. Interestingly, this was the only site resident within an AMPK-related kinase consensus motif that was consistently down regulated in this analysis. Importantly, the inhibitory phosphorylation site on GSK3 $\beta$  Ser-9 was also reduced upon HTH-01-015 and there was a corresponding increase in the phosphorylation of numerous GSK3 $\beta$  targets (Figure 5.11).

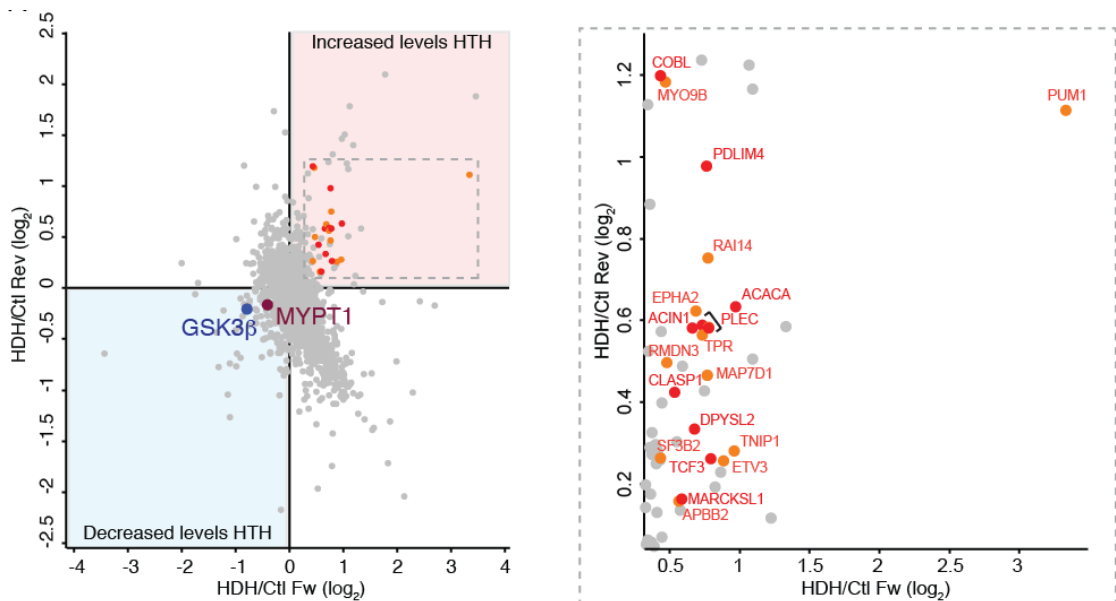


### Figure 5.11 - NUAK1 is necessary for the inhibitory phosphorylation of GSK3 $\beta$ Ser-9

Summary of phospho-proteomic changes induced in U2OS cells upon treatment with 10 $\mu$ M HTH-01-015 for 1hr. Left panel depicts the comparison of “forward” (X-axis) with “reverse” (Y-axis) SILAC labeled cells. Phosphorylation sites in the lower left quadrant thus show consistent reduction in levels while those in the upper right quadrant show consistently higher phosphorylation levels detected by mass spectrometry. The previously validated NUAK1 substrate MYPT1 was used to set a threshold for acceptance/rejection of modulated phosphorylations. Right panel shows zoom of the inset from left panel, with known (red) and predicted (orange) GSK3 $\beta$  substrates highlighted. This analysis was performed by Tiziana Monteverde in collaboration with Dr. Sara Zanivan and the Beatson Proteomics Facility.

### 5.2.4.2 NUAK1’s effect on GSK3 $\beta$ is conserved to SW480 cells and is independent of upstream AKT signalling

Activation of AKT at Thr-308 and Ser-473 leads to AKT-mediated phosphorylation of GSK3 $\beta$  and its subsequent inhibition in many cellular settings including that of NRF2 regulation. In the presence of oxidative stress, cytoplasmic GSK3 $\beta$  must be

phosphorylated, and thereby inactivated, in order to release NRF2 from negative regulation and allow it to accumulate in the nucleus and consequently upregulate the anti-oxidant response pathway (Rojo et al., 2008).

To examine this mechanism in the context of NUA1 depletion in SW480 cells, nuclear and cytoplasmic fractions were investigated once again with and without acute H<sub>2</sub>O<sub>2</sub> treatment. As expected, cytoplasmic AKT was activated and GSK3 $\beta$  phosphorylated at Ser-9 in response to peroxide (Figure 5.12, right panel). Upon depletion of NUA1 however, cytoplasmic GSK3 $\beta$  Ser-9 was strongly reduced, corroborating the phospho-proteomics analysis, while AKT phosphorylation was unaffected. This data confirms that NUA1 has a conserved regulatory role in the phosphorylation of GSK3 $\beta$  Ser-9 and consequently, releases NRF2 from negative regulation, to upregulate the oxidative response pathway.

Interestingly both AKT and GSK3 $\beta$  protein appeared to increase in the nuclear fraction upon H<sub>2</sub>O<sub>2</sub>, and this effect was reduced in NUA1 depleted conditions (Figure 5.12, left panel). It is currently unclear what NUA1's role is in nuclear accumulation of these proteins and how this effects their functions there.

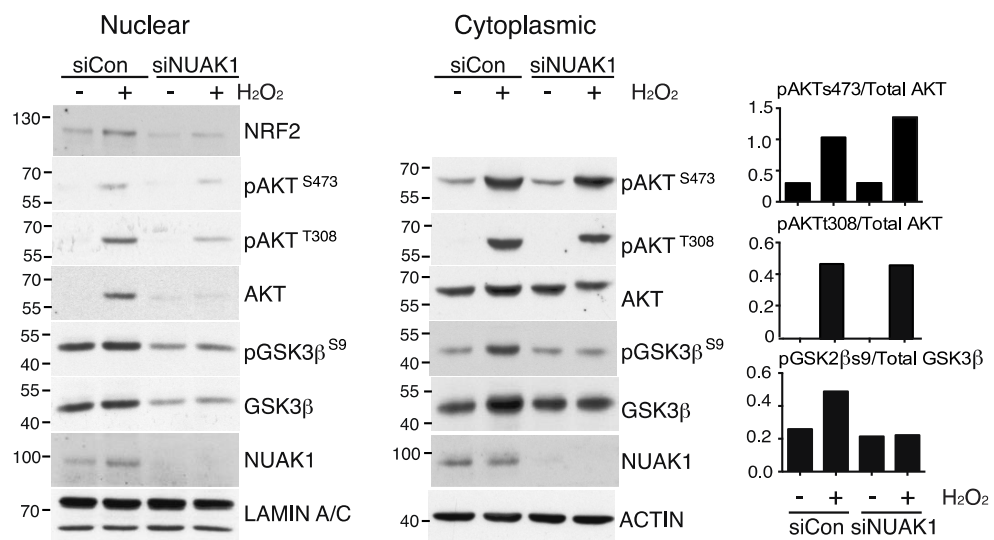


**Figure 5. 12 - NUA1's regulation of GSK3 $\beta$  is conserved to SW480 cells and is independent of upstream AKT signalling**

Immunoblots of Nuclear (left panel) versus Cytoplasmic (right panel) fractions isolated from SW480 cells with or without NUA1 depletion and treatment with 500 $\mu$ M H<sub>2</sub>O<sub>2</sub> (30 mins), cytoplasmic densitometry (far right panel) calculated by ImageJ, N=3. siNUAK1 sequence #2 used.

#### 5.2.4.4 Pharmacological or genetic abrogation of GSK3 $\beta$ rescues nuclear accumulation of NRF2

These investigations have shown that the inhibitory phosphorylation of GSK3 $\beta$  is impaired in NUA1 depleted cells; therefore it was assessed whether GSK3 $\beta$  inhibition by small molecule inhibitor could rescue nuclear accumulation of NRF2. Conclusively, inhibition of GSK3 $\beta$  with either BIO-acetoxime or CHIR99021 was able to rescue nuclear accumulation of NRF2 in NUA1 deficient SW480 cells (Figure 5.13).

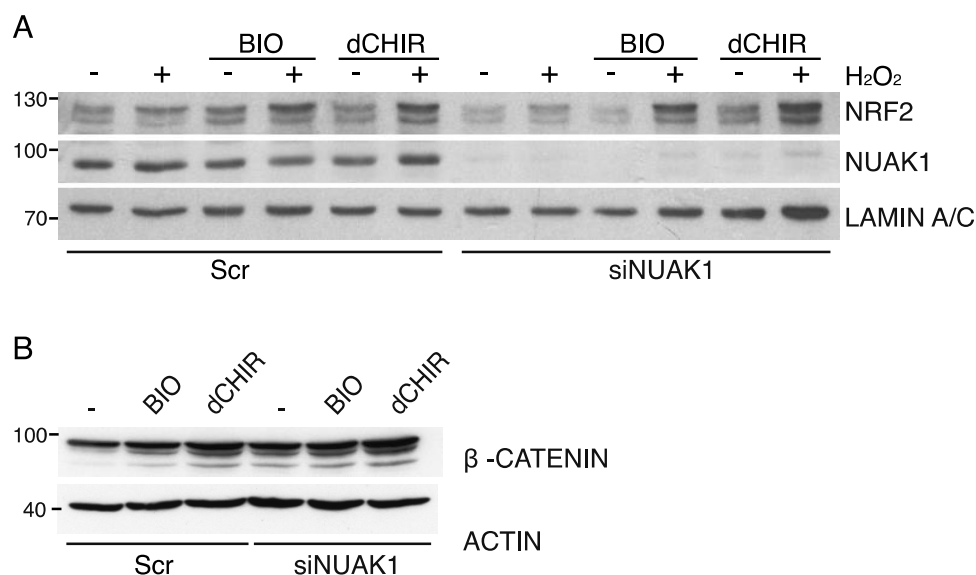


**Figure 5. 13 - Pharmacological or genetic abrogation of GSK3 $\beta$  rescues nuclear accumulation of NRF2**

(A) Immunoblots showing 6 hours pre-treatment of NUA1 depleted SW480 cells with GSK3 $\beta$  inhibitors BIO-acetoxime (BIO; 1 $\mu$ M) or CHIR99021 (dCHIR; 5 $\mu$ M) restores H<sub>2</sub>O<sub>2</sub>-induced NRF2 nuclear translocation (H<sub>2</sub>O<sub>2</sub> - 500 $\mu$ M, 30 mins) in nuclear extracts. (B) Immunoblots showing the accumulation of  $\beta$ -Catenin as a result of GSK3 $\beta$  inhibition with each inhibitor in whole cell extracts. siNUAK1 sequence #2 used.

#### 5.2.5 MYPT1 responds to ROS in a NUA1 dependent manner

NUA1-mediated phosphorylation of MYPT1 at Ser-445 inhibits PP1 $\beta$  activity as reported by Zagorska et al, 2010. Furthermore, PP1 $\beta$  has been linked to GSK3 $\beta$  activity; specifically PP1 $\beta$  can dephosphorylate and subsequently activate GSK3 $\beta$  (Hernández et al., 2010, Mobasher et al., 2013). This suggests that ROS co-ordinately activates AKT and inactivates PP1 $\beta$  via NUA1 to suppress GSK3 $\beta$ . Interestingly, phosphorylation of MYPT1 Ser-445 responded to H<sub>2</sub>O<sub>2</sub> treatment in U2OS and SW480 cells (Figure 5.14). When NUA1 was depleted in these cells, the activation was almost completely abrogated in U2OS suggesting that NUA1 is the upstream kinase responding to increasing ROS.

This effect was present, however less evident in SW480 cells suggesting that there may be another kinase compensating for NUA1 depletion.

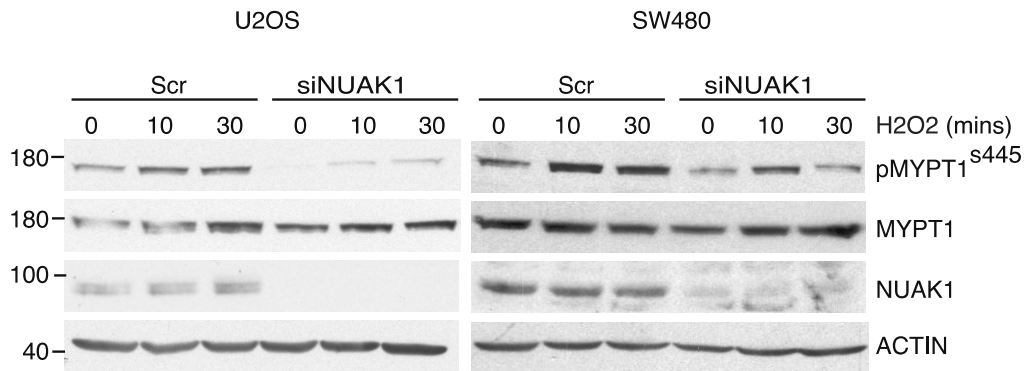


**Figure 5. 14 - MYPT1 responds to peroxide treatment in a NUA1 dependent manner**

Immunoblots showing MYPT1 Ser-445 phosphorylation in response to H<sub>2</sub>O<sub>2</sub> treatment (500µM, 10, 30 mins) after depletion of NUA1 by siRNA sequence #2 in whole cell extracts from U2OS (left panel) and SW480 (right panel) cells.

### **5.2.6 NUA1 is activated by ROS oxidisation of cysteine residues**

NRF2 regulator, KEAP1, contains cysteine residues which are targeted for oxidisation in the presence of ROS leading to the dissociation of KEAP1 to NRF2 (Dinkova-Kostova et al., 2002). Therefore one possible way that NUA1 is responsive to ROS is that it contains similar cysteine residues. Dimedone is a chemical reagent which forms adducts with oxidised groups in proteins (Rudyk & Eton, 2014). In order to detect possible cysteine oxidation by ROS, dimedone was used as a labelling agent in SW480 cells expressing FLAG-tagged NUA1 after acute H<sub>2</sub>O<sub>2</sub> treatment. Treatment with increasing doses of H<sub>2</sub>O<sub>2</sub> resulted in increased dimedone labelling of FLAG-immunoprecipitated (IP) NUA1 as well as increased phosphorylation of NUA1 (Figure 5.15A).

According to the NCBI reference sequence there are nine possible cysteine residues present in NUA1 (NP\_055655.1). A less crude and more accurate method of measuring cysteine oxidization is Mass Spectrometry analysis of iodoacetamide labelled proteins. Iodoacetamide differentially labels cysteine residues under both normal and oxidative stress conditions; cysteines that become oxidized exhibit a decreased iodoacetamide labeling due to the lessened nucleophilicity of the sulfur atom. Iodoacetamide labelling of FLAG-NUA1 IPs from cells treated for 5 minutes with H<sub>2</sub>O<sub>2</sub> similarly revealed increased oxidation of all nine NUA1 cysteine's, as compared with untreated controls (Figure 5.15B & C). Collectively, this data suggests a model wherein ROS-dependent activation of

NUAK1 coordinates inhibition of PP1 $\beta$  with activation of AKT in order to counteract suppression of nuclear NRF2 by GSK3.

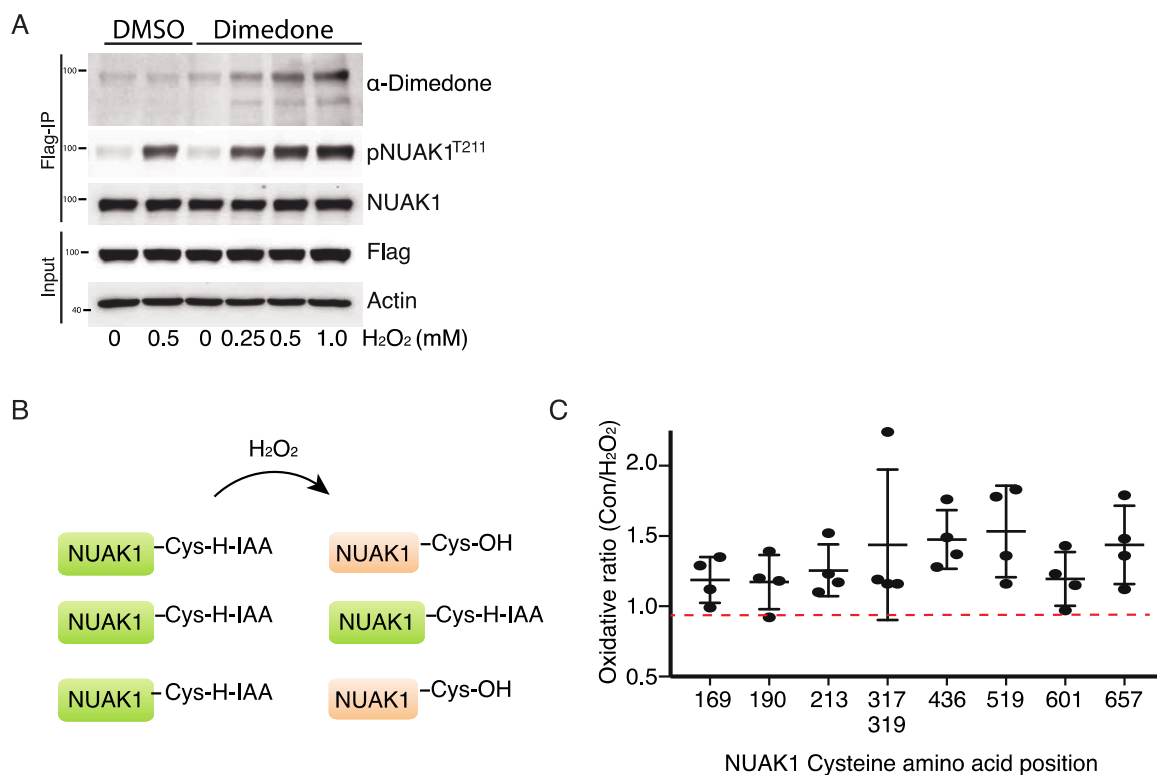


**Figure 5. 15 - NUA1 is activated by ROS oxidation of cysteine residues**

(A) Oxidation of NUA1 protein detected by dimedone labeling of U2OS cells expressing FLAG-tagged NUA1 and treated for 5 minutes with H<sub>2</sub>O<sub>2</sub> (0.25, 0.5, and 1.0mM). (B) Identification of oxidised cysteines in FLAG-tagged NUA1 by mass spectrometry analysis of Iodoacetamide labelling of U2OS-FLAG-NUAK1 cells treated with/without H<sub>2</sub>O<sub>2</sub> for 5 minutes. Lysates were labelled with heavy (13C) or light (12C) iodoacetamide, followed by immunoprecipitation of FLAG-NUAK1. Plot shows analysis of reciprocally labeled samples from 2 independent experiments. Mean and SD indicated.

## 5.3 Discussion

The primary role of NRF2 is to induce the transcription of a wide array of genes that are involved in the detoxification of cellular ROS and thereby prevent the harmful effects of extrinsic and intrinsic insults (Moi et al., 1994). GSK3 $\beta$  is known to negatively regulate NRF2 by two independent mechanisms, 1) GSK3 $\beta$  is a major regulator in the export of NRF2 from the nucleus (Salazar et al., 2006, Rojo et al., 2008) and 2) GSK3 $\beta$  can phosphorylate NRF2 directly to target it for proteosomal degradation via SCF/ $\beta$ -TrCP (Chowdhry et al., 2013, Rada et al., 2011).

The investigations of this chapter have demonstrated that NUAK1 regulates nuclear accumulation of NRF2. Interestingly, recent unpublished data from the lab suggests that NUAK2 can also regulate NRF2's localisation to the nucleus. This is not entirely surprising as NUAK2 can also regulate the PP1 $\beta$ <sup>MYPT1</sup> complex, however what is surprising is that NUAK1 and NUAK2 cannot compensate for loss of the other in this context. It should be noted that all siRNAs used were analysed for on-target silencing and did not silence the other NUAK isoform. Furthermore, H<sub>2</sub>O<sub>2</sub> stimulated phosphorylation of MYPT1 in U2OS cells, is almost completely abrogated after NUAK1 depletion suggesting that NUAK1 is the dominant NUAK isoform in these cells in this context. On the other hand, although markedly reduced, the effect was not so dramatic in SW480 cells suggesting that indeed NUAK2 or another AMPK-RK may also be able to phosphorylate MYPT1 in response to H<sub>2</sub>O<sub>2</sub> however not as efficiently as NUAK1. According to the literature, NUAK1 and NUAK2 are the only AMPK-RKs to bind to PP1 $\beta$  and phosphorylate MYPT1 via the conserved GILK motif (Banerjee et al., 2014b). As mentioned previously, the NUAK phosphorylation sites on MYPT1 lie within an optimal AMPK consensus motif LX(R/K)(S/T)X(pS)XXX(L/I) (Dale et al., 1995). Indeed, there is some evidence to suggest that AMPK is also able to phosphorylate MYPT1 at these residues (Murphy lab; unpublished). Therefore, further analysis would be required to investigate whether or not other AMPK-RKs can also take part in NRF2 regulation in the absence of the NUAK isoforms, and whether or not there is a biochemical difference in the NUAK isoforms that prevents them from compensating either *in vitro* or *in vivo*.

NUAK1 is necessary for the nuclear accumulation of NRF2 by counteracting negative regulation of this process by GSK3 $\beta$ , and direct inhibition of GSK3 $\beta$  can restore NRF2 nuclear accumulation in NUAK1 deficient cells. GSK3 $\beta$  is a constitutively activated kinase, which is controlled by inhibitory phosphorylation at Ser-9. AKT is the major

upstream kinase of this phosphorylation site and thereby mediates GSK3 $\beta$  activity (Beurel et al., 2015). In the context of oxidative stress, ROS activates phosphoinositide-3-kinase (PI3K) to amplify downstream AKT signalling, and simultaneously inactivates the phosphatase and tensin homolog (PTEN), which inhibits activation of AKT, by the oxidation of cysteine residues within PTEN (Lee et al., 2002, Zhang and Yang, 2013). This leads to inhibition of GSK3 $\beta$  by phosphorylation at Ser-9 and the consequent release of NRF2 from GSK3 $\beta$ -dependent negative regulation (Rojo et al., 2008) (Lee et al., 2002). It has been shown here that activation of AKT by ROS is unaffected by NUA1 deficiency therefore modulation must occur at GSK3 $\beta$ , either by the interruption of AKT's ability to phosphorylate GSK3 $\beta$  or by the regulation of dephosphorylation of GSK3 $\beta$ .

Interestingly, PP1 $\beta$  was previously shown to promote GSK3 $\beta$ -dependent regulation of NRF2 by dephosphorylating GSK3 $\beta$  (Mobasher et al., 2013). Here, NUA1 dependent phosphorylation of MYPT1 was activated in response to H<sub>2</sub>O<sub>2</sub> providing evidence that activated NUA1 leads to the suppression of PP1 $\beta$  activity via MYPT1 phosphorylation in response to ROS. This in turn can inhibit dephosphorylation of GSK3 $\beta$  by PP1 $\beta$  thus allowing NRF2 to accumulate in the nucleus and upregulate the anti-oxidant response pathway. As NRF2 controls anti-oxidant transcription in order to detoxify ROS, and AMPK functions as a sensor for cellular stress, it seems plausible that the two mechanisms are linked. Indeed AMPK participates in the anti-oxidant defence indirectly by conserving NADPH levels via inhibition of lipid biosynthesis (Jeon et al., 2012). Additionally, AMPK is able to phosphorylate NRF2 directly at Ser-558, which is located in the canonical nuclear export signal (NES) sequence and is also a consensus AMPK motif and AMPK is able to concurrently phosphorylate GSK3 $\beta$  and inhibit its activity at Ser-9, thereby inhibiting negative regulation of NRF2 in times of oxidative stress (Joo et al., 2016). It is known that both AMPK and NUA1 can be activated by increased AMP levels therefore it is not unlikely that both AMPK and NUA1 are activated by an increase in AMP/ATP ratio in this context, which frequently occurs prior to oxidative stress (Joo et al., 2016, Suzuki et al., 2003b). On the other hand, redox signalling is more direct and involves H<sub>2</sub>O<sub>2</sub>-mediated oxidation of cysteine residues within proteins such as NRF2 regulator, KEAP1 (Rhee, 2006). Exposure to H<sub>2</sub>O<sub>2</sub> has been reported to induce the oxidation of cysteine residues on AMPK, which subsequently results in AMPK activation through auto-phosphorylation (Zmijewski et al., 2010). Therefore, another possible mechanism of activation would be that NUA1 contains cysteine residues susceptible to oxidation. Indeed in this study, NUA1 is activated by ROS-dependent oxidation of cysteine residues.

This study has accumulated evidence to suggest that the NRF2 anti-oxidant response pathway is compromised upon loss of NUA1. Firstly, loss of NUA1 leads to elevated ROS levels in U2OS and the CRC cell lines, in transformed spheroids and acute loss of Nuak1 *in vivo* results in ROS within tumours. Secondly, hypersensitisation to oxidative stress-induced apoptosis was demonstrated in the CRC cell lines. Thirdly, NUA1 inhibitor, HTH-01-015-mediated cell death was rescued by the exogenous addition of anti-oxidant 6-hydroxy-2,5,7,8-tetramethylchroman-2-carboxylic acid (Trolox) in both U2OS and CRC cell lines and transformed small intestine- and colon-derived spheroids. This was confirmed *in vivo* as provision of NAC was able to rescue loss of tumour burden in mice after acute Nuak1 loss. This confirms that cytotoxic levels of ROS are responsible for cell death. However, it must be noted that in no case was the rescue 100%. This implies that inhibition of NUA1 may be compromising other essential cellular processes. Once again, this is not surprising as NUA1 has been implicated in proliferation and DNA damage response (Hou et al., 2011), adhesion (Zagorska et al., 2010), senescence (Humbert et al., 2010), and apoptosis (Suzuki et al., 2003) as mentioned previously. However it is unclear how these would result in cell death. On the other hand, phospho-proteomic analysis indicated modulation of multiple GSK3 $\beta$  targets in addition to NRF2, therefore NUA1's regulation of GSK3 $\beta$  may be pleiotropic and undiscovered functions are likely to exist. This has enormous implications as GSK3 $\beta$  has been reported to phosphorylate about 100 proteins so far (Sutherland, 2011) and this study has only investigated one downstream consequence of NUA1 modulation. Investigation of the nuclear population of GSK3 $\beta$  and AKT showed that NUA1 mediates both at protein level in the nuclear fraction and therefore may indicate an additional NUA1 mediated function. GSK3 $\beta$  is considered a cytosolic protein however it has been reported to be present in the nucleus and mitochondria (Bijur & Jope, 2003). Translocation and specific localisation of GSK3 $\beta$  govern its participation in signalling pathways, control its interaction with substrates and involvement in protein complex formation and impact gene expression and transcription (Thotala and Yazlovitskaya, 2011). GSK3 $\beta$  localises to the nucleus via an intrinsic nuclear localization sequence in GSK3 $\beta$  (Meares and Jope, 2007), and nuclear levels of GSK3 $\beta$  have been reported to rapidly increase in response to some apoptotic stimuli (Bijur and Jope, 2001). In the nucleus, GSK3 $\beta$  can affect gene expression, nuclear functions, as well as regulate the epigenetics of the cell (Beurel et al., 2015). Therefore this data reiterates NUA1's role in the regulation of multiple downstream GSK3 $\beta$  targets and suggests that loss of NUA1 has far-reaching

implications for a cell or tumour. It would be interesting to delve deeper into the subset of GSK3B targets that were modulated upon NUA1 inhibition.

Depletion of NUA1 by siRNA in all cell lines leads to significant sensitisation to peroxide challenge, resulting in increased levels of cell death in U2OS and the CRC cell lines. However, the levels of cell death in NUA1 depleted cells (not treated with H<sub>2</sub>O<sub>2</sub>) was not consistent with the levels of cell death observed when the same cell lines were treated with small molecule inhibitor HTH-01-015 in Chapter 1 (Section 3.2.3, Figure 3.4). It could be reasoned that this might be due to insufficient depletion, as shown in Figure 5.5. Another possibility is that the pharmacodynamics of the small molecule inhibitor are immediate and synchronous; therefore cells do not have time to adapt to inhibition of NUA1 resulting in pro-apoptotic pathways being induced. Whereas depletion by siRNA takes much longer and depletion in every cell is varied suggesting that non-synchronicity results in investigation of a mixed population of NUA1 replete and deplete cells. Finally, it must be considered that the inhibitor is having a NUA1 independent, toxic off-target effect at the dose used, however cell death was observed in tumours acutely depleted of NUA1 *in vivo* in the previous chapter (Section 4.2.6.1, Figure 4.15) and this correlated with elevated ROS in this chapter, therefore drug toxicity seems unlikely. Further analysis is required to eliminate these possibilities and emphasises the importance of investigation using both pharmacological and genetic approaches as has been done in this study.

The osteosarcoma cell line, U2OS has been used extensively in this analysis in addition to the colorectal cell lines SW480, SW620, HCT116 and LS174T and NUA1-dependent perturbation of NRF2 function in each case. The mechanism of NRF2 regulation and the proteins involved are highly conserved across mammalian cell types and species, therefore NUA1 regulation of NRF2 is likely to be broadly applicable and not restricted to colorectal cancer. The U2OS cell line has the advantage of not expressing the closely related NUA2, which has exhibited similar functions with NUA1, the most relevant being in the regulation of PP1 $\beta$  activity via MYPT1 (Banerjee et al., 2014b) and more recently, the regulation of NRF2 accumulation in the nucleus. NUA2 levels in U2OS cells have been confirmed both at protein level (Section 3.2.3, Figure 3.4) and at RNA level in our RNA sequencing analysis. The absence of NUA2 allows the investigator to focus primarily on NUA1 function providing cleaner data and easier interpretation of results than is the case in the CRC cell lines due to their varying levels of NUA2. On the other hand, suppression of NUA1 leads to an increase in cellular ROS and interestingly in NUA1 high cell lines, U2OS and SW480 had greater fold increase in ROS than

NUAK1 low cell lines SW620, and LS174T. However, NUA1 levels did not appear to correlate with sensitivity to inhibition of NUA1 by inhibitor (Section 3.2.3, Figure 3.4) or sensitivity to peroxide treatment under NUA1 depleted conditions. Furthermore, all cell lines were dependent upon NUA1 for the translocation of NRF2 to the nucleus after peroxide stimulation suggesting that basal NUA1 levels have no effect on NUA1's role here. Therefore in this context, it is unlikely that NUA1 and NUA2 levels correlate with activity and further investigation of kinase activity is required.

In conclusion, this data proposes a new mechanism of redox signal transduction in which ROS-dependent activation of NUA1 coordinates PP1 $\beta$ <sup>MYPT1</sup> inhibition, with AKT activation in order to suppress GSK3 $\beta$ -dependent inhibition of NRF2 nuclear import (Figure 5.15). Loss of NUA1, both *in vitro* and *in vivo*, leads to a compromised NRF2-dependent oxidative stress response, resulting in an increase in cytotoxic ROS levels that cells cannot sustain.

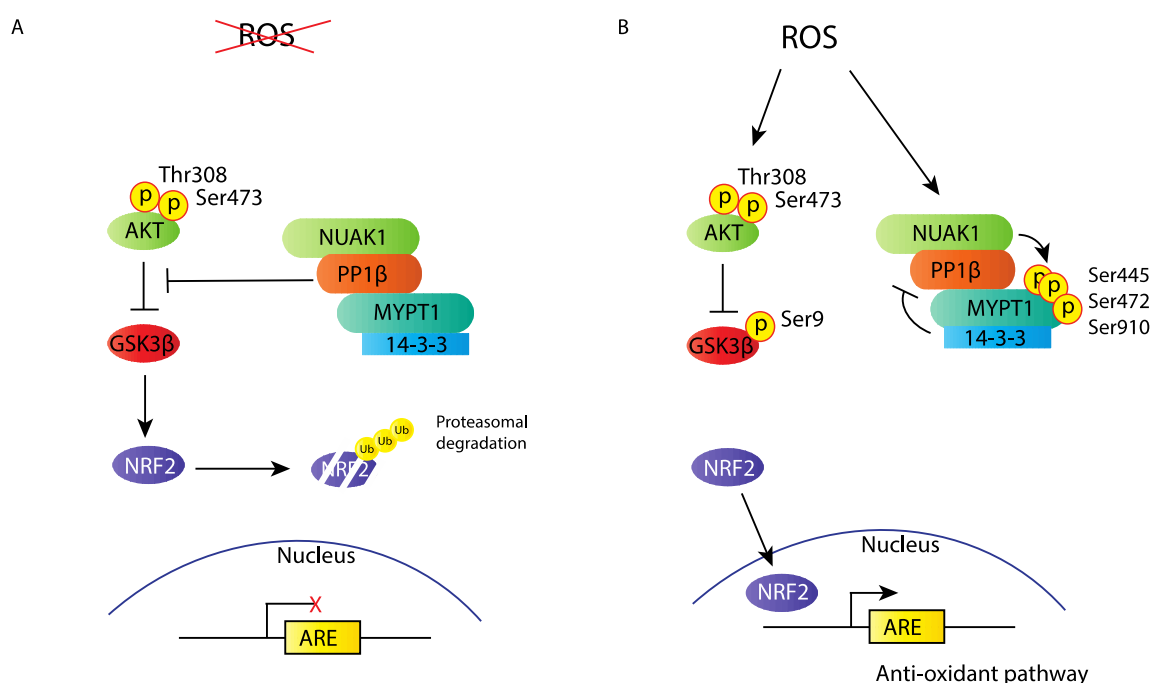


**Figure 5. 16 - NUA1 regulation of the anti-oxidant response pathway**

(A) Schematic of basal conditions, where ROS levels are low, NUA1 is inactive, therefore PP1 $\beta$  is able to dephosphorylate GSK3 $\beta$  and consequently target NRF2 for degradation by the proteasome. (B) ROS activation of NUA1 and AKT simultaneously results in phosphorylation of AKT and downstream inhibitory phosphorylation of GSK3 $\beta$ . This prevents NRF degradation and allows NRF2 to localise to the nucleus where it upregulates the anti-oxidant response pathway to detoxify the ROS. In tandem, activated NUA1 in complex with PP1 $\beta$  and MYPT1, phosphorylates MYPT1 and consequently inhibits GSK3 $\beta$  dephosphorylation by PP1 $\beta$ .

## Chapter 6 Discussion, Conclusions and Future work

Colorectal cancer (CRC) is the fourth most common cancer in the UK with over 40,000 new cases annually, and 110 cases diagnosed daily (CRUK, 2013). Worldwide, CRC is the third most commonly occurring cancer in men and the second most commonly occurring cancer in women (World Cancer Research Fund International, 2012). About two-thirds of CRC cases occur in the developed world, however incidence rates are expected to increase due to the adoption of westernised diet and lifestyle globally. Promisingly, since the 1970s mortality rates have decreased by 43% in the UK and rates are projected to fall by a further 23% by 2035 due to more appropriate and available information, earlier diagnosis and improvements in surgical, adjuvant and palliative treatment (CRUK, 2013). Our improved understanding of CRC has uncovered a number of novel CRC-associated proteins, and genomic-based technologies have demonstrated that CRC can be a very heterogeneous disease (Johnston, 2014). Therefore, there is still a requirement to apply molecule-based therapeutic approaches in addition to the combination of targeted therapies with chemotherapy in the treatment of CRC (Van Schaeybroeck et al., 2011).

NUAK1 is a member of the AMPK-related kinase (AMPK-RK) family based on its sequence homology to essential cellular energy sensor, AMPK (Bright et al., 2009). NUAK1 shares 47 and 45.8% homology to AMPK- $\alpha$ 1 and AMPK- $\alpha$ 2 respectively (Suzuki et al., 2003b). AMPK is activated by rising AMP:ATP ratio and acts to inhibit anabolic processes and promote catabolic processes in order to maintain cellular energy homeostasis (Hardie et al., 2012). NUAK1 has been reported to share many characteristics in common with AMPK including its phosphorylation and activation by upstream kinase, LKB1, its activation by rising AMP levels, as well as its ability to phosphorylate SAMs peptide, a synthetic substrate for AMPK-RKs (Suzuki et al., 2003a, Suzuki et al., 2003b, Suzuki et al., 2006). Notably, it is unknown if NUAK1 can function heterotrimerically similar to AMPK, therefore it is currently unclear how AMP can stimulate NUAK1 in a similar manner to AMPK. On the other hand, NUAK1 has also been implicated in the regulation of energy homeostasis in the context of overexpressed MYC, where both AMPK and NUAK1 were discovered to be synthetic lethal with MYC overexpression (Liu et al., 2012). NUAK1 can phosphorylate MYPT1 at residues that lie within a conserved AMPK consensus motif (Zagorska et al., 2010) indeed, the Murphy lab has evidence to suggest the AMPK can also phosphorylate this site. This indicates possible similarity or over-lap in NUAK1 and AMPK function. In relation to the findings in this study, both NUAK1 and

AMPK can release NRF2 from negative regulation, albeit by different mechanism, in response to rising cellular ROS. Together, this data suggests that like AMPK, NUA1 has an important role in the regulation of cellular metabolic plasticity by acting as a metabolic checkpoint. Thereby NUA1 confers tumour cells a growth advantage by providing the ability to adapt to metabolic stress.

By definition, a metabolic checkpoint is a cellular mechanism that ensures the accurate response based on a cell's metabolic status and is composed of a metabolic signal, sensors, transducers and effectors (Wang and Green, 2012). Metabolic signals indicate fluctuations in the extracellular nutrient environment or intracellular metabolic status and include ATP, NADP<sup>+</sup>-NADPH, acetyl-CoA as well as ROS. The sensors of a metabolic checkpoint are proteins that can physically interact with and respond to metabolic signals, and can subsequently initiate the appropriate downstream signalling cascades (Wang and Green, 2012). AMPK is a well-established metabolic checkpoint sensor of bioenergetic status, and the Murphy lab previously showed that NUA1 can also function as a sensor of bioenergetic status via the mTOR pathway (Liu et al., 2012) (Monteverde, Accepted for publication). In this study, new evidence suggests that NUA1 is also a sensor of oxidative stress status. The final stage of the metabolic checkpoint includes the activation of signal transduction pathways and their downstream effectors that prompt appropriate cellular responses. This often involves metabolic 'rewiring', cell differentiation, proliferation, and death (Wang and Green, 2012). Concurrently, NUA1 expression is normally highest in more oxidative tissues (Inazuka et al., 2010). Overall this suggests that protecting cells from oxidative stress is a major physiological role of NUA1.

However, this presents an important question: why do two or more proteins exist when they appear to have very similar functions? Throughout evolution, genes that do not confer a survival advantage and are thereby redundant are often lost. Therefore, NUA1 must have a unique function that neither AMPK, nor any other AMPK-RK including NUA2, can compensate for.

NUA1 has also been associated with cell survival, invasion and metastasis and poor prognosis in many tumour types. Interestingly, the alteration frequency of NUA1 in cancer is relatively low, however elevated expression has been observed in multiple tumour types including CRC (Liu et al., 2012). Furthermore, NUA1 expression level correlates with more advanced stages of CRC and is enriched in liver metastasis (Kusakai et al., 2004). Taken together, NUA1 is a novel tumour progression-associated factor in

cancer, however prior to this study, its primary functions in this context and its use as a potential therapeutic target in human CRC remained unclear. This study shows that NUA1 is a prognostic factor in human CRC. Patients with high NUA1 expression had significantly reduced overall survival in three independent cohorts. Furthermore, TCGA analysis confirmed that NUA1 levels are higher in more aggressive disease, and in patients with lymph node involvement. This suggests that NUA1 is a valuable molecular biomarker for progressed CRC that may be used as a diagnostic tool. In agreement with analysis performed on online datasets, it has been shown that NUA1 expression is elevated in human CRC using a human TMA and NUA1 RNA *in situ* hybridisation, and expression strongly correlates with advanced tumour stage and increased lymph node metastasis.

In this study, a mouse model for sporadic intestinal cancer has shown that Nuak1 is essential for tumour initiation. Additionally, Nuak1 is essential for the survival of established colorectal tumours. Tumours depleted of Nuak1 demonstrated increased levels of cell death and ROS damage, concurrent with reduced cell proliferation. In both contexts, there appeared to be a selective pressure for cells to retain Nuak1, which then conveys a survival advantage. This was corroborated in 3D organoid culture, where Nuak1 was required for the formation and viability of transformed spheroids, and that Nuak1 retaining cells could out-compete Nuak1 deficient cells.

Importantly, the requirement for Nuak1 does not extend to healthy wildtype cells of the intestine. In this study, loss of Nuak1 did not appear to affect normal intestine homeostasis; mice could sustain Nuak1 depletion over a long period without any apparent detrimental side effects; and wildtype organoids were resistant to Nuak1 inhibition. This data strengthens NUA1's position as a candidate for targeted therapy, suggesting that inhibition of NUA1 in cancer patients would have limited side effects.

The requirement for NUA1 in cancer cells in this investigation was attributed to the regulation of NRF2 and the anti-oxidant response pathway. It has been demonstrated that NUA1 is necessary for the nuclear accumulation of NRF2 by counteracting negative regulation of this process by GSK3 $\beta$ , and that direct inhibition of GSK3 $\beta$  is able to restore NRF2 nuclear accumulation in NUA1 deficient cells. Furthermore, direct activation of NUA1, by cysteine oxidation, in response to ROS led to activation of MYPT1 and the consequent suppression of PP1 $\beta$  activity. This in turn inhibits dephosphorylation of

GSK3 $\beta$  by PP1 $\beta$  thus allowing NRF2 to accumulate in the nucleus and upregulate the anti-oxidant response pathway (Figure 6.1A & B).

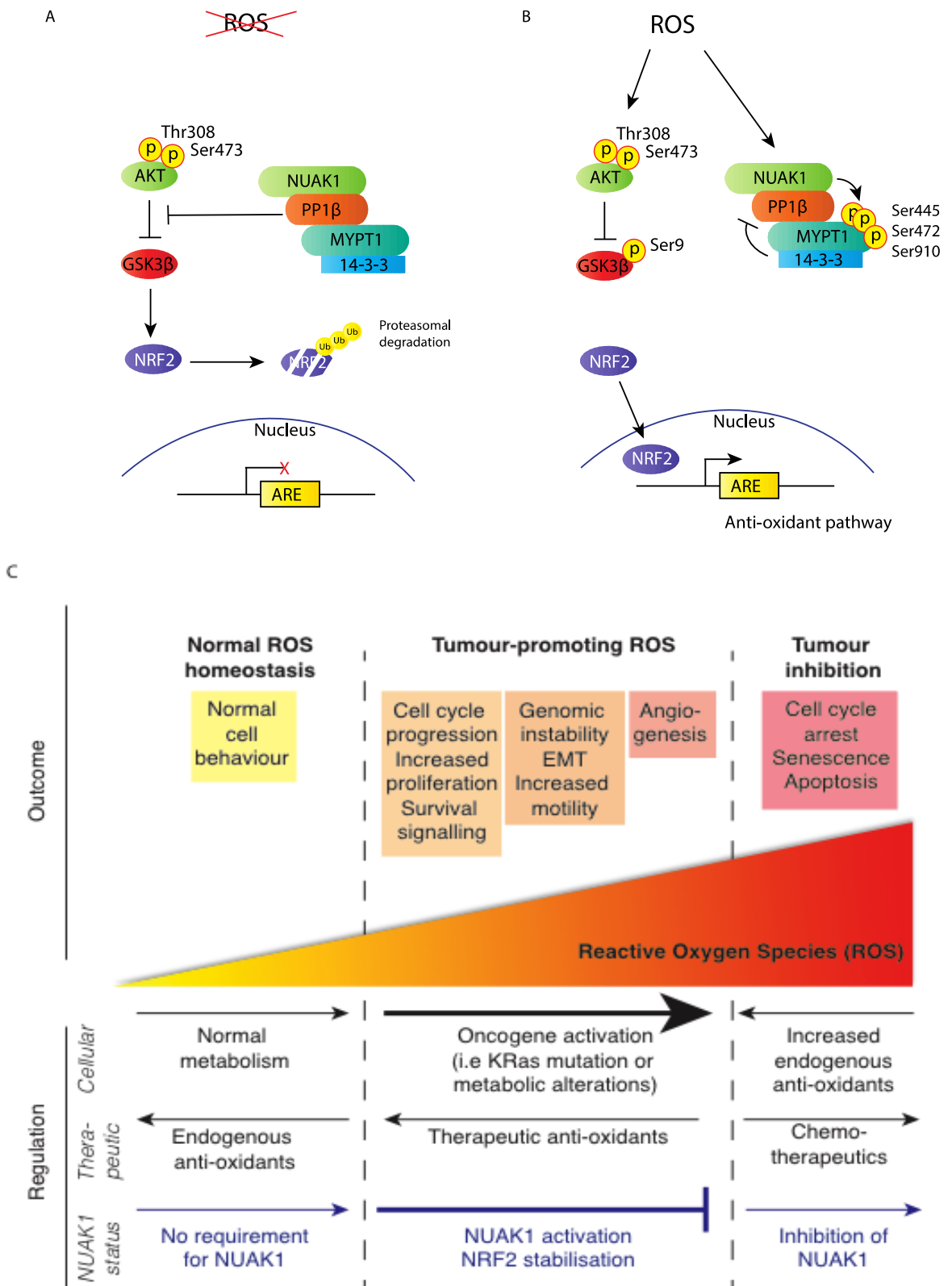


**Figure 6.1 - NUA1 and the anti-oxidant stress response**

(A) Schematic of basal conditions, where ROS levels are low, NUA1 is inactive, therefore PP1 $\beta$  is able to dephosphorylate GSK3 $\beta$  and consequently target NRF2 for degradation by the proteasome. (B) ROS activation of NUA1 and AKT simultaneously results in phosphorylation of AKT and downstream inhibitory phosphorylation of GSK3 $\beta$ . This prevents NRF degradation and allows NRF2 to localise to the nucleus where it upregulates the anti-oxidant response pathway to detoxify the ROS. In tandem, activated NUA1 in complex with PP1 $\beta$  and MYPT1, phosphorylates MYPT1 and consequently inhibits GSK3 $\beta$

dephosphorylation by PP1 $\beta$ . (C) A schematic of the generation, regulation and effects of cellular ROS. ROS are produced in normal cellular processes, and cells express anti-oxidants to detoxify the free radical. Tumourigenic events including oncogene activation can increase intracellular ROS and promote tumour initiation and progression. These pro-tumourigenic ROS levels can result in cell cycle progression, increased proliferation and survival signalling, however these can be targeted therapeutically by anti-oxidants. Excessive increases in ROS can be cytotoxic by inducing cell cycle arrest, senescence or cell death of tumour cells, however it is possible that the tumour cells are able to upregulate expression of endogenous anti-oxidant to combat cytotoxicity. NUAK1 is activated in response to rising ROS levels and maintains redox homeostasis within the pro-tumourigenic bracket by stabilisation of NRF2. Loss of NUAK1 can be therapeutic as it removes this regulation and ROS levels become cytotoxic. Figure adapted from (Liou and Storz, 2010).

NRF2 is known to be a major defence mechanism and regulator of cell survival (Jaramillo and Zhang, 2013). In healthy cells, NRF2 protects against tumour initiation and progression by reducing genotoxic compounds that arise both intrinsically and extrinsically. On the other hand, activation of the NRF2-dependent anti-oxidant response pathway can promote the survival of both healthy and cancer cells by generating optimal conditions for cell growth. Elevated levels of oxidative stress have been detected in almost all cancers as a consequence of the altered characteristics of tumour cells and their environment. These include increased metabolic activity, mitochondrial dysfunction, peroxisome activity, increased cellular receptor signalling, oncogene activity, increased activity of oxidase, cyclooxygenases, lipoxigenases and thymidine phosphorylase or through cross talk with infiltrating immune cells (Storz, 2005, Szatrowski and Nathan, 1991, Liou and Storz, 2010, Babior, 1999). Indeed, cancer cells often show elevated expression of NRF2 and anti-oxidant defence to counteract the potentially lethal increases in ROS that accompany tumour progression (D'Autreaux and Toledano, 2007, Trachootham et al., 2009, DeNicola et al., 2015, Comerford et al., 2016, Menegon et al., 2016). Interestingly, differential expression and activity of NRF2 has been observed in healthy intestinal cells when compared to CRC tumour cells (Chang et al., 2013, Hayes and McMahon, 2009). Thus, colorectal cancer is no exception to NRF2's protective nature. Overexpression of NRF2 in response to excessive ROS was shown to result in inflammation of the colon tissue and promote tumourigenesis (Stachel et al., 2014). Additionally, following APC loss, c-MYC has been shown to promote ROS (Cheung et al., 2016). Therefore, the evidence presented here suggests that transformed cells can upregulate NUAK1 expression and consequently, activate NRF2 transcriptional activity to protect tumour cells from rising oxidative stress. This facilitates tumour genesis and progression. Thus NUAK1 is not a classical oncogene, its function facilitates, rather than drives tumourigenesis. Loss of Nuak1 in established tumours led to an increase in ROS levels that were concurrent with reduced proliferation and increased cell death. This suggests that tumour cells cannot sustain the rising levels of ROS without Nuak1-mediated

regulation of Nrf2 (summarised in Figure 6.1C). Low levels of ROS are pro-tumourigenic and high levels of ROS are cytotoxic, therefore a fine balance of NRF2 regulation is required (Liou and Storz, 2010). This is reflected in this study demonstrating that NUAK1 expression increases with progressing tumour stage; it is likely that as the requirement for the anti-oxidant response increases so does the selective pressure for tumour cells to overexpress NUAK1.

Furthermore, high expression of NRF2 in tumours have been correlated with poor prognosis in cancer patients partly due to an increase in NRF2 dependent cell proliferation and resistance to chemotherapy and radiotherapy (Shibata et al., 2008a, Solis et al., 2010b, Sasaki et al., 2013, Kang et al., 2014, Kang et al., 2016). Using online datasets, high NUAK1 expression also significantly reduced overall survival in three independent cohorts of human CRC patients. In agreement, high NRF2 expression also correlated with a significant reduction in patient survival in two out of the three of these datasets. Therefore, patients with high NUAK1 may have poor prognosis due to consequential NRF2 activity.

Exploiting the heightened sensitivity of tumour cells to ROS is emerging as a plausible strategy for cancer therapy. Many chemotherapeutic and radiotherapeutic strategies are designed to excessively increase ROS levels to induce irreparable damages consequently resulting in tumour cell death (Liou and Storz, 2010, Alexandre et al., 2006, Bairati et al., 2005, Llobet et al., 2008). Additionally, Sulindac is an FDA approved, non-steroidal and anti-inflammatory drug currently being investigated for its potential use in tumour therapy. Sulindac modulates ROS levels and renders colon and lung cancers more sensitive to H<sub>2</sub>O<sub>2</sub>-triggered apoptosis (Marchetti et al., 2009). More recently, intravenous injection of high doses of di-hydro-Ascorbate was revealed to suppress colorectal tumour formation by saturating ROS scavengers (Yun et al., 2015), and further work by Schoenfeld et al. confirms that this therapeutic strategy may have clinical benefit (Schoenfeld et al., 2017). Furthermore, Wang et al. found that the downregulation of NRF2 makes cancer cells more sensitive to chemotherapeutic drugs such as cisplatin, doxorubicin and etoposide (Wang et al., 2008b). Based on these studies and the data within this thesis, inhibiting the anti-oxidant response via transient inhibition of NUAK1 may offer a new strategy for reducing acquired resistance to chemotherapeutic drugs and improve therapeutic outcomes in CRC.

It must be considered that NRF2 has a very complex role in tumourigenesis, and the literature suggests that NRF2 can be both pro-tumourigenic and anti-tumourigenic depending on the tumour type and stage (Menegon et al., 2016). This suggests that

therapeutic inhibition of NRF2 via NUA1 may not be as straightforward as the data above suggests. As alluded to earlier, regulation of NRF2 requires a fine balance during tumourigenesis, and to use it therapeutically, temporal consideration is required. In CRC, inhibition of NRF2 has also been linked to increased risk of CRC (Li et al., 2008). Recently, silencing of Nrf2 was shown to increase the number of aberrant crypts, resulting in the formation of adenoma and the progression of CRC (Yokoo et al., 2016). Additionally, other studies have demonstrated that Nrf2 knockout mice are more susceptible to treatments that cause inflammation and ulcerative colitis including DSS and, as in the previous study, form more aberrant crypts (Khor et al., 2006, Osburn et al., 2007a). Notably, this effect was not observed in the model presented in this study as Nua1 depletion was induced post DSS treatment and tumour formation. Arlt et al. observed that NRF2 expression is beneficial in preventing early stage tumourigenesis, however can contribute to progression in the colon at later stages (Arlt et al., 2009), and as such NRF2 is now considered both a tumour suppressor gene and an oncogene (Menegon et al., 2016, Sporn and Liby, 2012). Therefore, in order to be effective, therapeutic inhibition of NRF2 via NUA1 must occur in progressed tumours where NRF2 is oncogenic. Importantly, most patients present at the clinic with symptoms associated with developed colorectal tumours therefore in most cases, inhibition of NUA1 could indeed improve current CRC treatments.

c-MYC is a proto-oncogene that has been implicated in the pathogenesis of the majority of human cancers. In healthy cells activation of c-MYC is usually restrained by controlled checkpoint mechanisms, however when c-MYC activation occurs via epigenetic and/or genetic alterations, c-MYC contributes to many hallmarks of cancer. These include uninhibited cell proliferation and growth, DNA replication, protein biogenesis, altered global metabolism, angiogenesis, and a restriction of host immune response (Gabay et al., 2014). As mentioned previously, MYC has been shown to also promote ROS in the gut (Cheung et al., 2016). Solid tumours rapidly outgrow existing vasculature and despite angiogenesis, experience depletion of nutrients and hypoxia leading to further cellular ROS and endoplasmic reticulum (ER) stress. The metabolic challenges of malignant growth result in cancer cell vulnerabilities related to irregular nutrient supply and incessant growth. Taking together that c-MYC is essential for CRC formation (Sansom et al., 2007), and that CRC cell lines demonstrated increased susceptibility to inhibition of NUA1 when compared to U2OS and wildtype mouse embryonic fibroblasts (MEFs), it appears that requirement for NUA1 remains associated with MYC-dependent phenotypes. Therefore, this data strongly suggests that NUA1 is one of the aforementioned

vulnerabilities and that cells with overexpressed c-MYC become addicted to NUA1 for its tumour protective roles in a changing metabolic environment, not only for ATP homeostasis, but also for the oxidative stress response.

The data presented in this thesis has confirmed that NUA1 is involved in redox regulation and tumour survival. However, there are many further questions to be answered. Currently, no NUA1 small molecule inhibitors have been validated *in vivo*. The development of a NUA1 inhibitor that is potent *in vivo* will be the next step in this investigation to assess Nuak1 inhibition in GEMMs of CRC and other tumour models. Additionally, there are drawbacks to the models used in this study. The ultimate goal when utilising a mouse model for cancer research is that the model recapitulates the human disease. Thus, to predict CRC patient response accurately, a mouse model that forms metastasis is required. Furthermore, the current literature suggests that NUA1 is enriched in liver metastasis (Kusakai et al., 2004). Therefore, future plans for this project include the investigation of Nuak1 in a metastatic CRC GEMM, *VillinCreER; KRas<sup>G12D/+</sup>; P53<sup>fl/fl</sup>; Nid1<sup>LSL/+</sup>*. This model develops metastatic disease with 100% penetrance in the lymph nodes, liver and/or lungs, and have a median survival of about 180 days. It would also be interesting and important to investigate NUA1-dependent regulation of NRF2 in other tumour types as there is evidence of a conserved mechanism between osteosarcoma-derived cell line, U2OS and colorectal adenocarcinoma-derived cell lines. Finally, the contribution of other AMPK-RKs including NUA2, to this mechanism is still unclear and will require further investigation.

In conclusion, this study has established a new and exciting role for NUA1 in the regulation of the NRF2-dependent oxidative stress response, which appears to leave tumours vulnerable to therapeutic intervention. Thereby, inhibition of NUA1 may offer a new strategy to improve therapeutic outcomes in colorectal cancer patients.

## Bibliography

2010. The Universal Protein Resource (UniProt) in 2010. *Nucleic Acids Res*, 38, D142-8.
2017. *A Study of LGK974 in Patients With Malignancies Dependent on Wnt Ligands* [Online]. ClinicalTrials.gov. Available: <https://clinicaltrials.gov/ct2/show/NCT01351103> [Accessed 30 July 2017 2017].
- ACKERMAN, D. & SIMON, M. C. 2014. Hypoxia, lipids, and cancer: surviving the harsh tumor microenvironment. *Trends Cell Biol*, 24, 472-8.
- AGUIRRE-GAMBOA, R., GOMEZ-RUEDA, H., MARTINEZ-LEDESMA, E., MARTINEZ-TORTEYA, A., CHACOLLA-HUARINGA, R., RODRIGUEZ-BARRIENTOS, A., TAMEZ-PENA, J. G. & TREVINO, V. 2013. SurvExpress: an online biomarker validation tool and database for cancer gene expression data using survival analysis. *PLoS One*, 8, e74250.
- ALEXANDRE, J., BATTEUX, F., NICCO, C., CHEREAU, C., LAURENT, A., GUILLEVIN, L., WEILL, B. & GOLDWASSER, F. 2006. Accumulation of hydrogen peroxide is an early and crucial step for paclitaxel-induced cancer cell death both in vitro and in vivo. *Int J Cancer*, 119, 41-8.
- AMADO, R. G., WOLF, M., PEETERS, M., VAN CUTSEM, E., SIENA, S., FREEMAN, D. J., JUAN, T., SIKORSKI, R., SUGGS, S., RADINSKY, R., PATTERSON, S. D. & CHANG, D. D. 2008. Wild-type KRAS is required for panitumumab efficacy in patients with metastatic colorectal cancer. *J Clin Oncol*, 26, 1626-34.
- ANASTAS, J. N. & MOON, R. T. 2013. WNT signalling pathways as therapeutic targets in cancer. *Nat Rev Cancer*, 13, 11-26.
- ANDREU, P., COLNOT, S., GODARD, C., GAD, S., CHAFEY, P., NIWAKAWAKITA, M., LAURENT-PUIG, P., KAHN, A., ROBINE, S., PERRET, C. & ROMAGNOLO, B. 2005. Crypt-restricted proliferation and commitment to the Paneth cell lineage following Apc loss in the mouse intestine. *Development*, 132, 1443-51.
- ARLT, A., BAUER, I., SCHAFMAYER, C., TEPEL, J., MUERKOSTER, S. S., BROSCHE, M., RODER, C., KALTHOFF, H., HAMPE, J., MOYER, M. P., FOLSCH, U. R. & SCHAFER, H. 2009. Increased proteasome subunit protein expression and proteasome activity in colon cancer relate to an enhanced activation of nuclear factor E2-related factor 2 (Nrf2). *Oncogene*, 28, 3983-96.
- ARTALE, S., SARTORE-BIANCHI, A., VERONESE, S. M., GAMBI, V., SARNATARO, C. S., GAMBACORTA, M., LAURICELLA, C. & SIENA, S. 2008. Mutations of KRAS and BRAF in primary and matched metastatic sites of colorectal cancer. *J Clin Oncol*, 26, 4217-9.
- ARVANITIS, C. & FELSHER, D. W. 2005. Conditionally MYC: insights from novel transgenic models. *Cancer Lett*, 226, 95-9.
- ASC. 2005-2007. *Colorectal Cancer: Stages* [Online]. Available: <http://www.cancer.net/cancer-types/colorectal-cancer/stages> [Accessed 16/07/17].
- AU, H. J., KARAPETIS, C. S., O'CALLAGHAN, C. J., TU, D., MOORE, M. J., ZALCBERG, J. R., KENNECKE, H., SHAPIRO, J. D., KOSKI, S., PAVLAKIS, N., CHARPENTIER, D., WYLD, D., JEFFORD, M., KNIGHT, G. J., MAGOSKI, N. M., BRUNDAGE, M. D. & JONKER, D. J. 2009. Health-related quality of life in patients with advanced colorectal cancer treated with cetuximab: overall and KRAS-specific results of the NCIC CTG and AGITG CO.17 Trial. *J Clin Oncol*, 27, 1822-8.
- BABIOR, B. M. 1999. NADPH oxidase: an update. *Blood*, 93, 1464-76.

- BAIRATI, I., MEYER, F., GELINAS, M., FORTIN, A., NABID, A., BROCHET, F., MERCIER, J. P., TETU, B., HAREL, F., ABDOUS, B., VIGNEAULT, E., VASS, S., DEL VECCHIO, P. & ROY, J. 2005. Randomized trial of antioxidant vitamins to prevent acute adverse effects of radiation therapy in head and neck cancer patients. *J Clin Oncol*, 23, 5805-13.
- BANERJEE, S., BUHRLAGE, SARA J., HUANG, H.-T., DENG, X., ZHOU, W., WANG, J., TRAYNOR, R., PRESCOTT, ALAN R., ALESSI, DARIO R. & GRAY, NATHANAEEL S. 2014a. Characterization of WZ4003 and HTH-01-015 as selective inhibitors of the LKB1-tumour-suppressor-activated NUA1 kinases. *Biochemical Journal*, 457, 215-225.
- BANERJEE, S., ZAGORSKA, A., DEAK, M., CAMPBELL, D. G., PRESCOTT, A. R. & ALESSI, D. R. 2014b. Interplay between Polo kinase, LKB1-activated NUA1 kinase, PP1betaMYPT1 phosphatase complex and the SCFbetaTrCP E3 ubiquitin ligase. *Biochem J*, 461, 233-45.
- BARKER, N., RIDGWAY, R. A., VAN ES, J. H., VAN DE WETERING, M., BEGTHEL, H., VAN DEN BORN, M., DANENBERG, E., CLARKE, A. R., SANSOM, O. J. & CLEVERS, H. 2009. Crypt stem cells as the cells-of-origin of intestinal cancer. *Nature*, 457, 608-11.
- BARON, J. A., COLE, B. F., SANDLER, R. S., HAILE, R. W., AHNEN, D., BRESALIER, R., MCKEOWN-EYSSSEN, G., SUMMERS, R. W., ROTHSTEIN, R., BURKE, C. A., SNOVER, D. C., CHURCH, T. R., ALLEN, J. I., BEACH, M., BECK, G. J., BOND, J. H., BYERS, T., GREENBERG, E. R., MANDEL, J. S., MARCON, N., MOTT, L. A., PEARSON, L., SAIBIL, F. & VAN STOLK, R. U. 2003. A randomized trial of aspirin to prevent colorectal adenomas. *N Engl J Med*, 348, 891-9.
- BAUR, J. A., PEARSON, K. J., PRICE, N. L., JAMIESON, H. A., LERIN, C., KALRA, A., PRABHU, V. V., ALLARD, J. S., LOPEZ-LLUCH, G., LEWIS, K., PISTELL, P. J., POOSALA, S., BECKER, K. G., BOSS, O., GWINN, D., WANG, M., RAMASWAMY, S., FISHBEIN, K. W., SPENCER, R. G., LAKATTA, E. G., LE COUTEUR, D., SHAW, R. J., NAVAS, P., PUIGSERVER, P., INGRAM, D. K., DE CABO, R. & SINCLAIR, D. A. 2006. Resveratrol improves health and survival of mice on a high-calorie diet. *Nature*, 444, 337-42.
- BELL, R. E., KHALED, M., NETANELY, D., SCHUBERT, S., GOLAN, T., BUXBAUM, A., JANAS, M. M., POSTOLSKY, B., GOLDBERG, M. S., SHAMIR, R. & LEVY, C. 2014. Transcription factor/microRNA axis blocks melanoma invasion program by miR-211 targeting NUA1. *J Invest Dermatol*, 134, 441-51.
- BETTENCOURT-DIAS, M., GIET, R., SINKA, R., MAZUMDAR, A., LOCK, W. G., BALLOUX, F., ZAFIROPOULOS, P. J., YAMAGUCHI, S., WINTER, S., CARTHEW, R. W., COOPER, M., JONES, D., FRENZ, L. & GLOVER, D. M. 2004. Genome-wide survey of protein kinases required for cell cycle progression. *Nature*, 432, 980-7.
- BEUREL, E., GRIECO, S. F. & JOPE, R. S. 2015. Glycogen synthase kinase-3 (GSK3): regulation, actions, and diseases. *Pharmacol Ther*, 148, 114-31.
- BIJUR, G. N. & JOPE, R. S. 2001. Proapoptotic stimuli induce nuclear accumulation of glycogen synthase kinase-3 beta. *J Biol Chem*, 276, 37436-42.
- BLOEMENDAAL, A. L., BUCHS, N. C., GEORGE, B. D. & GUY, R. J. 2016. Intestinal stem cells and intestinal homeostasis in health and in inflammation: A review. *Surgery*, 159, 1237-48.

- BOKEMEYER, C., BONDARENKO, I., HARTMANN, J. T., DE BRAUD, F., SCHUCH, G., ZUBEL, A., CELIK, I., SCHLICHTING, M. & KORALEWSKI, P. 2011. Efficacy according to biomarker status of cetuximab plus FOLFOX-4 as first-line treatment for metastatic colorectal cancer: the OPUS study. *Ann Oncol*, 22, 1535-46.
- BOKEMEYER, C., BONDARENKO, I., MAKHSON, A., HARTMANN, J. T., APARICIO, J., DE BRAUD, F., DONEA, S., LUDWIG, H., SCHUCH, G., STROH, C., LOOS, A. H., ZUBEL, A. & KORALEWSKI, P. 2009. Fluorouracil, leucovorin, and oxaliplatin with and without cetuximab in the first-line treatment of metastatic colorectal cancer. *J Clin Oncol*, 27, 663-71.
- BOLT, A. B., PAPANIKOLAOU, A., DELKER, D. A., WANG, Q. S. & ROSENBERG, D. W. 2000. Azoxymethane induces KI-ras activation in the tumor resistant AKR/J mouse colon. *Mol Carcinog*, 27, 210-8.
- BOSMAN, F. T., DE BRUINE, A., FLOHIL, C., VAN DER WURFF, A., TEN KATE, J. & DINJENS, W. W. 1993. Epithelial-stromal interactions in colon cancer. *Int J Dev Biol*, 37, 203-11.
- BRABLETZ, T., JUNG, A. & KIRCHNER, T. 2002.  $\beta$ -Catenin and the morphogenesis of colorectal cancer. *Virchows Archiv*, 441, 1-11.
- BRAZIL, D. P., PARK, J. & HEMMING, B. A. 2002. PKB binding proteins. Getting in on the Akt. *Cell*, 111, 293-303.
- BRIGHT, N. J., CARLING, D. & THORNTON, C. 2008. Investigating the regulation of brain-specific kinases 1 and 2 by phosphorylation. *J Biol Chem*, 283, 14946-54.
- BRIGHT, N. J., THORNTON, C. & CARLING, D. 2009. The regulation and function of mammalian AMPK-related kinases. *Acta Physiol (Oxf)*, 196, 15-26.
- CALON, A., LONARDO, E., BERENQUER-LLERGO, A., ESPINET, E., HERNANDOMOMBLONA, X., IGLESIAS, M., SEVILLANO, M., PALOMO-PONCE, S., TAURIELLO, D. V., BYROM, D., CORTINA, C., MORRAL, C., BARCELO, C., TOSI, S., RIERA, A., ATTOLINI, C. S., ROSSELL, D., SANCHO, E. & BATLLE, E. 2015. Stromal gene expression defines poor-prognosis subtypes in colorectal cancer. *Nat Genet*, 47, 320-9.
- CARTER, B. S., FLETCHER, J. S. & THOMPSON, R. C. 2010. Analysis of messenger RNA expression by in situ hybridization using RNA probes synthesized via in vitro transcription. *Methods*, 52, 322-31.
- CHANG, L. C., FAN, C. W., TSENG, W. K., CHEN, J. R., CHEIN, H. P., HWANG, C. C. & HUA, C. C. 2013. Immunohistochemical study of the Nrf2 pathway in colorectal cancer: Nrf2 expression is closely correlated to Keap1 in the tumor and Bach1 in the normal tissue. *Appl Immunohistochem Mol Morphol*, 21, 511-7.
- CHANG, X. Z., YU, J., LIU, H. Y., DONG, R. H. & CAO, X. C. 2012. ARK5 is associated with the invasive and metastatic potential of human breast cancer cells. *J Cancer Res Clin Oncol*, 138, 247-54.
- CHEN, P., LI, K., LIANG, Y., LI, L. & ZHU, X. 2013. High NUA1 expression correlates with poor prognosis and involved in NSCLC cells migration and invasion. *Exp Lung Res*, 39, 9-17.
- CHEUNG, E. C., LEE, P., CETECI, F., NIXON, C., BLYTH, K., SANSOM, O. J. & VOUSDEN, K. H. 2016. Opposing effects of TIGAR- and RAC1-derived ROS on Wnt-driven proliferation in the mouse intestine. *Genes & Development*, 30, 52-63.
- CHOWDHRY, S., ZHANG, Y., MCMAHON, M., SUTHERLAND, C., CUADRADO, A. & HAYES, J. D. 2013. Nrf2 is controlled by two distinct beta-TrCP recognition motifs in its Neh6 domain, one of which can be modulated by GSK-3 activity. *Oncogene*, 32, 3765-81.
- CIOMBOR, K. K., WU, C. & GOLDBERG, R. M. 2015. Recent therapeutic advances in the treatment of colorectal cancer. *Annu Rev Med*, 66, 83-95.

- CLARK, D. A. & COKER, R. 1998. Transforming growth factor-beta (TGF-beta). *Int J Biochem Cell Biol*, 30, 293-8.
- COMERFORD, S. A., HINNANT, E. A., CHEN, Y., BANSAL, H., KLAPPROTH, S., RAKHEJA, D., FINEGOLD, M. J., LOPEZ-TERRADA, D., O'DONNELL, K. A., TOMLINSON, G. E. & HAMMER, R. E. 2016. Hepatoblastoma modeling in mice places Nrf2 within a cancer field established by mutant beta-catenin. *JCI Insight*, 1, e88549.
- CORTON, J. M., GILLESPIE, J. G., HAWLEY, S. A. & HARDIE, D. G. 1995. 5-aminoimidazole-4-carboxamide ribonucleoside. A specific method for activating AMP-activated protein kinase in intact cells? *Eur J Biochem*, 229, 558-65.
- COX, J. & MANN, M. 2008. MaxQuant enables high peptide identification rates, individualized p.p.b.-range mass accuracies and proteome-wide protein quantification. *Nat Biotechnol*, 26, 1367-72.
- COX, J., NEUHAUSER, N., MICHALSKI, A., SCHELTEMA, R. A., OLSEN, J. V. & MANN, M. 2011. Andromeda: a peptide search engine integrated into the MaxQuant environment. *J Proteome Res*, 10, 1794-805.
- CUI, J., YU, Y., LU, G. F., LIU, C., LIU, X., XU, Y. X. & ZHENG, P. Y. 2013. Overexpression of ARK5 is associated with poor prognosis in hepatocellular carcinoma. *Tumour Biol*, 34, 1913-8.
- D'AUTREAUX, B. & TOLEDANO, M. B. 2007. ROS as signalling molecules: mechanisms that generate specificity in ROS homeostasis. *Nat Rev Mol Cell Biol*, 8, 813-24.
- DALE, S., WILSON, W. A., EDELMAN, A. M. & HARDIE, D. G. 1995. Similar substrate recognition motifs for mammalian AMP-activated protein kinase, higher plant HMG-CoA reductase kinase-A, yeast SNF1, and mammalian calmodulin-dependent protein kinase I. *FEBS letters*, 361, 191-195.
- DANG, C. V., LE, A. & GAO, P. 2009. MYC-induced cancer cell energy metabolism and therapeutic opportunities. *Clin Cancer Res*, 15, 6479-83.
- DANG, C. V., RESAR, L. M., EMISON, E., KIM, S., LI, Q., PRESCOTT, J. E., WONSEY, D. & ZELLER, K. 1999. Function of the c-Myc oncogenic transcription factor. *Exp Cell Res*, 253, 63-77.
- DANIELSEN, S. A., LIND, G. E., BJORNSLETT, M., MELING, G. I., ROGNUM, T. O., HEIM, S. & LOTHE, R. A. 2008. Novel mutations of the suppressor gene PTEN in colorectal carcinomas stratified by microsatellite instability- and TP53 mutation-status. *Hum Mutat*, 29, E252-62.
- DATTA, S. R., DUDEK, H., TAO, X., MASTERS, S., FU, H., GOTOH, Y. & GREENBERG, M. E. 1997. Akt phosphorylation of BAD couples survival signals to the cell-intrinsic death machinery. *Cell*, 91, 231-41.
- DE ROSA, M., REGA, D., COSTABILE, V., DURATURO, F., NIGLIO, A., IZZO, P., PACE, U. & DELRIO, P. 2016. The biological complexity of colorectal cancer: insights into biomarkers for early detection and personalized care. *Therap Adv Gastroenterol*, 9, 861-886.
- DE SOUZA-PINTO, N. C., EIDE, L., HOGUE, B. A., THYBO, T., STEVNSNER, T., SEEBERG, E., KLUNGLAND, A. & BOHR, V. A. 2001. Repair of 8-oxodeoxyguanosine lesions in mitochondrial dna depends on the oxoguanine dna glycosylase (OGG1) gene and 8-oxoguanine accumulates in the mitochondrial dna of OGG1-defective mice. *Cancer research*, 61, 5378-5381.
- DEACU, E., MORI, Y., SATO, F., YIN, J., OLARU, A., STERIAN, A., XU, Y., WANG, S., SCHULMANN, K., BERKI, A., KAN, T., ABRAHAM, J. M. & MELTZER, S. J. 2004. Activin type II receptor restoration in ACVR2-deficient colon cancer cells induces transforming growth factor-beta response pathway genes. *Cancer Res*, 64, 7690-6.

- DEKHUIJZEN, P. N. 2004. Antioxidant properties of N-acetylcysteine: their relevance in relation to chronic obstructive pulmonary disease. *Eur Respir J*, 23, 629-36.
- DELCOMMENNE, M., TAN, C., GRAY, V., RUE, L., WOODGETT, J. & DEDHAR, S. 1998. Phosphoinositide-3-OH kinase-dependent regulation of glycogen synthase kinase 3 and protein kinase B/AKT by the integrin-linked kinase. *Proc Natl Acad Sci U S A*, 95, 11211-6.
- DELKER, D. A., WANG, Q. S., PAPANIKOLAOU, A., WHITELEY, H. E. & ROSENBERG, D. W. 1999. Quantitative assessment of azoxymethane-induced aberrant crypt foci in inbred mice. *Exp Mol Pathol*, 65, 141-9.
- DENICOLA, G. M., CHEN, P. H., MULLARKY, E., SUDDERTH, J. A., HU, Z., WU, D., TANG, H., XIE, Y., ASARA, J. M., HUFFMAN, K. E., WISTUBA, II, MINNA, J. D., DEBERARDINIS, R. J. & CANTLEY, L. C. 2015. NRF2 regulates serine biosynthesis in non-small cell lung cancer. *Nat Genet*, 47, 1475-81.
- DENICOLA, G. M., KARRETH, F. A., HUMPTON, T. J., GOPINATHAN, A., WEI, C., FRESE, K., MANGAL, D., YU, K. H., YEO, C. J., CALHOUN, E. S., SCRIMIERY, F., WINTER, J. M., HRUBAN, R. H., IACOBUIZIO-DONAHUE, C., KERN, S. E., BLAIR, I. A. & TUVESON, D. A. 2011. Oncogene-induced Nrf2 transcription promotes ROS detoxification and tumorigenesis. *Nature*, 475, 106-9.
- DEY, D., SAXENA, M., PARANJAPPE, A. N., KRISHNAN, V., GIRADDI, R., KUMAR, M. V., MUKHERJEE, G. & RANGARAJAN, A. 2009. Phenotypic and Functional Characterization of Human Mammary Stem/Progenitor Cells in Long Term Culture. *PLoS ONE*, 4, e5329.
- DINKOVA-KOSTOVA, A. T., HOLTZCLAW, W. D., COLE, R. N., ITOH, K., WAKABAYASHI, N., KATO, Y., YAMAMOTO, M. & TALALAY, P. 2002. Direct evidence that sulfhydryl groups of Keap1 are the sensors regulating induction of phase 2 enzymes that protect against carcinogens and oxidants. *Proc Natl Acad Sci U S A*, 99, 11908-13.
- DOW, L. E., PREMSRIRUT, P. K., ZUBER, J., FELLMANN, C., MCJUNKIN, K., MIETHING, C., PARK, Y., DICKINS, R. A., HANNON, G. J. & LOWE, S. W. 2012. A pipeline for the generation of shRNA transgenic mice. *Nat. Protocols*, 7, 374-393.
- DOWNWARD, J. 2003. Targeting RAS signalling pathways in cancer therapy. *Nat Rev Cancer*, 3, 11-22.
- DREWES, G., EBNETH, A., PREUSS, U., MANDELKOW, E. M. & MANDELKOW, E. 1997. MARK, a novel family of protein kinases that phosphorylate microtubule-associated proteins and trigger microtubule disruption. *Cell*, 89, 297-308.
- DROST, J., VAN JAARSVELD, R. H., PONSIOEN, B., ZIMBERLIN, C., VAN BOXTEL, R., BUIJS, A., SACHS, N., OVERMEER, R. M., OFFERHAUS, G. J., BEGTHEL, H., KORVING, J., VAN DE WETERING, M., SCHWANK, G., LOGTENBERG, M., CUPPEN, E., SNIPPERT, H. J., MEDEMA, J. P., KOPS, G. J. & CLEVERS, H. 2015. Sequential cancer mutations in cultured human intestinal stem cells. *Nature*, 521, 43-7.
- DUNCAN, R., CARPENTER, B., MAIN, L. C., TELFER, C. & MURRAY, G. I. 2008. Characterisation and protein expression profiling of annexins in colorectal cancer. *Br J Cancer*, 98, 426-33.
- EADEN, J. A., ABRAMS, K. R. & MAYBERRY, J. F. 2001. The risk of colorectal cancer in ulcerative colitis: a meta-analysis. *Gut*, 48, 526-35.
- EGAN, B. & ZIERATH, J. R. 2009. Hunting for the SNARK in metabolic disease. *Am J Physiol Endocrinol Metab*, 296, E969-72.
- EILERS, M. & EISENMAN, R. N. 2008. Myc's broad reach. *Genes Dev*, 22, 2755-66.

- EL MARJOU, F., JANSSEN, K. P., CHANG, B. H., LI, M., HINDIE, V., CHAN, L., LOUVARD, D., CHAMBON, P., METZGER, D. & ROBINE, S. 2004. Tissue-specific and inducible Cre-mediated recombination in the gut epithelium. *Genesis*, 39, 186-93.
- EPPERT, K., SCHERER, S. W., OZCELIK, H., PIRONE, R., HOODLESS, P., KIM, H., TSUI, L. C., BAPAT, B., GALLINGER, S., ANDRULIS, I. L., THOMSEN, G. H., WRANA, J. L. & ATTISANO, L. 1996. MADR2 maps to 18q21 and encodes a TGFbeta-regulated MAD-related protein that is functionally mutated in colorectal carcinoma. *Cell*, 86, 543-52.
- ESUMI, H., IZUSHI, K., KATO, K., HASHIMOTO, K., KURASHIMA, Y., KISHIMOTO, A., OGIURA, T. & OZAWA, T. 2002. Hypoxia and nitric oxide treatment confer tolerance to glucose starvation in a 5'-AMP-activated protein kinase-dependent manner. *J Biol Chem*, 277, 32791-8.
- EVANS, G. S., FLINT, N., SOMERS, A. S., EYDEN, B. & POTTEN, C. S. 1992. The development of a method for the preparation of rat intestinal epithelial cell primary cultures. *J Cell Sci*, 101 ( Pt 1), 219-31.
- FAHEY, J. W., HARISTOY, X., DOLAN, P. M., KENSLER, T. W., SCHOLTUS, I., STEPHENSON, K. K., TALALAY, P. & LOZNIEWSKI, A. 2002. Sulforaphane inhibits extracellular, intracellular, and antibiotic-resistant strains of *Helicobacter pylori* and prevents benzo [a] pyrene-induced stomach tumors. *Proceedings of the National Academy of Sciences*, 99, 7610-7615.
- FANG, L., ZHU, Q., NEUENSCHWANDER, M., SPECKER, E., WULF-GOLDENBERG, A., WEIS, W. I., VON KRIES, J. P. & BIRCHMEIER, W. 2016. A Small-Molecule Antagonist of the beta-Catenin/TCF4 Interaction Blocks the Self-Renewal of Cancer Stem Cells and Suppresses Tumorigenesis. *Cancer Res*, 76, 891-901.
- FEARON, E. R. & VOGELSTEIN, B. 1990. A genetic model for colorectal tumorigenesis. *Cell*, 61, 759-67.
- FELLMANN, C., HOFFMANN, T., SRIDHAR, V., HOPFGARTNER, B., MUHAR, M., ROTH, M., LAI, D. Y., BARBOSA, I. A., KWON, J. S., GUAN, Y., SINHA, N. & ZUBER, J. 2013. An optimized microRNA backbone for effective single-copy RNAi. *Cell Rep*, 5, 1704-13.
- FELLMANN, C., ZUBER, J., MCJUNKIN, K., CHANG, K., MALONE, C. D., DICKINS, R. A., XU, Q., HENGARTNER, M. O., ELLEDGE, S. J., HANNON, G. J. & LOWE, S. W. 2011. Functional identification of optimized RNAi triggers using a massively parallel sensor assay. *Mol Cell*, 41, 733-46.
- FELSHER, D. W. & BISHOP, J. M. 1999. Reversible tumorigenesis by MYC in hematopoietic lineages. *Mol Cell*, 4, 199-207.
- FERNANDEZ, P. C., FRANK, S. R., WANG, L., SCHROEDER, M., LIU, S., GREENE, J., COCITO, A. & AMATI, B. 2003. Genomic targets of the human c-Myc protein. *Genes & development*, 17, 1115-1129.
- FISHER, J. S., JU, J.-S., OPPELT, P. J., SMITH, J. L., SUZUKI, A. & ESUMI, H. 2005. Muscle contractions, AICAR, and insulin cause phosphorylation of an AMPK-related kinase. *American journal of physiology. Endocrinology and metabolism*, 289, E986-E992.
- FLORES, I., MURPHY, D. J., SWIGART, L. B., KNIES, U. & EVAN, G. I. 2004. Defining the temporal requirements for Myc in the progression and maintenance of skin neoplasia. *Oncogene*, 23, 5923-30.
- FODDE, R., EDELMANN, W., YANG, K., VAN LEEUWEN, C., CARLSON, C., RENAULT, B., BREUKEL, C., ALT, E., LIPKIN, M., KHAN, P. M. & ET AL. 1994. A targeted chain-termination mutation in the mouse Apc gene results in multiple intestinal tumors. *Proc Natl Acad Sci U S A*, 91, 8969-73.

- FODDE, R. & KHAN, P. M. 1995. Genotype-phenotype correlations at the adenomatous polyposis coli (APC) gene. *Critical Reviews™ in Oncogenesis*, 6.
- FUJII, M., SHIMOKAWA, M., DATE, S., TAKANO, A., MATANO, M., NANKI, K., OHTA, Y., TOSHIMITSU, K., NAKAZATO, Y., KAWASAKI, K., URAOKA, T., WATANABE, T., KANAI, T. & SATO, T. 2016. A Colorectal Tumor Organoid Library Demonstrates Progressive Loss of Niche Factor Requirements during Tumorigenesis. *Cell Stem Cell*, 18, 827-38.
- FUKAMACHI, H. 1992. Proliferation and differentiation of fetal rat intestinal epithelial cells in primary serum-free culture. *J Cell Sci*, 103 ( Pt 2), 511-9.
- GABAY, M., LI, Y. & FELSHER, D. W. 2014. MYC Activation Is a Hallmark of Cancer Initiation and Maintenance. *Cold Spring Harbor Perspectives in Medicine*, 4, a014241.
- GARRAWAY, I. P., SUN, W., TRAN, C. P., PERNER, S., ZHANG, B., GOLDSTEIN, A. S., HAHM, S. A., HAIDER, M., HEAD, C. S., REITER, R. E., RUBIN, M. A. & WITTE, O. N. 2010. Human Prostate Sphere-Forming Cells Represent a Subset of Basal Epithelial Cells Capable of Glandular Regeneration in Vivo. *The Prostate*, 70, 491-501.
- GOSSEN, M. & BUJARD, H. 1992. Tight control of gene expression in mammalian cells by tetracycline-responsive promoters. *Proceedings of the National Academy of Sciences of the United States of America*, 89, 5547-5551.
- GRADY, W. M., MYEROFF, L. L., SWINLER, S. E., RAJPUT, A., THIAGALINGAM, S., LUTTERBAUGH, J. D., NEUMANN, A., BRATTAIN, M. G., CHANG, J., KIM, S. J., KINZLER, K. W., VOGELSTEIN, B., WILLSON, J. K. & MARKOWITZ, S. 1999. Mutational inactivation of transforming growth factor beta receptor type II in microsatellite stable colon cancers. *Cancer Res*, 59, 320-4.
- GRADY, W. M. & PRITCHARD, C. C. 2014. Molecular alterations and biomarkers in colorectal cancer. *Toxicol Pathol*, 42, 124-39.
- GRODEN, J., THLIVERIS, A., SAMOWITZ, W., CARLSON, M., GELBERT, L., ALBERTSEN, H., JOSLYN, G., STEVENS, J., SPIRIO, L., ROBERTSON, M. & ET AL. 1991. Identification and characterization of the familial adenomatous polyposis coli gene. *Cell*, 66, 589-600.
- GUINNEY, J., DIENSTMANN, R., WANG, X., DE REYNIES, A., SCHLICKER, A., SONESON, C., MARISA, L., ROEPMAN, P., NYAMUNDANDA, G., ANGELINO, P., BOT, B. M., MORRIS, J. S., SIMON, I. M., GERSTER, S., FESSLER, E., DE SOUSA, E. M. F., MISSIAGLIA, E., RAMAY, H., BARRAS, D., HOMICKO, K., MARU, D., MANYAM, G. C., BROOM, B., BOIGE, V., PEREZ-VILLAMIL, B., LADERAS, T., SALAZAR, R., GRAY, J. W., HANAHAN, D., TABERNEIRO, J., BERNARDS, R., FRIEND, S. H., LAURENT-PUIG, P., MEDEMA, J. P., SADANANDAM, A., WESSELS, L., DELORENZI, M., KOPETZ, S., VERMEULEN, L. & TEJPAR, S. 2015. The consensus molecular subtypes of colorectal cancer. *Nat Med*, 21, 1350-6.
- HAASE, P., COWEN, D. M. & KNOWLES, J. C. 1973. Histogenesis of colonic tumours in mice induced by dimethyl hydrazine. *J Pathol*, 109, Px.
- HAMAD, I., ARDA, N., PEKMEZ, M., KARAER, S. & TEMIZKAN, G. 2010. Intracellular scavenging activity of Trolox (6-hydroxy-2,5,7,8-tetramethylchromane-2-carboxylic acid) in the fission yeast, *Schizosaccharomyces pombe*. *J Nat Sci Biol Med*, 1, 16-21.
- HARDIE, D. G. 2003. Minireview: the AMP-activated protein kinase cascade: the key sensor of cellular energy status. *Endocrinology*, 144, 5179-83.
- HARDIE, D. G. & HAWLEY, S. A. 2001. AMP-activated protein kinase: the energy charge hypothesis revisited. *Bioessays*, 23, 1112-9.
- HARDIE, D. G., ROSS, F. A. & HAWLEY, S. A. 2012. AMPK: a nutrient and energy sensor that maintains energy homeostasis. *Nat Rev Mol Cell Biol*, 13, 251-62.

- HARDIE, D. G., SALT, I. P., HAWLEY, S. A. & DAVIES, S. P. 1999. AMP-activated protein kinase: an ultrasensitive system for monitoring cellular energy charge. *Biochem J*, 338 ( Pt 3), 717-22.
- HASHIMOTO, K., KATO, K., IMAMURA, K., KISHIMOTO, A., YOSHIKAWA, H., TAKETANI, Y. & ESUMI, H. 2002. 5-amino-4-imidazolecarboxamide riboside confers strong tolerance to glucose starvation in a 5'-AMP-activated protein kinase-dependent fashion. *Biochem Biophys Res Commun*, 290, 263-7.
- HAWLEY, S. A., BOUDEAU, J., REID, J. L., MUSTARD, K. J., UDD, L., MAKELA, T. P., ALESSI, D. R. & HARDIE, D. G. 2003. Complexes between the LKB1 tumor suppressor, STRAD alpha/beta and MO25 alpha/beta are upstream kinases in the AMP-activated protein kinase cascade. *J Biol*, 2, 28.
- HAWLEY, S. A., DAVISON, M., WOODS, A., DAVIES, S. P., BERI, R. K., CARLING, D. & HARDIE, D. G. 1996. Characterization of the AMP-activated protein kinase kinase from rat liver and identification of threonine 172 as the major site at which it phosphorylates AMP-activated protein kinase. *J Biol Chem*, 271, 27879-87.
- HAWLEY, S. A., PAN, D. A., MUSTARD, K. J., ROSS, L., BAIN, J., EDELMAN, A. M., FRENGUELLI, B. G. & HARDIE, D. G. 2005. Calmodulin-dependent protein kinase kinase-beta is an alternative upstream kinase for AMP-activated protein kinase. *Cell Metab*, 2, 9-19.
- HAWLEY, S. A., ROSS, F. A., CHEVTZOFF, C., GREEN, K. A., EVANS, A., FOGARTY, S., TOWLER, M. C., BROWN, L. J., OGUNBAYO, O. A., EVANS, A. M. & HARDIE, D. G. 2010. Use of cells expressing gamma subunit variants to identify diverse mechanisms of AMPK activation. *Cell Metab*, 11, 554-65.
- HAYASHI, S. & MCMAHON, A. P. 2002. Efficient recombination in diverse tissues by a tamoxifen-inducible form of Cre: a tool for temporally regulated gene activation/inactivation in the mouse. *Dev Biol*, 244, 305-18.
- HAYES, J. D. & MCMAHON, M. 2009. NRF2 and KEAP1 mutations: permanent activation of an adaptive response in cancer. *Trends in biochemical sciences*, 34, 176-188.
- HAYES, J. D., MCMAHON, M., CHOWDHRY, S. & DINKOVA-KOSTOVA, A. T. 2010. Cancer chemoprevention mechanisms mediated through the Keap1-Nrf2 pathway. *Antioxid Redox Signal*, 13, 1713-48.
- HERNÁNDEZ, F., LANGA, E., CUADROS, R., AVILA, J. & VILLANUEVA, N. 2010. Regulation of GSK3 isoforms by phosphatases PP1 and PP2A. *Molecular and cellular biochemistry*, 344, 211-215.
- HERRERO- MARTÍN, G., HØYER- HANSEN, M., GARCÍA- GARCÍA, C., FUMAROLA, C., FARKAS, T., LÓPEZ- RIVAS, A. & JÄÄTTELÄ, M. 2009. TAK1 activates AMPK- dependent cytoprotective autophagy in TRAIL- treated epithelial cells. *The EMBO journal*, 28, 677-685.
- HIGUCHI, M., MASUYAMA, N., FUKUI, Y., SUZUKI, A. & GOTOH, Y. 2001. Akt mediates Rac/Cdc42-regulated cell motility in growth factor-stimulated cells and in invasive PTEN knockout cells. *Curr Biol*, 11, 1958-62.
- HIRANO, M., KIYONARI, H., INOUE, A., FURUSHIMA, K., MURATA, T., SUDA, Y. & AIZAWA, S. 2006. A new serine/threonine protein kinase, Omphk1, essential to ventral body wall formation. *Dev Dyn*, 235, 2229-37.
- HIRAYAMA, A., YOH, K., NAGASE, S., UEDA, A., ITOH, K., MORITO, N., HIRAYAMA, K., TAKAHASHI, S., YAMAMOTO, M. & KOYAMA, A. 2003. EPR imaging of reducing activity in Nrf2 transcriptional factor-deficient mice. *Free Radical Biology and Medicine*, 34, 1236-1242.
- HOHENBERGER, W., WEBER, K., MATZEL, K., PAPADOPOULOS, T. & MERKEL, S. 2009. Standardized surgery for colonic cancer: complete mesocolic excision and central ligation--technical notes and outcome. *Colorectal Dis*, 11, 354-64; discussion 364-5.

- HONG, S.-P., LEIPER, F. C., WOODS, A., CARLING, D. & CARLSON, M. 2003. Activation of yeast Snf1 and mammalian AMP-activated protein kinase by upstream kinases. *Proceedings of the National Academy of Sciences*, 100, 8839-8843.
- HORIKE, N., TAKEMORI, H., KATOH, Y., DOI, J., MIN, L., ASANO, T., SUN, X. J., YAMAMOTO, H., KASAYAMA, S., MURAOKA, M., NONAKA, Y. & OKAMOTO, M. 2003. Adipose-specific expression, phosphorylation of Ser794 in insulin receptor substrate-1, and activation in diabetic animals of salt-inducible kinase-2. *J Biol Chem*, 278, 18440-7.
- HOU, X., LIU, J. E., LIU, W., LIU, C. Y., LIU, Z. Y. & SUN, Z. Y. 2011. A new role of NUA1: directly phosphorylating p53 and regulating cell proliferation. *Oncogene*, 30, 2933-42.
- HUMBERT, N., NAVARATNAM, N., AUGERT, A., DA COSTA, M., MARTIEN, S., WANG, J., MARTINEZ, D., ABBADIE, C., CARLING, D., DE LAUNOIT, Y., GIL, J. & BERNARD, D. 2010. Regulation of ploidy and senescence by the AMPK-related kinase NUA1. *Embo j*, 29, 376-86.
- HURWITZ, H., FEHRENBACHER, L., NOVOTNY, W., CARTWRIGHT, T., HAINSWORTH, J., HEIM, W., BERLIN, J., BARON, A., GRIFFING, S., HOLMGREN, E., FERRARA, N., FYFE, G., ROGERS, B., ROSS, R. & KABBINAVAR, F. 2004. Bevacizumab plus irinotecan, fluorouracil, and leucovorin for metastatic colorectal cancer. *N Engl J Med*, 350, 2335-42.
- HWANG, S. Y., DENG, X., BYUN, S., LEE, C., LEE, S. J., SUH, H., ZHANG, J., KANG, Q., ZHANG, T., WESTOVER, K. D., MANDINOVA, A. & LEE, S. W. 2016. Direct Targeting of beta-Catenin by a Small Molecule Stimulates Proteasomal Degradation and Suppresses Oncogenic Wnt/beta-Catenin Signaling. *Cell Rep*, 16, 28-36.
- INAZUKA, F., SUGIYAMA, N., TOMITA, M., ABE, T., SHIOI, G. & ESUMI, H. 2012. Muscle-specific knock-out of NUA1 family SNF1-like kinase 1 (NUAK1) prevents high fat diet-induced glucose intolerance. *J Biol Chem*, 287, 16379-89.
- INOMATA, M., OCHIAI, A., AKIMOTO, S., KITANO, S. & HIROHASHI, S. 1996. Alteration of  $\beta$ -catenin expression in colonic epithelial cells of familial adenomatous polyposis patients. *Cancer Research*, 56, 2213-2217.
- ITO, M., NAKANO, T., ERDODI, F. & HARTSHORNE, D. J. 2004. Myosin phosphatase: structure, regulation and function. *Mol Cell Biochem*, 259, 197-209.
- ITOH, K., WAKABAYASHI, N., KATOH, Y., ISHII, T., IGARASHI, K., ENGEL, J. D. & YAMAMOTO, M. 1999. Keap1 represses nuclear activation of antioxidant responsive elements by Nrf2 through binding to the amino-terminal Neh2 domain. *Genes & development*, 13, 76-86.
- IZUISHI, K., KATO, K., OGURA, T., KINOSHITA, T. & ESUMI, H. 2000. Remarkable tolerance of tumor cells to nutrient deprivation: possible new biochemical target for cancer therapy. *Cancer Res*, 60, 6201-7.
- JACKSON, E. L., WILLIS, N., MERCER, K., BRONSON, R. T., CROWLEY, D., MONTOYA, R., JACKS, T. & TUVESON, D. A. 2001. Analysis of lung tumor initiation and progression using conditional expression of oncogenic K-ras. *Genes Dev*, 15, 3243-8.
- JACKSTADT, R. & SANSOM, O. J. 2016. Mouse models of intestinal cancer. *J Pathol*, 238, 141-51.
- JALEEL, M., VILLA, F., DEAK, M., TOTH, R., PRESCOTT, A. R., VAN AALTEN, D. M. & ALESSI, D. R. 2006. The ubiquitin-associated domain of AMPK-related kinases regulates conformation and LKB1-mediated phosphorylation and activation. *Biochem J*, 394, 545-55.

- JANSSEN, K. P., EL-MARJOU, F., PINTO, D., SASTRE, X., ROUILLARD, D., FOUQUET, C., SOUSSI, T., LOUVARD, D. & ROBINE, S. 2002. Targeted expression of oncogenic K-ras in intestinal epithelium causes spontaneous tumorigenesis in mice. *Gastroenterology*, 123, 492-504.
- JARAMILLO, M. C. & ZHANG, D. D. 2013. The emerging role of the Nrf2-Keap1 signaling pathway in cancer. *Genes Dev*, 27, 2179-91.
- JASPERSON, K. W., TUOHY, T. M., NEKLASON, D. W. & BURT, R. W. 2010. Hereditary and familial colon cancer. *Gastroenterology*, 138, 2044-58.
- JAWHAR, N. M. T. 2009. Tissue Microarray: A rapidly evolving diagnostic and research tool. *Annals of Saudi Medicine*, 29, 123-127.
- JEON, S.-M., CHANDEL, N. S. & HAY, N. 2012. AMPK regulates NADPH homeostasis to promote tumour cell survival during energy stress. *Nature*, 485, 661-665.
- JIANG, T., CHEN, N., ZHAO, F., WANG, X.-J., KONG, B., ZHENG, W. & ZHANG, D. D. 2010. High levels of Nrf2 determine chemoresistance in type II endometrial cancer. *Cancer research*, 70, 5486-5496.
- JOHNSON, L., MERCER, K., GREENBAUM, D., BRONSON, R. T., CROWLEY, D., TUVESON, D. A. & JACKS, T. 2001. Somatic activation of the K-ras oncogene causes early onset lung cancer in mice. *Nature*, 410, 1111-6.
- JOHNSTON, P. G. 2014. Identification of clinically relevant molecular subtypes in colorectal cancer: the dawning of a new era. *The oncologist*, 19, 568-573.
- JOO, M. S., KIM, W. D., LEE, K. Y., KIM, J. H., KOO, J. H. & KIM, S. G. 2016. AMPK facilitates nuclear accumulation of Nrf2 by phosphorylating at serine 550. *Molecular and cellular biology*, 36, 1931-1942.
- JORISSEN, R. N., GIBBS, P., CHRISTIE, M., PRAKASH, S., LIPTON, L., DESAI, J., KERR, D., AALTONEN, L. A., ARANGO, D., KRUGHØFFER, M., ØRNTOFT, T. F., ANDERSEN, C. L., GRUIDL, M., KAMATH, V. P., ESCHRICHS, S., YEATMAN, T. J. & SIEBER, O. M. 2009. Metastasis-associated gene expression changes predict poor outcomes in patients with Dukes' stage B and C colorectal cancer. *Clinical cancer research : an official journal of the American Association for Cancer Research*, 15, 7642-7651.
- JUNG, P., SATO, T., MERLOS-SUAREZ, A., BARRIGA, F. M., IGLESIAS, M., ROSSELL, D., AUER, H., GALLARDO, M., BLASCO, M. A., SANCHO, E., CLEVERS, H. & BATLLE, E. 2011. Isolation and in vitro expansion of human colonic stem cells. *Nat Med*, 17, 1225-7.
- KAHN, M. 2014. Can we safely target the WNT pathway? *Nat Rev Drug Discov*, 13, 513-32.
- KALLURI, R. & ZEISBERG, M. 2006. Fibroblasts in cancer. *Nature reviews. Cancer*, 6, 392.
- KANG, K. A., PIAO, M. J., KIM, K. C., KANG, H. K., CHANG, W. Y., PARK, I. C., KEUM, Y. S., SURH, Y. J. & HYUN, J. W. 2014. Epigenetic modification of Nrf2 in 5-fluorouracil-resistant colon cancer cells: involvement of TET-dependent DNA demethylation. *Cell Death Dis*, 5, e1183.
- KANG, K. A., PIAO, M. J., RYU, Y. S., KANG, H. K., CHANG, W. Y., KEUM, Y. S. & HYUN, J. W. 2016. Interaction of DNA demethylase and histone methyltransferase upregulates Nrf2 in 5-fluorouracil-resistant colon cancer cells. *Oncotarget*, 7, 40594-40620.
- KATAJISTO, P., VALLENIUS, T., VAAHTOMERI, K., EKMAN, N., UDD, L., TIAINEN, M. & MAKELA, T. P. 2007. The LKB1 tumor suppressor kinase in human disease. *Biochim Biophys Acta*, 1775, 63-75.
- KATO, K., OGURA, T., KISHIMOTO, A., MINEGISHI, Y., NAKAJIMA, N., MIYAZAKI, M. & ESUMI, H. 2002. Critical roles of AMP-activated protein kinase in constitutive tolerance of cancer cells to nutrient deprivation and tumor formation. *Oncogene*, 21, 6082-90.

- KATOH, Y., TAKEMORI, H., LIN, X. Z., TAMURA, M., MURAOKA, M., SATOH, T., TSUCHIYA, Y., MIN, L., DOI, J., MIYAUCHI, A., WITTERS, L. A., NAKAMURA, H. & OKAMOTO, M. 2006. Silencing the constitutive active transcription factor CREB by the LKB1-SIK signaling cascade. *Febs j*, 273, 2730-48.
- KENNEDY, S. G., WAGNER, A. J., CONZEN, S. D., JORDAN, J., BELLACOSA, A., TSICHLIS, P. N. & HAY, N. 1997. The PI 3-kinase/Akt signaling pathway delivers an anti-apoptotic signal. *Genes Dev*, 11, 701-13.
- KESSLER, J. D., KAHLE, K. T., SUN, T., MEERBREY, K. L., SCHLABACH, M. R., SCHMITT, E. M., SKINNER, S. O., XU, Q., LI, M. Z., HARTMAN, Z. C., RAO, M., YU, P., DOMINGUEZ-VIDANA, R., LIANG, A. C., SOLIMINI, N. L., BERNARDI, R. J., YU, B., HSU, T., GOLDING, I., LUO, J., OSBORNE, C. K., CREIGHTON, C. J., HILSENBECK, S. G., SCHIFF, R., SHAW, C. A., ELLEDGE, S. J. & WESTBROOK, T. F. 2012. A SUMOylation-dependent transcriptional subprogram is required for Myc-driven tumorigenesis. *Science*, 335, 348-53.
- KHOR, T. O., HUANG, M.-T., PRAWAN, A., LIU, Y., HAO, X., YU, S., CHEUNG, W. K. L., CHAN, J. Y., REDDY, B. S. & YANG, C. S. 2008. Increased susceptibility of Nrf2 knockout mice to colitis-associated colorectal cancer. *Cancer prevention research*, 1, 187-191.
- KHOR, T. O., HUANG, M. T., KWON, K. H., CHAN, J. Y., REDDY, B. S. & KONG, A. N. 2006. Nrf2-deficient mice have an increased susceptibility to dextran sulfate sodium-induced colitis. *Cancer Res*, 66, 11580-4.
- KIM, J. H., KIM, W. S. & PARK, C. 2008. SNARK, a novel downstream molecule of EBV latent membrane protein 1, is associated with resistance to cancer cell death. *Leuk Lymphoma*, 49, 1392-8.
- KIM, Y. R., OH, J. E., KIM, M. S., KANG, M. R., PARK, S. W., HAN, J. Y., EOM, H. S., YOO, N. J. & LEE, S. H. 2010. Oncogenic NRF2 mutations in squamous cell carcinomas of oesophagus and skin. *The Journal of pathology*, 220, 446-451.
- KINZLER, K. W., NILBERT, M. C., SU, L. K., VOGELSTEIN, B., BRYAN, T. M., LEVY, D. B., SMITH, K. J., PREISINGER, A. C., HEDGE, P., MCKECHNIE, D. & ET AL. 1991. Identification of FAP locus genes from chromosome 5q21. *Science*, 253, 661-5.
- KISHI, M., PAN, Y. A., CRUMP, J. G. & SANES, J. R. 2005. Mammalian SAD kinases are required for neuronal polarization. *Science*, 307, 929-32.
- KOERA, K., NAKAMURA, K., NAKAO, K., MIYOSHI, J., TOYOSHIMA, K., HATTA, T., OTANI, H., AIBA, A. & KATSUKI, M. 1997. K-ras is essential for the development of the mouse embryo. *Oncogene*, 15, 1151-9.
- KUGA, W., TSUCHIHARA, K., OGURA, T., KANEHARA, S., SAITO, M., SUZUKI, A. & ESUMI, H. 2008. Nuclear localization of SNARK; its impact on gene expression. *Biochem Biophys Res Commun*, 377, 1062-6.
- KUSAKAI, G., SUZUKI, A., OGURA, T., MIYAMOTO, S., OCHIAI, A., KAMINISHI, M. & ESUMI, H. 2004. ARK5 expression in colorectal cancer and its implications for tumor progression. *Am J Pathol*, 164, 987-95.
- KYRIAKOS, M. 1985. The President's cancer, the Dukes classification, and confusion. *Arch Pathol Lab Med*, 109, 1063-6.
- LEE, S. R., YANG, K. S., KWON, J., LEE, C., JEONG, W. & RHEE, S. G. 2002. Reversible inactivation of the tumor suppressor PTEN by H<sub>2</sub>O<sub>2</sub>. *J Biol Chem*, 277, 20336-42.
- LEFEBVRE, D. L., BAI, Y., SHAHMOLKY, N., SHARMA, M., POON, R., DRUCKER, D. J. & ROSEN, C. F. 2001. Identification and characterization of a novel sucrose-non-fermenting protein kinase/AMP-activated protein kinase-related protein kinase, SNARK. *Biochem J*, 355, 297-305.

- LEFEBVRE, D. L. & ROSEN, C. F. 2005. Regulation of SNARK activity in response to cellular stresses. *Biochim Biophys Acta*, 1724, 71-85.
- LEGEMBRE, P., SCHICKEL, R., BARNHART, B. C. & PETER, M. E. 2004. Identification of SNF1/AMP kinase-related kinase as an NF-kappaB-regulated anti-apoptotic kinase involved in CD95-induced motility and invasiveness. *J Biol Chem*, 279, 46742-7.
- LESSARD, S. J., RIVAS, D. A., SO, K., KOH, H.-J., QUEIROZ, A. L., HIRSHMAN, M. F., FIELDING, R. A. & GOODYEAR, L. J. 2016. The AMPK-related kinase SNARK regulates muscle mass and myocyte survival. *The Journal of Clinical Investigation*, 126, 560-570.
- LEVY, D. B., SMITH, K. J., BEAZER-BARCLAY, Y., HAMILTON, S. R., VOGELSTEIN, B. & KINZLER, K. W. 1994. Inactivation of both APC alleles in human and mouse tumors. *Cancer Res*, 54, 5953-8.
- LEWANDOSKI, M., WASSARMAN, K. M. & MARTIN, G. R. 1997. Zp3-cre, a transgenic mouse line for the activation or inactivation of loxP-flanked target genes specifically in the female germ line. *Current Biology*, 7, 148-151.
- LI, W., KHOR, T. O., XU, C., SHEN, G., JEONG, W. S., YU, S. & KONG, A. N. 2008. Activation of Nrf2-antioxidant signaling attenuates NFkappaB-inflammatory response and elicits apoptosis. *Biochem Pharmacol*, 76, 1485-9.
- LIOU, G.-Y. & STORZ, P. 2010. Reactive oxygen species in cancer. *Free radical research*, 44, 10.3109/10715761003667554.
- LIU, L., ULBRICH, J., MULLER, J., WUSTEFELD, T., AEGERHARD, L., KRESS, T. R., MUTHALAGU, N., RYCAK, L., RUDALSKA, R., MOLL, R., KEMPA, S., ZENDER, L., EILERS, M. & MURPHY, D. J. 2012. Deregulated MYC expression induces dependence upon AMPK-related kinase 5. *Nature*, 483, 608-12.
- LIZCANO, J. M., GORANSSON, O., TOTH, R., DEAK, M., MORRICE, N. A., BOUDEAU, J., HAWLEY, S. A., UDD, L., MAKELA, T. P., HARDIE, D. G. & ALESSI, D. R. 2004. LKB1 is a master kinase that activates 13 kinases of the AMPK subfamily, including MARK/PAR-1. *Embo j*, 23, 833-43.
- LLOBET, D., ERITJA, N., ENCINAS, M., SOROLLA, A., YERAMIAN, A., SCHOENENBERGER, J. A., LLOMBART-CUSSAC, A., MARTI, R. M., MATIAS-GUIU, X. & DOLCET, X. 2008. Antioxidants block proteasome inhibitor function in endometrial carcinoma cells. *Anticancer Drugs*, 19, 115-24.
- LOMBARDI, L., NEWCOMB, E. W. & DALLA-FAVERA, R. 1987. Pathogenesis of Burkitt lymphoma: expression of an activated c-myc oncogene causes the tumorigenic conversion of EBV-infected human B lymphoblasts. *Cell*, 49, 161-70.
- LOVE, M. I., HUBER, W. & ANDERS, S. 2014. Moderated estimation of fold change and dispersion for RNA-seq data with DESeq2. *Genome Biol*, 15, 550.
- LU, S., NIU, N., GUO, H., TANG, J., GUO, W., LIU, Z., SHI, L., SUN, T., ZHOU, F., LI, H., ZHANG, J. & ZHANG, B. 2013. ARK5 promotes glioma cell invasion, and its elevated expression is correlated with poor clinical outcome. *Eur J Cancer*, 49, 752-63.
- MA, Q. 2013. Role of nrf2 in oxidative stress and toxicity. *Annual review of pharmacology and toxicology*, 53, 401-426.
- MADAN, B., KE, Z., HARMSTON, N., HO, S. Y., FROIS, A. O., ALAM, J., JEYARAJ, D. A., PENDHARKAR, V., GHOSH, K., VIRSHUP, I. H., MANOHARAN, V., ONG, E. H., SANGTHONGPITAG, K., HILL, J., PETRETTO, E., KELLER, T. H., LEE, M. A., MATTER, A. & VIRSHUP, D. M. 2016. Wnt addiction of genetically defined cancers reversed by PORCN inhibition. *Oncogene*, 35, 2197-207.
- MALLADI, S., MACALINAO, D. G., JIN, X., HE, L., BASNET, H., ZOU, Y., DE STANCHINA, E. & MASSAGUE, J. 2016. Metastatic Latency and Immune Evasion through Autocrine Inhibition of WNT. *Cell*, 165, 45-60.

- MANNING, G., WHYTE, D. B., MARTINEZ, R., HUNTER, T. & SUDARSANAM, S. 2002. The protein kinase complement of the human genome. *Science*, 298, 1912-34.
- MARCHETTI, M., RESNICK, L., GAMLIEL, E., KESARAJU, S., WEISSBACH, H. & BINNINGER, D. 2009. Sulindac enhances the killing of cancer cells exposed to oxidative stress. *PLoS One*, 4, e5804.
- MARTIN, M. S., MARTIN, F., MICHIELS, R., BASTIEN, H., JUSTRABO, E., BORDES, M. & VIRY, B. 1973. An experimental model for cancer of the colon and rectum. Intestinal carcinoma induced in the rat 1,2-dimethylhydrazine. *Digestion*, 8, 22-34.
- MATANO, M., DATE, S., SHIMOKAWA, M., TAKANO, A., FUJII, M., OHTA, Y., WATANABE, T., KANAI, T. & SATO, T. 2015. Modeling colorectal cancer using CRISPR-Cas9-mediated engineering of human intestinal organoids. *Nat Med*, 21, 256-62.
- MCCORMICK, F. 2015. KRAS as a Therapeutic Target. *Clin Cancer Res*, 21, 1797-801.
- MEARES, G. P. & JOPE, R. S. 2007. Resolution of the Nuclear Localization Mechanism of Glycogen Synthase Kinase-3 FUNCTIONAL EFFECTS IN APOPTOSIS. *Journal of Biological Chemistry*, 282, 16989-17001.
- MENEGON, S., COLUMBANO, A. & GIORDANO, S. 2016. The Dual Roles of NRF2 in Cancer. *Trends Mol Med*, 22, 578-93.
- MILLER, D. M., THOMAS, S. D., ISLAM, A., MUENCH, D. & SEDORIS, K. 2012. c-Myc and Cancer Metabolism. *Clinical cancer research : an official journal of the American Association for Cancer Research*, 18, 5546-5553.
- MOBASHER, M. A., GONZALEZ-RODRIGUEZ, A., SANTAMARIA, B., RAMOS, S., MARTIN, M. A., GOYA, L., RADA, P., LETZIG, L., JAMES, L. P., CUADRADO, A., MARTIN-PEREZ, J., SIMPSON, K. J., MUNTANE, J. & VALVERDE, A. M. 2013. Protein tyrosine phosphatase 1B modulates GSK3beta/Nrf2 and IGFIR signaling pathways in acetaminophen-induced hepatotoxicity. *Cell Death Dis*, 4, e626.
- MOI, P., CHAN, K., ASUNIS, I., CAO, A. & KAN, Y. W. 1994. Isolation of NF-E2-related factor 2 (Nrf2), a NF-E2-like basic leucine zipper transcriptional activator that binds to the tandem NF-E2/AP1 repeat of the beta-globin locus control region. *Proceedings of the National Academy of Sciences*, 91, 9926-9930.
- MONTEVERDE, T., TAIT-MULDHER, J., HEDLEY, A., KNIGHT, J., SANSOM, O.J., MURPHY, D.J. Accepted for publication. Calcium Signalling links MYC to NUA1. *Oncogene*.
- MORITO, N., YOH, K., ITOH, K., HIRAYAMA, A., KOYAMA, A., YAMAMOTO, M. & TAKAHASHI, S. 2003. Nrf2 regulates the sensitivity of death receptor signals by affecting intracellular glutathione levels. *Oncogene*, 22, 9275.
- MOSER, A. R., DOVE, W. F., ROTH, K. A. & GORDON, J. I. 1992. The Min (multiple intestinal neoplasia) mutation: its effect on gut epithelial cell differentiation and interaction with a modifier system. *J Cell Biol*, 116, 1517-26.
- MOSER, A. R., PITOT, H. C. & DOVE, W. F. 1990. A dominant mutation that predisposes to multiple intestinal neoplasia in the mouse. *Science*, 247, 322-4.
- MOTTA, G., NAHUM, M. A., TESTA, T. & SPINELLI, E. 1995. [TNM staging system of lung carcinoma: historical notes, limitations and controversies]. *Ann Ital Chir*, 66, 425-32.
- NAGASE, T., ISHIKAWA, K., SUYAMA, M., KIKUNO, R., HIROSAWA, M., MIYAJIMA, N., TANAKA, A., KOTANI, H., NOMURA, N. & OHARA, O. 1998. Prediction of the coding sequences of unidentified human genes. XII. The complete sequences of 100 new cDNA clones from brain which code for large proteins in vitro. *DNA Res*, 5, 355-64.

- NAGY, A. 2000. Cre recombinase: the universal reagent for genome tailoring. *Genesis*, 26, 99-109.
- NAMIKI, T., YAGUCHI, T., NAKAMURA, K., VALENCIA, J. C., COELHO, S. G., YIN, L., KAWAGUCHI, M., VIEIRA, W. D., KANEKO, Y., TANEMURA, A., KATAYAMA, I., YOKOZEKI, H., KAWAKAMI, Y. & HEARING, V. J. 2015. NUA2 amplification coupled with PTEN deficiency promote melanoma development via CDK activation. *Cancer research*, 75, 2708-2715.
- NESBIT, C. E., TERSAK, J. M. & PROCHOWNIK, E. V. 1999. MYC oncogenes and human neoplastic disease. *Oncogene*, 18, 3004-16.
- NGUYEN, D. X., CHIANG, A. C., ZHANG, X. H., KIM, J. Y., KRIS, M. G., LADANYI, M., GERALD, W. L. & MASSAGUE, J. 2009a. WNT/TCF signaling through LEF1 and HOXB9 mediates lung adenocarcinoma metastasis. *Cell*, 138, 51-62.
- NGUYEN, T., NIOI, P. & PICKETT, C. B. 2009b. The Nrf2-antioxidant response element signaling pathway and its activation by oxidative stress. *J Biol Chem*, 284, 13291-5.
- OHMURA, T., SHIOI, G., HIRANO, M. & AIZAWA, S. 2012. Neural tube defects by NUA1 and NUA2 double mutation. *Developmental Dynamics*, 241, 1350-1364.
- ORIAN, A., VAN STEENSEL, B., DELROW, J., BUSSEMAKER, H. J., LI, L., SAWADO, T., WILLIAMS, E., LOO, L. W., COWLEY, S. M. & YOST, C. 2003. Genomic binding by the Drosophila Myc, Max, Mad/Mnt transcription factor network. *Genes & development*, 17, 1101-1114.
- OSBURN, W. O., KARIM, B., DOLAN, P. M., LIU, G., YAMAMOTO, M., HUSO, D. L. & KENSLER, T. W. 2007a. Increased colonic inflammatory injury and formation of aberrant crypt foci in Nrf2-deficient mice upon dextran sulfate treatment. *Int J Cancer*, 121, 1883-91.
- OSBURN, W. O., KARIM, B., DOLAN, P. M., LIU, G., YAMAMOTO, M., HUSO, D. L. & KENSLER, T. W. 2007b. Increased colonic inflammatory injury and formation of aberrant crypt foci in Nrf2- deficient mice upon dextran sulfate treatment. *International Journal of Cancer*, 121, 1883-1891.
- OSHIMA, H., OSHIMA, M., KOBAYASHI, M., TSUTSUMI, M. & TAKETO, M. M. 1997. Morphological and molecular processes of polyp formation in Apc(delta716) knockout mice. *Cancer Res*, 57, 1644-9.
- OSHIMA, M., OSHIMA, H., KITAGAWA, K., KOBAYASHI, M., ITAKURA, C. & TAKETO, M. 1995. Loss of Apc heterozygosity and abnormal tissue building in nascent intestinal polyps in mice carrying a truncated Apc gene. *Proc Natl Acad Sci U S A*, 92, 4482-6.
- PEETERS, M., PRICE, T. J., CERVANTES, A., SOBRERO, A. F., DUCREUX, M., HOTKO, Y., ANDRE, T., CHAN, E., LORDICK, F., PUNT, C. J., STRICKLAND, A. H., WILSON, G., CIULEANU, T. E., ROMAN, L., VAN CUTSEM, E., TZEKOVA, V., COLLINS, S., OLINER, K. S., RONG, A. & GANSERT, J. 2010. Randomized phase III study of panitumumab with fluorouracil, leucovorin, and irinotecan (FOLFIRI) compared with FOLFIRI alone as second-line treatment in patients with metastatic colorectal cancer. *J Clin Oncol*, 28, 4706-13.
- PHIPPEN, N. T., BATEMAN, N. W., WANG, G., CONRADS, K. A., AO, W., TENG, P.-N., LITZI, T. A., OLIVER, J., MAXWELL, G. L., HAMILTON, C. A., DARCY, K. M. & CONRADS, T. P. 2016. NUA1 (ARK5) Is Associated with Poor Prognosis in Ovarian Cancer. *Frontiers in Oncology*, 6, 213.
- PINO, M. S. & CHUNG, D. C. 2010. The chromosomal instability pathway in colon cancer. *Gastroenterology*, 138, 2059-72.
- PINTO, D. & CLEVERS, H. 2005. Wnt, stem cells and cancer in the intestine. *Biology of the Cell*, 97, 185-196.

- POWELL, S. M., ZILZ, N., BEAZER-BARCLAY, Y., BRYAN, T. M., HAMILTON, S. R., THIBODEAU, S. N., VOGELSTEIN, B. & KINZLER, K. W. 1992. APC mutations occur early during colorectal tumorigenesis. *Nature*, 359, 235-7.
- PREMSRIRUT, P. K., DOW, L. E., KIM, S. Y., CAMIOLO, M., MALONE, C. D., MIETHING, C., SCUOPPO, C., ZUBER, J., DICKINS, R. A., KOGAN, S. C., SHROYER, K. R., SORDELLA, R., HANNON, G. J. & LOWE, S. W. 2011. A rapid and scalable system for studying gene function in mice using conditional RNA interference. *Cell*, 145, 145-58.
- QUESADA, C. F., KIMATA, H., MORI, M., NISHIMURA, M., TSUNEYOSHI, T. & BABA, S. 1998. Piroxicam and acarbose as chemopreventive agents for spontaneous intestinal adenomas in APC gene 1309 knockout mice. *Jpn J Cancer Res*, 89, 392-6.
- RADA, P., ROJO, A. I., CHOWDHRY, S., MCMAHON, M., HAYES, J. D. & CUADRADO, A. 2011. SCF/ $\beta$ -TrCP promotes glycogen synthase kinase 3-dependent degradation of the Nrf2 transcription factor in a Keap1-independent manner. *Mol Cell Biol*, 31, 1121-33.
- RAJAGOPALAN, H., NOWAK, M. A., VOGELSTEIN, B. & LENGAUER, C. 2003. The significance of unstable chromosomes in colorectal cancer. *Nat Rev Cancer*, 3, 695-701.
- RAMOS-GOMEZ, M., KWAK, M. K., DOLAN, P. M., ITOH, K., YAMAMOTO, M., TALALAY, P. & KENSLER, T. W. 2001. Sensitivity to carcinogenesis is increased and chemoprotective efficacy of enzyme inducers is lost in nrf2 transcription factor-deficient mice. *Proc Natl Acad Sci U S A*, 98, 3410-5.
- RAPPSILBER, J., MANN, M. & ISHIHAMA, Y. 2007. Protocol for micro-purification, enrichment, pre-fractionation and storage of peptides for proteomics using StageTips. *Nat Protoc*, 2, 1896-906.
- RAZIS, E., BRIASOULIS, E., VRETTOU, E., SKARLOS, D. V., PAPAMICHAEL, D., KOSTOPOULOS, I., SAMANTAS, E., XANTHAKIS, I., BOBOS, M., GALANIDI, E., BAI, M., GIKONTI, I., KOUKOUMA, A., KAFIRI, G., PAKAKOSTAS, P., KALOGERAS, K. T., KOSMIDIS, P. & FOUNTZILAS, G. 2008. Potential value of PTEN in predicting cetuximab response in colorectal cancer: an exploratory study. *BMC Cancer*, 8, 234.
- REID, S. E., KAY, E. J., NEILSON, L. J., HENZE, A. T., SERNEELS, J., MCGHEE, E. J., DHAYADE, S., NIXON, C., MACKAY, J. B., SANTI, A., SWAMINATHAN, K., ATHINEOS, D., PAPALAZAROU, V., PATELLA, F., ROMAN-FERNANDEZ, A., ELMAGHLOOB, Y., HERNANDEZ-FERNAUD, J. R., ADAMS, R. H., ISMAIL, S., BRYANT, D. M., SALMERON-SANCHEZ, M., MACHESKY, L. M., CARLIN, L. M., BLYTH, K., MAZZONE, M. & ZANIVAN, S. 2017. Tumor matrix stiffness promotes metastatic cancer cell interaction with the endothelium. *Embo j*, 36, 2373-2389.
- RHEE, S. G. 2006. H<sub>2</sub>O<sub>2</sub>, a necessary evil for cell signaling. *Science*, 312, 1882-1883.
- ROJO, A. I., SAGARRA, M. R. & CUADRADO, A. 2008. GSK-3 $\beta$  down-regulates the transcription factor Nrf2 after oxidant damage: relevance to exposure of neuronal cells to oxidative stress. *J Neurochem*, 105, 192-202.
- ROSENBERG, D. W., GIARDINA, C. & TANAKA, T. 2009. Mouse models for the study of colon carcinogenesis. *Carcinogenesis*, 30, 183-96.
- RYNER, L., GUAN, Y., FIRESTEIN, R., XIAO, Y., CHOI, Y., RABE, C., LU, S., FUENTES, E., HUW, L. Y., LACKNER, M. R., FU, L., AMLER, L. C., BAIS, C. & WANG, Y. 2015. Upregulation of Periostin and Reactive Stroma Is Associated with Primary Chemoresistance and Predicts Clinical Outcomes in Epithelial Ovarian Cancer. *Clin Cancer Res*, 21, 2941-51.
- SABATINI, D. M. 2006. mTOR and cancer: insights into a complex relationship. *Nat Rev Cancer*, 6, 729-34.

- SAGAR, J. 2011. Colorectal stents for the management of malignant colonic obstructions. *Cochrane Database Syst Rev*, Cd007378.
- SAKAMOTO, K., GORANSSON, O., HARDIE, D. G. & ALESSI, D. R. 2004. Activity of LKB1 and AMPK-related kinases in skeletal muscle: effects of contraction, phenformin, and AICAR. *Am J Physiol Endocrinol Metab*, 287, E310-7.
- SALAZAR, M., ROJO, A. I., VELASCO, D., DE SAGARRA, R. M. & CUADRADO, A. 2006. Glycogen synthase kinase-3beta inhibits the xenobiotic and antioxidant cell response by direct phosphorylation and nuclear exclusion of the transcription factor Nrf2. *J Biol Chem*, 281, 14841-51.
- SAMOWITZ, W. S., POWERS, M. D., SPIRIO, L. N., NOLLET, F., VAN ROY, F. & SLATTERY, M. L. 1999.  $\beta$ -catenin mutations are more frequent in small colorectal adenomas than in larger adenomas and invasive carcinomas. *Cancer research*, 59, 1442-1444.
- SAMUELS, Y., WANG, Z., BARDELLI, A., SILLIMAN, N., PTAK, J., SZABO, S., YAN, H., GAZDAR, A., POWELL, S. M., RIGGINS, G. J., WILLSON, J. K., MARKOWITZ, S., KINZLER, K. W., VOGELSTEIN, B. & VELCULESCU, V. E. 2004. High frequency of mutations of the PIK3CA gene in human cancers. *Science*, 304, 554.
- SANCAK, Y., THOREEN, C. C., PETERSON, T. R., LINDQUIST, R. A., KANG, S. A., SPOONER, E., CARR, S. A. & SABATINI, D. M. 2007. PRAS40 is an insulin-regulated inhibitor of the mTORC1 protein kinase. *Mol Cell*, 25, 903-15.
- SANCHO, E., BATLLE, E. & CLEVERS, H. 2003. Live and let die in the intestinal epithelium. *Curr Opin Cell Biol*, 15, 763-70.
- SANSOM, O. J., MENIEL, V., WILKINS, J. A., COLE, A. M., OIEN, K. A., MARSH, V., JAMIESON, T. J., GUERRA, C., ASHTON, G. H., BARBACID, M. & CLARKE, A. R. 2006. Loss of Apc allows phenotypic manifestation of the transforming properties of an endogenous K-ras oncogene in vivo. *Proc Natl Acad Sci U S A*, 103, 14122-7.
- SANSOM, O. J., MENIEL, V. S., MUNCAN, V., PHESSSE, T. J., WILKINS, J. A., REED, K. R., VASS, J. K., ATHINEOS, D., CLEVERS, H. & CLARKE, A. R. 2007. Myc deletion rescues Apc deficiency in the small intestine. *Nature*, 446, 676-9.
- SANSOM, O. J., REED, K. R., HAYES, A. J., IRELAND, H., BRINKMANN, H., NEWTON, I. P., BATLLE, E., SIMON-ASSMANN, P., CLEVERS, H., NATHKE, I. S., CLARKE, A. R. & WINTON, D. J. 2004. Loss of Apc in vivo immediately perturbs Wnt signaling, differentiation, and migration. *Genes & Development*, 18, 1385-1390.
- SARTORE-BIANCHI, A., MARTINI, M., MOLINARI, F., VERONESE, S., NICHELATTI, M., ARTALE, S., DI NICOLANTONIO, F., SALETTI, P., DE DOSSO, S., MAZZUCHELLI, L., FRATTINI, M., SIENA, S. & BARDELLI, A. 2009. PIK3CA mutations in colorectal cancer are associated with clinical resistance to EGFR-targeted monoclonal antibodies. *Cancer Res*, 69, 1851-7.
- SASAI, H., MASAKI, M. & WAKITANI, K. 2000. Suppression of polypogenesis in a new mouse strain with a truncated Apc(Delta474) by a novel COX-2 inhibitor, JTE-522. *Carcinogenesis*, 21, 953-8.
- SASAKI, H., SUZUKI, A., SHITARA, M., HIKOSAKA, Y., OKUDA, K., MORIYAMA, S., YANO, M. & FUJII, Y. 2013. Genotype analysis of the NRF2 gene mutation in lung cancer. *Int J Mol Med*, 31, 1135-8.
- SATO, T., STANGE, D. E., FERRANTE, M., VRIES, R. G., VAN ES, J. H., VAN DEN BRINK, S., VAN HOUDT, W. J., PRONK, A., VAN GORP, J., SIERSEMA, P. D. & CLEVERS, H. 2011. Long-term expansion of epithelial organoids from human colon, adenoma, adenocarcinoma, and Barrett's epithelium. *Gastroenterology*, 141, 1762-72.

- SATO, T., VRIES, R. G., SNIPPERT, H. J., VAN DE WETERING, M., BARKER, N., STANGE, D. E., VAN ES, J. H., ABO, A., KUJALA, P., PETERS, P. J. & CLEVERS, H. 2009. Single Lgr5 stem cells build crypt-villus structures in vitro without a mesenchymal niche. *Nature*, 459, 262-5.
- SCHEPERS, A. & CLEVERS, H. 2012. Wnt Signaling, Stem Cells, and Cancer of the Gastrointestinal Tract. *Cold Spring Harbor Perspectives in Biology*, 4, a007989.
- SCHOENFELD, J. D., SIBENALLER, Z. A., MAPUSKAR, K. A., WAGNER, B. A., CRAMER-MORALES, K. L., FURQAN, M., SANDHU, S., CARLISLE, T. L., SMITH, M. C., ABU HEJLEH, T., BERG, D. J., ZHANG, J., KEECH, J., PAREKH, K. R., BHATIA, S., MONGA, V., BODEKER, K. L., AHMANN, L., VOLLSTEDT, S., BROWN, H., KAUFFMAN, E. P. S., SCHALL, M. E., HOHL, R. J., CLAMON, G. H., GREENLEE, J. D., HOWARD, M. A., SCHULTZ, M. K., SMITH, B. J., RILEY, D. P., DOMANN, F. E., CULLEN, J. J., BUETTNER, G. R., BUATTI, J. M., SPITZ, D. R. & ALLEN, B. G. 2017. O<sub>2</sub>- and H<sub>2</sub>O<sub>2</sub>-Mediated Disruption of Fe Metabolism Causes the Differential Susceptibility of NSCLC and GBM Cancer Cells to Pharmacological Ascorbate. *Cancer Cell*, 32, 268.
- SCHUBBERT, S., SHANNON, K. & BOLLAG, G. 2007. Hyperactive Ras in developmental disorders and cancer. *Nat Rev Cancer*, 7, 295-308.
- SCREATON, R. A., CONKRIGHT, M. D., KATOH, Y., BEST, J. L., CANETTIERI, G., JEFFRIES, S., GUZMAN, E., NIESSEN, S., YATES, J. R., 3RD, TAKEMORI, H., OKAMOTO, M. & MONTMINY, M. 2004. The CREB coactivator TORC2 functions as a calcium- and cAMP-sensitive coincidence detector. *Cell*, 119, 61-74.
- SEHGAL, R. & COFFEY, J. C. 2014. Historical development of mesenteric anatomy provides a universally applicable anatomic paradigm for complete/total mesocolic excision. *Gastroenterol Rep (Oxf)*, 2, 245-50.
- SEOW, H. F., YIP, W. K. & FIFIS, T. 2016. Advances in targeted and immunobased therapies for colorectal cancer in the genomic era. *Oncotargets Ther*, 9, 1899-920.
- SHAMSUDDIN, A. K. & PHILLIPS, R. M. 1981. Preneoplastic and neoplastic changes in colonic mucosa in Crohn's disease. *Arch Pathol Lab Med*, 105, 283-6.
- SHAW, R. J., KOSMATKA, M., BARDEESY, N., HURLEY, R. L., WITTERS, L. A., DEPINHO, R. A. & CANTLEY, L. C. 2004. The tumor suppressor LKB1 kinase directly activates AMP-activated kinase and regulates apoptosis in response to energy stress. *Proc Natl Acad Sci U S A*, 101, 3329-35.
- SHIBATA, H., TOYAMA, K., SHIOYA, H., ITO, M., HIROTA, M., HASEGAWA, S., MATSUMOTO, H., TAKANO, H., AKIYAMA, T., TOYOSHIMA, K., KANAMARU, R., KANEGAE, Y., SAITO, I., NAKAMURA, Y., SHIBA, K. & NODA, T. 1997. Rapid colorectal adenoma formation initiated by conditional targeting of the Apc gene. *Science*, 278, 120-3.
- SHIBATA, T., KOKUBU, A., GOTOH, M., OJIMA, H., OHTA, T., YAMAMOTO, M. & HIROHASHI, S. 2008a. Genetic alteration of Keap1 confers constitutive Nrf2 activation and resistance to chemotherapy in gallbladder cancer. *Gastroenterology*, 135, 1358-1368. e4.
- SHIBATA, T., KOKUBU, A., SAITO, S., NARISAWA-SAITO, M., SASAKI, H., AOYAGI, K., YOSHIMATSU, Y., TACHIMORI, Y., KUSHIMA, R. & KIYONO, T. 2011. NRF2 mutation confers malignant potential and resistance to chemoradiation therapy in advanced esophageal squamous cancer. *Neoplasia*, 13, 864IN24-873IN26.
- SHIBATA, T., OHTA, T., TONG, K. I., KOKUBU, A., ODOGAWA, R., TSUTA, K., ASAMURA, H., YAMAMOTO, M. & HIROHASHI, S. 2008b. Cancer related mutations in NRF2 impair its recognition by Keap1-Cul3 E3 ligase and promote malignancy. *Proceedings of the National Academy of Sciences*, 105, 13568-13573.

- SIDERIS, M. & PAPAGRIGORIADIS, S. 2014. Molecular biomarkers and classification models in the evaluation of the prognosis of colorectal cancer. *Anticancer Res*, 34, 2061-8.
- SINGH, A., MISRA, V., THIMMULAPPA, R. K., LEE, H., AMES, S., HOQUE, M. O., HERMAN, J. G., BAYLIN, S. B., SIDRANSKY, D. & GABRIELSON, E. 2006. Dysfunctional KEAP1–NRF2 interaction in non-small-cell lung cancer. *PLoS medicine*, 3, e420.
- SMITH, J. J., DEANE, N. G., DHAWAN, P. & BEAUCHAMP, R. D. 2008. Regulation of metastasis in colorectal adenocarcinoma: a collision between development and tumor biology. *Surgery*, 144, 353-66.
- SMITS, R., KARTHEUSER, A., JAGMOHAN-CHANGUR, S., LEBLANC, V., BREUKEL, C., DE VRIES, A., VAN KRANEN, H., VAN KRIEKEN, J. H., WILLIAMSON, S., EDELMANN, W., KUCHERLAPATI, R., KHANPM & FODDE, R. 1997. Loss of Apc and the entire chromosome 18 but absence of mutations at the Ras and Tp53 genes in intestinal tumors from Apc1638N, a mouse model for Apc-driven carcinogenesis. *Carcinogenesis*, 18, 321-7.
- SOLIS, L. M., BEHRENS, C., DONG, W., SURAOOKAR, M., OZBURN, N., MORAN, C., CORVALAN, A. H., BISWAL, S., SWISHER, S. G. & BEKELE, B. N. 2010a. Nrf2 and Keap1 abnormalities in non-small cell lung carcinoma and association with clinicopathologic features. *Clinical Cancer Research*, clincanres. 3352. subyr.
- SOLIS, L. M., BEHRENS, C., DONG, W., SURAOOKAR, M., OZBURN, N. C., MORAN, C. A., CORVALAN, A. H., BISWAL, S., SWISHER, S. G., BEKELE, B. N., MINNA, J. D., STEWART, D. J. & WISTUBA, II 2010b. Nrf2 and Keap1 abnormalities in non-small cell lung carcinoma and association with clinicopathologic features. *Clin Cancer Res*, 16, 3743-53.
- SOUCEK, L., WHITFIELD, J., MARTINS, C. P., FINCH, A. J., MURPHY, D. J., SODIR, N. M., KARNEZIS, A. N., SWIGART, L. B., NASI, S. & EVAN, G. I. 2008. Modelling Myc inhibition as a cancer therapy. *Nature*, 455, 679-83.
- SPARKS, A. B., MORIN, P. J., VOGELSTEIN, B. & KINZLER, K. W. 1998. Mutational analysis of the APC/β-catenin/Tcf pathway in colorectal cancer. *Cancer research*, 58, 1130-1134.
- SPORN, M. B. & LIBY, K. T. 2012. NRF2 and cancer: the good, the bad and the importance of context. *Nat Rev Cancer*, 12, 564-71.
- STACHEL, I., GEISMANN, C., ADEN, K., DEISINGER, F., ROSENSTIEL, P., SCHREIBER, S., SEBENS, S., ARLT, A. & SCHAFER, H. 2014. Modulation of nuclear factor E2-related factor-2 (Nrf2) activation by the stress response gene immediate early response-3 (IER3) in colonic epithelial cells: a novel mechanism of cellular adaption to inflammatory stress. *J Biol Chem*, 289, 1917-29.
- STEINBACH, G., LYNCH, P. M., PHILLIPS, R. K., WALLACE, M. H., HAWK, E., GORDON, G. B., WAKABAYASHI, N., SAUNDERS, B., SHEN, Y., FUJIMURA, T., SU, L. K., LEVIN, B., GODIO, L., PATTERSON, S., RODRIGUEZ-BIGAS, M. A., JESTER, S. L., KING, K. L., SCHUMACHER, M., ABBRUZZESE, J., DUBOIS, R. N., HITTELMAN, W. N., ZIMMERMAN, S., SHERMAN, J. W. & KELLOFF, G. 2000. The effect of celecoxib, a cyclooxygenase-2 inhibitor, in familial adenomatous polyposis. *N Engl J Med*, 342, 1946-52.
- STORZ, P. 2005. Reactive oxygen species in tumor progression. *Front Biosci*, 10, 1881-96.
- SUN, X., GAO, L., CHIEN, H. Y., LI, W. C. & ZHAO, J. 2013. The regulation and function of the NUA family. *J Mol Endocrinol*, 51, R15-22.
- SUTHERLAND, C. 2011. What are the bona fide GSK3 substrates? *International journal of Alzheimer's Disease*, 2011.

- SUZUKI, A., KUSAKAI, G., KISHIMOTO, A., LU, J., OGURA, T. & ESUMI, H. 2003a. ARK5 suppresses the cell death induced by nutrient starvation and death receptors via inhibition of caspase 8 activation, but not by chemotherapeutic agents or UV irradiation. *Oncogene*, 22, 6177-82.
- SUZUKI, A., KUSAKAI, G., KISHIMOTO, A., LU, J., OGURA, T., LAVIN, M. F. & ESUMI, H. 2003b. Identification of a novel protein kinase mediating Akt survival signaling to the ATM protein. *J Biol Chem*, 278, 48-53.
- SUZUKI, A., KUSAKAI, G., KISHIMOTO, A., MINEGICHI, Y., OGURA, T. & ESUMI, H. 2003c. Induction of cell-cell detachment during glucose starvation through F-actin conversion by SNARK, the fourth member of the AMP-activated protein kinase catalytic subunit family. *Biochem Biophys Res Commun*, 311, 156-61.
- SUZUKI, A., OGURA, T. & ESUMI, H. 2006. NDR2 acts as the upstream kinase of ARK5 during insulin-like growth factor-1 signaling. *J Biol Chem*, 281, 13915-21.
- SUZUKI, T., SHIBATA, T., TAKAYA, K., SHIRAIISHI, K., KOHNO, T., KUNITOH, H., TSUTA, K., FURUTA, K., GOTO, K. & HOSODA, F. 2013. Regulatory nexus of synthesis and degradation deciphers cellular Nrf2 expression levels. *Molecular and cellular biology*, 33, 2402-2412.
- SZATROWSKI, T. P. & NATHAN, C. F. 1991. Production of large amounts of hydrogen peroxide by human tumor cells. *Cancer Res*, 51, 794-8.
- TABERNERO, J., VAN CUTSEM, E., LAKOMY, R., PRAUSOVA, J., RUFF, P., VAN HAZEL, G. A., MOISEYENKO, V. M., FERRY, D. R., MCKENDRICK, J. J., SOUSSAN-LAZARD, K., CHEVALIER, S. & ALLEGRA, C. J. 2014. Aflibercept versus placebo in combination with fluorouracil, leucovorin and irinotecan in the treatment of previously treated metastatic colorectal cancer: prespecified subgroup analyses from the VELOUR trial. *Eur J Cancer*, 50, 320-31.
- TAKAKU, K., OSHIMA, M., MIYOSHI, H., MATSUI, M., SELDIN, M. F. & TAKETO, M. M. 1998. Intestinal tumorigenesis in compound mutant mice of both Dpc4 (Smad4) and Apc genes. *Cell*, 92, 645-56.
- TAMMELA, T., SANCHEZ-RIVERA, F. J., CETINBAS, N. M., WU, K., JOSHI, N. S., HELENIUS, K., PARK, Y., AZIMI, R., KERPER, N. R., WESSELHOEFT, R. A., GU, X., SCHMIDT, L., CORNWALL-BRADY, M., YILMAZ, O. H., XUE, W., KATAJISTO, P., BHUTKAR, A. & JACKS, T. 2017. A Wnt-producing niche drives proliferative potential and progression in lung adenocarcinoma. *Nature*, 545, 355-359.
- THAKER, A. I., SHAKER, A., RAO, M. S. & CIORBA, M. A. 2012. Modeling colitis-associated cancer with azoxymethane (AOM) and dextran sulfate sodium (DSS). *J Vis Exp*.
- THOTALA, D. K. & YAZLOVITSKAYA, E. M. 2011. GSK3B (glycogen synthase kinase 3 beta).
- TOBIAS JEFFREY S., H., DANIEL 2013. *Cancer and its Management*, Wiley-Blackwell.
- TOYOSHIMA, M., HOWIE, H. L., IMAKURA, M., WALSH, R. M., ANNIS, J. E., CHANG, A. N., FRAZIER, J., CHAU, B. N., LOBODA, A., LINSLEY, P. S., CLEARY, M. A., PARK, J. R. & GRANDORI, C. 2012. Functional genomics identifies therapeutic targets for MYC-driven cancer. *Proc Natl Acad Sci U S A*, 109, 9545-50.
- TRACHOOTHAM, D., ALEXANDRE, J. & HUANG, P. 2009. Targeting cancer cells by ROS-mediated mechanisms: a radical therapeutic approach? *Nat Rev Drug Discov*, 8, 579-91.
- TSUCHIHARA, K., OGURA, T., FUJIOKA, R., FUJII, S., KUGA, W., SAITO, M., OCHIYA, T., OCHIAI, A. & ESUMI, H. 2008. Susceptibility of Snark-deficient mice to azoxymethane-induced colorectal tumorigenesis and the formation of aberrant crypt foci. *Cancer Sci*, 99, 677-82.

- TVEIT, K. M., GUREN, T., GLIMELIUS, B., PFEIFFER, P., SORBYE, H., PYRHONEN, S., SIGURDSSON, F., KURE, E., IKDAHL, T., SKOVLUND, E., FOKSTUEN, T., HANSEN, F., HOFSLI, E., BIRKEMEYER, E., JOHNSON, A., STARKHAMMAR, H., YILMAZ, M. K., KELDSEN, N., ERDAL, A. B., DAJANI, O., DAHL, O. & CHRISTOFFERSEN, T. 2012. Phase III trial of cetuximab with continuous or intermittent fluorouracil, leucovorin, and oxaliplatin (Nordic FLOX) versus FLOX alone in first-line treatment of metastatic colorectal cancer: the NORDIC-VII study. *J Clin Oncol*, 30, 1755-62.
- TYANOVA, S., TEMU, T., SINITCYN, P., CARLSON, A., HEIN, M. Y., GEIGER, T., MANN, M. & COX, J. 2016. The Perseus computational platform for comprehensive analysis of (prote)omics data. *Nat Methods*, 13, 731-40.
- VAN CUTSEM, E., KOHNE, C. H., HITRE, E., ZALUSKI, J., CHANG CHIEN, C. R., MAKHSON, A., D'HAENS, G., PINTER, T., LIM, R., BODOKY, G., ROH, J. K., FOLPRECHT, G., RUFF, P., STROH, C., TEJPAR, S., SCHLICHTING, M., NIPPGEN, J. & ROUGIER, P. 2009. Cetuximab and chemotherapy as initial treatment for metastatic colorectal cancer. *N Engl J Med*, 360, 1408-17.
- VAN CUTSEM, E., TABERNERO, J., LAKOMY, R., PRENEN, H., PRAUSOVA, J., MACARULLA, T., RUFF, P., VAN HAZEL, G. A., MOISEYENKO, V., FERRY, D., MCKENDRICK, J., POLIKOFF, J., TELLIER, A., CASTAN, R. & ALLEGRA, C. 2012. Addition of aflibercept to fluorouracil, leucovorin, and irinotecan improves survival in a phase III randomized trial in patients with metastatic colorectal cancer previously treated with an oxaliplatin-based regimen. *J Clin Oncol*, 30, 3499-506.
- VAN DE WETERING, M., SANCHO, E., VERWEIJ, C., DE LAU, W., O Ving, I., HURLSTONE, A., VAN DER HORN, K., BATLLE, E., COUDREUSE, D., HARAMIS, A. P., TJON-PON-FONG, M., MOERER, P., VAN DEN BORN, M., SOETE, G., PALS, S., EILERS, M., MEDEMA, R. & CLEVERS, H. 2002. The beta-catenin/TCF-4 complex imposes a crypt progenitor phenotype on colorectal cancer cells. *Cell*, 111, 241-50.
- VAN DEN BIGGELAAR, M., HERNANDEZ-FERNAUD, J. R., VAN DEN ESHOF, B. L., NEILSON, L. J., MEIJER, A. B., MERTENS, K. & ZANIVAN, S. 2014. Quantitative phosphoproteomics unveils temporal dynamics of thrombin signaling in human endothelial cells. *Blood*, 123, e22-36.
- VAN SCHAEYBROECK, S., ALLEN, W. L., TURKINGTON, R. C. & JOHNSTON, P. G. 2011. Implementing prognostic and predictive biomarkers in CRC clinical trials. *Nature reviews Clinical oncology*, 8, 222-232.
- VANDER HAAR, E., LEE, S. I., BANDHAKAVI, S., GRIFFIN, T. J. & KIM, D. H. 2007. Insulin signalling to mTOR mediated by the Akt/PKB substrate PRAS40. *Nat Cell Biol*, 9, 316-23.
- VASEN, H. F., MOSLEIN, G., ALONSO, A., ARETZ, S., BERNSTEIN, I., BERTARIO, L., BLANCO, I., BULOW, S., BURN, J., CAPELLA, G., COLAS, C., ENGEL, C., FRAYLING, I., FRIEDL, W., HES, F. J., HODGSON, S., JARVINEN, H., MECKLIN, J. P., MOLLER, P., MYRHOI, T., NAGENGAST, F. M., PARC, Y., PHILLIPS, R., CLARK, S. K., DE LEON, M. P., RENKONEN-SINISALO, L., SAMPSON, J. R., STORMORKEN, A., TEJPAR, S., THOMAS, H. J. & WIJNEN, J. 2008. Guidelines for the clinical management of familial adenomatous polyposis (FAP). *Gut*, 57, 704-13.
- VOGELSTEIN, B., FEARON, E. R., HAMILTON, S. R., KERN, S. E., PREISINGER, A. C., LEPPERT, M., NAKAMURA, Y., WHITE, R., SMITS, A. M. & BOS, J. L. 1988. Genetic alterations during colorectal-tumor development. *N Engl J Med*, 319, 525-32.

- VOOIJIS, M., JONKERS, J. & BERNIS, A. 2001. A highly efficient ligand- regulated Cre recombinase mouse line shows that LoxP recombination is position dependent. *EMBO reports*, 2, 292-297.
- WALTHER, A., JOHNSTONE, E., SWANTON, C., MIDGLEY, R., TOMLINSON, I. & KERR, D. 2009. Genetic prognostic and predictive markers in colorectal cancer. *Nat Rev Cancer*, 9, 489-99.
- WANG, R. & GREEN, D. R. 2012. Metabolic checkpoints in activated T cells. *Nat Immunol*, 13, 907-15.
- WANG, X.-J., SUN, Z., VILLENEUVE, N. F., ZHANG, S., ZHAO, F., LI, Y., CHEN, W., YI, X., ZHENG, W. & WONDRAK, G. T. 2008a. Nrf2 enhances resistance of cancer cells to chemotherapeutic drugs, the dark side of Nrf2. *Carcinogenesis*, 29, 1235-1243.
- WANG, X. J., SUN, Z., VILLENEUVE, N. F., ZHANG, S., ZHAO, F., LI, Y., CHEN, W., YI, X., ZHENG, W., WONDRAK, G. T., WONG, P. K. & ZHANG, D. D. 2008b. Nrf2 enhances resistance of cancer cells to chemotherapeutic drugs, the dark side of Nrf2. *Carcinogenesis*, 29, 1235-43.
- WEINSTEIN, J. N., COLLISSON, E. A., MILLS, G. B., SHAW, K. R., OZENBERGER, B. A., ELLROTT, K., SHMULEVICH, I., SANDER, C. & STUART, J. M. 2013. The Cancer Genome Atlas Pan-Cancer analysis project. *Nat Genet*, 45, 1113-20.
- WIŚNIEWSKI, J. R., ZOUGMAN, A., NAGARAJ, N. & MANN, M. 2009. Universal sample preparation method for proteome analysis. *Nature methods*, 6, 359-362.
- WOODS, A., JOHNSTONE, S. R., DICKERSON, K., LEIPER, F. C., FRYER, L. G., NEUMANN, D., SCHLATTNER, U., WALLIMANN, T., CARLSON, M. & CARLING, D. 2003. LKB1 is the upstream kinase in the AMP-activated protein kinase cascade. *Curr Biol*, 13, 2004-8.
- WORLD CANCER RESEARCH FUND INTERNATIONAL, W. 2012. *Colorectal Cancer Statistics* [Online]. [Accessed 15/09/17 2017].
- YAMAMOTO, H., TAKASHIMA, S., SHINTANI, Y., YAMAZAKI, S., SEGUCHI, O., NAKANO, A., HIGO, S., KATO, H., LIAO, Y., ASANO, Y., MINAMINO, T., MATSUMURA, Y., TAKEDA, H. & KITAKAZE, M. 2008. Identification of a novel substrate for TNFalpha-induced kinase NUA2. *Biochem Biophys Res Commun*, 365, 541-7.
- YE, X. T., GUO, A. J., YIN, P. F., CAO, X. D. & CHANG, J. C. 2014. Overexpression of NUA1 is associated with disease-free survival and overall survival in patients with gastric cancer. *Med Oncol*, 31, 61.
- YOKOO, Y., KIJIMA, A., ISHII, Y., TAKASU, S., TSUCHIYA, T. & UMEMURA, T. 2016. Effects of Nrf2 silencing on oxidative stress-associated intestinal carcinogenesis in mice. *Cancer Med*, 5, 1228-38.
- YOUNG, M., ORDONEZ, L. & CLARKE, A. R. 2013. What are the best routes to effectively model human colorectal cancer? *Mol Oncol*, 7, 178-89.
- YOUNG, M. & REED, K. R. 2016. Organoids as a Model for Colorectal Cancer. *Current Colorectal Cancer Reports*, 12, 281-287.
- YU, M., TING, D. T., STOTT, S. L., WITTNER, B. S., OZSOLAK, F., PAUL, S., CICILIANO, J. C., SMAS, M. E., WINOKUR, D., GILMAN, A. J., ULMAN, M. J., XEGA, K., CONTINO, G., ALAGESAN, B., BRANNIGAN, B. W., MILOS, P. M., RYAN, D. P., SEQUIST, L. V., BARDEESY, N., RAMASWAMY, S., TONER, M., MAHESWARAN, S. & HABER, D. A. 2012. RNA sequencing of pancreatic circulating tumour cells implicates WNT signalling in metastasis. *Nature*, 487, 510-3.

- YUN, J., MULLARKY, E., LU, C., BOSCH, K. N., KAVALIER, A., RIVERA, K., ROPER, J., CHIO, II, GIANNOPOULOU, E. G., RAGO, C., MULEY, A., ASARA, J. M., PAIK, J., ELEMENTO, O., CHEN, Z., PAPPIN, D. J., DOW, L. E., PAPADOPOULOS, N., GROSS, S. S. & CANTLEY, L. C. 2015. Vitamin C selectively kills KRAS and BRAF mutant colorectal cancer cells by targeting GAPDH. *Science*, 350, 1391-6.
- ZAGORSKA, A., DEAK, M., CAMPBELL, D. G., BANERJEE, S., HIRANO, M., AIZAWA, S., PRESCOTT, A. R. & ALESSI, D. R. 2010. New roles for the LKB1-NUAK pathway in controlling myosin phosphatase complexes and cell adhesion. *Sci Signal*, 3, ra25.
- ZAROGOULIDIS, P., LAMPAKI, S., TURNER, J. F., HUANG, H., KAKOLYRIS, S., SYRIGOS, K. & ZAROGOULIDIS, K. 2014. mTOR pathway: A current, up-to-date mini-review (Review). *Oncology Letters*, 8, 2367-2370.
- ZHANG, D. D., LO, S. C., CROSS, J. V., TEMPLETON, D. J. & HANNINK, M. 2004. Keap1 is a redox-regulated substrate adaptor protein for a Cul3-dependent ubiquitin ligase complex. *Mol Cell Biol*, 24, 10941-53.
- ZHANG, P., SINGH, A., YEGNASUBRAMANIAN, S., ESOP, D., KOMBAIRAJU, P., BODAS, M., WU, H., BOVA, S. G. & BISWAL, S. 2010. Loss of Kelch-like ECH-associated protein 1 function in prostate cancer cells causes chemoresistance and radioresistance and promotes tumor growth. *Mol Cancer Ther*, 9, 336-46.
- ZHANG, Y. & YANG, J. H. 2013. Activation of the PI3K/Akt pathway by oxidative stress mediates high glucose-induced increase of adipogenic differentiation in primary rat osteoblasts. *J Cell Biochem*, 114, 2595-602.
- ZHOU, G., MYERS, R., LI, Y., CHEN, Y., SHEN, X., FENYK-MELODY, J., WU, M., VENTRE, J., DOEBBER, T., FUJII, N., MUSI, N., HIRSHMAN, M. F., GOODYEAR, L. J. & MOLLER, D. E. 2001. Role of AMP-activated protein kinase in mechanism of metformin action. *J Clin Invest*, 108, 1167-74.
- ZMIJEWSKI, J. W., BANERJEE, S., BAE, H., FRIGGERI, A., LAZAROWSKI, E. R. & ABRAHAM, E. 2010. Exposure to hydrogen peroxide induces oxidation and activation of AMP-activated protein kinase. *J Biol Chem*, 285, 33154-64.